AN INVESTIGATION OF *N*-HETEROCYCLIC CARBENE CARBOXYLATES: INSIGHT INTO DECARBOXYLATION, A TRANSCARBOXYLATION REACTION, AND SYNTHESIS OF HYDROGEN BONDING PRECURSORS

by

Bret Ryan Van Ausdall

A dissertation submitted to the faculty of
The University of Utah
in partial fulfillment of the requirement for the degree of

Doctor of Philosophy

Department of Chemistry

The University of Utah

May 2012

The University of Utah Graduate School

STATEMENT OF DISSERTATION APPROVAL

The dissertation of **Bret Ryan Van Ausdall**

has been approved by the following supervisory committee members:

Janis Louie	, Chair	**7-8-2011** Date Approved
Cynthia Burrows	, Member	**7-8-2011** Date Approved
Thomas Richmond	, Member	**7-8-2011** Date Approved
Matthew S. Sigman	, Member	**7-8-2011** Date Approved
Debra Mascaro	, Member	**7-8-2011** Date Approved

and by **Henry S. White** , Chair of the Department of **Chemistry**

and by Charles A. Wight, Dean of The Graduate School.

ABSTRACT

A series of 1,3-disubstituted-2-imidazolium carboxylates, an adduct of CO_2 and N-heterocyclic carbenes, was synthesized and characterized using single crystal X-ray, thermogravimetric, IR, and NMR analysis. The TGA analysis of the imidazolium carboxylates shows that as steric bulk on the N-substituent increases, the ability of the NHC-CO_2 to decarboxylate increases. Single crystal X-ray analysis shows that the torsional angle of the carboxylate group and the C-CO_2 bond length with respect to the imidazolium ring is dependent on the steric bulk of the N-substituent. Rotamers in the unit cell of a single crystal of I^{t}BuPrCO_2 (2_f) indicate that the C-CO_2 bond length increases as the N-substituents rotate toward the carboxylate moiety, which suggests that rotation of the N-substituents through the plane of the C-CO_2 bond may be involved in the bond breaking event to release CO_2.

Combination of *N*,*N*-bis(2,6-diisopropylphenyl)imidazolum-2-carboxylate (IPrCO_2) with the Lewis acids $MBPh_4$, where M=Li or Na, provided two separate complexes, a monomer and dimer, respectively. Combination of *N*,*N*-bis(2,4,6-trimethyllphenyl)imidazolum-2-carboxylate (IMesCO_2) with $LiBPh_4$ afforded a dimeric species that was similar in global structure to that of the IPrCO_2+$NaBPh_4$ dimer. Thermogravimetric analysis of the crystals demonstrated that decarboxylation occurred at lower temperatures than the decarboxylation temperature of the parent NHC·CO_2. Kinetic analysis of the transcarboxylation of IPrCO_2 to acetophenone with $NaBPh_4$ to

yield sodium benzoylacetate was performed. First order dependencies were observed for $IPrCO_2$ and acetophenone while zero order dependence was observed for $NaBPh_4$. Direct dicarboxylation of MeCN was observed after combination with I^tBuCO_2 in the absence of salts.

An imidazolium salt, 1-2,4,6-trimethylphenyl-3-lactamidebenzylimidazolium tosylate was synthesized and characterized by ^1H NMR, ^{13}C NMR, and single crystal x-ray analysis. The downfield shift of the amide protons in the ^1H NMR spectrum salt relative to the starting material lactamide-OTs indicate that hydrogen bonding was present in solution. The crystal structure of imidazolium tosylate showed a series of intermolecular hydrogen bonds between amide groups and tosylate anions. The amount of hydrogen bonding present in the carbene precursor is promising for attempts to observe intramolecular hydrogen bonding with a carbene and the carboxylate.

CONTENTS

LIST OF ABBREVIATIONS

Bn – benzyl

Boc – *tert*-butyl carbamate

BF_4^- – tetrafluoroborate

BPh_4 – tetraphenylborate

CO_2 – carbon dioxide

Cy – cyclohexyl

d – doublet

DMA – *N*, *N* – dimethylacetamide

DMF – *N*, *N* – dimethylformamide

DMC - dimethylcarbonate

DMSO – dimethylsulfoxide

ee – enantiomeric excess

Et – ethyl

IEt – 1,3-diethylimidazol-2-ylidene

$IEtCO_2$ – 1,3-diethylimidazolium-2-carboxylate

IEt_{Me} – 1,3-diethyl-4,5-dimethylimidazol-2-ylidene

$IEt_{Me}CO_2$ – 1,3-diethyl-4,5-dimethylimidazolium-2-carboxylate

I^iPr_{Me} – 1,3-isopropyl-4,5-dimethylimidazol-2-ylidene

$I^iPr_{Me}CO_2$ – 1,3-isopropyl-4,5-dimethylimidazolium-2-carboxylate

IMe – 1,3-dimethylimidazol-2-ylidene

$IMeCO_2$ – 1,3-dimethylimidazolium-2-carboxylate

IMe_{Me} – 1,3,4,5-tetramethylimidazol-2-ylidene

$IMe_{Me}CO_2$ – 1,3-tetramethylimidazolium-2-carboxylate

IMes – 1,3-bis-(2,4,6-trimethylphenyl)-imidazol-2-ylidene

$IMesCO_2$ – 1,3-bis-(2,4,6-trimethylphenyl)-imidazolium-2-carboxylate

$IMes_{Me}$ – 1,3-bis-(2,4,6-trimethylphenyl)-4,5-dimethylimidazol-2-ylidene

$IMes_{Me}CO_2$ – 1,3-bis-(2,4,6-trimethylphenyl)-4,5-dimethylimidazolium-2-carboxylate

IMe^{t}Bu – 1- *tert*-butylimidazolium-3-methylimidazol-2-ylidene

IMe^{t}BuCO_2 – 1- *tert*-butylimidazolium-3-methylimidazolium-2-carboxylate

IPr – 1,3-bis-(2,6-diisopropylphenyl)-imidazol-2-ylidene

$IPrCO_2$ – 1,3-bis-(2,6-diisopropylphenyl)-imidazolium-2-carboxylate

IPr_{Me} – 1,3-bis-(2,6-diisopropylphenyl)-imidazol-2-ylidene

IPr $_{Me}CO_2$ – 1,3-bis-(2,6-diisopropylphenyl)-4,5-dimethylimidazolium-2-carboxylate

I^{t}Bu – 1,3-di-*tert*-butylimidazol-2-ylidene

I^{t}BuCO_2 – 1,3-di-*tert*-butylimidazolium-2-carboxylate

I^{t}Bu$PrCO_2$ – 1- *tert*-butylimidazolium-3-bis-(2,6-diisopropylphenyl)-imidazolium-2-carboxylate

*i*Pr – isopropyl

IR – infra-red

M – metal

m – multiplet

MeCN – acetonitrile

MeOH – methanol

n-Bu – normal-butyl

NHC – *N*-heterocyclic carbene

NHC·CO_2 – *N*-heterocyclic carbene carboxylate

NMR – Nuclear Magnetic resonance

OTs^- – *para*-tolylsulfonate

Ph – phenyl

q – quartet

s – singlet

SIPr – 1,3-bis(2,6-diisopropylphenyl)-imidazolin-2-ylidene

SIPrCO_2 – 1,3-bis(2,6-diisopropylphenyl)-imidazolium-2-carboxylate

SIMes – 1,3-bis-(2,4,6-trimethylphenyl)-imidazol-2-ylidene

SIMesCO_2 – 1,3-bis-(2,4,6-trimethylphenyl)-imidazolium-2-carboxylate

t – triplet

^{t}Bu – *tert*-butyl

TEMPOH - 1-hydroxy-2,2,6,6-tetramethyl-piperidine

TGA – thermogravimetric analysis

THF- tetrahydrofuran

TMS – trimethylsilyl

X – halogen

ACKNOWLEDGEMENTS

Many thanks to Paul, Yolanda, Marten, and Scott Van Ausdall, my family, for supporting me through this arduous journey; if it were not for their support, finishing this journey would not have been possible. My brother Scott deserves a separate token of gratitude for moving to Salt Lake in his own quest for knowledge and ultimately providing me invaluable brotherhood in times of struggle. It is not possible to thank my family enough.

I also thank the many friends through the years helped me in times of good and bad, both in lab and out, who provided me the means to not only grow as a scientist, but as a person.

Brendan D'Souza, Kainan Zhang, Jorge de Freitas, and Dave Thomas were lab mates as well as indispensible friends who helped create a lab that was not only a fun place, but a great learning environment where they helped inspire creativity on a daily basis. Dr. Dawn Troast, Dr. Pramod Chopade, and Dr. Rodrigo Cella, post-doctoral researchers at various points in the Louie Lab, helped my development as a researcher and also made life in lab more enjoyable early in my PhD research.

The University of Utah and the Chemistry Department must be given thanks as well. The staff that made the Chemistry Department run were invaluable in my research. Dr. Peter Flynn proved to be a bastion of knowledge in designing NMR experiments and

also provided key insight into future endeavors. Kevin Teaford, our master glass blower, brought my imagination to life and made several pieces of glassware that were essential in several experiments. Dr. Atta Aarif was a good friend as well as an excellent x-ray crystallographer. Tomi Carr, our groups assistant, proved to be a good friend through the years.

My committee members, Dr. Matthew Sigman, Dr. Cynthia Burrows, Dr. Thomas Richmond, and Dr. Debra Mascaro must be given thanks for providing insight and valuable criticism into my research and ideas throughout my PhD.

To Dr. Janis Louie, my advisor, I give thanks for providing key advice throughout my graduate student career and providing the funding to perform research. Her focus on the skills to be effective in presenting ideas in a clean and concise manner, as well as allowing for our own individuality in our group member's research paths, has provided us all with an invaluable skill set.

CHAPTER 1

A SYSTEMATIC INVESTIGATION OF FACTORS INFLUENCING THE DECARBOXYLATION OF IMIDAZOLIUM CARBOXYLATES

Introduction

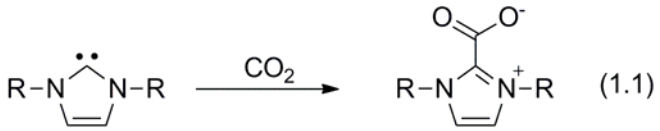

(1.1)

The capture of carbon dioxide by organic compounds has been a long-withstanding interest in organic chemistry.[1-30] Although the discovery of the reactivity of imidazolidenes to capture CO_2 was discovered a decade ago (Equation 1.1),[31-36] this reaction and the resulting imidazolium carboxylates remain underutilized. Initially, imidazolium carboxylates were used as an air stable precursor to imidazolidenes,[37,38] which are both highly synthetically useful ligands for transition metal catalysts[39-47] and potent nucleophilic organocatalysts.[48-52] In addition, the ability for NHCs to react with carbon dioxide (and other heterocumulenes) to afford stable zwitterions has been exploited to quench polymerizations catalyzed by NHCs.[53] More recently, imidazolium carboxylates themselves have demonstrated the ability to catalyze reactions such as the cyclotrimerization of isocyanates[54] and the coupling of epoxides and carbon dioxide.[55] Finally, imidazolium carboxylates have been shown to act as a CO_2 delivery agent in the carboxylation of acetophenone.[56,57] Despite these advances, the utility of imidazolium

carboxylates remains sparse. In an effort to increase the function of these interesting carboxylates, we have synthesized a large array of imidazolium carboxylates where we have systematically altered the *N*-substituent and studied their propensity to undergo thermal decarboxylation.

Results and Discussion

A series of imidazolium carboxylates were prepared (Scheme 1.1). The smallest carboxylate (**2a**) was synthesized using Crabtree's modification of a literature procedure.[37] In all other cases, we found imidazolium carboxylates (**2b-2h**) were generated cleanly and in excellent yields from direct carboxylation of the NHC precursors. Simple *N*-alkyl (**1b-1e**), aryl imidazole (**1f-1h**), and aryl imidazolin (**1i-1j**) carbenes were generated in situ from deprotonation of the corresponding imidazol(in)ium salt with potassium hexamethyldisilylazide (KHMDS) in toluene. Interestingly, the standard deprotonation methods such as catalytic amounts of KO^tBu with NaH[58] generally led to contaminated carboxylate. Furthermore, when a full equivalent of KO^tBu was used to deprotonate the imidazolium salts, the *tert*-butanol that was produced could not be separated effectively from the carbene. Ultimately, carboxylates that were determined to be pure by elemental analysis were obtained through the reaction of carbon dioxide and carbenes that were prepared in situ via the deprotonation of the imidazol(in)ium salts in toluene with KHMDS. Importantly, the carbenes were filtered away from the potassium halide salt by-product before exposure to carbon dioxide. This

Scheme 1.1 Synthesis of Imidazol(in)ium Carboxylates

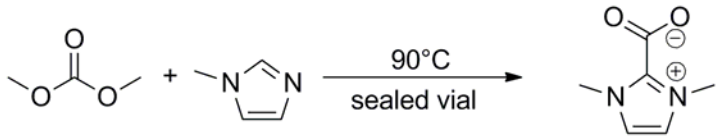

2a $IMeCO_2$

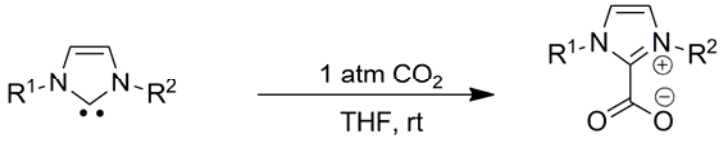

1b $R^1=R^2=$ Et (IEt)
1c $R^1=R^2=$ ^{i}Pr (I^iPr)
1d $R^1=R^2=$ ^{t}Bu (I^tBu)
1e $R^1=$ Me $R^2=$ ^{t}Bu (IMe^tBu)
1f $R^1=$ ^{t}Bu $R^2=$ 2,6-diisopropylphenyl (I^tBuIpr)
1g R = Mesityl (IMes)
1h R = 2,6-diisopropylphenyl (IPr)

2b $IEtCO_2$
2c I^iPrCO_2
2d I^tBuCO_2
2e IMe^tBuCO_2
2f $I^tBuIPrCO_2$
2g $IMesCO_2$
2h $IPrCO_2$

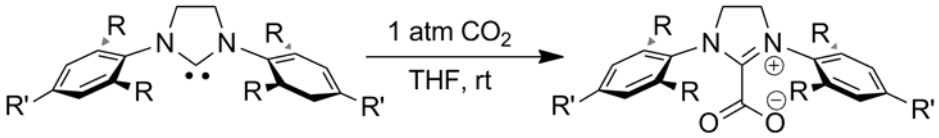

1i R = R' = Me (SIMes)
1j R = ^{i}Pr, R' = H (SIPr)

2i R = R' = Me ($SIMesCO_2$)
2j R = ^{i}Pr, R' = H ($SIPrCO_2$)

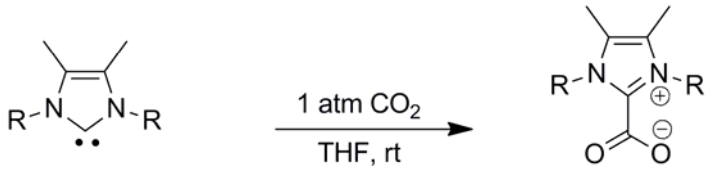

$1a_{Me}$ R = Me (IMe_{Me})
$1b_{Me}$ R = Et (IEt_{Me})
$1c_{Me}$ R = ^{i}Pr (I^iPr_{Me})
$1g_{Me}$ R = Mesityl (IMes)
$1h_{Me}$ R = 2,6-diisopropylphenyl (IPr)

$2a_{Me}$ $IMe_{Me}CO_2$
$2b_{Me}$ $IEt_{Me}CO_2$
$2c_{Me}$ $I^iPr_{Me}CO_2$
$2g_{Me}$ $IMes_{Me}CO_2$
$2h_{Me}$ $IPr_{Me}CO_2$

step is critical to obtain pure, salt-free imidazoylium carboxylates (**2b** – **2j**, *vide infra*). *N*-Alkyl carbenes that possess a methylated backbone (**1a$_{Me}$** – **1c$_{Me}$**) were prepared from the reduction of the corresponding thiourea with potassium and isolated prior to carboxylation.[59]

Reactions with Water

The stability of the imidazolium carboxylates toward water was evaluated. When H_2O was introduced to a CD_2Cl_2 solution of IMeCO_2 (**2a**), IEtCO_2 (**2b**), I^{i}PrCO_2 (**2c**), or I^{t}BuCO_2 (**2d**), protonation occurred within minutes as indicated by the appearance of a new singlet at 9.10 ppm in the respective ^{1}H NMR spectra (Equation 1.2). Interestingly, an imidazolium carbonate was formed, resulting from decarboxylation and subsequent protonation of the formed carbene.[60] Rogers and coworkers have prepared **3a$_{OCOOH}$** through a two-step reaction of **2a** and aqueous carbonic acid.

In contrast to N-alkyl imidazolium carboxylates, decarboxylation does not readily occur when water is added to N-aryl imidazolium carboxylates. Specifically, when H_2O was added to a solution of **2h** in CD_2Cl_2, the signature imidazolium proton signal at 9.10 ppm that was observed with the alkyl carboxylates **2a-2d** did not appear. Instead, a new set of signals for the aryl and backbone protons was observed alongside the original signals for starting carboxylate, **2h**. The backbone, -*ortho*, and -*meta* aryl protons all moved downfield, shifting from 7.17 ppm to 7.83 ppm, 7.28 ppm to 7.37 ppm, and 7.51 ppm to 7.6 ppm, respectively. We tentatively assign this species to an imidazolium carboxylate where the carboxylate is hydrogen bonded to a water molecule

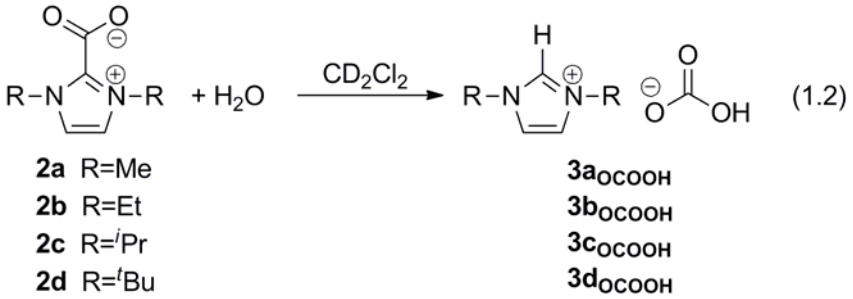

(Equation 1.3). The same phenomenon was observed when H_2O was added to aryl carboxylate $IMesCO_2$ (**2g**).

The addition of water to **2h** and **2a** in the presence of $NaBPh_4$ led to rapid and smooth decarboxylation (Equation 1.4). $IPrBPh_4$ and $IMeBPh_4$, which both possess a distinct acidic proton (~9 ppm in the ^1H NMR spectrum), and sodium carbonate were formed quantitatively.

IR Frequency Analysis

The imidazolium carboxylates display distinct carbonyl stretching frequencies (Table 1.1). *N*-Alkyl imidazolium carboxylates (**2a**-**2e**) have COO^- asymmetric stretching frequencies that are in the low to mid 1600 cm^{-1}. A slight trend relating the stretching frequencies and the size of the *N*-substituent was observed. As the alkyl substituent changes from Me to Et to *i*Pr (**2a, 2b, 2c**), the C=O stretching frequencies gradually increase. However, when the alkyl substituent is replaced with the bulky ^{t}Bu group (**2d**), the C=O stretching dramatically decreases by 37 cm^{-1}. The hybrid NHC-CO_2 **2e** has an intermediate frequency of 1647 cm^{-1}, in between $IMeCO_2$ (**2a**) and I^tBuCO_2 (**2d**).

Table 1.1. IR stretching frequencies of imidazol(in)ium carboxylates.

Entry	Carboxylate	ν_{COasym} (cm^{-1})
	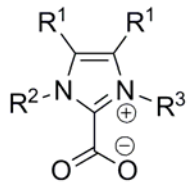	
1	**2a** R^1=H R^2=R^3=Me ($IMeCO_2$)	1653
2	**2b** R^1=H R^2=R^3=Et ($IEtCO_2$)	1654
3	**2c** R^1=H R^2=R^3=^{i}Pr (I^iPrCO_2)	1666
4	**2d** R^1=H R^2=R^3=^{t}Bu (I^tBuCO_2)	1629
5	**2e** R^1=H R^2=Me R^3= ^{t}Bu (IMe^tBuCO_2)	1647
6	**2a$_{Me}$** R^1=Me R^2=R^3=Me ($IMe_{Me}CO_2$)	1669
7	**2b$_{Me}$** R^1=Me R^2=R^3=Et ($IEt_{Me}CO_2$)	1657
8	**2c$_{Me}$** R^1=Me R^2=R^3=*i*Pr ($Ii Pr_{Me}CO_2$)	1662
9	**2f** R^1=^{t}Bu R^2= 2,6-diisopropylphenyl ($I^tBuIprCO_2$)	1675
10	**2g** R^1=H R^2=R^3=Me ($IMesCO_2$)	1675
11	**2g$_{Me}$** R^1=Me R^2=R^3=Me ($IMes_{Me}CO_2$)	1674
12	**2h** R^1=H R^2=R^3=2,6-diisopropylphenyl ($IPrCO_2$)	1678
13	**2h$_{Me}$** R^1=Me R^2=R^3=2,6-diisopropylphenyl ($IPr_{Me}CO_2$)	1683
	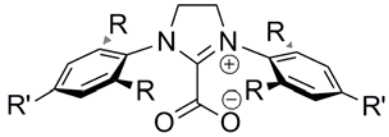	
11	**2i** R = R' = Me ($SIMesCO_2$)	1680
12	**2j** R = *i*Pr, R' = H ($SIPrCO_2$)	1683

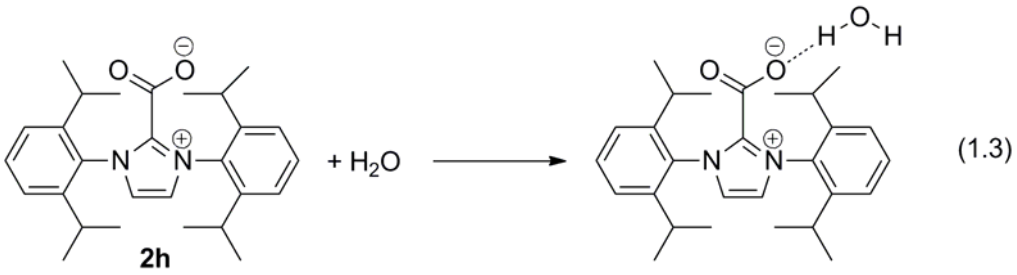

N-Aryl imidazolium carboxylates have higher C=O stretching frequencies than their *N*-alkyl counterparts. Interestingly, the stretching frequencies of $IMesCO_2$ (**2g**) and $IPrCO_2$ (**2h**) are almost identical, which suggests that the carbon-oxygen bond is less affected by the ortho-substituents (i.e., the methyl of the $IMesCO_2$ and the *i*Pr of the $IPrCO_2$) than in the *N*-alkyl series (i.e., **2a** vs. **2c**).

Modification of the imidazolium backbone, through either methylation or saturation, does not have a large influence on the C=O stretching frequencies. For example, the stretching frequency of **2b** and $\mathbf{2b_{Me}}$ differ by only 3 cm^{-1}. In addition, methylation of the backbone causes the C=O stretching frequency to increase for $\mathbf{2a_{Me}}$ (relative to **2a**) but causes a decrease for $\mathbf{2c_{Me}}$ (relative to **2c**). Imidazolinium carboxylates (**2i** and **2j**) displayed stretching frequencies that were only 5 cm^{-1} higher than their unsaturated analogs.

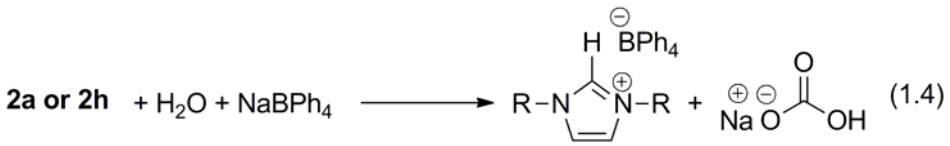

Thermogravimetric Analysis (TGA)

The imidazolium carboxylates were each evaluated by thermogravimetric analysis (TGA). During the investigation, we found that the amount of imidazolium carboxylate that was subjected to TGA had a profound effect on the results. For example, the TGA analysis of larger samples of $IPrCO_2$ (**2h**) afforded higher decarboxylation temperatures than smaller samples.[61] As such, subsequent TGA's were consistently performed with 3.5 mg of imidazolium carboxylate.

TGA of *N*-alkyl Imidazolium Carboxylates (2a-2d)

The TGA analysis of a series of *N*-alkyl carboxylates where the size of the *N*-alkyl substituent was increased in size (i.e., Me (**2a**), Et (**2b**), *i*Pr (**2c**), and ^{t}Bu (**2d**)) is shown in Figure 1.1. It is clear that an increase in substituent size leads to a decrease in decarboxylation temperature. At the two extremes, $IMeCO_2$ (**2a**) begins to decompose at 162 °C whereas I^tBuCO_2 (**2d**) loses CO_2 and decomposes at a much lower temperature (71 °C) for a difference in decarboxylation temperatures of 91 °C. Only $IEtCO_2$ (**2b**) does not seem to follow this trend and undergoes decarboxylation at 128 °C, i.e. 12 °C lower than the decarboxylation temperature of I^iPrCO_2 (**2c**). Interestingly, only I^tBuCO_2 displays a biphasic TGA curve suggesting that a short-lived intermediate, presumably I^tBu, is generated. Nevertheless, CO_2 was detected via mass spectrometry at the onset of weight loss in each TGA analysis of **2a**-**2d**.

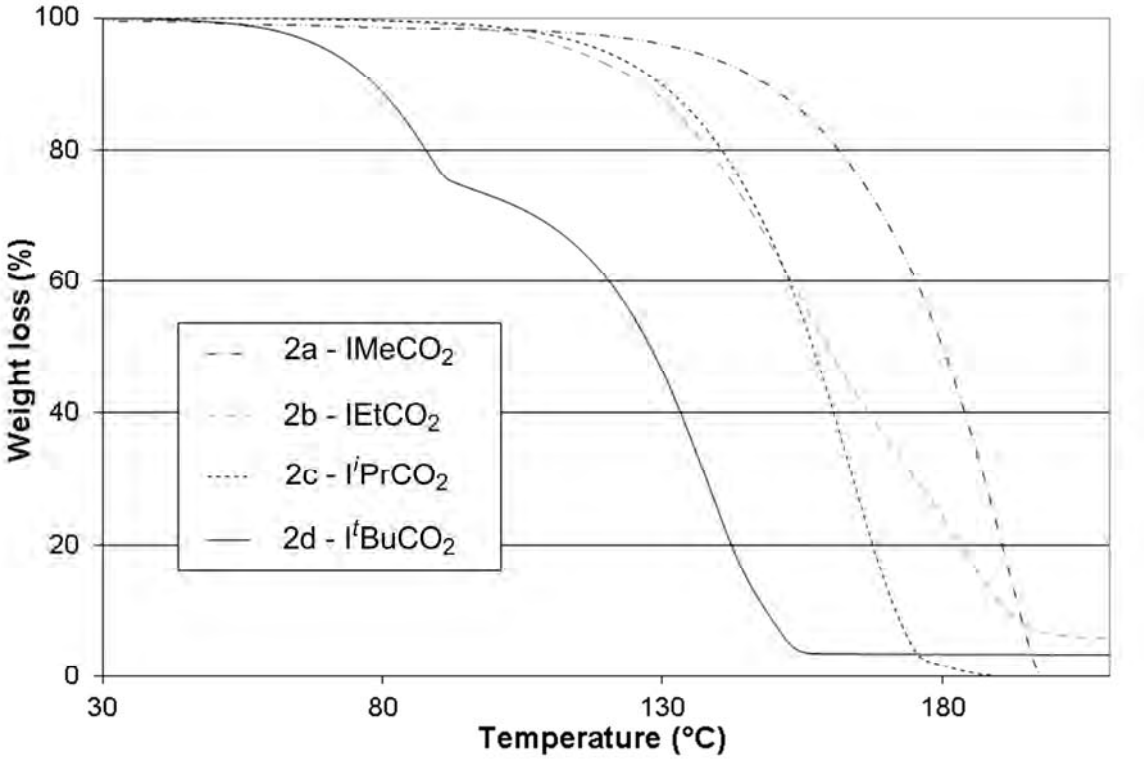

Figure 1.1. TGA of alkyl carboxylates **2a**-**2d**.

TGA of *N*-alkyl Imidazolium Carboxylates Possessing a Methylated Backbone ($2a_{Me}$-$2d_{Me}$)

The collective TGA spectra of the 4,5-dimethyl *N*-alkyl NHC·CO_2 compounds $\mathbf{2a_{Me}}$-$\mathbf{2c_{Me}}$ as well as **2a-2c** are shown in Figure 1.2 and are summarized in Table 1.2. In general, imidazolium carboxylates possessing increasing steric hinderance of the N-alkyl substituent displayed lower decarboxylation temperatures. For example, decarboxylation began at 182 °C for $IMe_{Me}CO_2$ ($\mathbf{2a_{Me}}$) and at 139 °C for $I\mathit{i}Pr_{Me}CO_2$ ($\mathbf{2c_{Me}}$).

An interesting effect caused by the methylation of the backbone of the carboxylates was also observed. The TGA of $\mathbf{2a_{Me}}$ displayed a 20 °C increase in the decarboxylation/decomposition temperatures over **2a** (i.e., 182 °C and 162 °C,

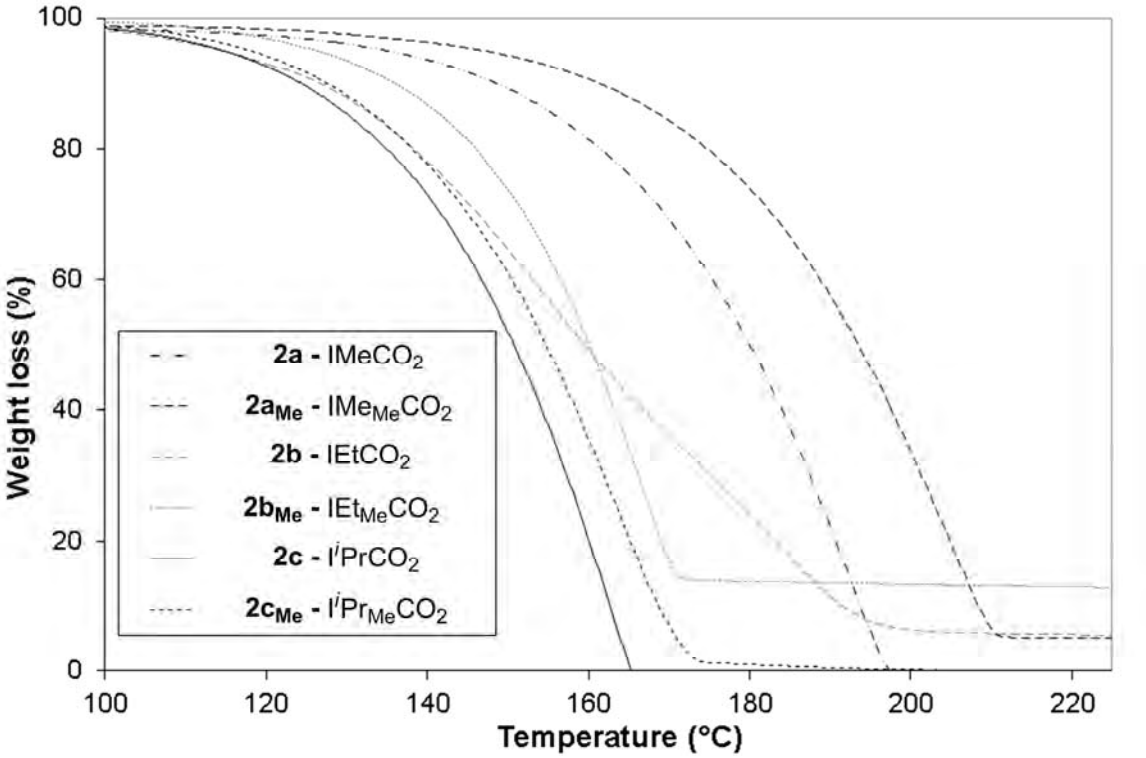

Figure 1.2. TGA analysis of alkyl carboxylates **2a$_{Me}$**-**2c$_{Me}$** and **2a**-**2c**.

respectively). In contrast, **2c$_{Me}$** and **2c**, both of which possess isopropyl *N*-substituents, have almost identical decarboxylation/decomposition temperatures (i.e., a difference of only 1°C, entries 4 and 5, Table 1.2).

Table 1.2. Calculated pK_a of carboxylate precursor carbenes with decarboxylation temperatures of the corresponding NHC-CO_2.

Entry	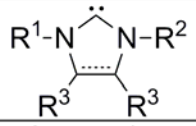	pK_a	-CO_2 of NHC·CO_2 (°C)
1	R^1=R^2=Me; R^3=H (**1a**)	27.4±0.4	162
2	R^1=R^2=Me; R^3=Me (**1a$_{Me}$**)	29.5±0.3	182
3	R^1=R^2=Me, R^3=saturated	28.5±0.4	-
4	R^1=R^2=^{i}Pr; R^3=H (**1c**)	28.2 0.3	140
5	R^1=R^2=^{i}Pr; R^3=Me (**1c$_{Me}$**)	30.4 0.3	139
6	R^1=R^2=^{t}Bu; R^3=H (**1d**)	28.3±0.1	71

Computations performed by Yates et al. have shown that methylation of the backbone increases the basicity of a carbene relative to that of the unsaturated parent carbene (Table 1.2).[62] As electron density of a particular carbene increases, the NHC·CO_2 would most likely possess a stronger $C_{carbene}$-CO_2 bond, which would result in an elevated decarboxylation temperature. Thus, the higher decarboxylation temperature and inferred increased C-CO_2 bond strength of **2a$_{Me}$** (182 °C) relative to **2a** (162 °C) may be attributed to the higher pK_a of the parent carbene (i.e., **1a$_{Me}$** versus **1a**). Although **1c$_{Me}$** has a higher pK_a than **1c**, their corresponding carboxylates, **2c** and **2c$_{Me}$**, decarboxylate at almost identical temperatures. Thus, as the *N*-substituents become larger, the steric bulk of the highly branched *N*-substituents overrides the enhanced stability of the $C_{carbene}$-CO_2 bond provided by the extra electron density at the carbene.

With carboxylates **2g-2j**, **2g$_{Me}$**, and **2h$_{Me}$** in hand, the TGAs of structurally similar, but electronically different, aryl carboxylates could be compared (Figure 1.3). As noted above, methylation of the backbone on the imidazole ring results in an increased pK_a. In the computational study by Yates, saturation of the backbone purportedly leads to a loss in aromaticity in the imidazole ring thereby also resulting in a higher pK_a. The NHC·CO_2 series (**2h**, **2h$_{Me}$**, and **2j**) possessing *N*-(2,6-diisopropyl)phenyl substituents (i.e., IPr) displays decarboxylation temperatures that correlate directly to the increased electron density in the imidazole ring. For example, both SIPrCO_2 (**2j**) and IPr$_{Me}CO_2$ (**2h$_{Me}$**) possess higher decarboxylation temperatures than IPrCO_2 (**2h**). SIPrCO_2 (**2j**) decarboxylates at 136 °C and IPr$_{Me}CO_2$ (**2h$_{Me}$**) decarboxylates at 120 °C while IPrCO_2 (**2h**) decarboxylates at 108 °C. Biphasic

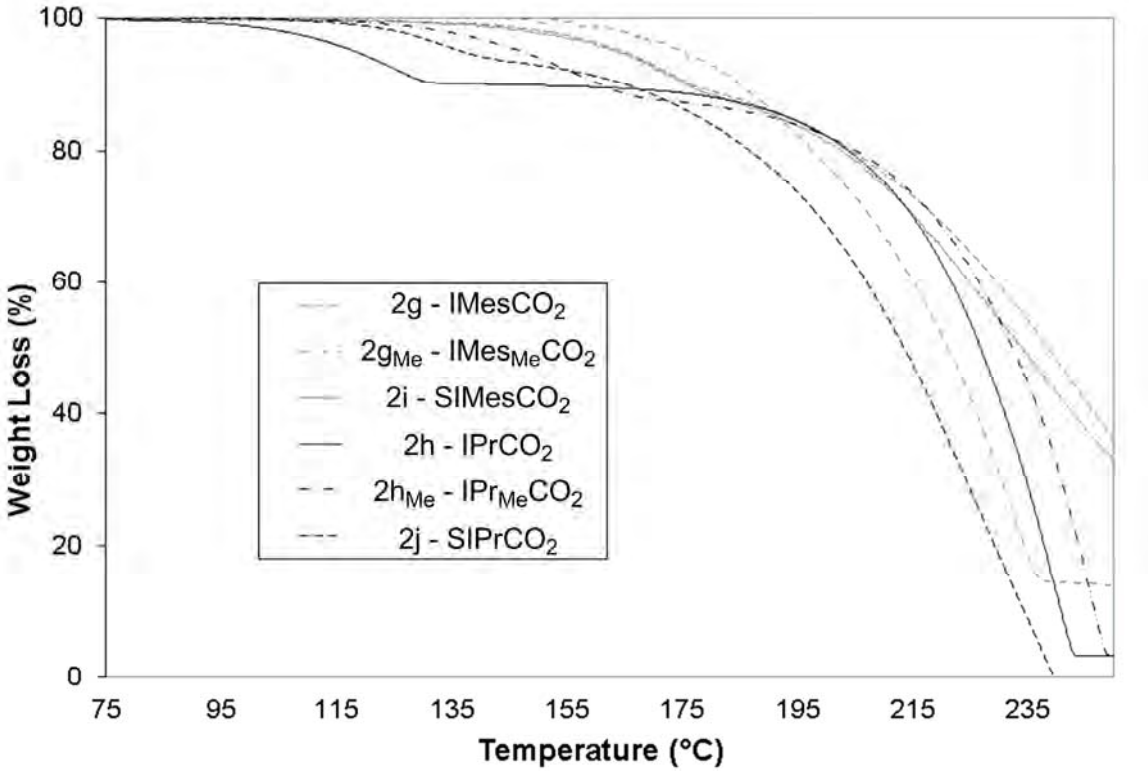

Figure 1.3. TGA analysis of aryl carboxylates **2g**-**2j**, $\mathbf{2g_{Me}}$, and $\mathbf{2h_{Me}}$.

decomposition was observed in all cases similar to what was observed in the TGA analysis of I^{t}BuCO$_2$ (**2d**). The biphasic decomposition suggests that a stable intermediate is formed after decarboxylation. Indeed, when the TGA of IPrCO$_2$ **2h** was interrupted at 108 °C, the ^{1}H NMR analysis of the residual solid displayed a spectrum identical to an authentic sample of the parent NHC, IPr. Thus, in some cases, decarboxylation occurs at a lower temperature than the decomposition of the parent carbenes.

When the *N*-substituent is replaced with (2,4,6-trimethyl)phenyl groups (i.e., IMes), the decarboxylation temperature for IMes$_{Me}$CO$_2$ ($\mathbf{2h_{Me}}$), which possesses a methylated backbone, is once again higher than for IMesCO$_2$ (**2h**) (193 °C and 155 °C, respectively). However, the saturated analog SIMesCO$_2$ (**2j**) decarboxylates at 156 °C, a temperature that is not markedly different from the decarboxylation temperature of

IMesCO$_2$ (**2h**). Thus, simple pK_a effects may not be the only factor that determines the ease of decarboxylation of the NHC·CO$_2$ complexes. Alternatively, the difference in electron density of saturated and unsaturated NHCs may not be significant. Indeed, Nolan et al. reported the CO stretching frequencies of various saturated and unsatured NHC-ligated metal carbonyl were almost identical suggesting similar σ-donor capabilities of saturated and unsaturated NHCs.[63] Furthermore, conflicting reports regarding the effect of saturation on the electron density of the NHC exist.[64,65]

TGA of asymmetric imidazolium carboxylates 2e and 2f

The TGA of asymmetric imidazolium carboxylates IMeI^{t}BuCO$_2$ (**2e**) and I^{t}BuIPrCO$_2$ (**2f**) were also evaluated (Figure 1.4). Not surprisingly, decarboxylation/decomposition of IMeI^{t}BuCO$_2$ (**2e**) occurred at 117 °C, a temperature in between the decarboxylation temperatures of IMeCO$_2$ (**2a**) and I^{t}BuCO$_2$ (**2d**). In addition, a one-step decarboxylation/decomposition was observed for **2e**. However, the low decomposition temperature of **2e** relative to other N-alkyl imidazolium carboxylates **2a**-**2c** suggests that the one *t*-butyl group plays a significant role in the lowering the decarboxylation temperature of **2e**. Despite the increased bulkiness of the ^{t}Bu group relative to the 2,6-diisopropylphenyl group,[63] the decarboxylation temperature of **2f** was strikingly similar to that of IPrCO$_2$ (**2h**). However, no prolonged carbene intermediate was observed.

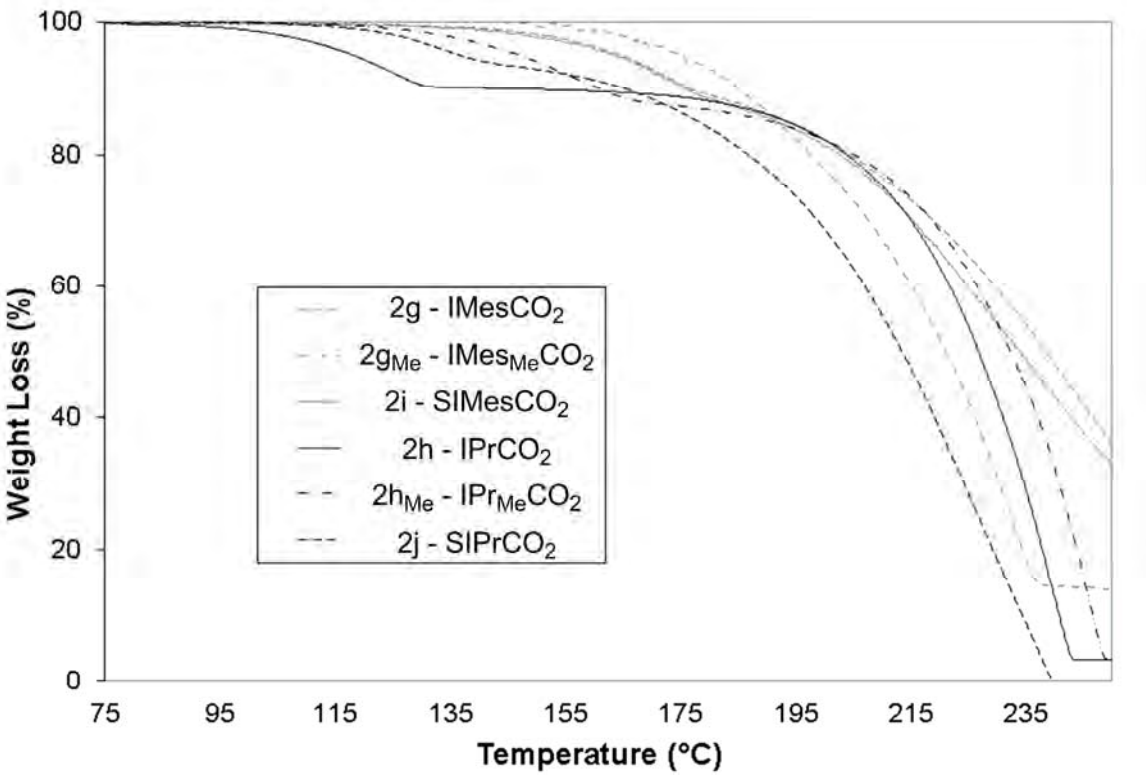

Figure 1.4. TGA analysis of asymmetric NHC-carboxylates **2e** and **2f**.

Single crystal x-ray analysis

The structures of **2a$_{Me}$**, **2b$_{Me}$**, **2i$_{Me}$**, and **2f** were solved using single crystal X-ray crystallography. Selected bond lengths, bond angles, dihedral angles, and structures of all solved carboxylates are listed in Table 1.4. For comparison, a summary of all of the decarboxylation temperatures, IR stretching frequencies, and C-CO_2 lengths are listed in Table 1.3. An increase in the size of the N-alkyl substituent causes the N-C_2 bond length to decrease. Specifically, this bond length decreases from 1.359(1) Å to 1.341(1) Å to 1.336 Å in **2a$_{Me}$** IMe$_{Me}$CO$_2$, **2b$_{Me}$** IEt$_{Me}$CO$_2$, and **2c$_{Me}$** I^{i}Pr$_{Me}$CO$_2$, respectively. In contrast, the N_1- C_2-N_2 bond angle steadily increases from 105.32(10)° in **2a$_{Me}$** to 108.02° in **2c$_{Me}$**. Less of an effect is observed on the C_6-O bond lengths. For example, **2b$_{Me}$** and

Table 1.3. IR, Decarboxylation Temperature, and C-CO_2 bond lengths of the imidazolium carboxylates.

Entry	Carboxylate	ν_{COasym} (cm^{-1})	-CO_2 Temp. (°C)	C-CO_2 Bond Length (Å)
1	**2a**	1653	162	1.523
2	**2b**	1654	128	*NA*
3	**2c**	1666	140	*NA*
4	**2d**	1629	71	*NA*
5	**2e**	1647	117	*NA*
6	**2a$_{Me}$**	1669	182	1.521(3)
7	**2b$_{Me}$**	1657	144	1.535(1)
8	**2c$_{Me}$**	1662	139	1.536
9	**2f**	1675	129	1.525 -1.544
10	**2g**	1675	155	*NA*
11	**2g$_{Me}$**	1674	193	*NA*
12	**2h**	1678	108	1.536
13	**2h$_{Me}$**	1683	136	1.542(2)
14	**2i**	1680	156	*NA*
15	**2j**	1683	120	1.535(2)

2c$_{Me}$, respectively, are longer than the C_2-C_6 bond length of **2a$_{Me}$** (1.521(5) Å). A direct correlation exists between the C_2-C_6 bond lengths and decarboxylation/decomposition temperature. **2a$_{Me}$** has both a significantly smaller bond length and higher decarboxylation temperature than **2b$_{Me}$** and **2c$_{Me}$** (Table 1.4). However, the differences in C_2-C_6 bond lengths as well as decarboxylation temperatures are small between **2b$_{Me}$** and **2c$_{Me}$**.

Methylation of the backbone appears to cause predictable changes to the structure. Both N-C_2 bond lengths of **2a$_{Me}$** $IMe_{Me}CO_2$ and **2h$_{Me}$** $IPr_{Me}CO_2$ are longer by 0.014 Å than their unmethylated counterparts **2a** $IMeCO_2$ and **2h** $IPrCO_2$. In addition, both C_6-O bond lengths of **2a$_{Me}$** and **2h$_{Me}$** are shorter by 0.010 Å. Interestingly, less of a difference is observed between the C_2-C_6 bond lengths (i.e. 0.002 Å and 0.006 Å differences, respectively).

Table 1.4. Structural features of **2a**, **2a$_{Me}$**, **2b$_{Me}$**, **2c$_{Me}$**, **2i**, **2i$_{Me}$**, **2g**, and the rotamer of **2g**.

NHC·CO_2	Bond Lengths (Å)		Bond/Dihedral Angles (°)		Structure
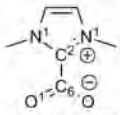 **2a** IMeCO_2	N_1-C_2	1.345	N_1-C_2-N_2	107.15	
	N_3-C_2	-	O_1-C_1-O_2	129.78	
	C_6-O_1	1.240	N_1-C_2-C_6-O_1	29.03	
	C_6-O_2	-	C_2-N_1-C_7-H_c	61.49	
	C_2-C_6	1.523			
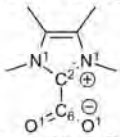 **2a$_{Me}$** IMe$_{Me}CO_2$	N_1-C_2	1.359(1)	N_1-C_2-N_2	105.32(10)	
	N_3-C_2	-	O_1-C_1-O_2	129.52(11)	
	C_6-O_1	1.230(1)	N_1-C_2-C_6-O_1	22.40(10)	
	C_6-O_2	-	C_2-N_1-C_7-H_c	7.18(11)	
	C_2-C_6	1.521(5)			
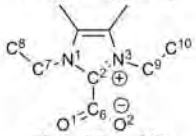 **2b$_{Me}$** IEt$_{Me}CO_2$	N_1-C_2	1.341(1)	N_1-C_2-N_2	107.49(9)	
	N_3-C_2	1.338(1)	O_1-C_1-O_2	130.69(11)	
	C_6-O_1	1.244(1)	N_1-C_2-C_6-O_1	47.54(12)	
	C_6-O_2	1.239(1)	N_3-C_2-C_6-O_2	50.78(12)	
	C_2-C_6	1.535(1)	C_2-N_1-C_7-C_8	78.50(14)	
			C_2-N_1-C_9-C_{10}	79.94(14)	
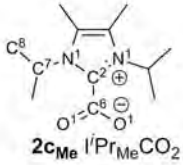 **2c$_{Me}$** I^{i}Pr$_{Me}CO_2$	N_1-C_2	1.336	N_1-C_2-N_2	108.02	
	N_3-C_2	-	O_1-C_1-O_2	131.25	
	C_6-O_1	1.244	N_1-C_2-C_6-O_1	68.96	
	C_6-O_2	-	N_3-C_2-C_6-O_2	-	
	C_2-C_6	1.536	C_2-N_1-C_7-C_8	100.99	
			C_2-N_1-C_9-C_{10}	-	
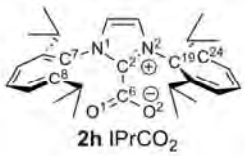 **2h** IPrCO_2	N_1-C_2	1.335	N_1-C_2-N_2	107.09	
	N_3-C_2	1.332	O_1-C_1-O_2	129.88	
	C_6-O_1	1.222	N_1-C_2-C_6-O_1	88.14	
	C_6-O_2	1.225	N_3-C_2-C_6-O_2	89.75	
	C_2-C_6	1.536	C_2-N_1-C_7-C_8	90.64	
			C_2-N_1-C_{19}-C_{24}	88.75	
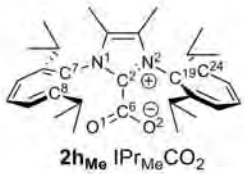 **2h$_{Me}$** IPr$_{Me}CO_2$	N_1-C_2	1.341(1)	N_1-C_2-N_2	107.22(9)	
	N_3-C_2	1.338(1)	O_1-C_1-O_2	131.31(11)	
	C_6-O_1	1.232(2)	N_1-C_2-C_6-O_1	46.72(16)	
	C_6-O_2	1.233(2)	N_3-C_2-C_6-O_2	49.46(16)	
	C_2-C_6	1.542(2)	C_2-N_1-C_7-C_8	84.16(13)	
			C_2-N_1-C_{19}-C_{24}	81.69(13)	
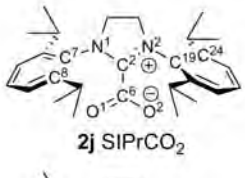 **2j** SIPrCO_2	N_1-C_2	1.326(2)	N_1-C_2-N_2	111.94(13)	
	N_3-C_2	1.317(2)	O_1-C_1-O_2	131.78(15)	
	C_6-O_1	1.237(2)	N_1-C_2-C_6-O_1	57.99(17)	
	C_6-O_2	1.234(2)	N_3-C_2-C_6-O_2	59.85(17)	
	C_2-C_6	1.535(2)	C_2-N_1-C_7-C_8	80.28(19)	
			C_2-N_1-C_{19}-C_{24}	91.50(20)	
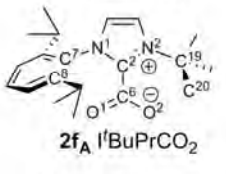 **2f$_A$** I^{t}BuPrCO_2	N_1-C_2	1.341(4)	N_1-C_2-N_2	107.1(3)	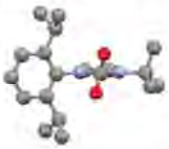
	N_3-C_2	1.348(4)	O_1-C_1-O_2	130.4(4)	
	C_6-O_1	1.243(4)	N_1-C_2-C_6-O_1	79.5(5)	
	C_6-O_2	1.222(5)	N_3-C_2-C_6-O_2	76.7(4)	
	C_2-C_6	1.525(4)	C_2-N_1-C_7-C_8	86.8(4)	
			C_2-N_1-C_{19}-C_{20}	27.9(5)	
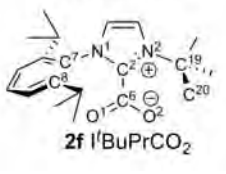 **2f** I^{t}BuPrCO_2	N_1-C_2	1.348(4)	N_1-C_2-N_2	107.8(3)	
	N_3-C_2	1.334(4)	O_1-C_1-O_2	130.7(3)	
	C_6-O_1	1.238(4)	N_1-C_2-C_6-O_1	79.0(4)	
	C_6-O_2	1.226(4)	N_3-C_2-C_6-O_2	79.1(4)	
	C_2-C_6	1.544(4)	C_2-N_1-C_7-C_8	91.1(4)	
			C_2-N_1-C_{19}-C_{20}	26.4(5)	

Saturation of the backbone also appears to cause changes to the structure. For example, the N-C_2 bond lengths of **2j** SIPrCO_2 is 0.009 Å shorter than that of **2h** IPrCO_2. The C_6-O bond lengths of **2j** SIPrCO_2 is 0.015 Å longer than that of **2h** IPrCO_2. However, no distinct difference is observed in the C_2-C_6 bond length of **2j** SIPrCO_2 and **2h** IPrCO_2. Thus, saturation appears to have the opposite effect on the structures of the imidazolium carboxylates than methylation of the backbone.

As steric bulk is introduced into the *N*-substituents of an NHC·CO_2, the cant of the CO_2 moiety becomes more pronounced with regard to the imidazole ring. The carboxylate torsional angles for alkyl carboxylates **2a$_{Me}$**, **2b$_{Me}$**, and **2c$_{Me}$** are 22.40(10)°, 49.16(12)°, and 68.96°, respectively. As the torsional angle of the carboxylate moiety of the NHC·CO_2 becomes larger, the lower the decarboxylation temperature of the NHC·CO_2. The decarboxylation temperatures for **2a$_{Me}$**, **2b$_{Me}$**, and **2c$_{Me}$** are 182 °C, 144 °C, and 139 °C, respectively. This is further exemplified with IPrCO_2 (**2h**), where the CO_2 group is rotated even more than **2c$_{Me}$** (i.e., 88°) and possesses a lower decarboxylation temperature of 108 °C.

Although **2h$_{Me}$** and **2j** possess very large N-substitutents, methylation and saturation of the imidazole backbone decrease the cant of the CO_2 with respect to the imidazole ring. That is, the carboxylate torsional angles for **2h$_{Me}$** IPr$_{Me}CO_2$ and **2j** SIPrCO_2 are 46.72(16)° and 57.99(17)° – significantly lower than the 88.14° observed in IPrCO_2 (**2h**). The decreased carboxylate torsional angles are exemplified in the decarboxylation temperatures. Indeed, **2h$_{Me}$** and **2j** decarboxylate at higher temperatures (i.e., 120° for **2j** and136° for **2h$_{Me}$**) than IPrCO_2 **2h** (108°).

When molecules **2a$_{Me}$** and **2b$_{Me}$** are compared, it is interesting to note the bond lengthening of the C-CO_2 bond from 1.521(5) Å in **2a$_{Me}$** to 1.535(1) Å in **2b$_{Me}$**. The decomposition temperatures of **2a$_{Me}$** to **2b$_{Me}$** are 182 °C and 144 °C, respectively. The C-CO_2 bond lengthening and decrease in decomposition temperature is due to the steric bulk provided by the ethyl group. Examining **2c$_{Me}$**, the C-CO_2 bond length is stretched marginally longer to 1.536 Å and provided a small decrease in the decomposition temperature of 6 °C. This suggests that the extra electronic density that strengthens the C-CO_2 bond provided by the methyls on the backbone has been nearly negated by the steric bulk of the *i*Pr *N*-substituents.

An interesting phenomenon of thermal stability and C-CO_2 bond length was observed with IPrCO_2 and IPr$_{Me}CO_2$. The phenyl rings in **2h$_{Me}$** have both rotated slightly in (84.16(13)° and 81.69(13)°) from the structure of **2h,** where the phenyl rings in **2h** are nearly perpendicular to the imidazole ring. This places the C^8 carbon of one phenyl ring and C^{24} of the other ring closer to the carboxylate. The steric bulk of the 4,5-methyl groups appears to cause the rotation of the 2,6-isopropyl groups away from the 4,5-methyl group, i.e., toward the carboxylate group (Figure 1.5). The combination of the isopropyl and phenyl ring rotation results in the two proximal methyls of the *ortho*-isopropyl groups moving from 4.305 Å and 4.250 Å from the carbon of the carboxylate (C_6) in **2h** to 3.784 Å (C_{14}) and 3.620 Å (C_{29}) from the carbon of the carboxylate (C_6) in **2h$_{Me}$**. Despite the elongation of the C-CO_2 bond and possible weakening of the C-CO_2 bond, the decarboxylation temperature of IPr$_{Me}CO_2$ is 26°C higher than IPrCO_2. This pronounced thermal stability is attributed to the electron density provided by the methyl groups on the imidazolium backbone.

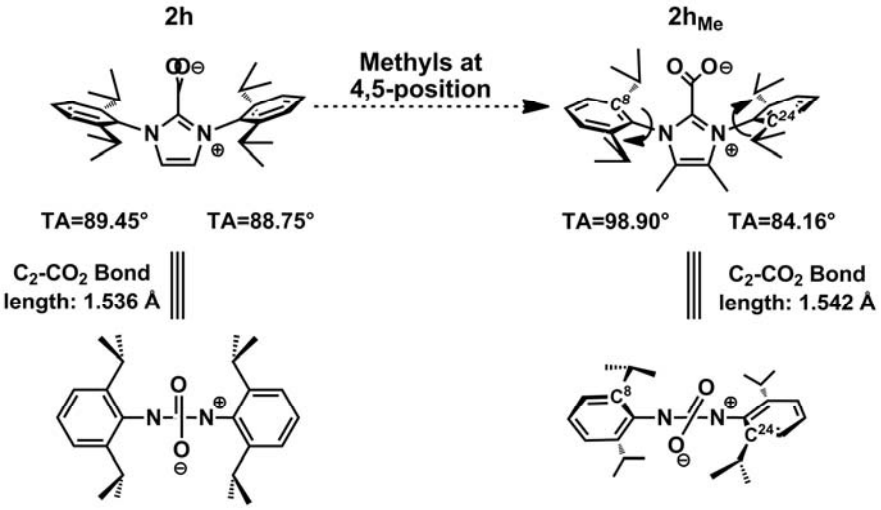

Figure 1.5. Torsional angles of phenyl rings and effects on the CO_2 moiety.

In the crystal structure of **2f**, where rotamers of **2f** are present, a C-CO_2 bond lengthening was observed. This lengthening was due to a small rotation the *tert*-butyl moiety. In **2f$_A$**, the methyl (C_{20}) in the *tert*-butyl group closest to the carbon of the carboxylate moiety is at an angle of 27.92° with respect to the imidazolium ring and is 2.995 Å from C_6, the carbon of the carboxylate group; in **2f**, the C_{20} methyl is at 26.45°, or 1.47° closer and 2.965 Å from C_6, making the methyl 0.030 Å closer in **2f** than in **2f$_A$** (see Table 1.4). Thus, it appears that the proximity of the methyl in **2f** has caused an elongation of the C_2-C_6 bond from **2f$_A$**, with bond lengths of 1.525(5) Å and 1.544(4) Å, respectively.

The bond lengthening in several NHC-CO_2 species by physical proximity of the *N*-substituents suggests that rotation of the *N*-substituents into the plane of the C_2-C_6 bond initiates bond breaking (*i.e.* decarboxylation). This is also supported by the TGA data from IMesCO_2 and IPrCO_2, where the zwitterions are structurally similar, but differ in the size of the *ortho* substituent (Figure 1.6). A larger *ortho* subsituent (*i*Pr vs Me) on the phenyl ring would be able to force CO_2 off more easily as the presence of the extra

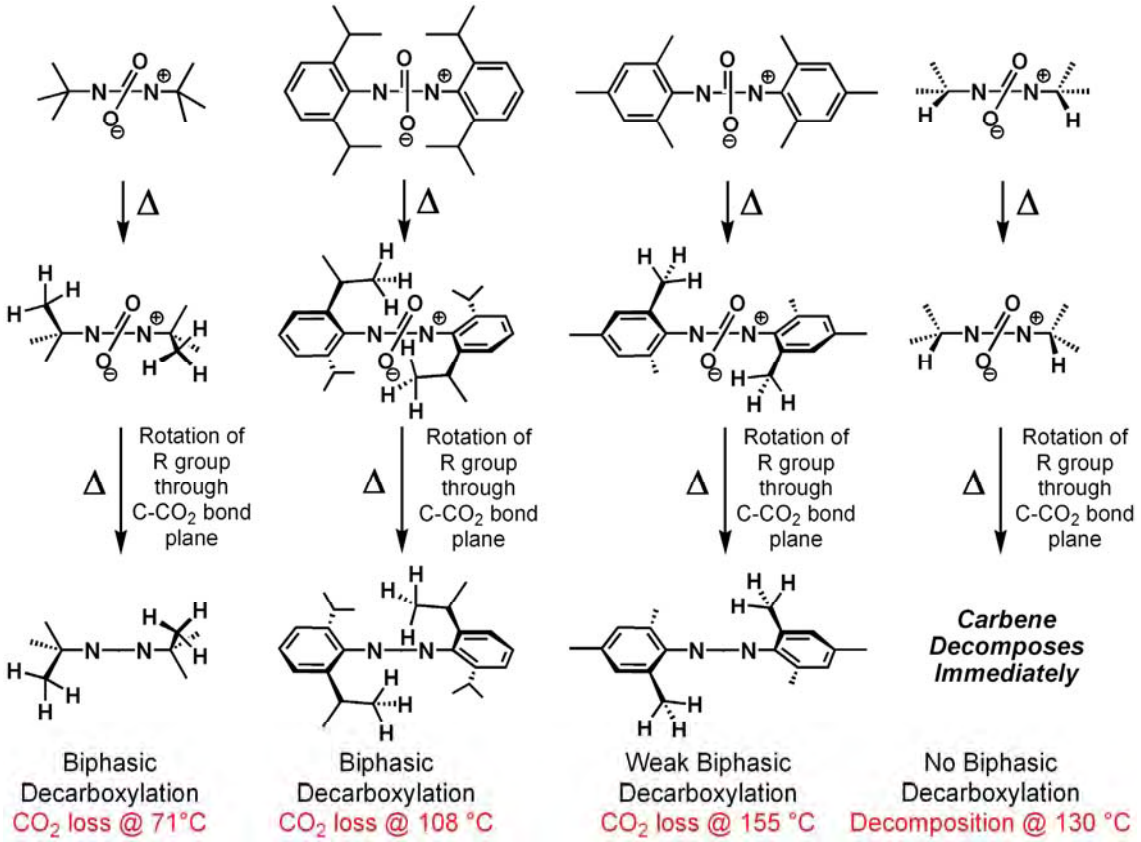

Figure 1.6. Imidazolium carboxylates and steric factors influencing decarboxylating ability.

methyl group is further into the plane of the C-CO_2 bond. This steric bulk in the bonding plane translates into a lower decarboxylation temperature observed for IPrCO_2 over IMesCO_2 (108° vs 155°).

The enhanced stability of the methylated aryl NHC·CO_2 analogues could be due to increased electron density, which also makes the rotation about the N-C_{phenyl} bond less facile. Preventing rotation of the *N*-aryl bond has been used recently by Grubbs et al. to isolate Ru-metathesis catalysts that were known to undergo C-H addition at the *ortho* hydrogens leading to inactive metathesis catalysts (Figure 1.7).[66] Installation of *gem*-dimethyl groups on the backbone of imidazolin carbenes prevents *N*-aryl bond rotation of the phenyl ring near the metal atom. The *gem*-dimethyl groups prevent rotation and thus

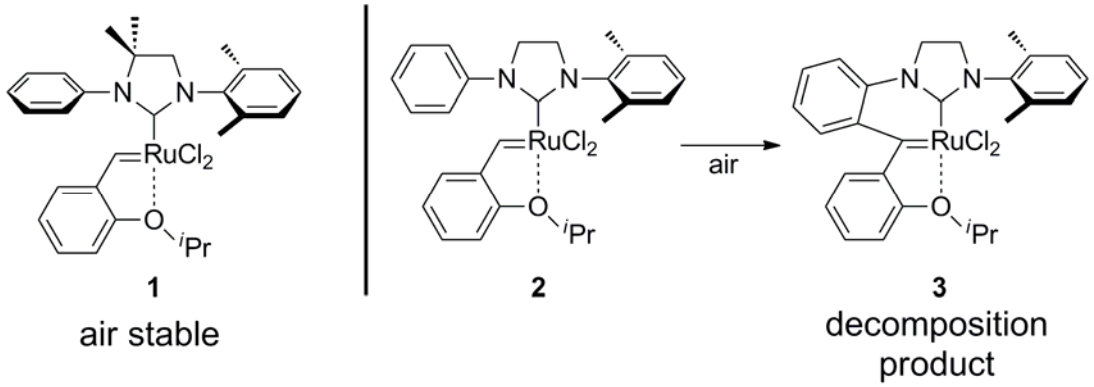

Figure 1.7. Prevention of *ortho*-C-H reaction by installation of gem-dimethyl groups at the carbene backbone.

prevents C-H activation and catalyst decomposition, allowing isolation of an effective ring-closing metathesis catalyst. The same effect is likely in effect here, where the phenyl rings cannot rotate through the C-CO_2 bond to cause a facile decarboxylation. With $IMes_{Me}CO_2$, a biphasic decomposition was not observed and the decomposition occurred at 196 °C, the highest temperature of all the carboxylates studied. In $IPr_{Me}CO_2$ a biphasic decomposition at 136 °C was still observed. This suggests that the *ortho*-*i*Pr groups on the phenyl rings can still rotate through the C-CO_2 bond plane to enact decarboxylation in a system where the phenyl ring rotation is constrained (Figure 1.8).

Conclusion

The synthesis of a series of imidazolium carboxylates from the reaction of *N*-heterocyclic carbene and carbon dioxide allowed for a thorough study of the decarboxylating ability of this class of molecules. Thermogravimetric analysis, single crystal x-ray crystallography, and IR analysis were used to study potential variables involved in a particular carboxylates ability to decarboxylate. TGA analysis of the

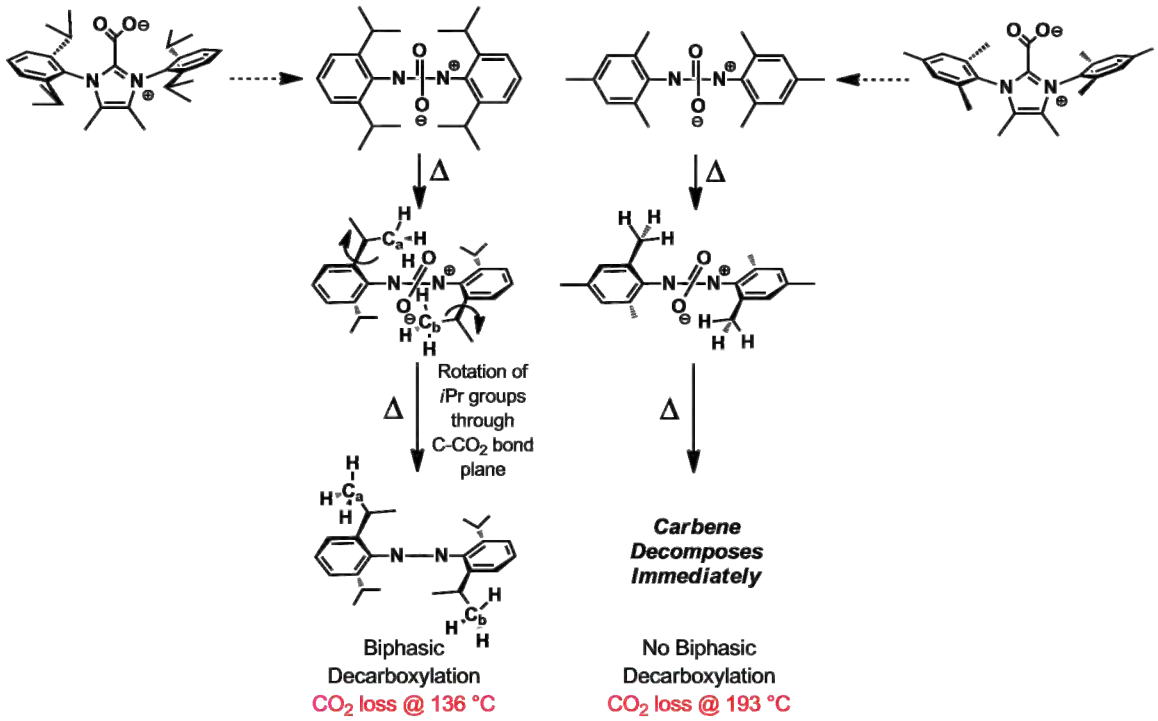

Figure 1.8. The rotation of *ortho*- groups in rotationally constrained carboxylates.

carboxylates clearly shows that the decarboxylating ability of an NHC-CO_2 is largely dependant on the steric bulk of the *N*-subsituent. The TGA analysis of **2a**-**2d** and **2a$_{Me}$**-**2c$_{Me}$** also shows that electronics in this system can be overridden by steric bulk. Single crystal x-ray analysis of a series of carboxylates indicates that the carbon-carbon bond breaking event may be caused by severe ring strain introduced by the *N*-substituents.

Experimental

General Information

All listed procedures were performed under a N_2 atmosphere unless otherwise stated. IR spectra were collected on a Bruker Tensor 27 instrument. Thermogravimetric analyses (TGA) were performed on a TA Instruments TGA2050. The TGA data was recorded using Therma Advantage, ver. 1.14. All TGA analyses were performed in a N_2

atmosphere at a heating rate of 5°C/min. All glassware was dried in an oven at 130 °C for 24 h prior to use. Elemental analyses were performed by Midwest Microlabs, LLC.

Materials

Solvents were purified and deoxygenated by passing through packed silica columns. All oil from NaH was removed by thorough washing with hexanes. KO^{t}Bu (98%) was purchased from Sigma-Aldrich and used without further purification. KHMDS (95%) was purchased from Sigma-Aldrich and used without further purification. All other reagents were purchased from the chemical provider without further purification, unless specified. All NMR solvents were thoroughly dried using standard procedures prior to use. The NHC-CO_2 **2a** was synthesized using a literature procedure.[38] Imidazolium salts **3g$_{Me}$** and **3h$_{Me}$** were synthesized using a literature procedure.[67] See Appendix A for IPrCO_2 TGA runs at different weights and the x-ray crystal structure reports for structures solved in this report.

General synthesis A for NHC-CO_2s 2b-2j, 2g$_{Me}$, and 2h$_{Me}$. The imidazolium salt (1 eq) and toluene was put into a 100-mL round bottom equipped with a stir-bar. To this suspension was added KHMDS (1 eq). The solution was allowed to stir for 2h before being filtered through Celite. The carbene solution was then transferred to a 100-mL Schlenk flask and CO_2 was introduced into the flask. The NHC-CO_2 precipitated as a white solid and was collected via filtration and then washed with ether and dried in vacuo.

2b: General synthesis A was used with 1,3-diethylimidazolium iodide (0.28 g, 1.2 mmol), toluene (50 mL), and KHMDS (0.25 g, 1.2 mmol) to afford 1,3-diethylimidazolium-2-carboxylate **2b** as a white powder (0.06 g, 35%); ^{1}H NMR (300

MHz, CD_2Cl_2): δ 7.05 (s, 2H), 4.57 (quartet, 4H, *J*= 7.3 Hz), 1.49 (t, 6H, *J*= 7.3 Hz); ^{13}C NMR (75.6 MHz, CD_2Cl_2): δ 155.0, 143.4, 120.2, 45.6, 16.2. IR (KBr) 1654, 1507, 1385, 1350, 1216 cm^{-1}. Anal. Calcd for $C_8H_{12}N_2O_2$: C, 57.13; H, 7.19; N, 16.66; O, 19.03; Found: C, 56.79; H, 7.39; N, 16.77; O, 19.97.

2c: General synthesis A was used with 1,3-diisopropylimidazolium iodide (0.72 g, 2.6 mmol), toluene (75 mL), and KHMDS (0.54 g, 2.6 mmol) to afford 1,3-diisopropylimidazolium-2-carboxylate **2c** as a white powder (0.17 g, 29%); ^1H NMR (300 MHz, CD_2Cl_2): δ 7.12 (s, 2H), 5.55 (septet, 2H, *J*=6.6 Hz), 1.47 (d, 12H, *J*=6.7 Hz); ^{13}C NMR (75.6 MHz, CD_2Cl_2): δ 155.4, 144.0, 116.6, 51.5, 23.3. IR (KBr) 1666, 1487, 1371, 1329, 1220 cm^{-1}. Anal. Calcd for $C_{10}H_{16}N_2O_2$: C, 61.20; H, 8.22; N, 14.27; O, 16.31; Found: C, 61.35; H, 8.16; N, 14.28; O, 16.51.

2e: General synthesis A was used with 1-*tert*-butyl3-methylimidazolium iodide (0.69 g, 2.6 mmol), toluene (75 mL), and KHMDS (0.54 g, 2.6 mmol) to afford 1-methyl-3-*tert*-butylimidazolium-2-carboxylate **2e** as a gray powder (0.30 g, 48%); ^1H NMR (300 MHz, CD_3CN): δ 7.24 (d, 1H, $J_{H\text{-}H}$=2.0 Hz), 7.08 (d, 1H, $J_{H\text{-}H}$=2.0 Hz), 3.754 (s, 3H), 1.713 (s, 9H); ^{13}C NMR (75.6 MHz, CD_3CN): δ.147.7, 119.6, 116.8, 61.7, 36.1, 29.8; IR (KBr) 1647, 1437, 1385, 1342, 12119 cm^{-1}. Anal. Calcd for $C_9H_{14}N_2O_2$: C, 59.32; H, 7.74; N, 15.37; O, 17.56; Found: C, 59.30; H, 7.62; N, 15.34; O, 17.30.

2f: General synthesis A was used with 1-(2,6-diisopropylphenyl)-3-*tert*-butylimidazolium tetrefluoroborate (0.42 g, 1.1 mmol), toluene (75 mL), and KHMDS (0.24 g, 1.1 mmol) to afford 1-(2,6-diisopropylphenyl)-3-*tert*-butylimidazolium-2-carboxylate as a gray powder, (0.32 g, 87%); ^1H NMR (300 MHz, CD_3CN): δ 7.50 (t, 1H, *J*=7.8 Hz), 7.28 (d, 4H, *J*= 7.8 Hz), 6.88 (s, 2H), 2.44 (sept., 1H, *J*=6.6 Hz), 1.81 (s, 9H),

1.28 (d, 6H), 1.09 (d, 6H, *J*=6.9 Hz). ^{13}C NMR (75.6 MHz, CD_3CN): δ 148.9, 146.9, 131.5, 124.7, 120.8, 116.9, 29.9, 29.3, 25.5, 23.2. IR (KBr) 1675, 1632, 1478, 1462, 1321, 1303, 1208 cm^{-1}. Anal. Calcd for $C_{20}H_{28}N_2O_2$: C, 73.14; H, 8.59; N, 8.53; O, 9.74; Found: C, 72.85; H, 8.54; N, 8.42; O, 19.21.

2g$_{Me}$: General synthesis A was used with 1,3-bis(2,4,6-trimethylphenyl)-4,5-dimethyl-imidazolium chloride (0.50 g, 1.3 mmol), toluene (75 mL), and KHMDS (0.27 g, 1.3 mmol) to afford 1,3-bis(2,4,6-trimethylphenyl)-4,5-dimethyl-imidazolium-2-carboxylate as a white powder (0.38 g, 75%); ^{1}H NMR (300 MHz, CD_3CN): δ 7.09 (s, 4H), 2.35 (s, 6H), 2.10 (s, 12H), 1.91 (s, 6H); ^{13}C NMR (75.6 MHz, CD_2Cl_2): 154.5, 145.9, 140.8, 135.6, 130.8, 129.8, 124.8, 21.5, 17.8, 8.9; IR (KBr): 1674, 1494, 1301 cm^{-1}; Anal. Calcd for $C_{24}H_{28}N_2O_2$: C, 76.56; H, 7.50; N, 7.44; O, 8.50. Found: C, 76.37; H, 7.42; N, 7.48; O, 8.63.

2h$_{Me}$: General synthesis A was used with 1,3-bis(2,6-diisopropylphenyl)-4,5-methyl-3-imidazolium chloride (0.50 g, 1.1 mmol), toluene (75 mL), and KHMDS (0.22 g, 1.1 mmol) to afford1,3-bis(2,6-diisopropylphenyl)-4,5-methyl-3-imidazolium-2-carboxylate, (0.40 g, 75%); ^{1}H NMR (300 MHz, CD_2Cl_2): δ 7.540 (t, 2H, *J*= 6.8 Hz, 8.4 Hz), 7.31 (d, 4H, *J*=7.8), 2.38 (septet, 4H, *J*=7.05 Hz), 1.95 (s, 6H), 1.24 (d, 12H, *J*=7.0 Hz), 1.22 (d, 12H, *J*=6.9 Hz); ^{13}C NMR (75.6 MHz, CD_2Cl_2): 153.2, 146.6, 145.3, 135.5, 130.9, 126.9, 124.8, 29.7, 24.3, 23.9, 9.6; IR (KBr): 1683, 1549, 1467, 1298 cm^{-1}; Anal. Calcd for $C_{30}H_{40}N_2O_2$: C, 78.22; H, 8.75; N, 6.08; O, 6.95. Found: C, 77.95; H, 8.54; N, 6.05; O, 6.71.

General synthesis B for NHC-CO_2s 2a$_{Me}$-2c$_{Me}$. Carbenes **1a$_{Me}$-1c$_{Me}$** were synthesized via potassium reduction of the appropriate thiourea following a literature

procedure. The appropriate carbene (1 eq) was dissolved in THF in an airless flask and the N_2 atmosphere was removed and replaced with CO_2. The NHC-CO_2 precipitated out of solution upon CO_2 introduction. The reaction was allowed to stir for 2 h before filtering the white precipitate away.

$2a_{Me}$: General synthesis B was used with 1,3,4,5-methyl-imidazolylid (1.16 g, 9.3 mmol) and THF (100 mL) to afford 1,3,4,5-methyl-imidazolium-2-carboxylate as a white solid (1.23 g, 78%); ^{1}H NMR (300 MHz, CD_2Cl_2): δ 3.89 (s, 6H), 2.16 (s, 6H); ^{13}C NMR (75.6 MHz, CD_2Cl_2): 155.9, 142.8, 125.6, 33.5, 8.9; IR (KBr): 1669, 1510, 1440, 1423, 1315, 1230 cm^{-1}. Anal. Calcd for $C_8H_{12}N_2O_2$: C, 57.13; H, 7.19; N, 16.66; O, 19.03; Found: C, 56.85; H, 7.06; N, 16.76; O, 19.21.

$2b_{Me}$: General synthesis B was used with 1,3-diethyl-4,5-methyl-imidazolylid (0.24 g, 1.5 mmol) and THF (50 mL) to afford 1,3-diethyl-4,5-methyl-imidazolium-2-carboxylate as a white solid (0.16 g, 52%); ^{1}H NMR (300 MHz, CD_2Cl_2): δ 4.45 (quart, 4H, *J*=7.2Hz,), 2.20 (s, 6H), 1.38 (t, 6H, *J*=7.22Hz); ^{13}C NMR (75.6 MHz, CD_2Cl_2): 155.8, 142.5, 124.7, 41.9, 15.9, 8.7; IR (KBr): 1657, 1503, 1456, 1323, 1274, 1209 cm^{-1}; Anal. Calcd for $C_{10}H_{16}N_2O_2$: C, 61.20; H, 8.22; N, 14.27; O, 16.31. Found: C, 61.41; H, 8.27; N, 14.36; O, 16.41.

Reaction of IPrCO_2 with H_2O. A heterogenous solution of NHC-CO_2 in CD_3CN is made and a background spectrum is obtained. To the sample is added 25 eq. of H_2O and mixed thoroughly, forming a homogenous solution. Another spectrum is obtained. The spectra indicate that there is a small interaction with H_2O as noted above. All of the liquid in the sample is then removed in vacuo and another spectrum is obtained with CD_3CN, showing only NHC-CO_2 peaks.

Reactions of carboxylates+MX with H_2O. Carboxylates (1 eq) are mixed with any MX (M=Li, Na, or K; X=BPH_4, BF_4, Cl, or I) salt (1 eq) in CD_3CN. A background spectrum was obtained prior to injection of deoxygenated, deionized H_2O (10 eq). ^1H NMR shows the acidic imidazolium proton at ~9 ppm.

References

(1) Calabrese, J. C.; Herskovitz, T.; Kinney, J. B. *J. Am. Chem. Soc.* **1983**, *105*, 5914.

(2) Pérez, E. R.; Santos, R. H. A.; Gambardella, M. T. P.; de Macedo, L. G. M.; Rodrigues-Filho, U. P.; Launay, J.-C.; Franco, D. W. *The Journal of Organic Chemistry* **2004**, *69*, 8005.

(3) Heldebrant, D. J.; Jessop, P. G.; Thomas, C. A.; Eckert, C. A.; Liotta, C. L. *J. Org. Chem.* **2005**, *70*, 5335.

(4) Kolbe, H.; Lautemann, E. *Liebigs Ann. Chem.* **1860**, *113*, 125.

(5) Lindsey, A. S.; Jeskey, H. *Chem. Rev.* **1957**, *57*, 583.

(6) Schmitt, R. *Journal fuer Praktische Chemie/Chemiker-Zeitung* **1885**, *31*, 397.

(7) Zelinsky, N. *Berichte der Deutschen Chemischen Gesellschaft* **1902**, *35*, 2687.

(8) Hoffmann, R. W.; Holzer, B. *Chem. Commun.* **2001**, 491.

(9) Otsuii, Y.; Arakawa, M.; Matasamura, N.; Haruki, E. *Chem. Lett.* **1973**, 1193.

(10) Mizuno, T.; Ishino, Y. *Tetrahedron* **2002**, *58*, 3155.

(11) Sudo, A.; Morioka, Y.; Sanda, F.; Endo, T. *Tetrahedron Lett.* **2004**, *45*, 1363.

(12) Inoue, S.; Koinuma, H.; Tsuruta, T. *Die Makromokular* **1969**, *130*, 210.

(13) Sugimoto, H.; Ohtsuka, H.; Inoue, S. *J. Polym. Sci., Part A: Polym. Chem.* **2005**, *43*, 4172.

(14) Sugimoto, H.; Inoue, S. *Pure Appl. Chem.* **2006**, *78*, 1823.

(15) Robertson, N. J.; Qin, Z.; Dallinger, G. C.; Lobkovsky, E.; Lee, S.; Coates, G. W. *Dalton Transactions* **2006**, *45*, 5390.

(16) Darensbourg, D. J.; Fitch, S. B. *Inorg. Chem.* **2007**, *46*, 5474.

(17) Lu, X.-B.; Shi, L.; Wang, Y.-M.; Zhang, R.; Zhang, Y.-J.; Peng, X.-J.; Zhang, Z.-C.; Li, B. *J. Am. Chem. Soc.* **2006**, *128*, 1664.

(18) Sasaki, Y.; Inoue, Y.; Hashimoto, H. *Chem. Comm.* **1976**, 605.

(19) Inoue, Y.; Itoh, Y.; Hashimoto, H. *Chem. Lett.* **1977**, 855.

(20) Tsuda, T.; Chujo, Y.; Saegusa, T. *Synth. Commun.* **1979**, *9*, 427.

(21) Tsuda, T.; Morikawa, S.; Sumiya, R.; Saegusa, T. *J. Org. Chem.* **1988**, *53*, 3140.

(22) Takimoto, M.; Mori, M. *J. Am. Chem. Soc.* **2002**, *124*, 10008.

(23) Takimoto, M.; Kawamura, M.; Mori, M. *Org. Lett.* **2003**, *5*, 2599.

(24) Li, F.; Xia, C.; Sun, W.; Chen, G. *Chem. Comm.* **2003**, 2042.

(25) Himeda, Y.; Onozawa-Komatsuzaki, N.; Sugihara, H.; Kasuga, K. *J. Am. Chem. Soc.* **2005**, *127*, 13118.

(26) Kayaki, Y.; Yamamoto, M.; Ikariya, T. *Angew. Chem. Int. Ed.* **2009**, *48*, 4194.

(27) Riduan, S. N.; Zhang, Y.; Ying, J. Y. *Angew. Chem. Int. Ed.* **2009**, *48*, 3322.

(28) Clements, J. H. *Ind. Eng. Chem. Res.* **2003**, *42*, 663.

(29) Braunstein, P.; Matt, D.; Nobel, D. *Chem. Rev.* **1988**, *88*, 747.

(30) Belli Dell'Amico, D.; Calderazzo, F.; Labella, L.; Marchetti, F.; Pampaloni, G. *Chem. Rev. (Washington, DC, U. S.)* **2003**, *103*, 3857.

(31) Kuhn, N.; Steimann, M.; Weyers, G. *Z. Naturforsch., B: Chem. Sci.* **1999**, *54*, 427.

(32) Ishiguro, K.; Hirabayashi, K.; Nojima, T.; Sawaki, Y. *Chem. Lett.* **2002**, 796.

(33) Holbrey, J. D.; Reichert, W. M.; Tkatchenko, I.; Bouajila, E.; Walter, O.; Tommasi, I.; Rogers, R. D. *Chemical Communications (Cambridge, United Kingdom)* **2003**, 28.

(34) Duong, H. A.; Tekavec, T. N.; Arif, A. M.; Louie, J. *Chem. Commun.* **2004**, 112.

(35) Tudose, A.; Demonceau, A.; Delaude, L. *J. Organomet. Chem.* **2006**, *691*, 5356.

(36) Schoessler, W.; Regitz, M. *Chem. Ber.* **1974**, *107*, 1931.

(37) Voutchkova, A. M.; Appelhans, L. N.; Chianese, A. R.; Crabtree, R. H. *J. Am. Chem. Soc.* **2005**, *127*, 17624.

(38) Voutchkova, A. M.; Feliz, M.; Clot, E.; Eisenstein, O.; Crabtree, R. H. *J. Am. Chem. Soc.* **2007**, *129*, 12834.

(39) Weskamp, T.; Schattemann, W. C.; Spiegler, M.; Hermann, W. A. *Angew. Chem. Int. Ed. Engl.* **1998**, *37*, 2490.

(40) Scholl, M.; Ding, S.; Lee, C. W.; Grubbs, R. H. *Org. Lett.* **1999**, *1*, 953.

(41) Huang, J.; Stevens, E. D.; Nolan, S. P.; Petersen, J. L. *J. Am. Chem. Soc.* **1999**, *121*, 2674.

(42) Hoveyda, A. H.; Schrock, R. R. *Chem. Eur. J* **2001**, *7*, 945.

(43) Furstner, A. *Angew. Chem. Int. Ed. Engl.* **2000**, *39*, 3012.

(44) Trnka, T. M.; Grubbs, R. H. *Acc. Chem. Res.* **2000**, *34*, 18.

(45) Louie, J.; Gibby, J. E.; Farnworth, M. V.; Tekavec, T. N. *J. Am. Chem. Soc.* **2002**, *124*, 15188.

(46) Ho, C.-Y.; Jamison, T. F. *Angew. Chem., Int. Ed.* **2007**, *46*, 782.

(47) Veige, A. S. *Polyhedron* **2008**, *27*, 3177.

(48) Connor, E. F.; Nyce, G. W.; Myers, M.; Moeck, A.; Hedrick, J. L. *J. Am. Chem. Soc.* **2002**, *124*, 914.

(49) Suzuki, Y.; Yamauchi, K.; Muramatsu, K.; Sato, M. *Chem. Commun.* **2004**, 2770.

(50) Sohn, S. S.; Rosen, E. L.; Bode, J. W. *J. Am. Chem. Soc.* **2004**, *126*, 14370.

(51) Scholten, M. D.; Hedrick, J. L.; Waymouth, R. M. *Macromolecules* **2008**, *41*, 7399.

(52) Merino, P.; Marques-Lopez, E.; Tejero, T.; Herrera, R. P. *Tetrahedron* **2009**, *65*, 1219.

(53) Culkin, D. A.; Jeong, W.; Csihony, S.; Gomez, E. D.; Balsara, N. P.; Hedrick, J. L.; Waymouth, R. M. *Angew. Chem. Int. Ed.* **2007**, *46*, 2627.

(54) Duong, H. A.; Cross, M. J.; Louie, J. *Org. Lett.* **2004**, *6*, 4679.

(55) Zhou, H.; Zhang, W.-Z.; Liu, C.-H.; Qu, J.-P.; Lu, X.-B. *J. Org. Chem.* **2008**, *73*, 8039.

(56) Tommasi, I.; Sorrentino, F. *Tetrahedron Lett.* **2005**, *46*, 2141.

(57) Tommasi, I.; Sorrentino, F. *Tetrahedron Lett.* **2006**, *47*, 6453.

(58) Alcarazo, M.; Roseblade, S. J.; Cowley, A. R.; Fernández, R.; Brown, J. M.; Lassaletta, J. M. *J. Am. Chem. Soc.* **2005**, *127*, 3290.

(59) Kuhn, N.; Kratz, T. *Synthesis* **1993**, 561.

(60) Bridges, N. J.; Hines, C. C.; Smiglak, M.; Rogers, R. D. *Chem. Eur. J.* **2007**, *13*, 5207.

(61) See Appendix A for $IPrCO_2$ TGA data at varied masses.

(62) Magill, A. M.; Cavell, K. J.; Yates, B. F. *J. Am. Chem. Soc.* **2004**, *126*, 8717.

(63) Dorta, R.; Stevens, E. D.; Scott, N. M.; Costabile, C.; Cavallo, L.; Hoff, C. D.; Nolan, S. P. *J. Am. Chem. Soc.* **2005**, *127*, 2485.

(64) Khramov, D. M.; Lynch, V. M.; Bielawski, C. W. *Organometallics* **2007**, *26*, 6042.

(65) Khramov, D. M.; Rosen, E. L.; Lynch, V. M.; Bielawski, C. W. *Angew. Chem., Int. Ed.* **2008**, *47*, 2267.

(66) Chung, C. K.; Grubbs, R. H. *Org. Lett.* **2008**, *10*, 2693.

(67) Nolan, S. P. *U. S. Patent* **2003**, 653.

CHAPTER 2

RELEVANCE OF *N*HC·CO_2 BOUND $NaBPh_4$ COMPLEXES IN TRANSCARBOXYLATION REACTIONS

Introduction

The ability to utilize carbon dioxide as a chemical feedstock has been a long desired goal in synthetic chemistry.[1-7] Every year, billions of tons of CO_2 are released into the atmosphere as waste.[8] The ability to harness CO_2 from the point of origin into high-yielding fine chemical processes would likely be a lucrative one as the souce of carbon could be collected from point-source waste streams. This been achieved only recently with any large scale success. Darensbourg[9-11] and Coates[12-14] independently developed unique systems that copolymerize CO_2 with epoxides that afford biodegradable polycarbonate polymers which are adequate substitutes for bisphenol A based polymers. The synthesis of cyclic carbonates from the reaction of epoxides and CO_2 and with various catalysts has also received a large amount of attention in recent years due to the industrial significance of cyclic carbonates.[15-20]

The Kolbe-Schmitt and Grignard reactions are relevant reactions when discussing the topic of CO_2 incorporation into fine chemicals. However, both the reactions are largely limited to phenolic and halogenated substrates, respectively.[21-23] Transition metals have found a home in CO_2 incorportation chemistry: Nolan has recently discovered a protocol utilizing a hydroxy-gold-carbene species to carboxylate

heteroaromatic and activated nonphenolic aryl species;[24,25] cycloaddition of CO_2 with diynes was discovered by Saegusa[26] and developed into a more efficient reaction by our own group;[27] Rovis et al. developed a hydrocarboxylation of styrene and styrene analogues using a Ni catalyst with stoichiometric amounts of diethylzinc.[28] A number of other CO_2 incorporation reactions have been developed, but most reactions require a transition metal, involvement of a reactive compound to oxidatively add into or transmetalate with, and an activated unsaturated compound with which to react.[29-33] There are, however, only a handful accounts of tranisition metal free or organocatalyic incorporation of CO_2 with organic molecules to form noncyclic carbonate products.[34-40]

In 2005, Tommasi et al. demonstrated the fixing of carbon dioxide onto acetophenone to form benzoyl acetate (**1**), methanol to form monomethyl carbonate (**2**), and benzaldehyde to form (**3**) by employing imidazolium carboxylates as a trans-carboxylating reagent (Scheme 1). The scope was further expanded in 2006 and 2009 as other compounds containing acidic α-protons, such as acetone, cyclohexanone, and benzylcyanide. In 2009, Lu et al. applied *N*-heterocyclic carbene bound CO_2 complexes ($NHC{\cdot}CO_2$) as a catalyst to couple epoxides with CO_2 to form cyclic carbonates utilizing relatively mild reaction conditions.[41] It is quite clear from the work of Lu et al. and Tommasi et al. that carbenes and their corresponding carboxylates provide efficient platforms to mediate the transfer of carbon dioxide to organic molecules. DBU has performed the same and similar types of reactions, though the exact method with which

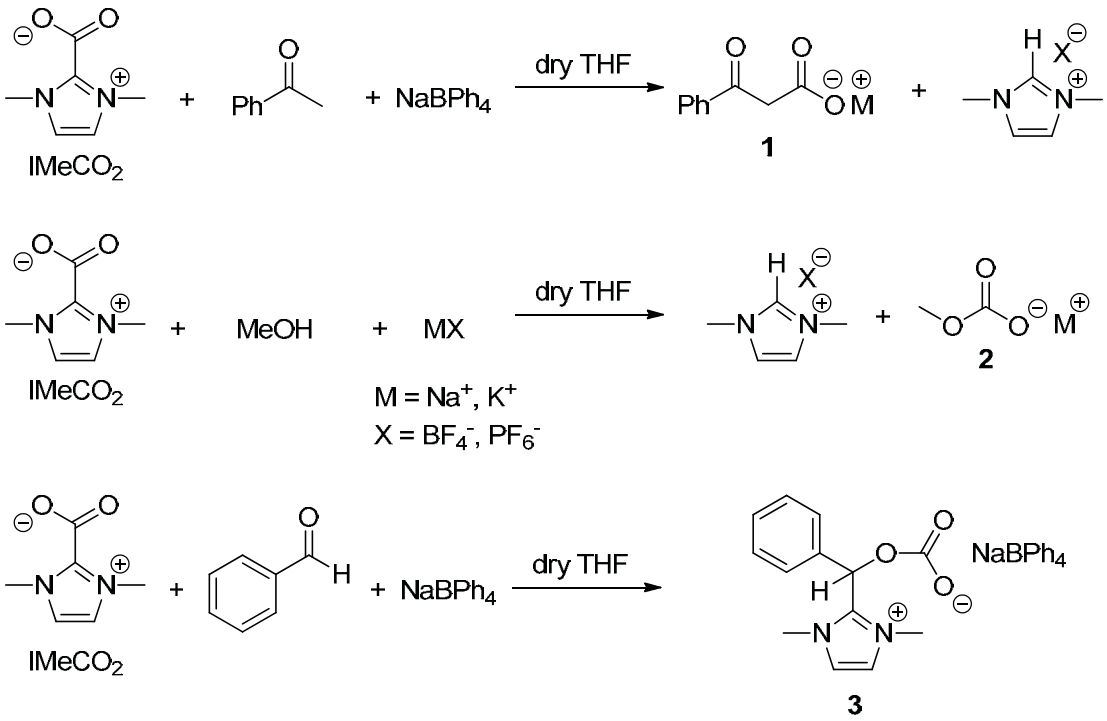

Scheme 2.1. Transcarboxylation reactions performed by Tommasi with NHC CO_2's.

DBU interacts with CO_2 was not known until recently.[42,43] The general lack of insight into DBU mediated reactions, however, has made them less attractive candidates as organocatalysts, with respect to NHCs, as mediators of CO_2 incorporating reactions due to the easy tunability of sterics and electronics of NHC's.[44] In an effort to design more effective NHC·CO_2 mediated carboxylation reactions, we embarked on an investigation of the mechanism of the transcarboxylation reaction.

Results and Discussion

Syntheses and Characterization of $(NHC{\cdot}CO_2){\cdot}MBPh_4$ Complexes

Carboxylation of acetophenone requires $NHC{\cdot}CO_2$ as well as $MBPh_4$. Thus, precomplexation of the $NHC{\cdot}CO_2$ with $MBPh_4$ could play an important role in carbon dioxide transfer. Although the original transcarboxylation reactions reported by Tomassi utilized 1,3-dimethylimidazolium-2-carboxylate ($IMeCO_2$), the insolubitily of $IMeCO_2$ led us to redirect our focus to more soluble $NHC{\cdot}CO_2$ adducts such as $IPrCO_2$ and $IMesCO_2$. Importantly, transcarboxylation reactions employing either $IPrCO_2$ or 1,3-bis-(2,4,6-trimethylphenyl)-imidazolium-2-carboxylate ($IMesCO_2$) afford product (**1**) in comparable yields to those obtained with $IMeCO_2$ (vide infra). Addition of $NaBPh_4$ to a suspension of $IPrCO_2$ in MeCN[45] led to a homogeneous solution. A layer of ether was added and allowed to slowly diffuse into the solution ultimately giving compound **4** as a crystalline solid in 96% yield (Scheme 2.2, Figure 2.1). Interestingly, compound **4** is dimeric where the carboxylate acts as a bridging ligand between two Na ions. A similar carboxylate complex (**5**) was formed when $IPrCO_2$ was added to $LiBPh_4$ in lieu of $NaBPh_4$. However, single crystal X-ray structural analysis showed that the complex was a monomer, not a dimer (Figure 2.2). Again, the cation (i.e., Li^+) binds, in this case, to only one oxygen of a single carboxylate group. Both complexes had distinctly different ^1H NMR shifts from noncomplexed $IPrCO_2$.

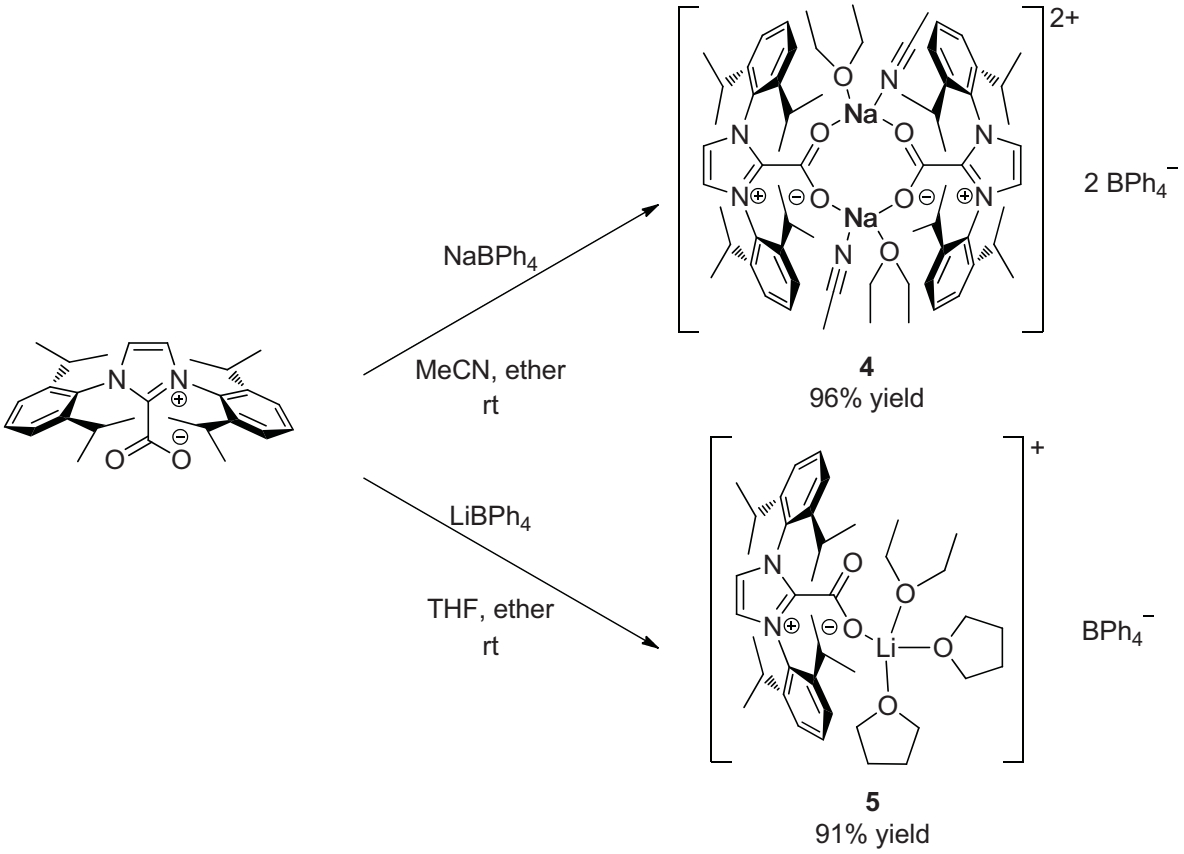

Scheme 2.1. Formation of $IPrCO_2$+$MBPh_4$ complexes **4** and **5**.

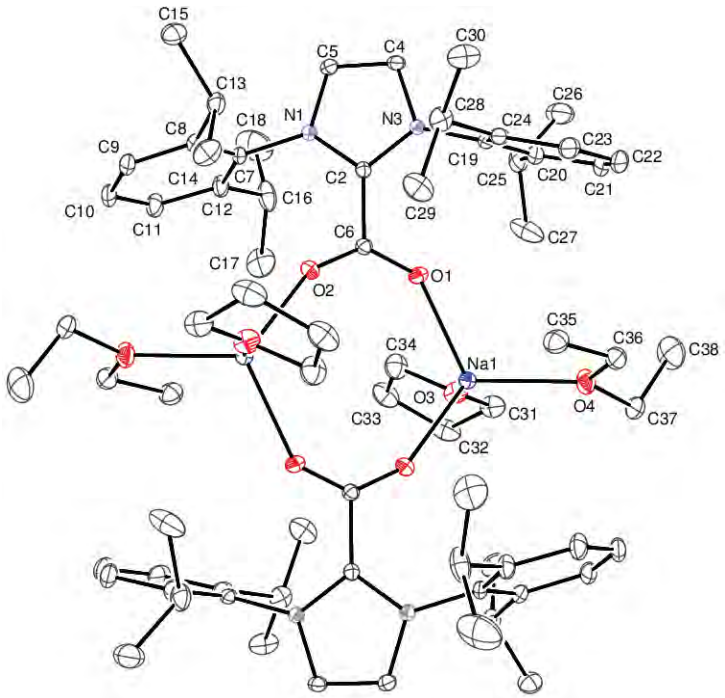

Figure 2.1. X-ray crystal structure of $IPrCO_2$+$NaBPh_4$ (**4**).

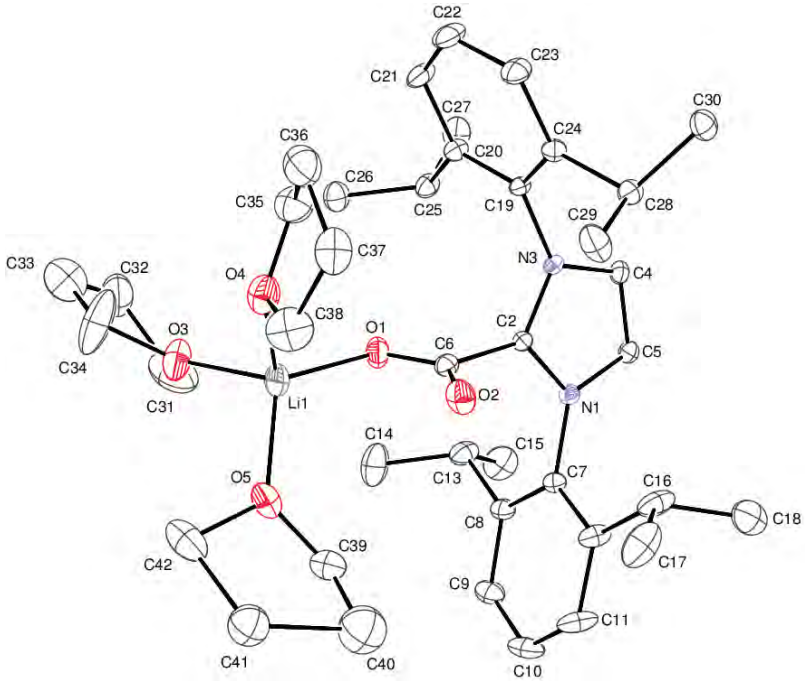

Figure 2.2. X-ray crystal structure of $IPrCO_2$+$LiBPh_4$ (**5**).

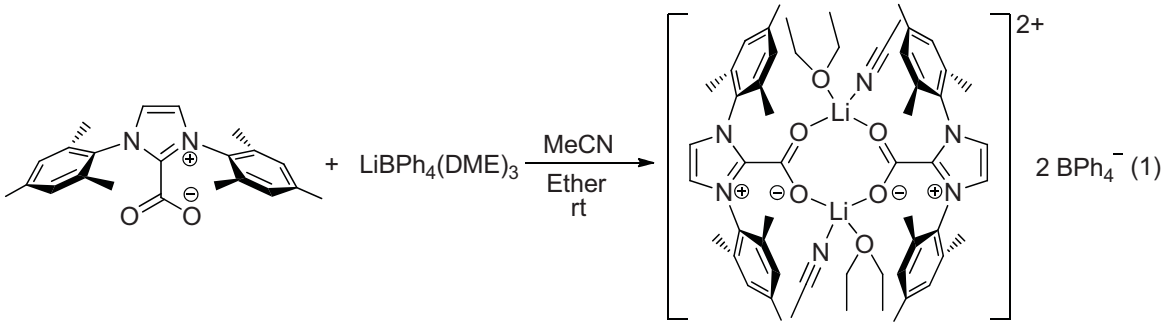

6
95% yield

In an effort to determine whether the formation of monomeric or dimeric complexes was a general phenomenon for NHC·CO_2+$MBPh_4$ compounds, reactions with $IMesCO_2$ were also evaluated. When $IMesCO_2$ was added to $LiBPh_4$ in acetonitrile and then crystallized via slow diffusion with ether, complex **6** was obtained in 95% yield (Equation 2.1, Figure 2.3). Structural analysis of **6** revealed that, in contrast to the reaction of $IPrCO_2$ with $LiBPh_4$, the reaction with $IMesCO_2$ with $LiBPh_4$ afforded a dimeric complex. Thus, although coordination of the NHC·CO_2 to the cation of $MBPh_4$ appears to be general, formation of either a monomer or a dimer can only be determined a posteriori.

A variety of salts were added to a series of carboxylates to examine possible trends in solubility (Table 2.1). All NHC·CO_2's alone were insoluble in THF and were either sparingly soluble in MeCN (entries 1-6, 8) or reacted with MeCN (entry 7, vide infra). When MX (where M^+=Li, Na, or K and X^-=BPh_4) was added to a suspension of $IMeCO_2$ in MeCN, no reaction occurred and only a suspended solid remained (entry 9). Addition of various salts to $IPrCO_2$ resulted in homogeneous solutions (entries 10-13, 15). As noted, addition of either $LiBPh_4$ or $NaBPh_4$ to $IPrCO_2$ led to the formation of

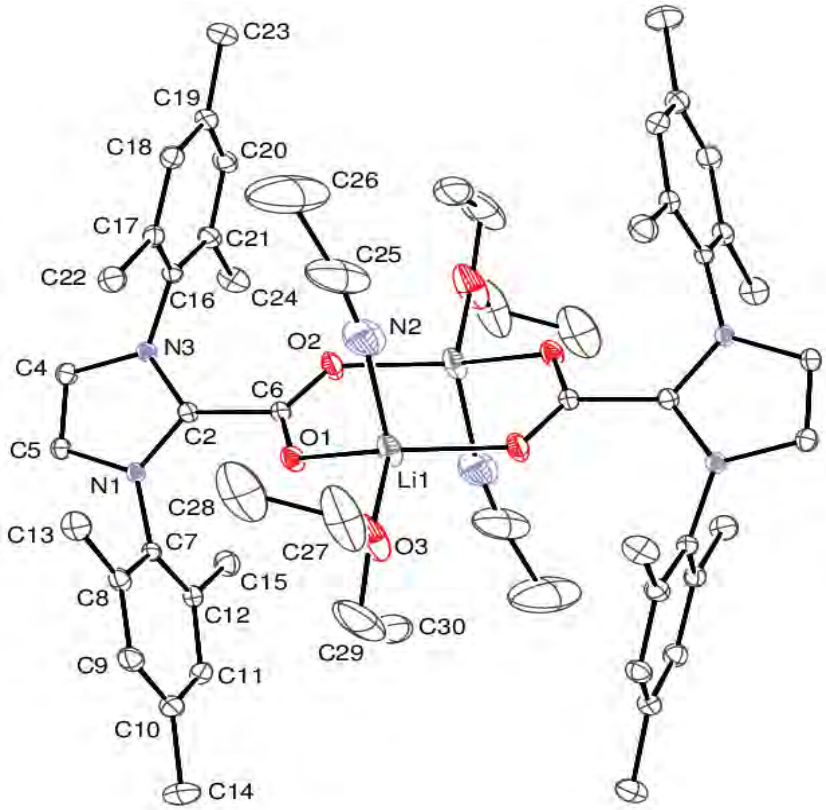

Figure 2.3. X-ray crystal structures of $IMesCO_2$+$LiBPh_4$ (**6**).

isolable compounds (**4** and **5**, respectively) that were amenable to crystallographic analysis (vide supra). The addition of $LiBF_4$, LiI, or NaI to $IPrCO_2$ in MeCN also led to homogeneous solutions (entries 13 and 15). Unfortunately, all attempts in isolating compounds suitable for X-ray analysis were unsuccessful. Interestingly, soluble complexes were not obtained upon the addition of $NaBF_4$, KBF_4, or KI salts to $IPrCO_2$ (entries 14 and 16). Homogeneous solutions were observed upon the addition of $LiBPh_4$ and LiI salts to $IMesCO_2$ (entries 17-18). Similarly, addition of $LiBPh_4$ or $NaBPh_4$ to

Table 2.1. Solubility of salts and carboxylates in various conditions.

entry	NHC•CO_2	salt	solvent[1]	solubility
1	$IPrCO_2$	None	THF	insoluble[2]
2	$IMesCO_2$	None	THF	insoluble[2]
3	I^tBuCO_2	None	THF	insoluble[2]
4	$IMeCO_2$	None	THF	insoluble[2]
5	$IPrCO_2$	None	MeCN	limited[3]
6	$IMesCO_2$	None	MeCN	limited[3]
7	I^tBuCO_2	None	MeCN	reaction with MeCN
8	$IMeCO_2$	None	MeCN	limited[3]
9	$IMeCO_2$	$MBPh_4$: M = Li, Na, K	THF or MeCN	insoluble
10	$IPrCO_2$	$LiBPh_4$ (**4**)	THF or MeCN	homogenous soln
11	$IPrCO_2$	$NaBPh_4$ (**5**)	THF or MeCN	homogenous soln
12	$IPrCO_2$	$KBPh_4$[4]	THF or MeCN	homogenous soln
13	$IPrCO_2$	$LiBF_4$[4]	MeCN	homogenous soln
14	$IPrCO_2$	MBF_4 (M = Na, K)	MeCN	insoluble
15	$IPrCO_2$	MI[4] (M = Li, Na)	MeCN	homogenous soln
16	$IPrCO_2$	KI	MeCN	insoluble
17	$IMesCO_2$	$LiBPh_4$ (**6**)	THF or MeCN	homogenous soln
18	$IMesCO_2$	LiI[4]	MeCN	homogenous soln
19	I^tBuCO_2	$MBPh_4$[4] (M = Li, Na)	THF	homogenous soln
20	I^tBuCO_2	$KBPh_4$[4]	THF	limited[3]

[1]These solvents solvated either the NHC·CO_2 or the salt. [2]No proton signals were observed in THF-d_8. [3]Proton signals were observed though the sample did not dissolve completely. [4]All attempts to grow crystals provided crystals of unsuitable quality for single crystal analysis.

Table 2.2. Bond lengths and torsional angles of $IPrCO_2$ and **4**, **5**, and **6**.

bond lengths (Å)	$IPrCO_2$	$IPrCO_2$+$LiBPh_4$ (**5**)	$IPrCO_2$+$NaBPh_4$ (**4**)	$IMesCO_2$+$LiBPh_4$ (**6**)
C_2-C_6	1.510	1.511	1.525	1.515
C_6-O_2	1.222	1.221	1.239	1.232
C_6-O_1	1.225	1.254	1.233	1.235
O_1-M_1	NA	1.951	2.244	1.906
O_2-M_2	NA	NA	2.236	1.887
N_1-C_2	1.335	1.345	1.344	1.342
N_3-C_2	1.332	1.336	1.333	1.338
Carboxylate Torsional Angle (°)				
N_1-C_2-C_6-O_1	89.75	78.61	27.66	36.47

I^{t}BuCO_2 also led to homogeneous solutions (entry 19). However, a complex with limited solubility formed when $KBPh_4$ was added (entry 20).

Selected bond lengths and the NHC·CO_2 torsional angles for compounds **4**-**6** as well as the parent $IPrCO_2$ are listed in Table 2.2. No structural data exist for $IMesCO_2$. However, given the electronic and overall steric similarities between $IMesCO_2$ and $IPrCO_2$, the structure of dimer **6** was compared to that of $IPrCO_2$. In all cases, complexation to either Li or Na affects the C_6-O bond length and, to a lesser extent, the C_2-C_6 bond length. In $IPrCO_2$, the C_6-O_1 and C_6-O_2 bond lengths are equivalent which reflects the existance of two equal resonance structures. For dimers **4** and **6**, the C_6-O_1 and C_6-O_2 bond lengths are again equivalent, as expected, yet are elongated with respect to uncomplexed $IPrCO_2$. In general, compounds **4**-**6** display both shortened C-O bond lengths (Average = 1.236 Å) as well as M-O bond lengths (Average = 1.915 Å for Li (**5**-**6**) and Average = 2.240 Å for Na (**4**)) relative to known M-carboxylates.[46-48] For example, the C-O and Na-O bond lengths of a similar Na *meta*-iodobenzoate complex are

1.260Å/1.264 Å and 2.476 Å, respectively. Furthermore, anhydrous lithium and sodium formate crystals possess carboxylate C-O bond lengths of 1.242 and 1.246 Å, respectively, and the Li-O and Na-O bond lengths of 1.950 and 2.451 Å, respectively.

The most marked structural change from complexes with either Na or Li is in the different torsional angles. That is, binding markedly lowers the N_1-C_2-C_6-O_1 torsional angle. For monomer **5**, the carboxylate moiety moved approximately 11 degrees toward planarity with the imidazolium ring (i.e., 89.75° in $IPrCO_2$ vs. 78.61° in **5**). An even more striking move toward planarity was observed in dimers **4** and **6**. Specifically, the torsional angles decreased over 50 degrees to 27.66° and 36.47°, respectively.

We recently evaluated a series of $NHC{\cdot}CO_2$ complexes and found that decarboxylation correlated closely to torsional angles.[49] Carboxylates possessing a larger torsional angle underwent decarboxylation at a lower temperature. As a consequence, binding to Li or Na in compounds **4**-**6** could stabilize the carboxylate thereby inhibiting decarboxylation. Surprisingly, TGA analyses of the $IPrCO_2$+$MBPh_4$ and $IMesCO_2{\cdot}LiBPh_4$ complexes revealed decarboxylation actually occurred at lower temperatures than the parent $IPrCO_2$ or $IMesCO_2$ (Figures 2.4 and 2.5). Decarboxylation of $IPrCO_2$ occurs at 108 °C.[50] In contrast, both $IPrCO_2$+$LiBPh_4$ (**5**) and $IPrCO_2$+$NaBPh_4$ (**4**) complexes lose CO_2 at temperatures below 100 °C (76 °C and 81 °C, respectively). In conjunction with the loss of CO_2, loss of coordinated solvent molecules (THF and ether) was also observed at these temperatures. Thus, coordination to Li or Na significantly lowers the temperature required for decarboxylation.

The activation of $IMesCO_2$ was also displayed in the $IMesCO_2$+$LiBPh_4$ complex (**6**) TGA. The $IMesCO_2$+$LiBPh_4$ complex had three stages of weight loss, the first one

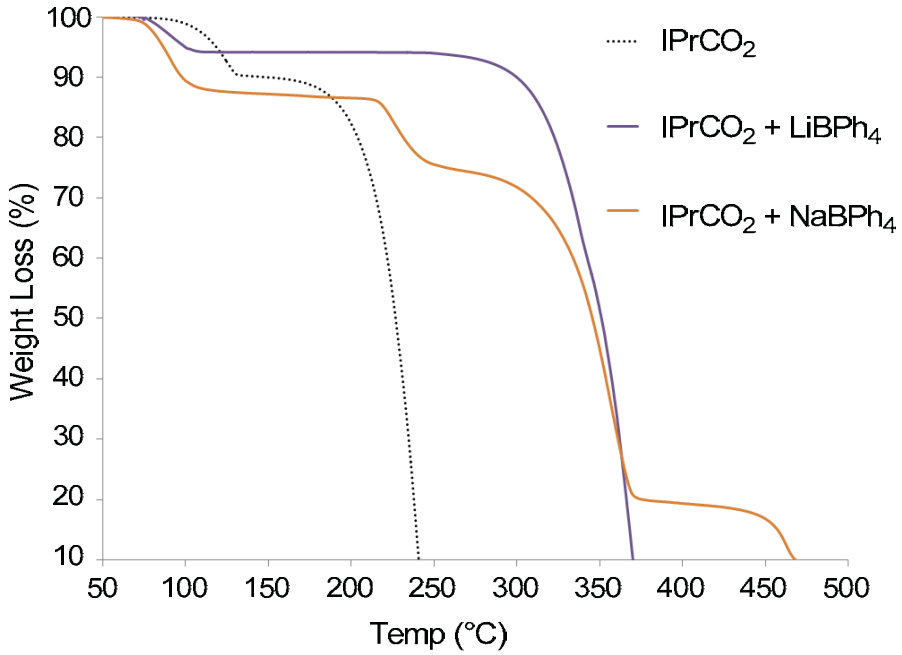

Figure 2.4. TGA curves of $IPrCO_2$, $IPrCO_2$+$LiBPh_4$, and $IPrCO_2$+$NaBPh_4$.

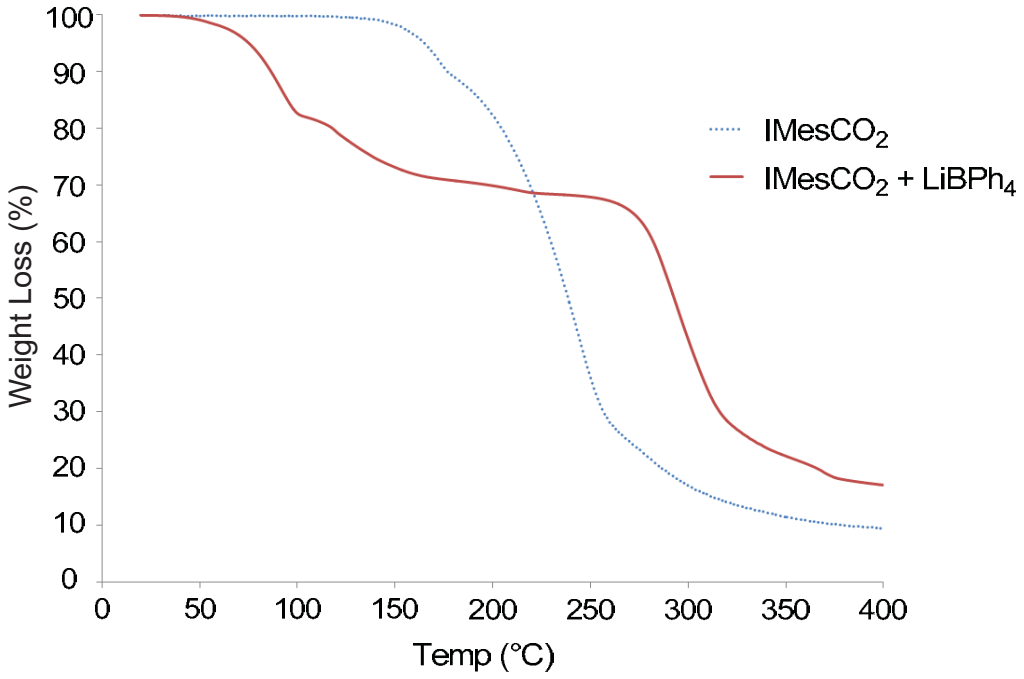

Figure 2.5. TGA plots of $IMesCO_2$ and $IMesCO_2$+$LiBPh_4$ complex.

Table 2.3. Mass percent lost and temperatures at each stage of decompositions for **4**, **5**, **6**, $IPrCO_2$ and $IMesCO_2$.

Decomposition Stage	Mass % lost, Temperature				
	$IPrCO_2$	$IPrCO_2$+$LiBPh_4$	$IPrCO_2$+$NaBPh_4$	$IMesCO_2$+$LiBPh_4$	$IMesCO_2$
1	9.8%, 109 °C	6.2%, 78 °C	22.1%, 104 °C	17.9%, 71 °C	9.6%, 155 °C
2	90.9%, 198 °C	93.0%, 339 °C	10.3%, 239 °C	11.5%, 115 °C	78.0%, 216 °C
3	NA	NA	54.5%, 329 °C	52.1%, 277 °C	NA
4	NA	NA	13.9%, 430 °C	NA	NA

occurring at 71 °C where CO_2, ether, and THF were detected on the mass spectrometer. This first decomposition is 84 °C lower than that of $IMesCO_2$. The TGA analysis indicates that there is activation of the NHC·CO_2 complexes where thermal decarboxylation is facilitated relative to that of the parent NHC·CO_2. The temperature at which each decomposition stage and the % of mass lost at each stage of weight loss is listed in Table 2.3.

Carboxylation Reactions with (NHC·CO_2)·$MBPh_4$ Complexes

Complex **4** was evaluated as a potential "all-in-one" carboxylating agent. When stoichiometric amounts of **4** were added to acetophenone in THF at 50 °C for 4 h, sodium benzoylacetate was formed in 71 % yield (Equation 2.2).

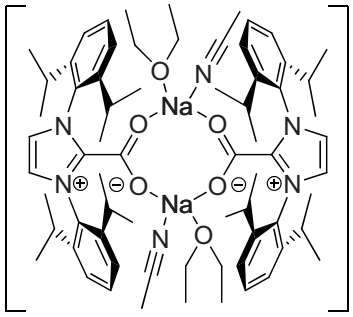

4

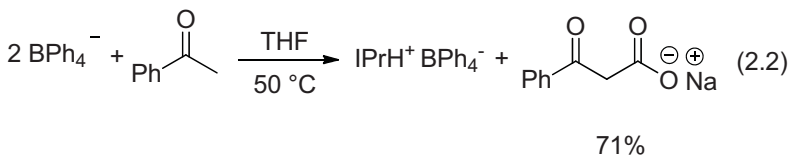

71% (2.2)

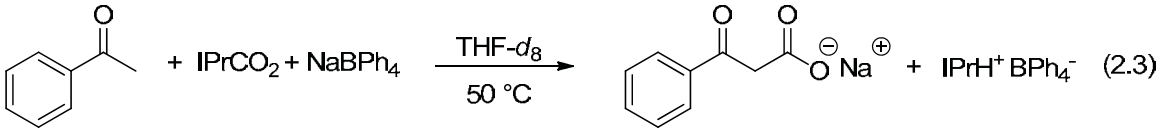

Kinetic Analysis

Kinetic analysis of the $IPrCO_2/NaBPh_4$-mediated carboxylation reaction of acetophenone at 50 °C in THF-d_8 was performed (eq 2.3, Table 2.4). Not surprisingly, carboxylation reactions were first order in acetophenone (Figure 2.6). However, our investigations revealed that the reaction was first order in $IPrCO_2$ (Figure 2.7) yet independent of $NaBPh_4$ (Figure 2.8) concentration. These results were particularly surprising given the dimer coordination mode we obtained from the individual reaction between $IPrCO_2$ and $NaBPh_4$ and the activation of the NHC·CO_2 with salts observed via

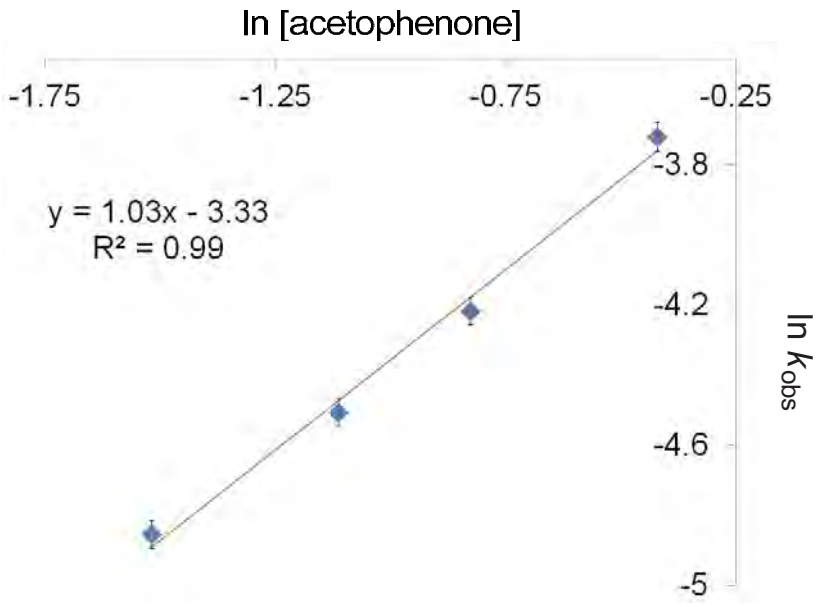

Figure 2.6. Plot of ln [acetophenone] vs ln k at 50.10 °C.

TGA. Interestingly, an equilibrium kinetic isotope effect of 1.57±0.14 was observed when acetophenone was replaced with acetophenone-d_3 in a carboxylation reaction (entry 1 vs. entry 9). In addition, a carboxylation reaction run under an atmosphere of CO_2 was an order of magnitude slower (entry 10).

Deuterium exchange reactions. A series of exchange reactions involving a 1:1 mixture of acetophenone and deuterated acetophenone were evaluated (Equation 2.4, Table 2.5). The control reaction of mixing acetophenone with deuterated acetophenone showed no exchange of deuterium, even at prolonged reaction times of 1 week (entry 1). When 1 equiv of 1,3,4,5-tetramethylimidazolylidene (IMe_{Me}) is added to a C_6D_6 solution containing the control mixture of acetophenone and acetophenone-d_3, scrambling of the enol proton occurred completely by the time the first NMR spectrum was obtained, which was within minutes (entry 2). When IMe_{Me} is substituted with less basic IPr (calculated

Table 2.4. Kinetic analysis of the carboxylation of acetophenone.

entry	[Acetophenone], equiv	[$NaBPh_4$], equiv	k_{obs} Rate constant (x 10^{-3} s^{-1})[b]
1	0.22 M, 5 equiv	0.23 M, 5.3 equiv	-7.8 ± 0.5
2	0.22 M, 5 equiv	0.35 M, 7.9 equiv	-7.7 ± 0.8
3	0.22 M, 5 equiv	0.46 M, 10.5 equiv	-7.8 ± 0.01
4	0.22 M, 5 equiv	0.69 M, 15.7 equiv	-8.0 ± 0.1
5	0.22 M, 5 equiv	0.46 M, 10.5 equiv	-7.8 ± 0.5
6	0.33 M, 7.5 equiv	0.46 M, 10.5 equiv	-10.5 ± 0.6
7	0.44 M, 10 equiv	0.46 M, 10.5 equiv	-13.7 ± 1.3
8	0.66 M, 15 equiv	0.46 M, 10.5 equiv	-23.9 ± 0.3
9	0.22 M, 5 eq[c]	0.23 M, 5.3 equiv	-4.9 ± 0.3
10	0.22 M, 5 eq	0.23 M, 5.3 equiv	-0.43 ± 0.06[d]

[a]Reaction conditions: [$IPrCO_2$] = 0.043 M (1 equiv) in THF-d_8, 50 °C. [b]All runs were performed at least twice. [c]Acetophenone-d_3 was used. [d]The rxn solution was sparged with CO_2 and the rxn was ran with a CO_2 atmosphere.

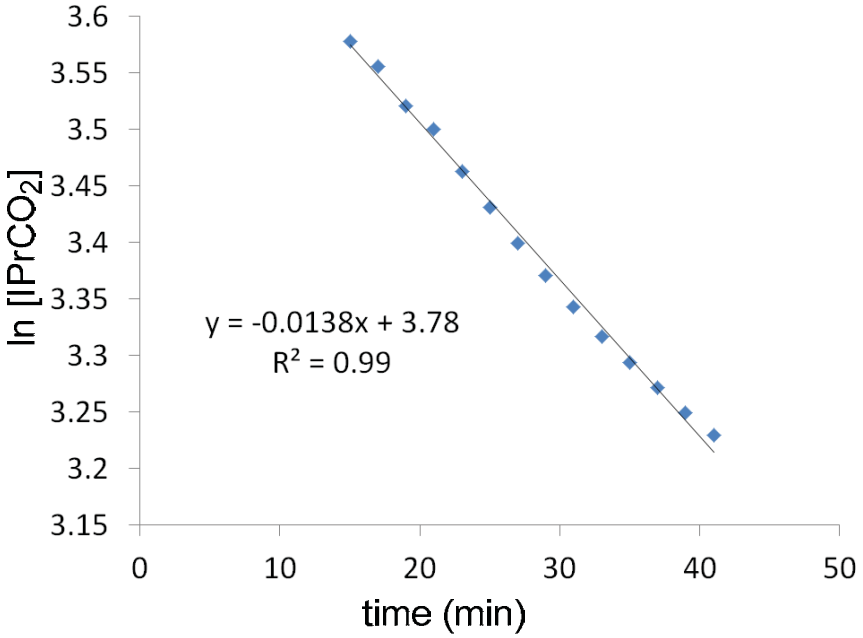

Figure 2.7. Plot of ln [$IPrCO_2$] vs time (min) at 50.10 °C.

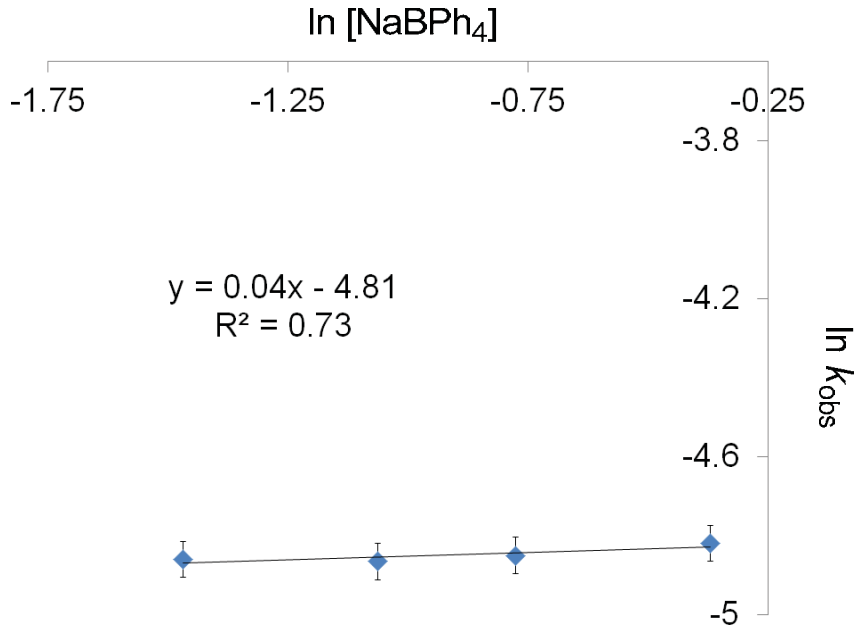

Figure 2.8. Plot of ln [$NaBPh_4$] vs ln *k* at 50.10 °C.

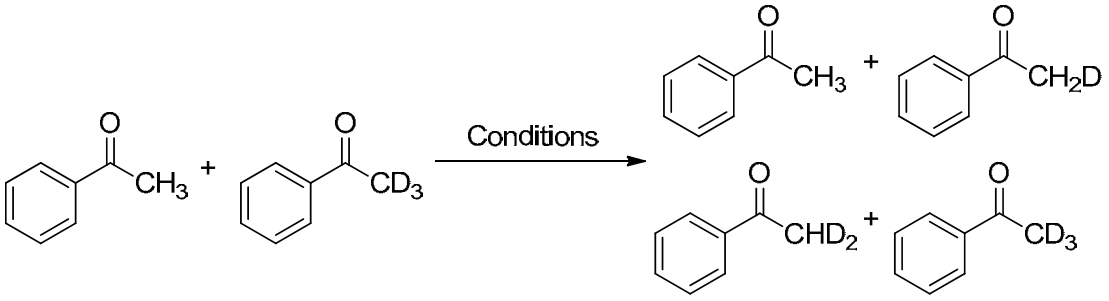

(2.4)

pK_a of 1,3-bis(2,6-dimethylphenyl) imidazolylidene = 16.8±0.09 in DMSO vs. 23.7±0.21 of IMe_{Me}), scrambling is still observed (entry 2), indicating that deprotonation and reprotonation occurs regardless of which NHC catalyst is added.

Interestingly, when 1 equiv of $IPrCO_2$ is added, either in the presence or absence of 1 equiv of $NaBPh_4$, proton/deuterium scrambling is still observed (entries 6-7). However, when $IPrCO_2$, again in the presence or absence of $NaBPh_4$, is added to the solution under an atmosphere of CO_2, scrambling does not occur (entries 8-9). Thus, the CO_2 atmosphere inhibits the buildup of IPr concentration (i.e., through a reversible decarboxylation of $IPrCO_2$) such that deprotonation of acetophenone cannot occur. Also

Table 2.5. NHC-catalyzed H/D Equation 4 exchange reaction conditions and results.

Entry	Conditions				H/D scrambling ($t_{1/2}$)
	Catalyst	Additives	Solvent	Temp	
1	None	None	C_6D_6	rt	Not observed
2	IMe_{Me}	None	C_6D_6	rt	<5 min
3	IPr	None	C_6D_6	rt	3 h
4	$IPrCO_2$	None	CD_3CN	50 °C	50 min
5	$IPrCO_2$	$NaBPh_4$	CD_3CN	50 °C	NA[a]
6	$IPrCO_2$	CO_2 (g)	CD_3CN	50 °C	Not observed
7	$IPrCO_2$	$NaBPh_4$, CO_2 (g)	CD_3CN	50 °C	Not observed

[a] Scrambling occurred, but slowly. Integration was not possible due to overlap of the IPr septet in the acetophenone methyl region. The point at which scrambling was detected was at 3 hours.

of interest, there was no indication that an imidazolium benzoylacetate product was formed when $IPrCO_2$ was put into solution with acetophenone with no MX salt. The aldol product that would form from an acetophenone enolate adding to acetophenone with either IMe_{Me} carbene, IPr carbene, or $IPrCO_2$ was also not observed.

Mechanistic Implications

Data that exists regarding NHC-CO_2 transcarboxylations to organic molecules comes from Lu et al. in the coupling of imidazolium bound CO_2 to epoxides.[41] Lu et al. has evidence that highlights two of three proposed paths (Scheme 2.3). The two paths being supported involve a nucleophilic attack either by a free carbene or attack via the oxyanion of the carboxylate onto the unhindered electrophilic carbon of the epoxide.

Louie et al. discovered that the CO_2 bound to $IPrCO_2$ exchanges freely with unbound $^{13}CO_2$ using ^{13}C NMR, indicating free NHC is generated from the NHC-CO_2 complex to facilitate the attack on a new $^{13}CO_2$ molecule.[50] Tommasi has possible evidence that would lend credence to carbene opening pathway B suggested by Lu et al. when compound **3** was isolated after reaction of benzaldehyde with a NHC-CO_2 and $NaBPh_4$ (Scheme 2.1).[35] This intermediate suggests that a carbene intermediate was formed after decarboxylation of NHC-CO_2 which then performs a nucleophilic attack at the electropositive carbon of the aldehyde, yielding the oxyanion that attacks CO_2 that would afford compound **3**. Waymouth et al. discovered a related intermediate when reacting SIMes carbene **7** with *ß*-butyrolactone, where the carbene attacked the lactone to generate proposed zwitterion **8**, which can then ring close to form the 5-membered spiro-ring **9** (Equation 2.5).[51]

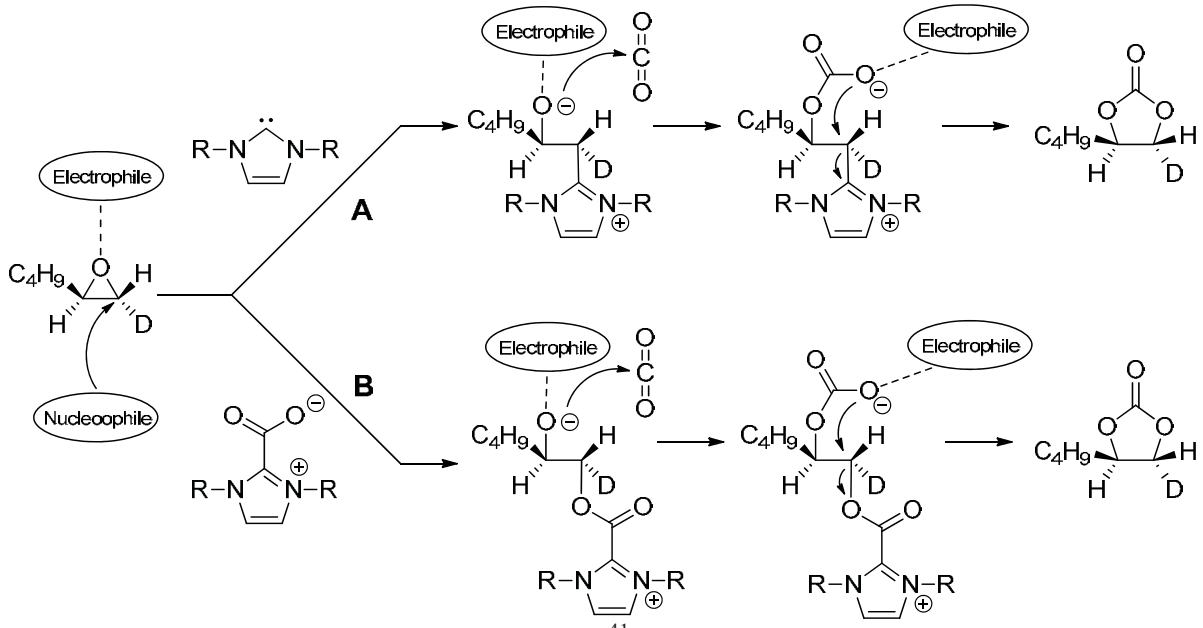

Scheme 2.3. Lu et al. proposed mechanisms[41] for coupling epoxides with CO_2 using SalenAlEt/NHC-CO_2 as the binary catalyst.

Tommasi et al. have proposed that a carbene may be necessary to deprotonate the acetophenone to form the nucleophilic enolate in the carboxylation of acetophenone with NHC-CO_2 and $NaBPh_4$. Indeed, the pK_a's of the carbenes involved in the reaction are high enough to deprotonate and enolize the substrates being carboxylated,[52-55] but this does not explain the role of the MX (M=Li, Na, or K; X=BPh_4 or I) in Tommasi et al. transcarboxylation reaction.

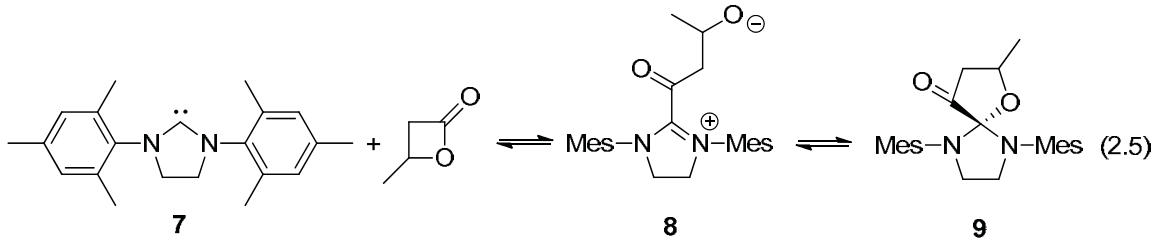

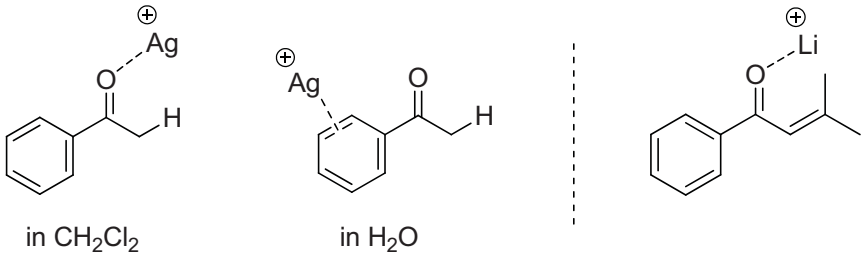

Potential structures observed by
^{13}C NMR by Crist[56] and House[57]

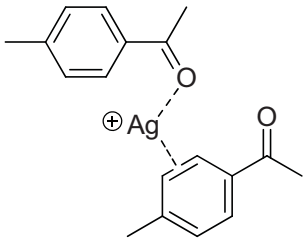

Structure Elucidated by Crist[56]

Figure 2.9. Potential interactions observed of acetophenone and analogues with Lewis acids and structures with metals solved.

It is known that monocations interact with the ketone substrates that Tommasi used in two ways: via the nonbonding sp^2-orbital electrons on oxygen in an *n*-type fashion or via the π-electrons in the benzene rings (Figure 2.9) as demonstrated by Crist and House.[56,57] Therefore it is possible that the MX present in Tommasi's transcarboxylation reactions are activating the acetophenone and assisting the formation of the more nucleophilic enol form of acetophenone (Equations 2.6 and 2.7), i.e. K_{eq} of equation 2.6 < K_{eq} equation 2.7.

In separate deuterium exchange studies performed by Crist et al. and House et al., it was determined that the observed rate constant for deuterium exchange of acetone in deuterated H_2O is larger in the presence of Lewis acids than without (Table 2.6). This phenomenon is largely attributed to the predominate ionic bonding nature of Li and Ag

Table 2.6. First Order Rate Constants for Catalyzed Hydrogen Exchange of Acetone.[56]

Catalyst	Rate ($10^6 k_{obsd}$, s^{-1})
No additive[a]	0.302 ± 0.20
[HNO_3], 0.250 M	19.3 ± 0.6
[KNO_3], 4.95 M	5.59 ± 0.14
[$AgNO_3$], 4.95 M	5.78 ± 0.14
[$LiNO_3$], 2.45 M[b]	5.43 ± 0.16

[a]enough KNO_3 to provide 0.5 M [b]No added KNO_3

cations to the oxygen and aryl ring, whereas the high charge density of H^+ polarizes the oxygen to the point of covalent bond formation, thus promoting the formation of the enol form of the keto-based substrates. House demonstrated with ^{13}C NMR studies that the ß-carbon shift of the enone was shifted downfield 4-5 ppm when excess $LiClO_4$ was added to ethereal solutions of the enone, suggesting reduction of electron density at the ß-carbon due to coordination of the Li cation by the ketone. The House and Crist studies show that there is a moderate activation of the carbonyl by Li^+, K^+, and Ag^+ thus potentially lowering the pK_a of the acetophenone or enabling the formation of more enol in the keto-enol equilibrium of acetophenone. Given such data, a potential mechanism where MX is involved in the transcarboxylation reaction is proposed in Scheme 2.4.

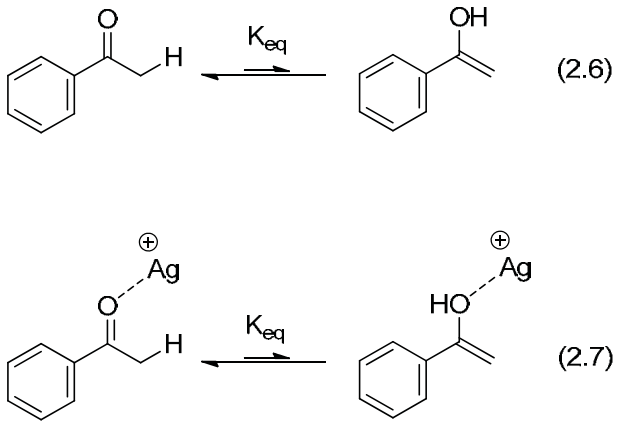

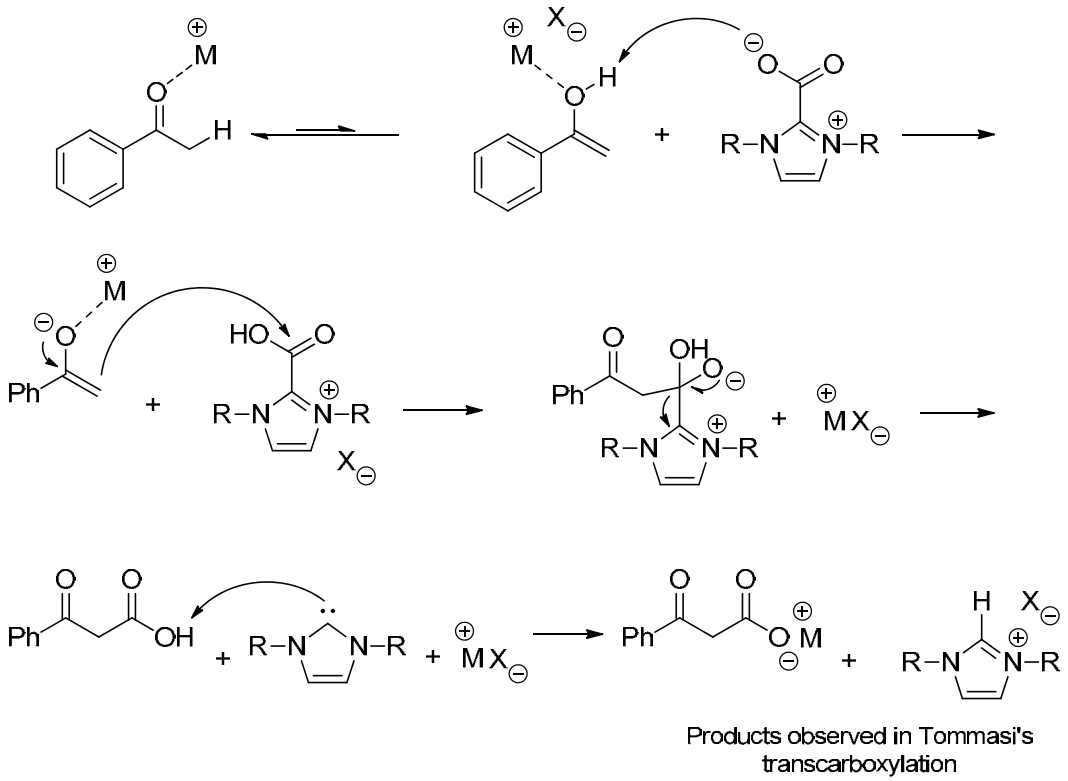

Scheme 2.4. Potential lowering of pK_a and stabilization of oxyanion by the MX salt to facilitate deprotonation and transcarboxylation.

Reaction of IPr·CO_2 and TMS enol

Given the lack of $NaBPh_4$ dependence determined from kinetic analysis, carboxylation reactions between a pre-formed enolate and $IPrCO_2$ were evaulated. Specifically, $IPrCO_2$, TMS enol (**10**), and CsF were combined in MeCN-d_3 and heated to 50 °C (Equation 2.9). After 24 h, no reaction of the $IPrCO_2$ was observed although complete consumption of the TMS enol occurred. Similar results were obtained when TBAF was used in lieu of CsF (Equation 2.10). The control reaction of direct carboxylation of acetophenone was performed by deprotonation of acetophenone with KO^{t}Bu at -78 °C, carboxylated by cannula transfer to dry ice, and acidified with 1.0 M HCl to yield the benzoyl acetic acid in 85% yield.[58]

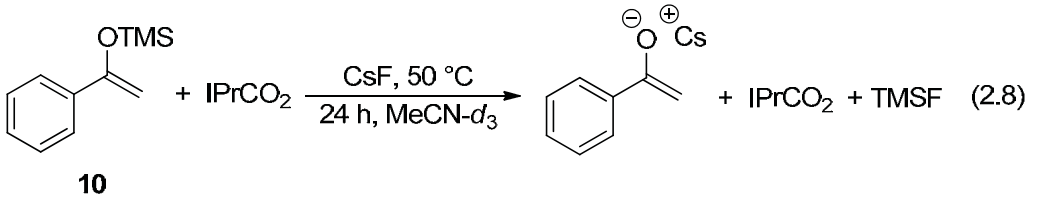

Reaction of I^{t}BuCO$_2$ with acetonitrile. Although no carboxylation products were detected between the reaction of IPrCO$_2$ and TMS enol **7**, direct carboxylation of MeCN does occur *in the absence of NaBPh$_4$*. During our attempts to recrystallize I^{t}BuCO$_2$ in MeCN and ether, single crystals of a dianionic,dicarboxylated ketenimide product were obtained (Equation 2.10, Figure 2.10). A proton from the acetonitrile is covalently bound to one oxygen (1.113 Å) and forms a strong hydrogen bond to the other oxyanion (1.323 Å) between the planar dicarboxylate moieties. A reaction mechanism for the formation of the ketenimide is proposed in Scheme 2.5. Carbon dioxide dissociation from I^{t}BuCO$_2$ affords the free carbene, I^{t}Bu, which then deprotonates the α-proton of MeCN to afford a ketenimide. Nucleophilic attack of either free carbon dioxide (shown) or of the initial I^{t}BuCO$_2$ gives rise to the carboxylate observed in salt **11**. The process is then repeated to ultimately afford the observed dicarboxylated product.

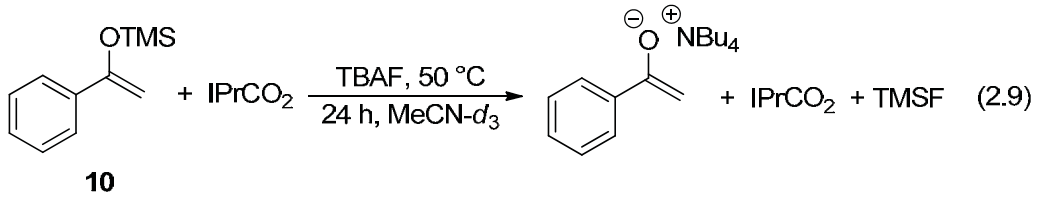

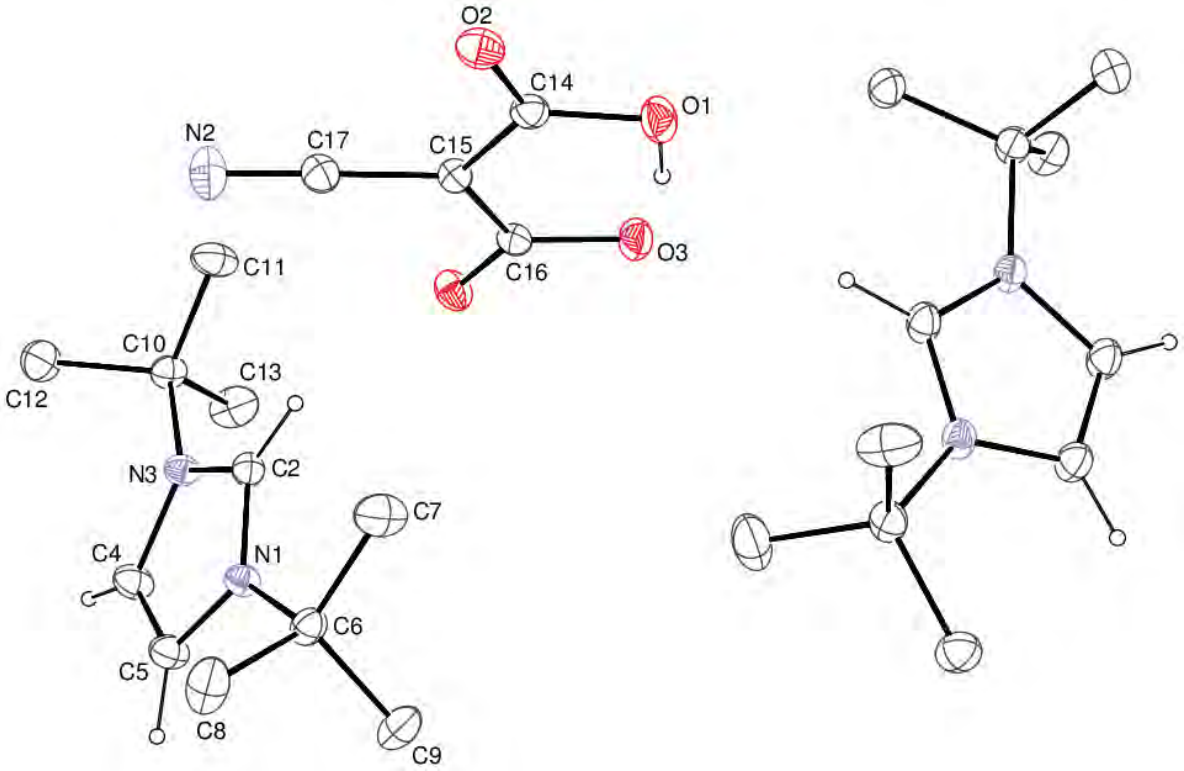

Figure 2.10. X-ray crystal structure of dicarboxylated acetonitrile and two I^{t}Bu imidazolium cations (**11**).

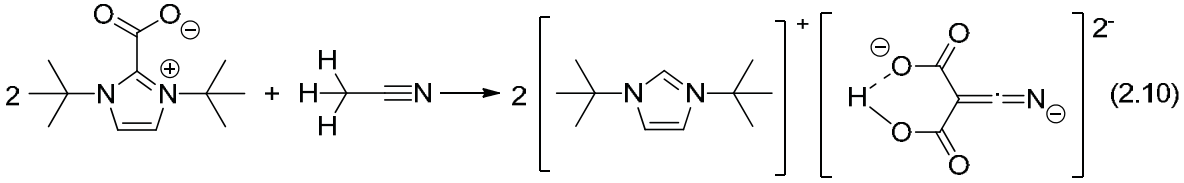

(2.10)

11

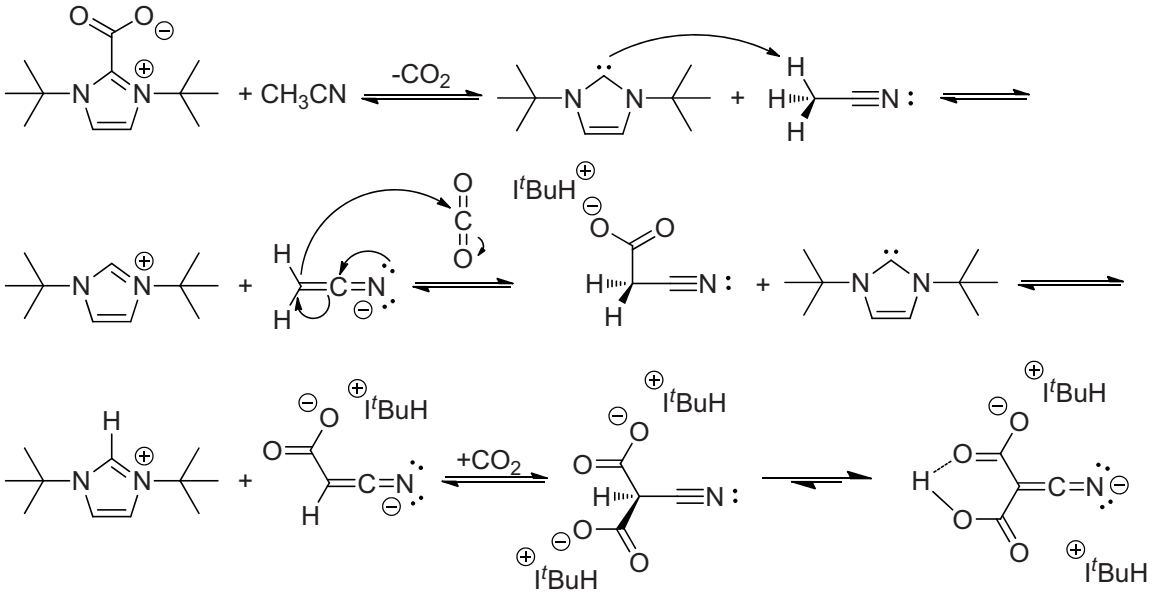

Scheme 2.5. Proposed mechanism for the formation of the dicarboxylato ketenimide from I^tBuCO_2 and acetonitrile.

Conclusion

Despite the isolation of a variety of interesting $NHC{\cdot}CO_2$+$MBPh_4$ complexes, our results suggest that the complexes do not remain aggregated during carboxylation. That is, carboxylation reaction rates were independent of $NaBPh_4$ concentration. This evidence also points away from a mechanism that involves a salt-assisted deprotonation of acetophenone (i.e., enhanced acidity of the α-proton through precoordination of the Na^+ to either the carbonyl or the arene).[56,57] In addition, facile carboxylation of MeCN occurred in the absence of added salt. Thus, the role of $NaBPh_4$ may be to help bring the $NHC{\cdot}CO_2$ into solution such that it is available to react. Indeed, our investigations indicate that the addition of salts to otherwise insoluble $NHC{\cdot}CO_2$ compounds led to homogeneous solutions. Given the propensity of the carboxylated product to undergo

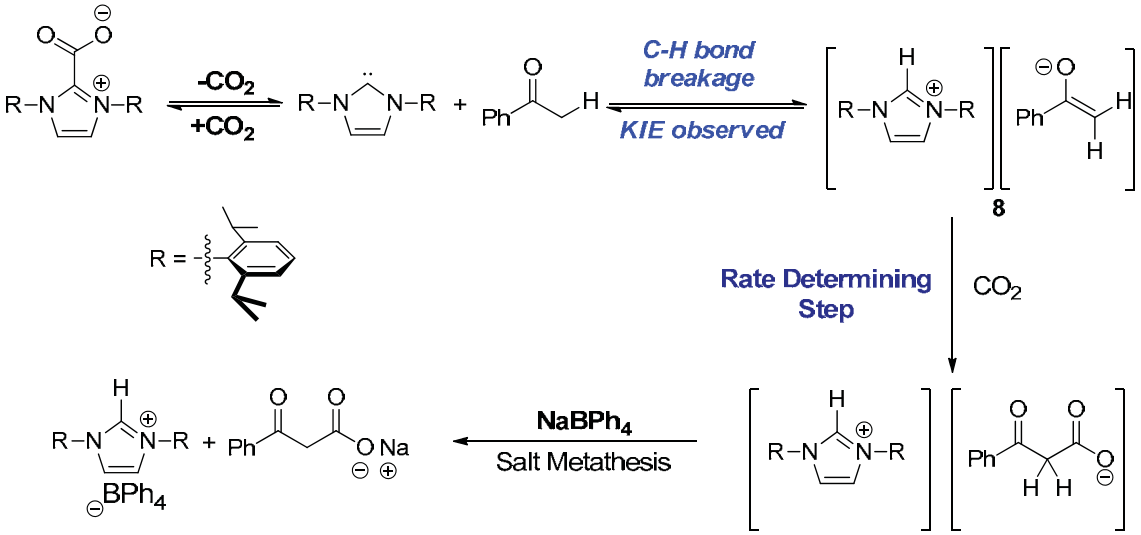

Scheme 2.6. The proposed reaction mechanism for the carboxylation of acetophenone.

spontaneous decarboxylation, the role of the $NaBPh_4$ may also serve to stabilize the product through ion-pairing. A proposed mechanism that is analogous to carboxylation of MeCN is shown in Scheme 2.6.

Experimental Section

General Information

All reactions and procedures were conducted under an atmosphere of N_2 using standard Schlenk techniques or in a N_2 filled glove-box unless otherwise noted. ^1H and ^{13}C Nuclear Magnetic Resonance spectra of pure compounds were acquired at 500 and 125 MHz, respectively, unless otherwise noted. All spectra are referenced to residual solvent peaks. The abbreviations s, d, dd, dt, dq, t, q, quint, sept., m stand for singlet, doublet, doublet of doublets, doublet of triplets, doublet of quartets, triplet, quartet, quintet, septet, and multiplet, in that order. All coupling constants, *J*, are reported in Hz. All ^{13}C NMR spectra were proton decoupled. IR spectra were recorded on a Bruker

Tensor 27 FT-IR spectrometer. Thermogravimetric analyses (TGA) were performed on a TA Instruments TGA2050. The TGA data were recorded using Therma Advantage, ver. 1.14. All TGA analyses were performed in a N_2 atmosphere at a heating rate of 5 °C/min.

Materials

Nondeuterated solvents were purified and deoxygenated by passing through packed silica columns. All oil from NaH was removed by thorough washing with hexanes. $LiBPh_4(DME)_3$, $KBPh_4$, LiI, NaI, KI, $LiBF_4$, $NaBF_4$, and KBF_4 were dried by placing in a 130 °C oven for several days and further dried and cooled under a vacuum over the solid for 30 minutes and stored in a N_2-filled glove box. $NaBPh_4$ was dried by dissolving in a minimal amount of THF and stirring with NaH for 30 min, filtering through Celite, and removing solvent in vacuo and stored under nitrogen. KO^tBu (98%) was purchased from Sigma-Aldrich and used without further purification. KHMDS (95%) was purchased from Sigma-Aldrich and used without further purification. All other reagents were purchased from the chemical provider without further purification, unless specified. All NMR solvents were thoroughly dried using standard procedures prior to use. All imidazolium carboxylates used were synthesized using previously reported procedures and citations therein.[49] Carboxylation of acetophenone was performed using a modification of an existing procedure.[58]

Deuterated solvents were purchased from Cambridge. CD_3CN was dried and distilled from CaH_2 and THF-d^8 was distilled from a benzophenone-Na ketyl radical still. All other reagents were purchased and used without further purification unless otherwise noted. See Appendix B for NMR spectra and x-ray crystal structure reports.

Preparation of $[(IPrCO_2Na)_2]^{2+}2[BPh_4]^{2-}$ (4). $IPrCO_2$ (0.025 g, 57 *u*mol, 1eq) and $NaBPh_4$ (0.020 g, 59 *u*mol, 1.03 eq) were weighed out into separate five vials and then mixed using a Pasteur pipette with a minimal amount of dry THF or MeCN until a homogenous solution was obtained. The vial containing the solution was then placed into a larger vial that contained diethyl ether and was capped. Within 12 h, enough diethyl ether had diffused into the THF or MeCN to yield 40 mg of colorless crystals (88 % yield) worthy of single crystal x-ray analysis. It should be duly noted that best efforts were given to dry solvents thoroughly and prevent the reaction of the complex with residual water when trying to characterize the compound, however, formation of the $IPrHBPh_4$ is observed to some degree in all attempts to obtain a ^1H or ^{13}C spectrum that contained unreacted **4**. THF and ether from the crystal lattice could not be removed via vacuum and is observed in the NMR spectrum in approximately a 1:9 ratio of $IPrH^+$:$IPrCO_2M^+$, as indicated by integration of the acidic C_2 proton of $IPrH^+$. ^1H NMR (THF-d_8, ppm) δ 7.43 (t, 2H, *J* = 7.8), 7.41 (s, 2H), 7.27 (d, 4H, *J* = 7.8), 7.23 (m, 8H), 6.77 (t, 8H, *J* = 7.5), 6.62 (t, 2H, *J* = 7.2), 3.36 (q, 3H, *J* = 7.0), 2.49 (sept., 4H, *J* = 6.9), 1.19 (d, 12H, *J* = 6.8), 1.16 (d, 12H, *J* = 7.0), 1.08 (t, 5H, *J* = 7.1) ^{13}C NMR (THF-d_8, ppm) δ 165.6, 165.2, 164.8, 164.4, 147.3, 146.2, 145.8, 137.4, 137.1, 136.9, 136.6, 132.5, 131.6, 130.97, 125.7, 125.2, 124.6, 124.1, 123.8, 122.2, 121.7, 121.4, 121.0, 68.0, 66.11, 30.1, 29.85, 26.1, 24.4, 24.3, 23.5, 23.41, 15.53, 15.44.

Preparation of $[IPrCO_2Li]^+[BPh_4]^-$ (5). $IPrCO_2$ (0.025 g, 57 *u*mol, 1eq) and $LiBPh_4(DME)_3$ (0.036 g, 59 *u*mol, 1.03 eq) were weighed out into separate five vials and then mixed using a Pasteur pipette with a minimal amount of dry THF or MeCN until a homogenous solution was obtained. The vial containing the solution was then placed into

a larger vial that contained diethyl ether and was capped. Within 12 h, enough diethyl ether had diffused into the THF or MeCN to yield 39 mg of colorless crystals (95 % yield) worthy of single crystal x-ray analysis. It should be duly noted that best efforts were given to dry solvents thoroughly and prevent the reaction of the complex with residual water when trying to characterize the compound, however, formation of the $IPrHBPh_4$ is observed to some degree in all attempts to obtain a ^1H or ^{13}C spectrum that contained unreacted **4**. THF and ether from the crystal lattice could not be removed via vacuum and is observed in the NMR spectrum in approximately a 1:9 ratio of $IPrH^+$:$IPrCO_2M^+$, as indicated by integration of the acidic C_2 proton of $IPrH^+$. ^1H NMR (THF-d_8, ppm) δ 7.46 (t, 2H, J = 7.8), 7.42 (s, 2H), 7.31 (d, 4H, J = 7.8), 7.23 (m, 8H), 6.79 (t, 8H, J = 7.3), 6.64 (t, 2H, J = 7.1), 3.57 (m, 3.4H), 3.35 (q, 0.6H, J = 7.0), 2.48 (sept., 4H, J = 6.9), 1.73 (m, 3.4H), 1.22 (d, 12H, J = 6.8), 1.17 (d, 12H, J = 7.0), 1.08 (t, 1.1H, J = 7.0) ^{13}C NMR (THF-d_8, ppm) δ 165.1, 164.8, 164.4, 155.8, 146.2, 145.8, 136.9, 132.7, 131.6, 124.5, 125.46, 125.44, 125.42, 125.40, 124.8, 124.7, 124.5, 68.0, 29.8, 26.1, 24.3, 23.3, 15.4.

Preparation of $[(IMesCO_2Li)_2]^{2+}2[BPh_4]^{2-}$ (6). $IMesCO_2$ (0.020 g, 57 *u*mol, 1eq) and $LiBPh_4(DME)_3$ (0.036 g, 59 *u*mol, 1.03 eq) were weighed out into separate five vials and then mixed using a Pasteur pipette with a minimal amount of dry THF or MeCN until a homogenous solution was obtained. The vial containing the solution was then placed into a larger vial that contained diethyl ether and was capped. Within 12 h, enough diethyl ether had diffused into the THF or MeCN to yield 33 mg of colorless crystals (85 % yield) worthy of single crystal x-ray analysis. It should be duly noted that best efforts were given to dry solvents thoroughly and prevent the reaction of the complex with

residual water when trying to characterize the compound. Therefore, formation of the $IMesHBPh_4$ is observed to some degree in all attempts to obtain a ^1H or ^{13}C spectrum that contained unreacted **6** and is observed in the NMR spectrum near a 1:8 ratio of $IMesH^+$:$IMesCO_2M^+$, as indicated by integration of the acidic C_2 proton of $IMesH^+$. THF and ether from the crystal lattice could not be removed via vacuum. ^1H NMR (THF-d_8, ppm) δ 7.26 (m, 8H), 7.07 (s, 2H), 7.02 (s, 4H), 6.81 (t, 8H, J = 7.1), 6.67 (t, 4H, J = 7.1), 3.61 (m, 6H), 3.39 (q, 0.8H, J = 7.0), 2.32 (s, 6H), 2.09 (s, 12H), 1.77 (m, 6H), 1.18 (t, 1.2H, J = 7.0). ^{13}C NMR (THF-d_8, ppm) δ 165.5, 165.1, 164.7, 164.4, 156.2, 145.9, 142.1, 141.2, 136.9, 135.7, 134.9, 132.6, 131.6, 130.4, 129.7, 169.6, 125.5, 125.4, 126.04, 122.9, 121.7, 121.5, 68.0, 26.2, 20.9, 20.8, 17.4, 17.2.

Preparation of $IPrCO_2$+$KBPh_4$. $IPrCO_2$ (0.020 g, 46 *u*mol, 1eq) and $KBPh_4$ (0.018 g, 48 *u*mol, 1.05 eq) were weighed out into separate vials and then mixed using a Pasteur pipette with a minimal amount of dry d^8-THF until a homogenous solution was obtained. Almost none of the $IPrCO_2$ had reacted with residual water. ^1H NMR (THF-d_8, ppm) δ 7.46 (t, 2H, J = 7.8), 7.44 (s, 2H), 7.32 (d, 4H, J = 7.8), 7.28 (m, 8H), 6.81 (t, 8H, J = 7.5), 6.67 (t, 4H, J = 7.2), 2.54 (sept, 4H, J = 6.8), 1.25 (d, 12H, J = 6.8), 1.20 (d, 12H, J = 6.8),. ^{13}C NMR (THF-d_8, ppm) δ 163.9, 163.5, 163.2, 162.8, 144.4, 135.3, 131.4, 129.8, 132.9, 123.8, 123.0, 122.5, 119.9, 28.2, 22.7, 21.9.

Preparation of $IPrCO_2$+$LiBF_4$. $IPrCO_2$ (0.020 g, 46 *u*mol, 1eq) and $LiBF_4$ (0.005 g, 48 *u*mol, 1.05 eq) were weighed out into separate vials and then mixed using a Pasteur pipette with a minimal amount of dry CD_3CN until a homogenous solution was obtained. The ratio of $IPrCO_2M$:IPrH detected from reaction with residual water was ~9:1. ^1H NMR (CD_3CN, ppm) δ 7.54 (s, 2H), 7.52 (t, 2H, J = 7.8), 7.34 (d, 4H, J = 7.8), 2.38

(sept, 4H, J = 6.8), 1.18 (d, 12H, J = 6.9), 1.20 (d, 12H, J = 6.7). ^{13}C NMR (THF-d_8, ppm) δ 155.0, 146.4, 145.6, 144.8, 133.3, 131.7, 131.5, 130.8, 125.6, 125.4, 125.1, 124.8, 30.1, 29.9, 24.5, 24.5, 23.6, 23.5.

Preparation of IPrCO$_2$+LiI. IPrCO$_2$ (0.020 g, 46 *u*mol, 1eq) and LiI (0.007 g, 48 *u*mol, 1.05 eq) were weighed out into separate vials and then mixed using a Pasteur pipette with a minimal amount of dry CD_3CN until a homogenous solution was obtained. The ratio of IPrCO$_2$M:IPrH detected from reaction with residual water was ~9:1. ^{1}H NMR (CD_3CN, ppm) δ 7.60 (s, 2H), 7.52 (t, 2H, J = 7.8), 7.34 (d, 4H, J = 7.8), 2.36 (sept, 4H, J = 6.8), 1.17 (d, 12H, J = 6.5), 1.13 (d, 12H, J = 6.7). ^{13}C NMR (THF-d_8, ppm) δ 155.5, 146.9, 146.1, 133.7, 132.2, 132.0, 131.3, 127.7, 127.5, 126.2, 126.0, 125.6, 125.3, 30.6, 30.4, 25.2, 25.1, 25.0, 24.4, 24.3, 24.1, 24.0.

Preparation of IPrCO$_2$+NaI. IPrCO$_2$ (0.020 g, 46 *u*mol, 1eq) and NaI (0.008 g, 48 *u*mol, 1.05 eq) were weighed out into separate vials and then mixed using a Pasteur pipette with a minimal amount of dry CD_3CN until a homogenous solution was obtained. The ratio of IPrCO$_2$M:IPrH detected from reaction with residual water was ~10:1. ^{1}H NMR (CD_3CN, ppm) δ 7.53 (s, 2H), 7.53 (t, 2H, J = 7.8), 7.37 (d, 4H, J = 7.8), 2.48 (sept, 4H, J = 6.9), 1.22 (d, 12H, J = 6.9), 1.20 (d, 12H, J = 6.9). ^{13}C NMR (THF-d_8, ppm) δ 155.5, 147.3, 146.9, 146.1, 133.9, 132.4, 132.2, 131.4, 125.0, 124.8, 30.8, 30.7, 30.6, 30.5, 30.2, 25, .9, 25.1, 25.0, 24.9, 25.2, 24.1, 23.2.

Preparation of IMesCO$_2$+LiI. IMesCO$_2$ (0.030 g, 86 *u*mol, 1eq) and LiI (0.012 g, 90 *u*mol, 1.05 eq) were weighed out into separate vials and then mixed using a Pasteur pipette with a minimal amount of dry CD_3CN until a homogenous solution was obtained. The ratio of IMesCO$_2$M:IMesH detected from reaction with residual water was ~8:1. ^{1}H

NMR (CD_3CN, ppm) δ 7.51 (s, 2H), 7.08 (s, 4H), 7.37 (d, 4H, J = 7.8), 2.34 (sept, 6H), 2.05 (s, 12H). ^{13}C NMR (THF-d_8, ppm) δ 154.9, 143.2, 141.5, 140.6, 137.5, 134.8, 134.6, 131.8, 130.8, 130.0, 129.8, 129.6, 129.4, 129.1, 128.8, 128.6, 125.0, 124.8, 123.6, 123.4, 123.2, 122.9, 20.40, 20.32, 20.26, 16.9, 16.8, 16.6, 16.4.

Preparation of I^{t}BuCO$_2$+LiBPh$_4$. I^{t}BuCO$_2$ (0.030 g, 130 *u*mol, 1eq) and $LiBPh_4(DME)_3$ (0.083 g, 140 *u*mol, 1.05 eq) were weighed out into separate vials and then mixed using a Pasteur pipette with a minimal amount of dry d^8-THF until a homogenous solution was obtained. The ratio of I^{t}BuCO$_2$M:I^{t}BuH detected from reaction with residual water was ~6:1. ^{1}H NMR (d^8-THF, ppm) δ 7.29 (m, 8H), 7.01 (s, 2H), 6.86 (s, 8H), 6.72 (t, 4H, J = 7.2), 3.42 (s, 4H), 3.26 (s, 6H), 1.58 (s, 18H). ^{13}C NMR (THF-d_8, ppm) δ 165.4, 164.2, 164.7, 164.5, 161.5, 144.5, 137.0, 136.9, 125.5, 121.7, 117.8, 117.6, 72.5, 62.4, 60.8, 58.7, 29.7, 29.6.

Preparation of I^{t}BuCO$_2$+NaBPh$_4$. I^{t}BuCO$_2$ (0.030 g, 130 *u*mol, 1eq) and $NaBPh_4$ (0.048 g, 140 *u*mol, 1.05 eq) were weighed out into separate vials and then mixed using a Pasteur pipette with a minimal amount of dry d^8-THF until a homogenous solution was obtained. The ratio of I^{t}BuCO$_2$M:I^{t}BuH detected from reaction with residual water was ~9:1. ^{1}H NMR (d^8-THF, ppm) δ 7.25 (m, 8H), 7.08 (s, 2H), 6.81 (t, 8H, J = 7.4), 6.67 (t, 4H, J = 7.2), 1.63 (s, 18H). ^{13}C NMR (THF-d_8, ppm) δ 165.6, 165.2, 164.8, 164.4, 161.9, 145.6, 137.1, 136.9, 125.5, 121.7, 117.3, 117.2, 68.0, 62.2, 60.8, 29.7.

Preparation of I^{t}BuCO$_2$+KBPh$_4$. I^{t}BuCO$_2$ (0.030 g, 130 *u*mol, 1eq) and $KBPh_4$ (0.050 g, 140 *u*mol, 1.05 eq) were weighed out into separate vials and then mixed using a Pasteur pipette with a minimal amount of dry d^8-THF until a homogenous solution was obtained. The ratio of I^{t}BuCO$_2$M:I^{t}BuH detected from reaction with residual water was

~9:1. ^{1}H NMR (d^{8}-THF, ppm) δ 7.29 (m, 8H), 7.13 (s, 2H), 6.86 (t, 8H, J = 7.4), 6.71 (t, 4H, J = 7.2), 1.52 (s, 18H). ^{13}C NMR (THF-d_8, ppm) δ 165.7, 165.3, 164.9, 164.5, 161.6, 146.8, 137.1, 137.0, 125.7, 121.8, 63.1, 62.1, 60.9, 60.3, 29.7, 29.5.

Preparation of 2[I^{t}BuH]$^{2+}$[dicarboxylatoketenimide]$^{2-}$ (11). I^{t}BuCO$_2$ (0.050 g, 0.222 mmol, 1eq) was weighed out into a vial and then dissolved with a minimal amount of dry acetonitrile until a homogenous solution was obtained. The vial containing the solution was then placed into a larger vial that contained diethyl ether and was capped. Within 12 h, enough diethyl ether had diffused into the THF or MeCN to yield 40 mg of colorless crystals (37 % yield) worthy of single crystal x-ray analysis. ^{1}H NMR (CD_3CN, ppm) δ 9.73 (s, 1H), 7.73 (s, 2H), 1.67 (s, 18H). ^{13}C NMR (MeCN-d_3, ppm) δ 164.5, 133.6, 120.9, 120.3, 61.1, 29.9, 27.7.

Pseudo-First Order Kinetic Studies with IPrCO$_2$+NaBPh$_4$+Acetophenone in d^{8}-THF: Order in IPrCO$_2$. IPrCO$_2$ (0.020 g, 46 *u*mol, 1.00 eq), NaBPh$_4$ (0.166 g, 485 *u*mol, 10.5 eq), and trimethoxybenzene (0.035 g, 21 *u*mol, 5 eq) were weighed into separate vials. Dry d^{8}-THF was then used to dissolve all three solids. The solution was transferred to a NMR tube and the vial rinsed thoroughly to ensure complete transfer of the IPrCO$_2$, NaBPh$_4$, and TMB. The final volume of this solution was 1.00 mL. To the 1.0 mL of solution was added 54 *u*L of acetophenone and the solution was sealed with parafilm, mixed thoroughly, and placed into an icebath. After heating the NMR spectrometer probe to 50.1 °C, the sample was inserted and initial rates of the reaction were used to determine that the consumption of IPrCO$_2$ was first-order.

Pseudo-First Order Kinetic Studies with IPrCO$_2$+NaBPh$_4$+Acetophenone in d^{8}-THF: Order in NaBPh$_4$. To determine the order of NaBPh$_4$ in the reaction, four

samples were made that varied only in the concentration of $NaBPh_4$. The amounts of $IPrCO_2$ (0.020 g, 46 *u*mol, 1.00 eq), acetophenone (27 *u*L, 231 *u*mol, 5 eq), and trimethoxybenzene (0.035 g, 21 *u*mol, 5 eq) stayed constant. The amounts of $NaBPh_4$ varied as follows: 0.083 g, 243 *u*mol, 5.25 eq; 0.124 g, 364 *u*mol, 7.88 eq; 0.166 g, 485 *u*mol, 10.5 eq; 0.249 g, 728 *u*mol, 15.8 eq. Dry d^8-THF was then used to make the samples, achieving 1.027 mL. The 1.027 mL of solution had 27 *u*L of acetophenone added and the solution was sealed with parafilm, mixed thoroughly, and placed into an icebath. After heating the NMR spectrometer probe to 50.1 °C, the sample was inserted, the temperature was allowed to equilibrate, and initial rates of $IPrCO_2$ loss were used to determine the reaction order of $NaBPh_4$. The following pseudo-first-order rate constants were obtained at different concentrations of acetophenone (-*k*, [$IPrCO_2$]), respectively: 7.8×10^{-3} M·s^{-1}, 7.7×10^{-3} M·s^{-1}, 7.8×10^{-3} M·s^{-1}, 8.1×10^{-3} M·s^{-1}.

Pseudo-First Order Kinetic Studies with $IPrCO_2$+$NaBPh_4$+Acetophenone in d^8-THF: Order in Acetophenone. To determine the order of acetophenone in the reaction, three samples were made that varied only in the concentration of acetophenone. The amounts of $IPrCO_2$ (0.020 g, 46 *u*mol, 1.00 eq), $NaBPh_4$ (0.166 g, 485 *u*mol, 10.5 eq), and trimethoxybenzene (0.035 g, 21 *u*mol, 5 eq) stayed constant. The amounts of acetophenone varied as follows: 27 *u*L, 231 *u*mol, 5 eq; 40 *u*L, 346 *u*mol, 7.5 eq; 54 *u*L, 460 *u*mol, 10 eq; 81 *u*L, 693 *u*mol, 15 eq. Dry d^8-THF was then used to make the samples: 1.027 mL THF required for the 5 eq sample, 1.014 mL THF needed for the 7.5 eq sample, 1.0 mL THF for the 10 eq sample, 0.973 mL THF needed for the 15 eq sample. The respective THF solutions then had the appropriate amount of acetophenone added and the solution was sealed with parafilm, mixed thoroughly, and placed into an

icebath. After heating the NMR spectrometer probe to 50.1 °C, the sample was inserted, the temperature was allowed to equilibrate, and initial rates of $IPrCO_2$ loss were used to determine the reaction order of acetophenone. The following pseudo-first-order rate constants were obtained at different concentrations of acetophenone (-*k*, [$IPrCO_2$]), respectively: 7.8×10^{-3} $M{\cdot}s^{-1}$, 11.0×10^{-3} $M{\cdot}s^{-1}$, 14.7×10^{-3} $M{\cdot}s^{-1}$, 24.1×10^{-3} $M{\cdot}s^{-1}$.

Effect of CO_2 (g) on reaction. An NMR sample containing $IPrCO_2$ (0.020 g, 46 *u*mol, 1 equiv), $NaBPh_4$ (0.083 g, 243 *u*mol, 5.3 equiv), acetophenone (27 *u*L, 231 *u*mol, 5 equiv), and trimethoxybenzene (0.035 g, 21 *u*mol, 5 equiv) in 1 mL dry THF-d_8 (Total volume is 1.054 mL) was prepared analogously to the method described above. The solution was cooled and the N_2 atmosphere was removed and replaced with CO_2 three times. The sample was inserted into a pre-heated NMR spectrometer probe at 50.1 °C and the initial loss of $IPrCO_2$ was monitored to give the following pseudo-first-order rate constants were: 0.39×10^{-3} $M{\cdot}s^{-1}$ and 0.43×10^{-3} $M{\cdot}s^{-1}$.

Acetophenone and d^3-Acetophenone Deuterium and Proton exchange reactions catalyzed by IMe_{Me} carbene. To a 0.8 mL C_6D_6 solution containing acetophenone (0.042 mL, 3.62 mmol, 3 eq), d^3-acetophenone (0.042 mL, 3.62 mmol, 3 eq), and trimethoxybenzene (60 mg, 3.62 mmol, 3 eq) was added 0.2 mL of C_6D_6 containing dissolved IMe_{Me} carbene (15 mg, 1.21 mmol, 1 eq). A spectrum was taken immediately after mixing, which showed that complete scrambling of the deuterated and the nondeuterated acetophenone happened within minutes of the carbene being introduced. ^1H NMR of reaction mixture (C_6D_6, ppm) δ 7.75 (d, 4H J = 7.1); 7.16 (t, 2H, J = 7.3); 7.07 (t, 4H, J = 7.6); 6.19 (s, 3H); 3.36 (s, 9H); 3.14 (s, 1H); 2.14 (s, 0.7H); 2.12 (t(^2H), 1.0H, J = 2.2); 2.10 (quint, 0.3H, J = 2.2); 1.36 (s, 1H).

Acetophenone and d^3-Acetophenone Deuterium and Proton exchange reactions catalyzed by IPr carbene. To a 0.8 mL C_6D_6 solution containing acetophenone (0.042 mL, 3.62 mmol, 3 eq), d^3-acetophenone (0.042 mL, 3.62 mmol, 3 eq), and trimethoxybenzene (60 mg, 3.62 mmol, 3 eq) was added 0.2 mL of C_6D_6 containing dissolved IPr carbene (46 mg, 1.21 mmol, 1 eq). A spectrum was taken immediately after mixing and every hour until the integration of the original acetophenone peak was half of the starting point, which was 4 h. ^{1}H NMR of completely exchanged mixture (C_6D_6, ppm) δ 7.73 (d, 4H *J* = 7.1); 7.27 (t, 0.7H, *J* = 7.8); 7.15 (d, 1.3H, *J* = 7.6); 7.13 (t, 2H, *J* = 7.3); 7.05 (t, 4H, *J* = 7.6); 6.66 (s, 0.7H); 6.18 (s, 3H); 3.33 (s, 9H); 2.90 (sept, 1.3H, *J* = 7.0); 2.10 (s, 0.8H); 2.09 (t(CH_2D), 1.0H, *J* = 2.2); 2.07 (quint(CHD_2), 0.3H, *J* = 2.2); 1.22 (d, 12H, *J* = 6.8); 1.14 (d, 12H, *J* = 6.8).

Acetophenone and d^3-Acetophenone Deuterium and Proton exchange reactions catalyzed by IPrCO_2+$NaBPh_4$. A NMR tube was filled with 0.8 mL d^8-THF solution containing IPrCO_2 (40 mg, 102 *u*mol, 1 eq), $NaBPh_4$ (37 mg, 108 *u*mol, 1.05 eq), acetophenone (0.012 mL, 102 *u*mol, 1 eq), and d^3-acetophenone (0.012 mL, 102 *u*mol, 1 eq). A spectrum was taken immediately after mixing, which showed no scrambling of the deuterated and the nondeuterated acetophenone. Heating of the reaction mixture to 50.1 °C and monitoring the reaction showed a steady loss of IPrCO_2 and steady deuterium exchange.

Exchange prevention by CO_2 (g). A J. Young NMR tube was filled with 0.78 mL d^8-THF solution containing IPrCO_2 (40 mg, 102 *u*mol, 1 eq), and $NaBPh_4$ (37 mg, 108 *u*mol, 1.05 eq). The liquid containing portion of the NMR tube was immersed into liquid N_2 and the N_2-atmosphere of the tube was removed in vacuo and replaced with CO_2 and

the solution was reheated to room temperature; this freeze-pump-thaw cycle was done 3 times. The J. Young NMR tube cap was quickly removed and the acetophenone (0.012 mL, 102 *u*mol, 1 eq) and d^3-acetophenone (0.012 mL, 102 *u*mol, 1 eq) were added. Another freeze-pump-thaw cycle was performed and then the NMR tube was filled with ~5 atm of CO_2. A spectrum was taken immediately after the last CO_2 infusion, which showed no scrambling of the deuterated and the nondeuterated acetophenone. Heating of the reaction mixture to 50.1 °C and monitoring the reaction via ^{1}H NMR showed a steady loss of $IPrCO_2$, however, even at prolonged reaction times there was no deuterium scrambling observed.

References

(1) *Carbon Dioxide as Chemical Feedstock*; Aresta, M., Ed.; Wiley-VCH: Weinheim, Germany, 2010.

(2) Patil, Y. P.; Tambade, P. J.; Jagtap, S. R.; Bhanage, B. M. *Front. Chem. Eng. China* **2010**, *4*, 213.

(3) Miller, J. E.; Diver, R. B.; Siegel, N. P.; Coker, E. N.; Ambrosini, A.; Dedrick, D. E.; Allendorf, M. D.; McDaniel, A. H.; Kellogg, G. L.; Hogan, R. E.; Chen, K. S.; Stechel, E. B.; Minerals, Metals & Materials Society: 2010, p 27.

(4) Mikkelsen, M.; Jorgensen, M.; Krebs, F. C. *Energy Environ. Sci.* **2010**, *3*, 43.

(5) Sakakura, T.; Choi, J.-C.; Yasuda, H. *Chem. Rev.* **2007**, *107*, 2365.

(6) Darensbourg, D. J. *Chem. Rev.* **2007**, *107*, 2388.

(7) Coates, G. W.; Moore, D. R. *Angew. Chem., Int. Ed.* **2004**, *43*, 6618.

(8) Tans, P., NOAA/ESRL (www.esrl.noaa.gov/gmd/ccgg/trends)

(9) Darensbourg, D. J.; Holtcamp, M. W. *Macromolecules* **1995**, *28*, 7577.

(10) Darensbourg, D. J.; Moncada, A. I.; Choi, W.; Reibenspies, J. H. *J. Am. Chem. Soc.* **2008**, *130*, 6523.

(11) Wu, G.-P.; Wei, S.-H.; Lu, X.-B.; Ren, W.-M.; Darensbourg, D. J. *Macromolecules* **2010**, *43*, 9202.

(12) Cheng, M.; Lobkovsky, E. B.; Coates, G. W. *J. Am. Chem. Soc.* **1998**, *120*, 11018.

(13) Cohen, C. T.; Chu, T.; Coates, G. W. *J. Am. Chem. Soc.* **2005**, *127*, 10869.

(14) Kim, J. G.; Cowman, C. D.; LaPointe, A. M.; Wiesner, U.; Coates, G. W. *Macromolecules* **2011**, *44*, 1110.

(15) North, M.; Villuendas, P.; Young, C. *Chem.--Eur. J.* **2009**, *15*, 11454.

(16) Sit, W. N.; Ng, S. M.; Kwong, K. Y.; Lau, C. P. *J. Org. Chem.* **2005**, *70*, 8583.

(17) Xie, Y.; Ding, K.; Liu, Z.; Li, J.; An, G.; Tao, R.; Sun, Z.; Yang, Z. *Chemistry – A European Journal* **2010**, *16*, 6687.

(18) Huang, J.-W.; Shi, M. *J. Org. Chem.* **2003**, *68*, 6705.

(19) Lu, X.-B.; Liang, B.; Zhang, Y.-J.; Tian, Y.-Z.; Wang, Y.-M.; Bai, C.-X.; Wang, H.; Zhang, R. *J. Am. Chem. Soc.* **2004**, *126*, 3732.

(20) Lichtenwalter, M.; Cooper, J. F.; Jefferson Chemical Co., Inc. . 1956.

(21) Gilman, H.; Kirby, R. H. *Organic Syntheses* **1932**, *Collective Vol. I*, 353.

(22) Lindsey, A. S.; Jeskey, H. *Chem. Rev.* **1957**, *57*, 583.

(23) Snaddon, T. N.; Buchgraber, P.; Schulthoff, S.; Wirtz, C.; Mynott, R.; Fuerstner, A. *Chem.--Eur. J.* **2010**, *16*, 12133.

(24) Boogaerts, I. I. F.; Nolan, S. P. *J. Am. Chem. Soc.* **2010**, *132*, 8858.

(25) Dalton, D. M.; Rovis, T. *Nat. Chem.* **2010**, *2*, 710.

(26) Tsuda, T.; Sumiya, R.; Saegusa, T. *Synth. Commun.* **1987**, *17*, 147.

(27) Louie, J.; Gibby, J. E.; Farnworth, M. V.; Tekavec, T. N. *J. Am. Chem. Soc.* **2002**, *124*, 15188.

(28) Williams, C. M.; Johnson, J. B.; Rovis, T. *J. Am. Chem. Soc.* **2008**, *130*, 14936.

(29) Zhang, Y.; Riduan, S. N. *Angew. Chem. Int. Ed.* **2011**, *50*, 6210.

(30) Ohishi, T.; Zhang, L.; Nishiura, M.; Hou, Z. *Angew. Chem. Int. Ed.* **2011**, n/a.

(31) Huang, K.; Sun, C.-L.; Shi, Z.-J. *Chem. Soc. Rev.* **2011**, *40*, 2435.

(32) Fujihara, T.; Xu, T.; Semba, K.; Terao, J.; Tsuji, Y. *Angew. Chem. Int. Ed.* **2011**, *50*, 523.

(33) Ohmiya, H.; Tanabe, M.; Sawamura, M. *Org. Lett.* **2011**, *13*, 1086.

(34) Kayaki, Y.; Yamamoto, M.; Ikariya, T. *Angew. Chem. Int. Ed.* **2009**, *48*, 4194.

(35) Tommasi, I.; Sorrentino, F. *Tetrahedron Lett.* **2005**, *46*, 2141.

(36) Tommasi, I.; Sorrentino, F. *Tetrahedron Lett.* **2006**, *47*, 6453.

(37) Tommasi, I.; Sorrentino, F. *Tetrahedron Lett.* **2009**, *50*, 104.

(38) Paddock, R. L.; Nguyen, S. T. *J. Am. Chem. Soc.* **2001**, *123*, 11498.

(39) Haruki, E.; Arakawa, M.; Matsumura, N.; Otsuji, Y.; Imoto, E. *Chem. Lett.* **1974**, 427.

(40) Mizuno, T.; Ishino, Y. *Tetrahedron* **2002**, *58*, 3155.

(41) Zhou, H.; Zhang, W.-Z.; Liu, C.-H.; Qu, J.-P.; Lu, X.-B. *J. Org. Chem.* **2008**, *73*, 8039.

(42) Heldebrant, D. J.; Jessop, P. G.; Thomas, C. A.; Eckert, C. A.; Liotta, C. L. *J. Org. Chem.* **2005**, *70*, 5335.

(43) Villiers, C.; Dognon, J.-P.; Pollet, R.; Thuery, P.; Ephritikhine, M. *Angew. Chem., Int. Ed.* **2010**, *49*, 3465.

(44) Benhamou, L.; Chardon, E.; Lavigne, G.; Bellemin-Laponnaz, S. p.; César, V. *Chem. Rev.* **2011**, *111*, 2705.

(45) THF can be used in lieu of MeCN.

(46) Van, D. R.; Ramaekers, J.; Nockemann, P.; Van, H. K.; Van, M. L.; Binnemans, K. *Eur. J. Inorg. Chem.* **2005**, 563.

(47) Kansikas, J.; Hermansson, K. *Acta Crystallogr., Sect. C: Cryst. Struct. Commun.* **1989**, *C45*, 187.

(48) Markila, P. L.; Rettig, S. J.; Trotter, J. *Acta Crystallogr., Sect. B* **1975**, *B31*, 2927.

(49) Van Ausdall, B. R.; Glass, J. L.; Wiggins, K. M.; Aarif, A. M.; Louie, J. *J. Org. Chem.* **2009**, *74*, 7935.

(50) Duong, H. A.; Tekavec, T. N.; Arif, A. M.; Louie, J. *Chem. Commun.* **2004**, 112.

(51) Jeong, W.; Hedrick, J. L.; Waymouth, R. M. *J. Am. Chem. Soc.* **2007**, *129*, 8414.

(52) Amyes, T. L.; Diver, S. T.; Richard, J. P.; Rivas, F. M.; Toth, K. *J. Am. Chem. Soc.* **2004**, *126*, 4366.

(53) Kim, Y.-J.; Streitwieser, A. *J. Am. Chem. Soc.* **2002**, *124*, 5757.

(54) Chu, Y.; Deng, H.; Cheng, J.-P. *J. Org. Chem.* **2007**, *72*, 7790.

(55) Magill, A. M.; Cavell, K. J.; Yates, B. F. *J. Am. Chem. Soc.* **2004**, *126*, 8717.

(56) Crist, D. R.; Hsieh, Z. H.; Quicksall, C. O.; Sun, M. K. *J. Org. Chem.* **1984**, *49*, 2478.

(57) House, H. O.; Chu, C.-Y. *J. Org. Chem.* **1976**, *41*, 3083.

(58) Flowers, B. J.; Gautreau-Service, R.; Jessop, P. G. In *Adv. Synth. Catal.*; Wiley-VCH Verlag GmbH & Co. KGaA: 2008; Vol. 350, p 2947.

CHAPTER 3

ADVENTURES IN CARBENE DESIGN: SYNTHESIS OF CHIRAL HYDROGEN BONDING BENZYLIMIDAZOLIUM SALTS, *N*-HETEROCYLCIC CARBENES, AND *N*HC·CARBOXYLATES

Introduction

The common synthetic approach in designing chiral *N*-heterocylcic carbenes (*N*HC's) is to fuse the chirality of the system into place using rings off one of the nitrogen and the backbone (Figure 3.1).[1-6] Effective induction of chirality into reactions catalyzed by chiral, non-ring-fused carbenes has been found to exhibit lower enantiomeric excesses (*ee*'s) than ring-fused counterparts, presumably due to rotation of the chiral arm of the system away from the reaction site in non-fused systems (Figure 3.2).[7,8] The use of sterics as one of the only factors with which to transfer chirality into products has been widespread. The steric bulk used in the vast majority of these carbene systems is passive in nature and works by protecting the addition of a reagent into a substrate from one face or another. In light of this, finding means to actively direct reagents to substrate via attractive forces may be of use in systems where carbenes with only chiral steric parameters fail to procure *ee*'s.[9] Thus, the impetus to introduce one of nature's most ubiquitous attractive forces, hydrogen bonding, into carbenes and carbene adducts is appropriate.

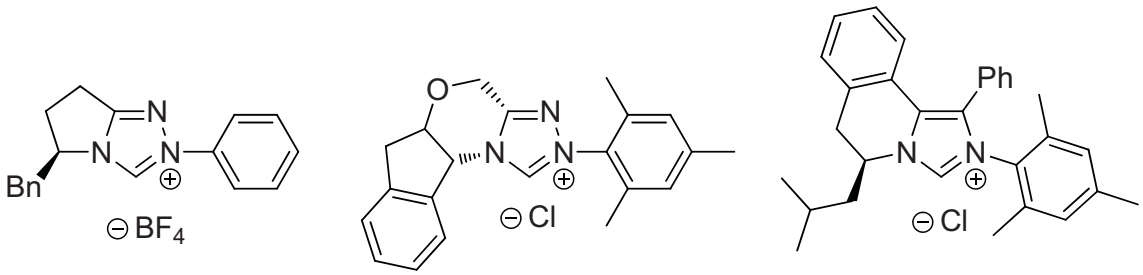

Rovis, 2005 Bode, 2009 Hong, 2010

Figure 3.1. Recent effective triazolium (Miller and Bode) and imidazolium (Hong) based chiral carbene precursors used in organocatalysis where fused rings are used to lock chirality.

Introducing hydrogen bonding into reactions catalyzed by carbenes may do more than just direct reagents to substrates, it may also stabilize reaction intermediates or transition states. Analysis of highly selective and efficient enzymatic systems has shown that hydrogen-bonding is critical in enzyme active sites, where the H-bonding is often stabilizing an intermediate or a proposed transient species in enzyme catalyzed reactions.[10-14] This concept has been used in organocatalytic chemistry and a plethora of reactions catalyzed or assisted by organic molecules which have the capacity to accept or

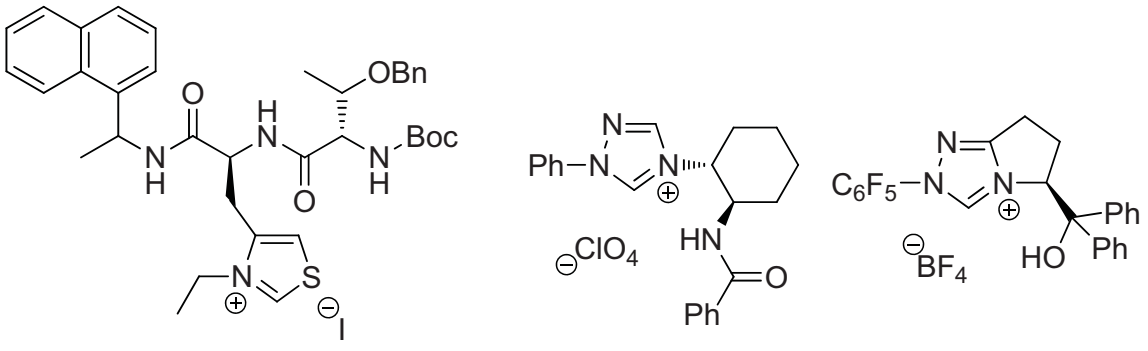

1 **2** **3**

Miller, 2005 Connon, 2009

Figure 3.2. Thiazolium (**1**) and triazolium (**2** and **3**) carbene precursors utilizing H-bonding for chirality induction in organocatalysis.

donate hydrogen bonds have been discovered.[15] The first citings to report hydrogen-bond assisted carbene catalysis was with thiazolium salts containing a peptide backbone (**1**, Figure 3.2) in an intermolecular Stetter reaction and an imino-aldehyde coupling reported by Miller et al in 2005.[16,17] However, no evidence for any hydrogen-bonding was given. Triazolium salts with hydrogen-bonding capacity (**2** and **3,** Figure 3.2) have been used in recent years to catalyze benzoin condensations with high *ee*'s.[7,18-21] Connon's seminal work with these reactions found **2** to provide reasonable yields of the benzoin condensation product, but poor *ee*'s; this is presumably attributed to the free rotation of the chiral arm away from the reactants. If the free alcohol in ring-fused imidazolium salt **3** is replaced with a silyl protecting group, both the yield and *ee*'s observed were halved, demonstrating the effect hydrogen bonding can have in these reaction system.

Triazolium based carbenes have been demonstrated to be effective in organocatalysis, but forming a complex with carbon dioxide has yet to be reported. In preleminary studies in our lab where a triazolium salt was deprotonated to the carbene and introduced to carbon dioxide did not form a carboxylated product. Previous work has demonstrated that imidazolium based carbenes react readily with carbon dioxide to form a stable carboxylate.[22-24] With a bound anionic species present in the form of the imidazolium carboxylate, such a system may present an opportunity to actively study and assess hydrogen bonding (Figure 3.3).

The purpose of this study is to synthesize chiral imidazolium salts that incorporate hydrogen bonding groups, preferably in a fashion that deviates from existing fused *N*HC architectures. H-bonding complexes derived thereafter, *N*HC's and *N*HC·CO_2's, may

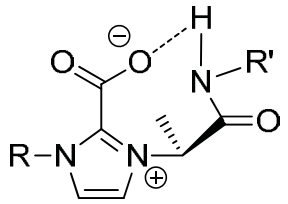

Figure 3.3. A potential intramolecular interaction *N*HC·CO_2 and a hydrogen bond donor.

provide a means with which to study hydrogen bonding in these systems. However, in order to effectively design such a system, a number of factors must be considered.

Carbene Design Rationale

Having a carbene and hydrogen bond donor exist in the same system without full deprotonation of the donors to an inactive imidazolium salt is critical. Evidence has shown that carbenes have the capacity to hydrogen bond with hydrogen bond donors and exists in several crystal structures: 1,3-bis-(2,4,6-trimethylphenyl)-imidazol-2-ylidene (IMes) with diphenylamine (**4**, Figure 3.4),[25] IMes carbene with methanol (**5,** Figure 3.4),[26] and IMes carbene with anhydrous TEMPO-H (**6,** Figure 3.4).[27] However, a crystal structure of IMes carbene having reacted with 2,6-di-*tert*-butyl-4-methylphenol shows a completely deprotonated alcohol group (**7**, Figure 3.5) has also been reported. A similar *N*HC, 1,3-bis(2,6-diisopropylphenyl)-imidazolin-2-ylidene (SIPr), was discovered not to H-bond with the alcohol group of TEMPO-H, but deprotonates it completely (**8**, Figure 3.5). The different complexes of TEMPO-H with similar carbenes IMes (**5**) and SIPr (**8**) indicate that appropriate design of any hydrogen-bond capable carbene system is requisite.

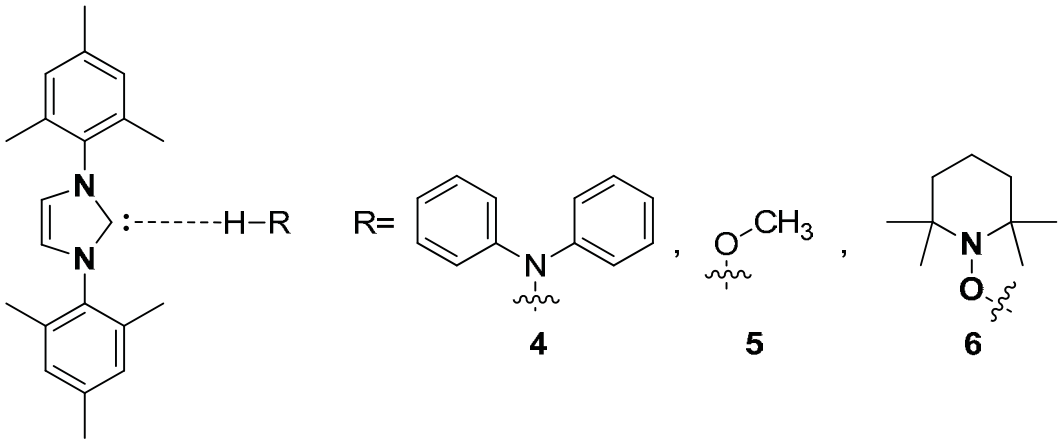

Figure 3.4. Isolated complexes of IMes with hydrogen bond donors.

Due to the sensitivity of carbenes to hydrogen bond donors, the choice of the hydrogen bonding donor/acceptor built into the carbene is critical. Species that can provide or accept hydrogen bonding, but will do little else to interfere with known carbene catalyzed reactions, are ideal. Alcohols, carboxylic acids, and thiols generally exhibit pK_a's that are well below that of diamino *N*-heterocyclic carbenes.[28-30] Hence, deprotonation of the hydrogen donor to anion and formation of the inactive imidazolium would occur as demonstrated with complexes **7** and **8**. Amines, with reasonably high pK_a's could play a role in such ligand design, however, the basicity and nucleophilicity of amines is too high with most compounds of interest (e.g., addition to halides, deprotonation at the alpha position of ketones or aldehydes, imine formation with ketones or aldehydes). The amide modality, however, appears to provide the means with which to start such a study due to the pK_a range amides exhibit[31] and the generally low nucleophilicity of amides. The amide group for implementation into a carbene with expectations of hydrogen bonding is apropos.

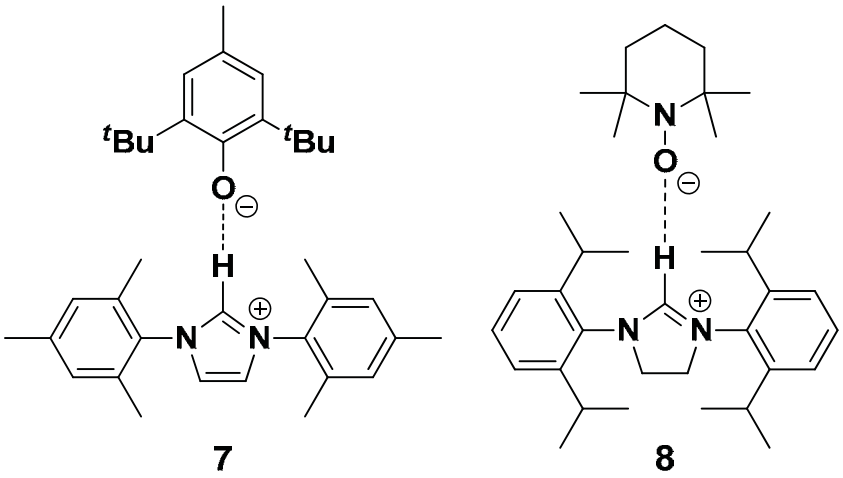

Figure 3.5. Isolated hydrogen bonding complexes of imidazol(in)ium cations with corresponding proton donor oxides.

Though carbenes have found use as organocatalysts and ligands as noted above, carbenes were discovered to activate carbon dioxide and has been the focus of a portion of our group's research portfolio. These *N*-heterocyclic carboxylates have been used to carboxylate a number of organic molecules with acidic C-H bonds; however, the reactions are slow and none have been discovered to facilitate the reaction enantioselectively. Choosing a chiral carboxylate that performs the reaction both at an appreciable speed and a high enantioselective excess would be the goal of any study in this realm.

In order to affect decarboxylation, and therefore reaction rate of a trans-carboxylation reaction, of asymmetric, carbene carboxylates without sacrificing enantioselectivity, careful selection of steric and chiral factors of the organocatalyst is required. A previous structural study elucidated factors that were intrinsic to facile decarboxylations,[32] most important being that the larger the *ortho*-substituent on a phenyl ring, the lower the decarboxylation temperature. This was true even in systems that were

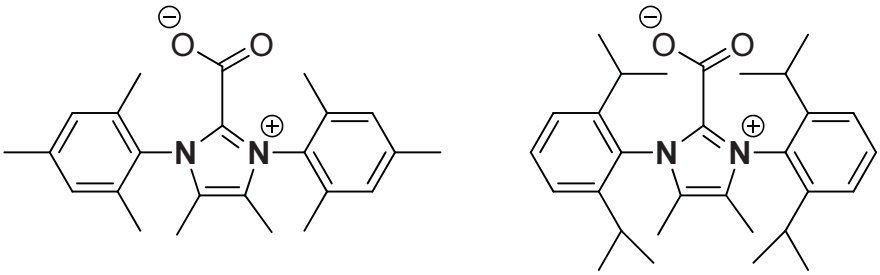

9
-CO_2 temp= 193 °C
monophasic decarboxylation

10
-CO_2 temp= 136 °C
biphasic decarboxylation

Figure 3.6. The known decarboxylation temperatures and decomposition patterns for carboxylates **9** and **10**.

rotationally confined, such as with **9** ($IMes_{Me}CO_2$, Figure 3.6) and **10** ($IPr_{Me}CO_2$, Figure 3.6), where 60 °C separates the two zwitterions decomposition temperatures. Henceforth, installation of a large *ortho*-substituted phenyl group in an asymmetric *N*HC-CO_2 was deemed essential. This is even more prudent when asymmetric carboxylate **11** (IPr^tBuCO_2, Figure 3.7), which contains two large but different *N*-substituents, has a decarboxylation/decomposition pattern and temperature that resembles the bis-2,6-diisopropylphenyl **12** ($IPrCO_2$, Figure 3.7) molecule more closely, not the di-^{t}Bu **13** (I^tBuCO_2, Figure 3.7), which suggests that the di-*ortho*-substituted substituent of **11** is controlling the decarboxylation.

Functional groups that are ideal for the success of this study have been drawn in benzimidazolium salt **14** (Figure 3.8): an *ortho*-^{t}Bu phenyl group that is likely to provide a low temperature decarboxylation of an *N*HC-CO_2; an amide group that should provide a molecule that will exhibit hydrogen bonding; and a methyl on the benzene backbone that should prevent rotation of the chiral arm and allow for induction of the chirality into

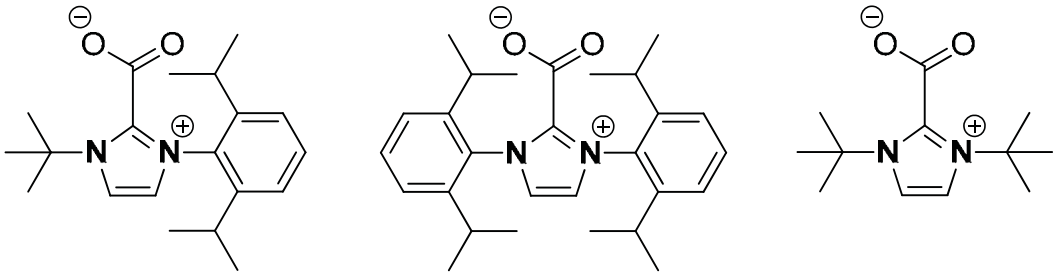

Figure 3.7. The structures and decarboxylation temperatures for carboxylates **11, 12**, and **13**.

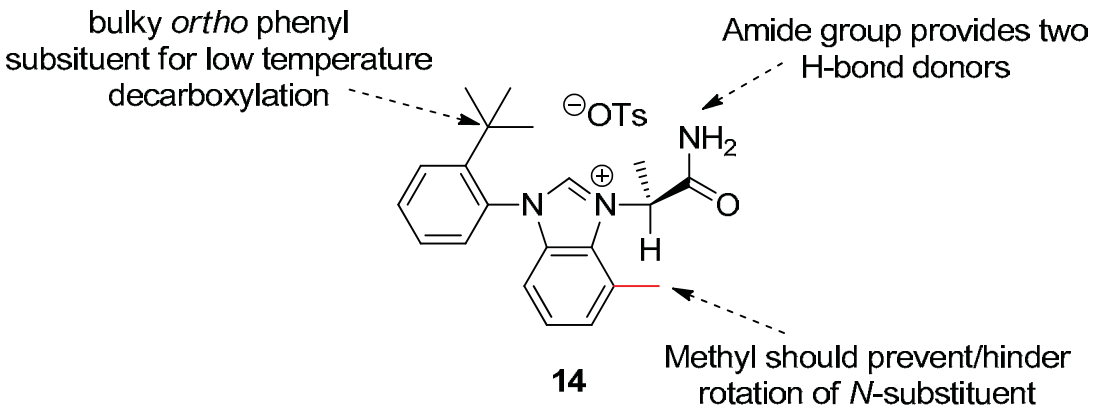

Figure 3.8. Highlighted design aspects of benzimidazolium salt **14**.

organocatalytic reactions. Benzimidazolium salt **14** can be synthesized via S_N2 addition of benzylimidazole **15** to lactamide-OTs **16** (Figure 3.9). The addition should be such that the hydrogen of the lactamide, the smallest component of the chiral center, should be rotated towards the methyl on the benzimidazole backbone to minimize steric interactions between the two reagents. The ^{t}Bu group of the *N*-aryl moiety will presumably be trans to the methyl group (i.e. the opposite face of the imidazolium ring).[33,34]

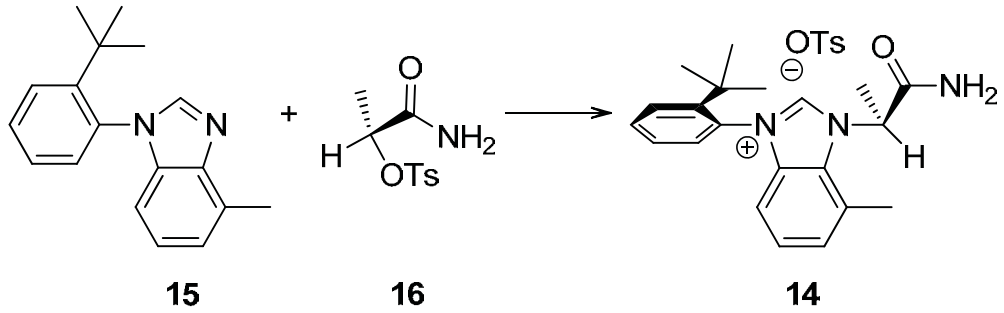

Figure 3.9. Addition of benzimidazole (**15**) to (*R*)-lactamide-OTs (**16**) and illustration of the locked conformation of chiral imidazolium salt **14** due to the benzyl methyl.

Results and Discussion

In order to determine if hydrogen bonding is indeed present in these species, a large amount of a benzimidazolium salt would be required to grow crystals of the starting salt, form and study the carbene, form and study the carbene carboxylate, and attempt to determine the efficacy of the carbene in various organocatalytic reactions. The precursor to salt **14**, *ortho*-^{t}Bu-phenyl formamidine **17**, was difficult to purify via column chromatography and the yield was 8% (Equation 3.1)..[35] The column purification for mesityl formamidine **18** was far more efficient and provided a higher yield of a benzimidazole precursor (35%) (Equation 3.1). The initial objective was to see if hydrogen bonding would occur at all, but due to the low yields of the **14** benzimidazole precursor, salt **14** would be synthesized only if hydrogen bonding was observed in other higher yielding species.

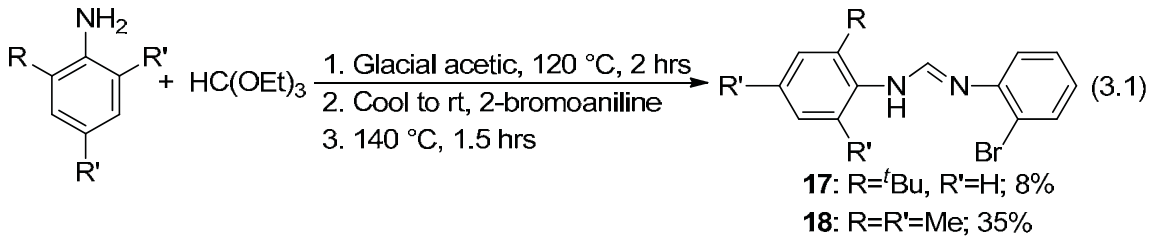

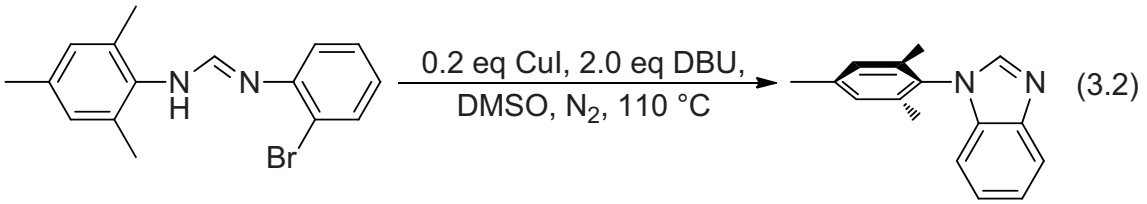

(3.2)

90%
19

Mesityl benzimidazole **19** was synthesized in 90% yield (32% overall yield) after ring closure via copper coupling (Equation 3.2).[35] The synthesis of the lactamide-OTs was performed using a tosylation protocol (Equation 3.3) of lactamide to afford tosylate **20** in 60% yield after two recrystallizations from CH_2Cl_2 and ether.[36] Combination of **19** and **20** in 1:1 MeCN/toluene solution at reflux for 24 hours (Equation 3.4) yielded a clear solution. Removal of most of the MeCN and introduction of ether provided a colorless precipitate. Filtration and washing of the precipitate with ether yielded salt **21** in 63% yield.

The ^{1}H NMR analysis of benzimidazolium salt **21** indicated a significant change in one of the amide protons that resulted in a large downfield shift from lactamide-OTs **20**. The amide protons in **20** were located at 6.33 and 5.89 ppm; the chemical shift of the amide protons in **21** were at 9.26 and 5.53 ppm. Similar large downfield shifts of alcohol protons were observed in the study of carbenes hydrogen bonding with the alcohol functionality.[26]

A crystal of sufficient quality for single crystal x-ray analysis was grown by dissolving solid **21** in MeCN and slowly diffusing ether into the MeCN solution. Single crystal x-ray analysis of **21** (Figure 3.10) showed that there was a network of intermolecular hydrogen bonding (Figure 3.11). Two hydrogen bonds were present with

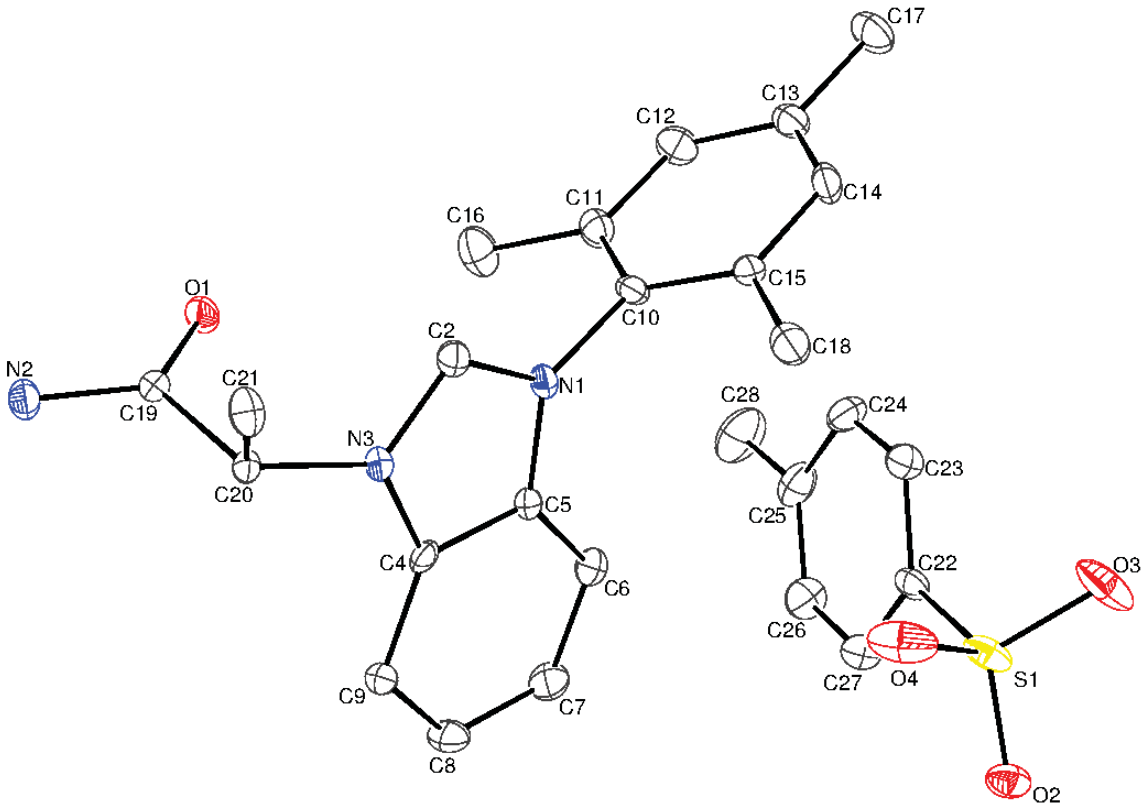

Figure 3.10. The x-ray crystal structure of **21**.

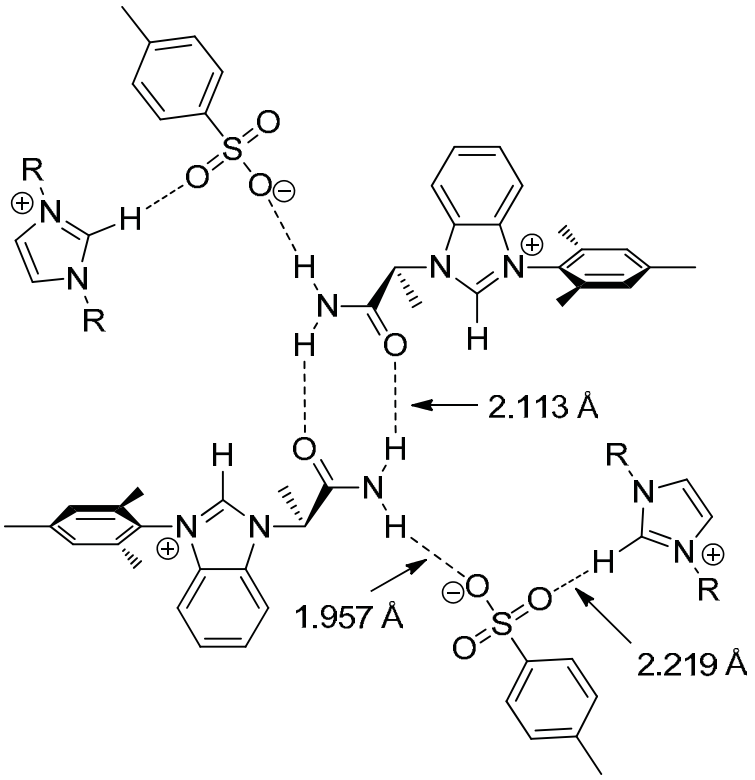

Figure 3.11. The hydrogen bonding network observed and the H-bond distances in the solved crystal structure for salt **21**.

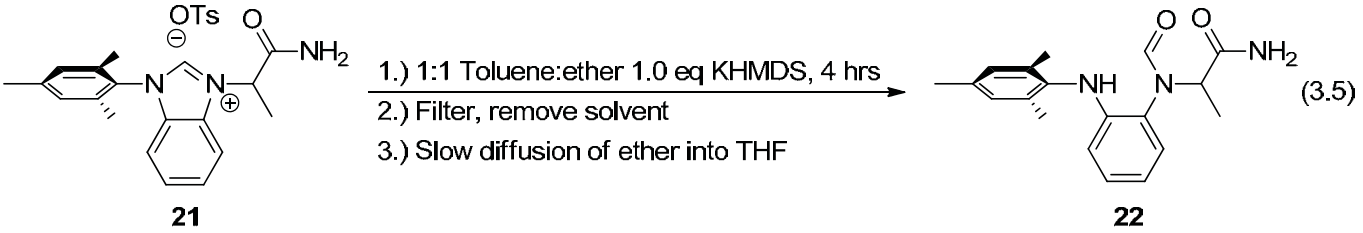

21 **22** (3.5)

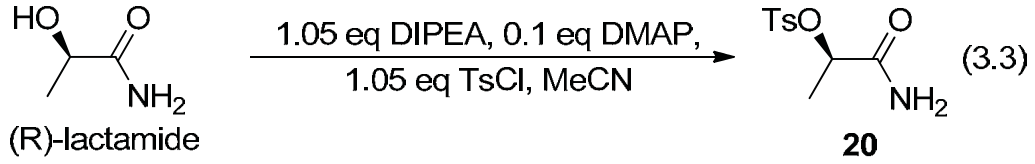

the amide protons: an intermolecular hydrogen bond with the amide oxygen of one **21** cation and amide proton of another **21** cation at 2.113 Å and an intermolecular hydrogen bond of the remaining amide proton to an oxygen of the tosylate anion at 1.957 Å. Another observed hydrogen bond measuring at 2.219 Å between the tosylate oxygen and the carbenic C_2 hydrogen (Figure 3.11). This hydrogen bonding was likely responsible for the observed shift in the ^{1}H NMR spectrum.

Deprotonation of the imidazolium salt was performed using KHMDS in a 1:1 toluene:ether solution (Equation 3.5). Filtration of the reaction solution through Celite after 4 hours of stirring yielded a clear solution. After removal of the solvent, this solution was used to grow crystals of the carbene. Upon crystal formation, a portion of the crystals were used for ^{1}H and ^{13}C NMR analysis. The crystals were of sufficient quality for solving structure **22** via single crystal x-ray analysis, and a structure was determined (Figure 3.12).

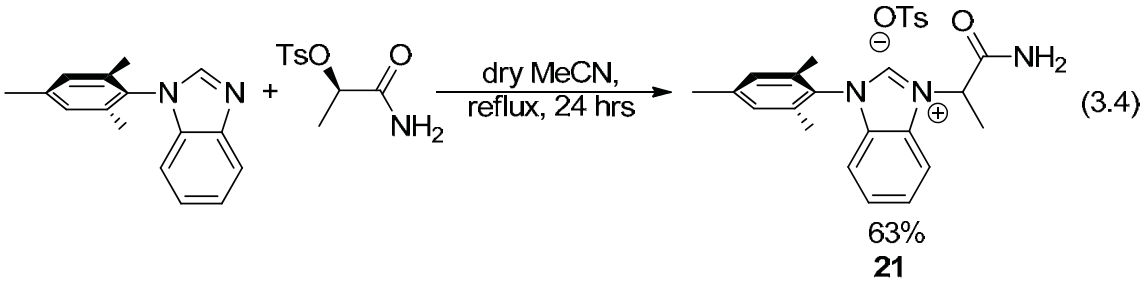

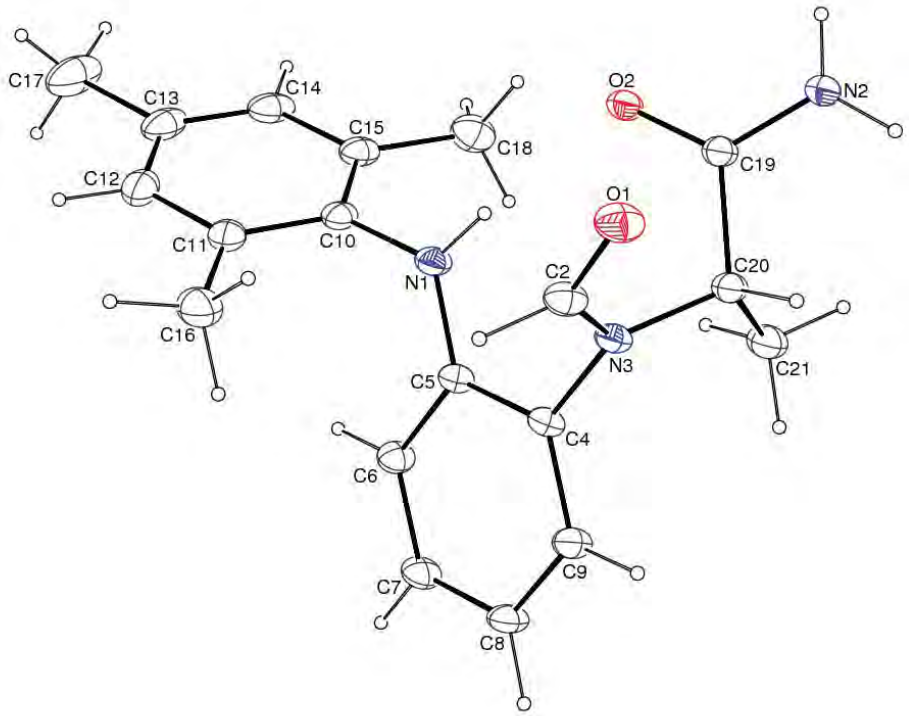

Figure 3.12. The x-ray crystal structure of **22**.

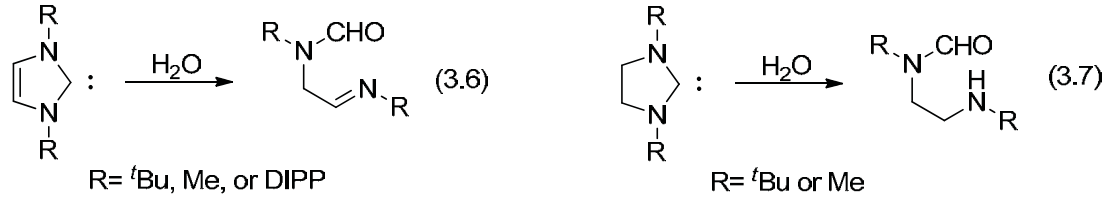

It is readily apparent that **22** is not the carbene that was sought upon deprotonation of **21**. It is likely that product **22** arises upon reaction with water. A potential mechanism is provided in Scheme 3.1. A similar carbene decomposition product was reported in previous studies by Nyulászi[37] et al and Polyakova et al.[38] Two earlier studies by Denk[39] and Amyes[40] with deuterium oxide in excess did not report the formation of hydrolysis or oxidation products. The Nyulászi study indicates that small amounts of water, with respect to that of the bulk organic solvent, allow for the formation

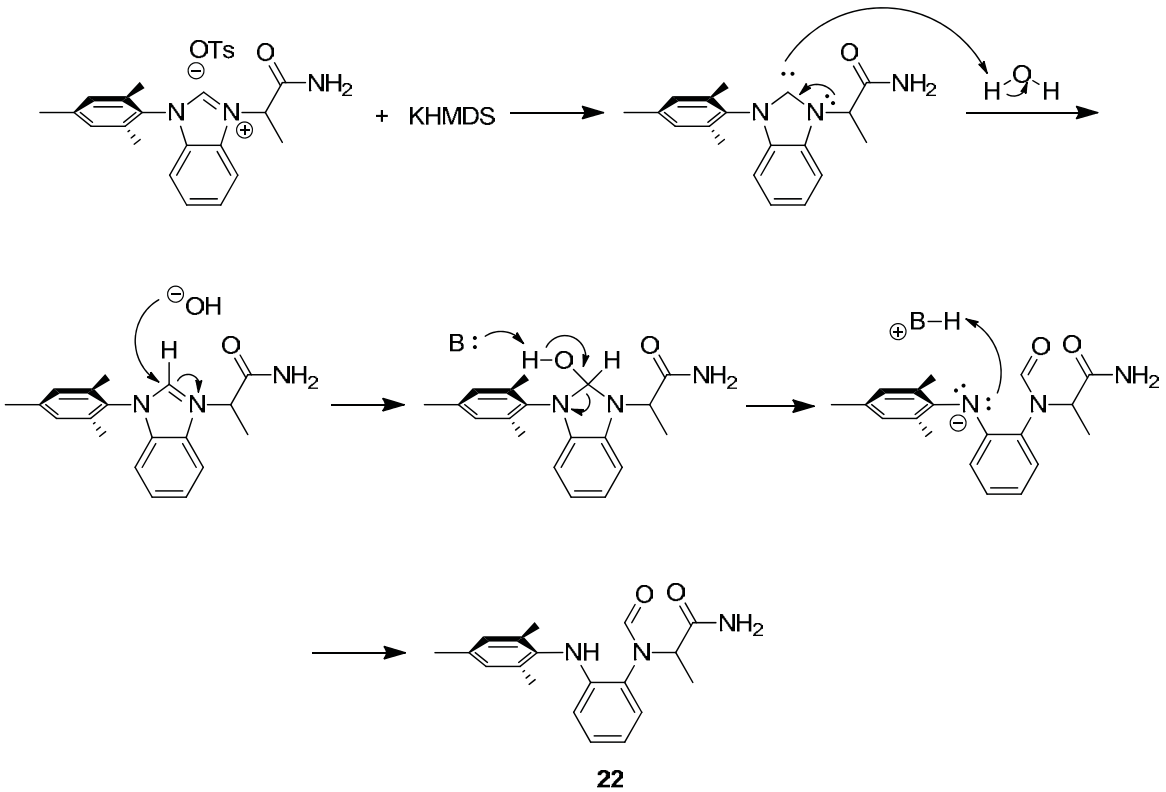

Scheme 3.1. Proposed mechanism of the formation of **22** from **21**.

of the formyl products (Equations 3.6 and 3.7). Nyulászi also reports that this reaction is more pronounced in THF. Amyes and Denk both conducted their studies in D_2O and reported no formation of the amide decomposition product. Extrapolating Nyulászi results into this work, it would suggest that the organic solvents in the glove box that were used have enough water to react the carbenes completely into the formamide product.

Interestingly, selective formation of the alkyl nitrogen formamide was observed; the diaryl nitrogen, by crystal structure analysis, was only protonated. This would suggest that the electron density of the alkylated nitrogen plays a role in the selective formation of this product. The hydrogen bonding amide group may also play a role in the selective formation of the formamide on the alkylated nitrogen. It is also possible that the hydrogen bonding the amide group provides may facilitate this sort of decomposition of carbenes in the presence of water. Nyulászi et al reports from their computational study that the insertion of the carbene into an O-H bond of water is more favorable when multiple water molecules are around due to hydrogen bonding stabilizing the corresponding hydroxide molecule formed. Due to the proximity of the amide hydrogens to the carbene, these may play a role in stabilizing a hydroxide formed after carbene insertion into an OH bond of the H_2O molecule.

Prior to the isolation of the formamide crystal and structure solving, an attempt at intercepting the carbene via reaction with CO_2 was attempted. The salt was deprotonated and after filtration, the reaction apparatus' N_2 atmosphere was removed and replaced with CO_2. No precipitate formed, though the solution turned yellow (Equation 3.8). After removal of the solvent, the yellow solid was taken up into d^8-THF and analyzed. ^1H

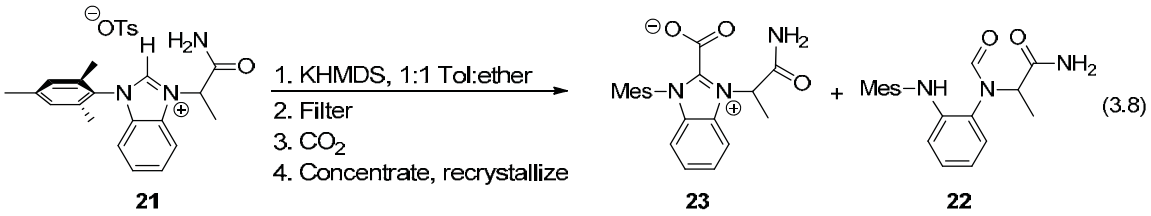

21 23 22

NMR analysis indicated that there was no benzimidazolium tosylate starting material left. There were, however, two sets of peaks present. One set corresponded to the ring opened product, and the second set with the larger integration value presumably corresponds to the carboxylate (**23**). The ratio of these peaks was approximately 3:1.

This data is intriguing for a number of reasons, the first being the likely instability of the carboxylate when intramolecular hydrogen-bonding is present. The introduction of CO_2 to the carbene was fast enough that carbene reaction with CO_2 should have taken place prior to any reaction with water. If so, all previous carboxylates formed in this lab have been largely stable when placed in THF with water.[32] The solvents for recrystallization in that study were handled and prepared in the same manner as this study; therefore, decomposition of the carboxylate to happen with a hydrogen-bonding carbene/carboxylate suggests an activation of the system versus that of the non-hydrogen bonding carboxylate. Reaction of these molecules in a dry system with acetophenone and $NaBPh_4$ may provide accelerated rates over nonhydrogen bonding systems. Further studies on this subject matter will require a thoroughly dry system.

Future Work

The amount and types of hydrogen bonding observed in **21** is a good indicator that hydrogen bonding in the carbene and the carboxylate compounds will be present. The amide protons interact with both a ketone lone-pair of electrons and a lone pair from an oxyanion; the carbene lone pair is a stronger electron donor than the amide ketone one pair and the carboxylate is an anion, like the tosylate in **21**. It is with this reasoning that hydrogen bonding motifs in **22** and **23** (Figure 3.13) are expected to be isolated after deprotonation to carbene (**22**) and formation of the carboxylate (**23**) after introducing the carbene to CO_2.

Benzimidazolium salts that contain electron donating and electron withdrawing groups on the amide will also be synthesized (**21** and **24-28**) to determine if the acidity of the amide hydrogen will play a role in the efficacy of the molecule to hydrogen bond (Figures 3.14 and 3.15). Previous studies in hydrogen bonding organocatalysis demonstrated that hydrogen acidity plays a distinct role in catalyst efficacy.[41] Removal of one amide proton will also test two things: the impact of having two hydrogen bonds available for catalysis and what happens to decarboxylation or reaction yields when steric bulk is placed on the amide group.

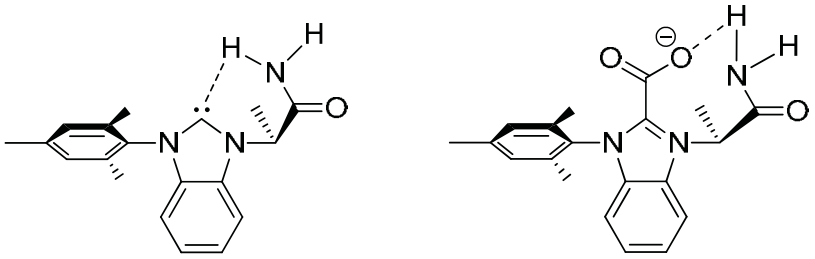

22 **23**

Figure 3.13. Proposed forms of H-bonding in the carbene (**22**) and carboxylate (**23**) analogues of benzimidazolium salt **21**.

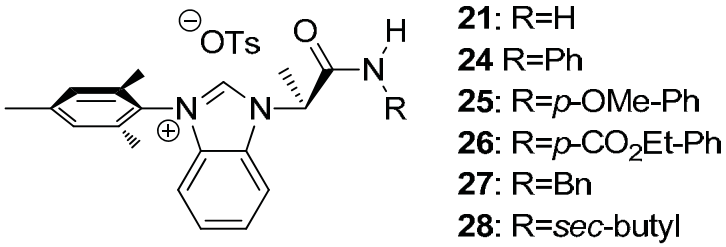

Figure 3.14. The series of salts to determine if amide proton acidity will affect the hydrogen bonding capacity of the molecule.

The substituted amides **41-43** can be synthesized directly from lactamide (Eq 3.9 and Eq 3.10). Buchwald established procedures for the substitution of amides by coupling amides with aryl halides catalyzed by copper and 1,2-diamine ligands that would allow for access of compounds **44-45** (Equation 3.9).[42] Synthesis of the alkyl substituted amides can be performed using *N*,*N*-dimethylformamide dimethyl acetal in transamidation chemistry developed by Myers et al. (Equation 3.10).[43] Tosylation of the substituted amides and formation of benzimidazolium salts will be performed as described above.

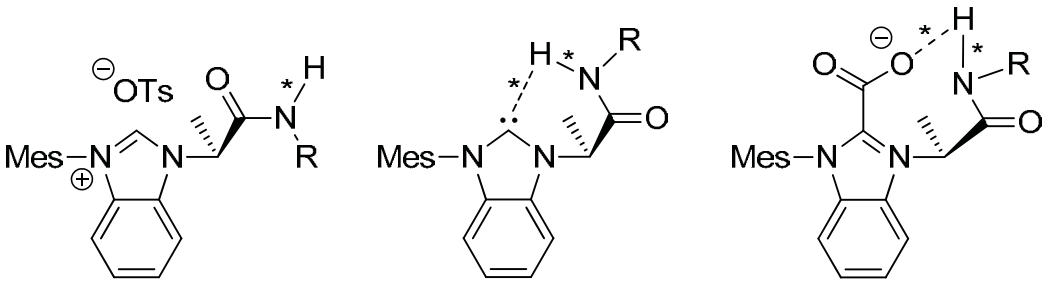

21, 24-28 **29**, **31-35** **30, 36-40**

Figure 3.15. The series of salts, carbenes, and carboxylates to determine if amide substitution and proton acidity will affect the hydrogen bonding and the indicated (*) bond lengths.

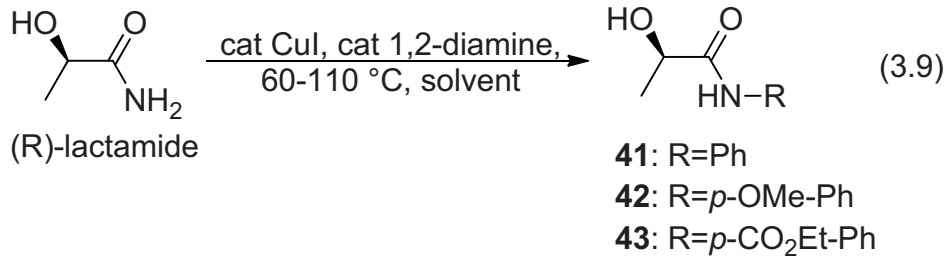

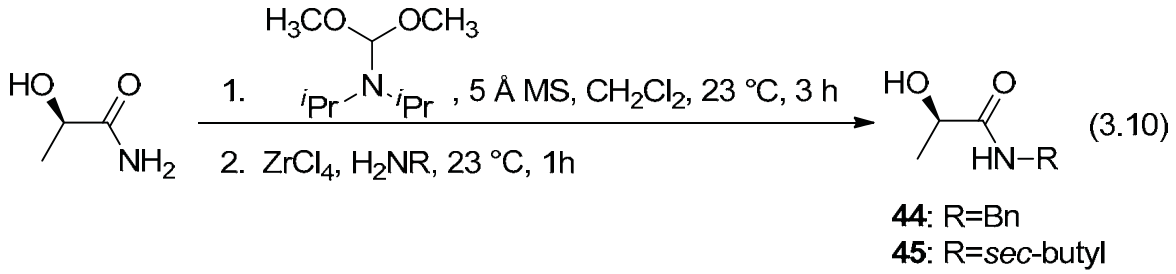

A series of benzylimidazoles and imidazoles will be synthesized and reacted with lactamide-OTs to determine further which factors are needed to prevent rotation of the *N*-substituents (Figure 3.16). Benzimidazolium **14**, with a large *ortho* group, will provide a means to see if the rotation is locked into position; benzimidazolium **46** will determine if the methyl group is needed to lock the molecule into place; benzimidazolium **47** may provide the insight into the importance of the tert-butyl moiety with respect to reaction yields, %*ee* in organocatalytic reactions, and decarboxylation temperatures of carboxylates; and imidazolium **48** should allow for proper contrast of the benzyl moiety on the rotational parameters, but may also provide insight into any electronic effects the benzene ring exhibits on carboxylate stability.

Synthesis of the **47** precursor *ortho*-methylphenylimidazole will be performed utilizing the route used by Glorius et al [44,45] and reacted with tosylate **20** to yield **47**. The imidazole precursor to imidazolium salt **48** will be synthesized using a modification of a literature procedure (Scheme 3.2) to yield *ortho*-^{t}Bu-phenyl imidazole **15**.[46] The imidazole will then be reacted with tosylate **20** to provide imidazolium salt **48**.

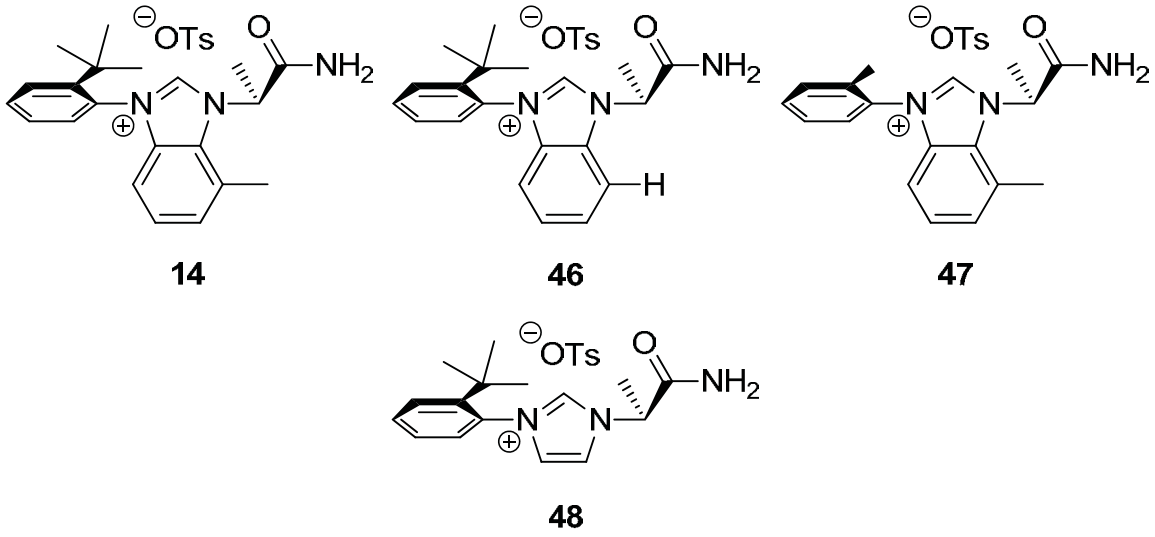

14 **46** **47**

48

Figure 3.16. The series of imidazolium salts to determine the role of steric bulk in the carbenes and the electronic impact of the benzene backbone.

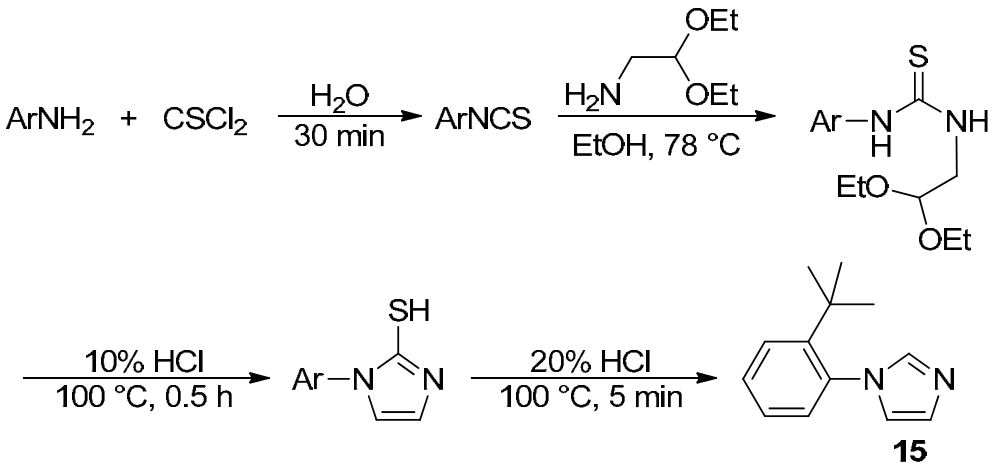

15

Scheme 3.2. Synthesis of the imidazolium salt **19** precursor imidazole.

All structures will be deprotonated with KHMDS in toluene or ether to form the carbene. Crystal growth of the carbene will be performed to try and obtain a crystal that will be worthy of single crystal x-ray analysis. Conversion of the carbenes to their carboxylates will be performed by exposing the carbenes to an atmosphere of CO_2 gas. Slow introduction of CO_2 may lead to crystal growth so that single crystal x-ray analysis can be performed.

Application of Hydrogen Bonding Carbenes

Reactions have been identified where chiral, hydrogen bonding carbenes should be able procure enantio-pure products.[9,47,48] One reaction of interest, discovered by Phillips et al. (Equation 3.11 and Equation 3.12 in Figure 3.17) is the IMes catalyzed conjugate addition of alcohols into enones to yield ether **49** and an intramolecular variant that yielded furan **50**.[9] Phillips et al. were able to demonstrate a slight enantio-enrichment with catalyst from salt **50**, but not with catalyst from salt **49**. The carbenes used by Phillips et al. are sufficient catalysts with regards to reaction yield, though improvement of the *ee*'s is desirable.

The proposed mechanism by which this reaction is thought to proceed through is shown in Scheme 3.3. The reasoning for which Phillips observed poor enantioselectivity with nonhydrogen bonding carbenes is that the addition of the alcohol into either face of the alkene is facile since chirality is exhibited in only one portion of the molecule (Figure 3.18). The sterics of the chiral portion of the catalyst push the reagents away and do not attract the reagents to the chirality as a hydrogen bonding catalyst would be able to do.

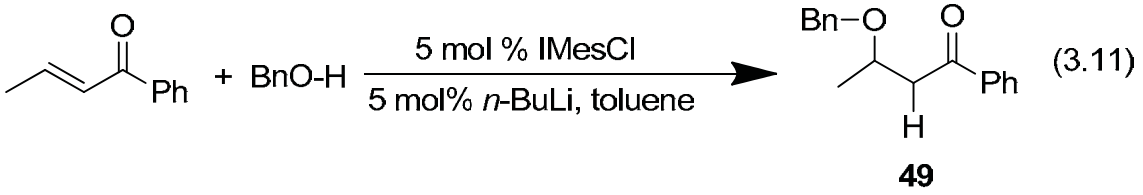

(3.11)

49

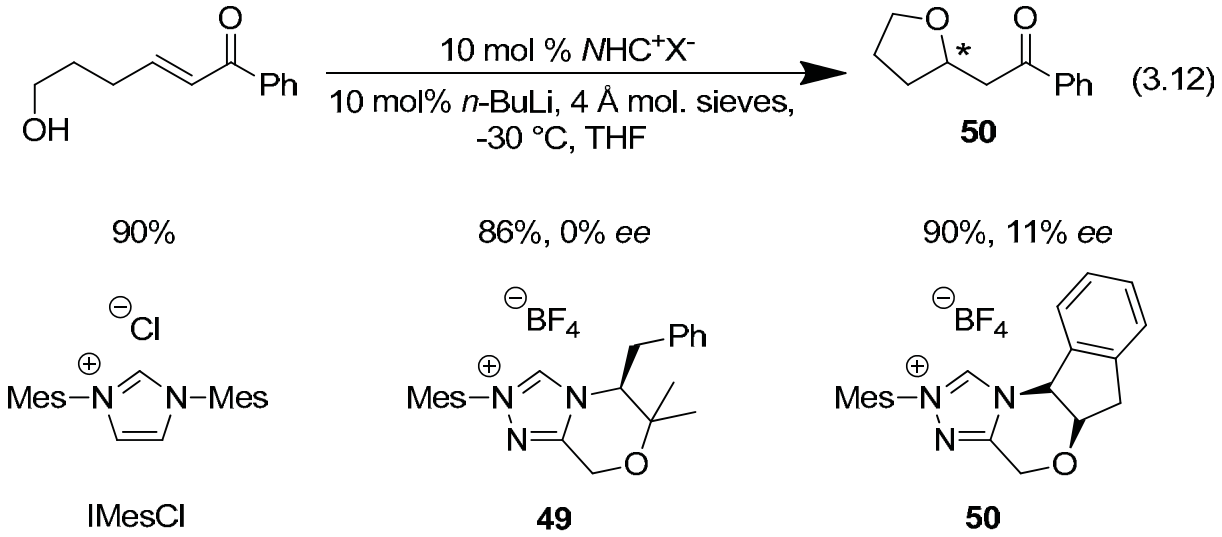

Figure 3.17. Carbenes catalyzed formation of tetrahydrofurans via intramolecular conjugate addition of alcohols to enones

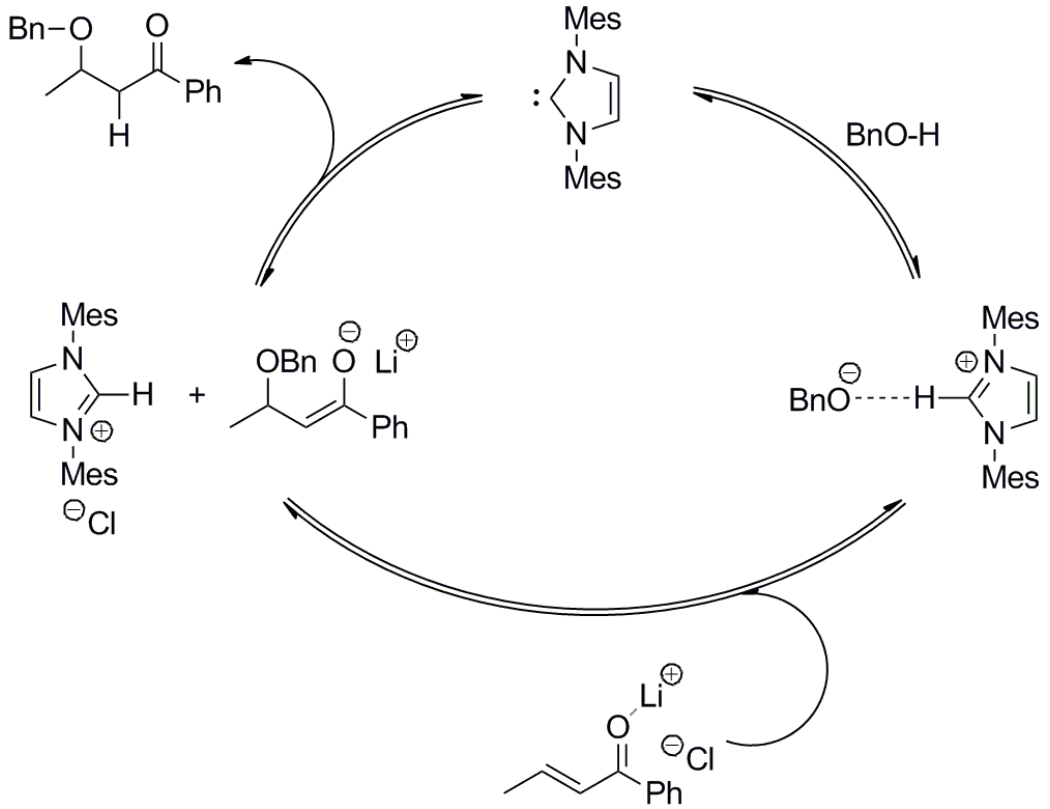

Scheme 3.3. The proposed mechanism of the conjugate addition of an alcohol into an enone.

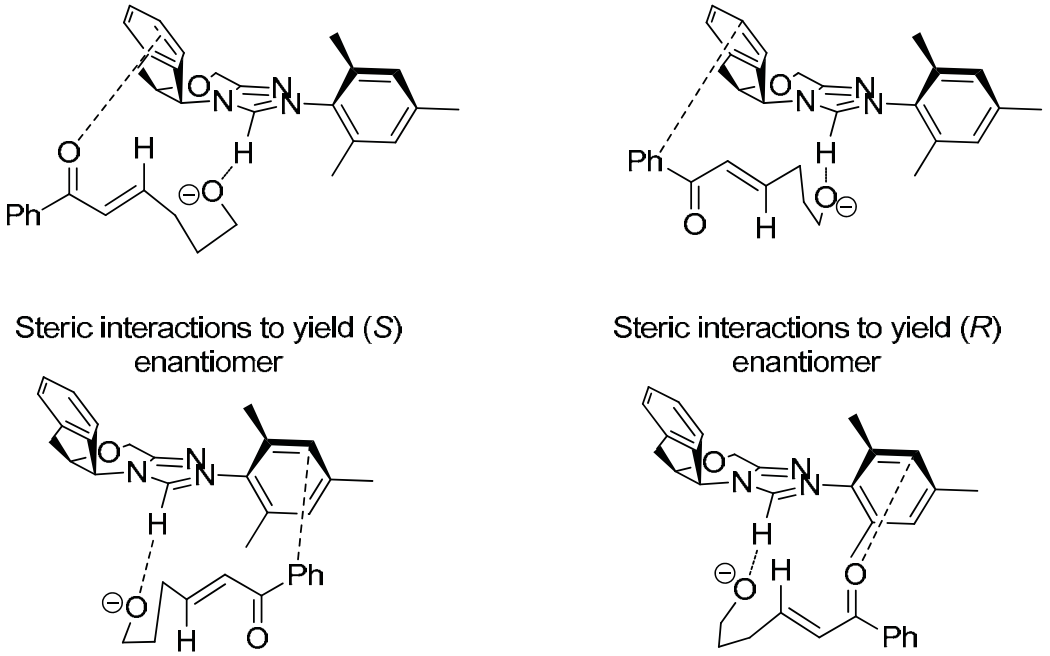

Figure 3.18. Proposed interactions of carbenes used by Scheidt with enone-alcohols.

The proposed hydrogen bonding scheme for the chiral (*S*)-carbenes used in this study to provide (*S*)-enantiomer products is depicted in Scheme 3.4. If the (*R*)-catalyst is used, the hydrogen bonding will be such that the face of the alkene is inverted (Scheme 3.5) yielding the (*R*)-tetrahydrofuran.

Other reactions where hydrogen bonding carbenes may be used to afford enantio-pure products have been identified; however, the conjugate addition of alcohols into enones to afford tetrahydrofurans provides a means for the study to start.

Conclusion

Benzimidazolium salt **21** has been synthesized and characterized by ^{1}H NMR, ^{13}C NMR, and single crystal x-ray analysis. The downfield shift of the amide protons in the ^{1}H NMR spectrum of **21** from the starting material lactamide-OTs indicate that hydrogen bonding may be present in solution. Similar observations were made with alcohol

protons when they were in solution with carbenes in previous studies. The crystal structure of **21** showed a series of intermolecular hydrogen bonds between amide groups and tosylate anions. The tosylate anion was also participating in a non-traditional hydrogen bond with the carbene C_2 hydrogen. The amount of hydrogen bonding present in the carbene precursor is promising for attempts to observe intramolecular hydrogen bonding with a carbene and the carboxylate. A carboxylate was likely formed after deprotonation of **21** and subsequent exposure to gaseous CO_2. Facile reaction with water of the carboxylate likely leads to **22**, which is a potential reason signals from **22** were observed in the spectrum of crystals of **23**.

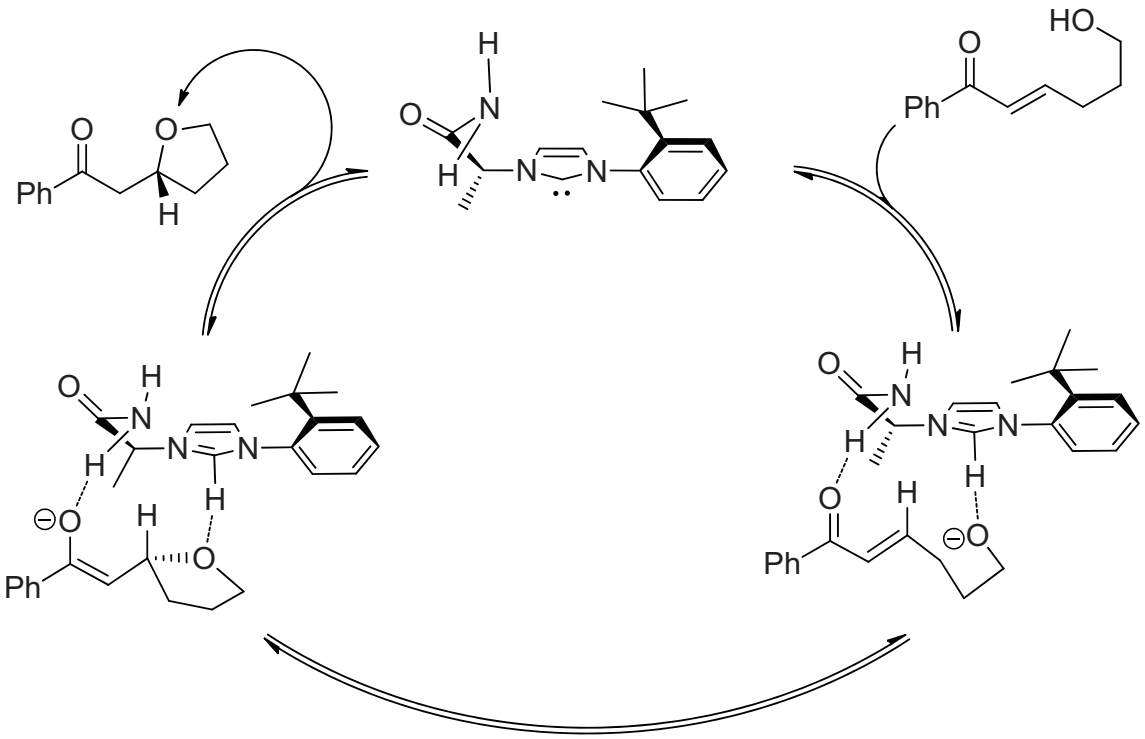

Scheme 3.4. Proposed mechanism for selective conjugate addition of alcohols into enones for the *S*-enantiomer (benzene backbone omitted for clarity).

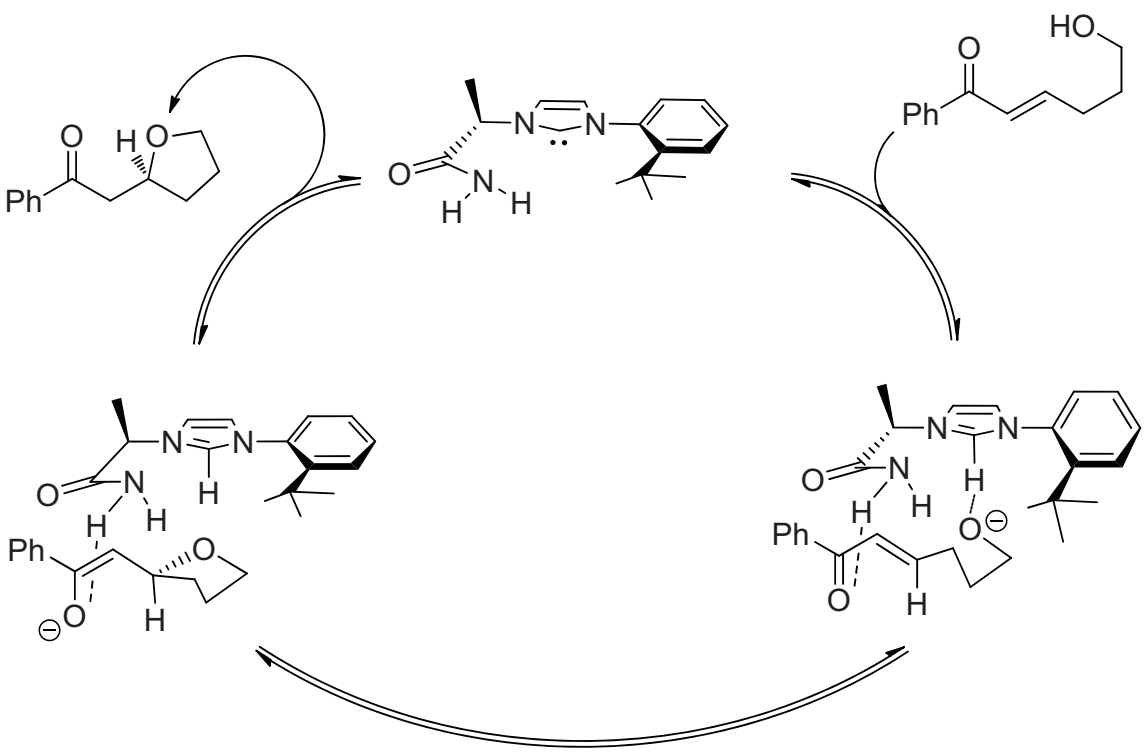

Scheme 3.5. Proposed mechanism for selective conjugate addition of alcohols into enones for the *R*-enantiomer (benzene backbone omitted for clarity).

Experimental Section

General Information

All reactions and procedures were conducted under an atmosphere of N_2 using standard Schlenk techniques or in a N_2 filled glove-box unless otherwise noted. ^1H and ^{13}C Nuclear Magnetic Resonance spectra of pure compounds were acquired at 500 and 125 MHz, respectively, unless otherwise noted. All spectra are referenced to residual solvent peaks. The abbreviations s, d, dd, dt, dq, t, q, quint, sept., m stand for singlet, doublet, doublet of doublets, doublet of triplets, doublet of quartets, triplet, quartet, quintet, septet, and multiplet, in that order. All coupling constants, *J*, are reported in Hz. All ^{13}C NMR spectra were proton decoupled. IR spectra were recorded on a Bruker

Tensor 27 FT-IR spectrometer. The x-ray crystal structure data was collected and solved by Dr. Atta Arif at the Department of Chemistry, University of Utah. The ^{1}H and ^{13}C NMR spectra are located in Appendix C along with the x-ray crystal structure report.

Nondeuterated solvents were purified and deoxygenated by passing through packed silica columns. KHMDS (95%) was purchased from Sigma-Aldrich and used without further purification. All other reagents were purchased from the chemical provider without further purification, unless specified. All NMR solvents were thoroughly dried using standard procedures prior to use. Synthesis of **17**, **18**, **19**,[49] and **20**[36] was performed using previously reported procedures.

Deuterated solvents were purchased from Cambridge. CD_3CN was dried and distilled from CaH_2. All other reagents were purchased and used without further purification unless otherwise noted.

Synthesis of *N*-2,4,6-trimethylphenyl-*N*-lactamidebenzimidazolium tosylate (21). *N*-mesityl benzimidazole **19** (0.250 g, 1 mmol, 1 eq) and lactamide **20** (0.257 g, 1 mmol, 1 eq) were weighed out and placed into a 50-mL round bottom that was equipped with a stir-bar. The round bottom was then charged with 3 mL of dry MeCN, 3 mL of dry toluene, equipped with a condenser and a flow of N_2, and the reaction was refluxed for 24 h. The reaction was allowed to cool and ~10 mL of MeCN was removed. After removal of most of the solvent in vacuo, the product was precipitated with ether, filtered, and washed with 3x10 mL ether washes, yielding 0.308 g of product (63% yield). ^{1}H NMR (500 MHz, $CDCl_3$): δ 9.96 (s, 1H), 9.26 (s, 1H), 8.55 (d, 1H, *J*=8.7 Hz), 7.79 (d, 2H, *J*=8.1 Hz), 7.71 (t, 1H, *J*=7.6 Hz), 7.60 (t, 1H, *J*=7.7 Hz), 7.23 (d, 1H, *J*=8.1 Hz), 7.10 (s, 2H), 6.58 (q, 1H, *J*=7.1 Hz), 5.53 (s, 1H), 2.43 (s, 3H), 2.36 (s, 3H), 2.02 (d, 3H,

J=7.1 Hz), 1.99 (s, 3H), 1.98 (s, 3H). ^{13}C (125 MHz, CD_2Cl_2): δ 169.8, 144.1, 142.4, 142.1, 139.9, 135.77, 135.76, 132.0, 131.4, 130.5, 129.0, 128.6, 128.4, 126.1, 116.3, 113.2, 57.2, 21.39, 21.36, 19.1, 17.5.

Synthesis of *N*-2,4,6-trimethylphenyl-*N*-lactamidebenzimidazolylide (22). Tosylate **21** (0.250 g, 0.52 mmol, 1 eq) was combined with 10 mL of ether, 10 mL of toluene, and a stir-bar in a 50-mL roundbottom flask. To this heterogenous solution, KHMDS (0.109 g, 0.52 mmol, 1 eq) was added. The solution was allowed to stir for 12 h before the reaction was poured through a pad of celite in a glass frit. The reaction solution was then evaporated in vacuo. The clear substance remaining was dissolved in THF and then ether was diffused slowly into the THF to form crystals 0.080 g of crystals. ^{13}C NMR analysis should be performed again with a more concentrated solution. ^{1}H NMR (500 MHz, d^8-THF): δ 9.01 (s, 1H), 8.12 (s, 1H), 7.16 (s, 1H), 7.00 (t, 2H, *J*=7.5 Hz), 6.90 (s, 2H), 6.63 (t, 1H, *J*=7.3 Hz), 6.56 (s, 1H), 6.09 (d, 1H, *J*=7.3 Hz), 4.64 (q, 1H, *J*=7.3 Hz), 2.27 (s, 3H), 2.14 (s, 3H), 2.07 (s, 3H), 1.29 (d, 2H, *J*=7.0 Hz). ^{13}C (125 MHz, d^8-THF): δ 164.1, 136.9, 133.2, 130.5, 129.9, 116.4, 112.8, 55.2, 21.1, 18.9, 18.6, 16.7.

Synthesis of *N*-2,4,6-trimethylphenyl-*N*-lactamidebenzimidazolium-2-carboxyalate (23). Tosylate **21** (0.250 g, 1 mmol, 1 eq) was combined with 10 mL of ether, 10 mL of toluene, and a stir-bar in a 50-mL round bottom flask. To this heterogenous solution, KHMDS (0.109 g, 0.52 mmol, 1 eq) was added. The solution was allowed to stir for 12 h before the reaction was poured through a pad of celite in a glass frit. The reaction solution was Schlenk flask and stoppered with a rubber stopper. The reaction was removed from the glove box and attached to a Schlenk line with dry

CO_2. The atmosphere above the reaction solution was removed and replaced with CO_2. The reaction was allowed to stir under this atmosphere for 24 h. The reaction had turned a slight yellow, remaining transparent, however. The flask was brought back into the glove box and the solvent was removed in vacuo, leaving a clear yellow film. The clear substance remaining was dissolved in THF and then ether was diffused slowly into the solution, providing what appeared to be two sets of crystals, one of which was clear like the ring opened formamide, and the other was a translucent yellow crystal. The ^{1}H NMR of the solution had two sets of peaks, one corresponding to the ring opened material and one corresponding to presumably the carboxylate. The ratio of the peaks was ~3:1, new species:ring opened material. If the carboxylate material is present, all 19 hydrogens, including amide hydrogens, were accounted for. A carbon spectrum was not collected due to the impurity indicated by the proton NMR spectrum. ^{1}H NMR (500 MHz, d^8-THF): δ 8.01 (s, 1H), 6.99 (s, 1H), 6.96 (s, 1H), 6.70 (d, 2H, *J*=7.6 Hz), 6.61 (t, 1H, *J*=7.5 Hz), 6.57 (t, 1H, *J*=7.5 Hz), 6.48 (s, 1H), 5.87 (d, 1H, *J*=7.3 Hz), 3.77 (q, 1H, *J*=7.2 Hz), 2.28 (s, 3H), 2.25 (s, 3H), 2.10 (s, 3H), 1.46 (d, 2H, *J*=7.0 Hz).

References

(1) Hirsch-Weil, D.; Abboud, K. A.; Hong, S. *Chem. Commun.* **2010**, *46*, 7525.

(2) Kaeobamrung, J.; Mahatthananchai, J.; Zheng, P.; Bode, J. W. *J. Am. Chem. Soc.* **2010**, *132*, 8810.

(3) Kerr, M. S.; Read, d. A. J.; Rovis, T. *J. Org. Chem.* **2005**, *70*, 5725.

(4) Enders, D.; Niemeier, O.; Balensiefer, T. *Angew. Chem., Int. Ed.* **2006**, *45*, 1463.

(5) Knight, R. L.; Leeper, F. J. *J. Chem. Soc., Perkin Trans. 1* **1998**, 1891.

(6) Suzuki, Y.; Muramatsu, K.; Yamauchi, K.; Morie, Y.; Sato, M. *Tetrahedron* **2005**, *62*, 302.

(7) O'Toole, S. E.; Connon, S. J. *Organic & Biomolecular Chemistry* **2009**, *7*, 3584.

(8) Suzuki, Y.; Yamauchi, K.; Muramatsu, K.; Sato, M. *Chem. Commun.* **2004**, 2770.

(9) Phillips, E. M.; Riedrich, M.; Scheidt, K. A. *J. Am. Chem. Soc.* **2010**, *132*, 13179.

(10) Papai, I.; Hamza, A.; Pihko, P. M.; Wierenga, R. K. *Chem.--Eur. J.* **2011**, *17*, 2859.

(11) Yang, X.; Hall, M. B. *J. Am. Chem. Soc.* **2009**, *131*, 10901.

(12) Amorati, R.; Catarzi, F.; Menichetti, S.; Pedulli, G. F.; Viglianisi, C. *J. Am. Chem. Soc.* **2008**, *130*, 237.

(13) Sharif, S.; Fogle, E.; Toney, M. D.; Denisov, G. S.; Shenderovich, I. G.; Buntkowsky, G.; Tolstoy, P. M.; Huot, M. C.; Limbach, H.-H. *J. Am. Chem. Soc.* **2007**, *129*, 9558.

(14) Kienhoefer, A.; Kast, P.; Hilvert, D. *J. Am. Chem. Soc.* **2003**, *125*, 3206.

(15) Doyle, A. G.; Jacobsen, E. N. *Chem. Rev.* **2007**, *107*, 5713.

(16) Mennen, S. M.; Blank, J. T.; Tran-Dube, M. B.; Imbriglio, J. E.; Miller, S. J. *Chem. Commun.* **2005**, 195.

(17) Mennen, S. M.; Gipson, J. D.; Kim, Y. R.; Miller, S. J. *J. Am. Chem. Soc.* **2005**, *127*, 1654.

(18) He, L.; Zhang, Y.-R.; Huang, X.-L.; Ye, S. *Synthesis* **2008**, 2825.

(19) Baragwanath, L.; Rose, C. A.; Zeitler, K.; Connon, S. J. *J. Org. Chem.* **2009**, *74*, 9214.

(20) Brand, J. P.; Siles, J. I. O.; Waser, J. *Synlett* **2010**, 881.

(21) O'Toole, S. E.; Rose, C. A.; Gundala, S.; Zeitler, K.; Connon, S. J. *J. Org. Chem.* **2010**, *76*, 347.

(22) Kuhn, N.; Steimann, M.; Weyers, G. *Z. Naturforsch., B: Chem. Sci.* **1999**, *54*, 427.

(23) Duong, H. A.; Tekavec, T. N.; Arif, A. M.; Louie, J. *Chem. Commun.* **2004**, 112.

(24) Holbrey, J. D.; Reichert, W. M.; Tkatchenko, I.; Bouajila, E.; Walter, O.; Tommasi, I.; Rogers, R. D. *Chemical Communications (Cambridge, United Kingdom)* **2003**, 28.

(25) Cowan, J. A.; Clyburne, J. A. C.; Davidson, M. G.; Harris, R. L. W.; Howard, J. A. K.; Küpper, P.; Leech, M. A.; Richards, S. P. *Angew. Chem. Int. Ed.* **2002**, *41*, 1432.

(26) Movassaghi, M.; Schmidt, M. A. *Org. Lett.* **2005**, *7*, 2453.

(27) Giffin, N. A.; Makramalla, M.; Hendsbee, A. D.; Robertson, K. N.; Sherren, C.; Pye, C. C.; Masuda, J. D.; Clyburne, J. A. C. *Organic & Biomolecular Chemistry* **2011**, *9*, 3672.

(28) Kim, Y.-J.; Streitwieser, A. *J. Am. Chem. Soc.* **2002**, *124*, 5757.

(29) Magill, A. M.; Cavell, K. J.; Yates, B. F. *J. Am. Chem. Soc.* **2004**, *126*, 8717.

(30) Chu, Y.; Deng, H.; Cheng, J.-P. *J. Org. Chem.* **2007**, *72*, 7790.

(31) Bordwell, F. G.; Fried, H. E.; Hughes, D. L.; Lynch, T. Y.; Satish, A. V.; Whang, Y. E. *J. Org. Chem.* **1990**, *55*, 3330.

(32) Van Ausdall, B. R.; Glass, J. L.; Wiggins, K. M.; Aarif, A. M.; Louie, J. *J. Org. Chem.* **2009**, *74*, 7935.

(33) Förster, H.; Vögtle, F. *Angew. Chem., Int. Ed.* **1977**, *16*, 429.

(34) Anslyn, E. V.; Dougherty, D. A. *Modern Organic Physical Chemistry*; University Science Books, 2006.

(35) Hirano, K.; Biju, A. T.; Glorius, F. *J. Org. Chem.* **2009**, *74*, 9570.

(36) Shaw, A. N.; Tedesco, R.; Bambal, R.; Chai, D.; Concha, N. O.; Darcy, M. G.; Dhanak, D.; Duffy, K. J.; Fitch, D. M.; Gates, A.; Johnston, V. K.; Keenan, R. M.; Lin-Goerke, J.; Liu, N.; Sarisky, R. T.; Wiggall, K. J.; Zimmerman, M. N. *Bioorg. Med. Chem. Lett.* **2009**, *19*, 4350.

(37) Hollóczki, O.; Terleczky, P. t.; Szieberth, D. n.; Mourgas, G.; Gudat, D.; Nyulászi, L. s. *J. Am. Chem. Soc.* **2010**, *133*, 780.

(38) Grishina, A. A.; Polyakova, S. M.; Kunetskiy, R. A.; Císařová, I.; Lyapkalo, I. M. *Chemistry – A European Journal* **2011**, *17*, 96.

(39) Denk, M. K.; Rodezno, J. M.; Gupta, S.; Lough, A. J. *J. Organomet. Chem.* **2001**, *617-618*, 242.

(40) Amyes, T. L.; Diver, S. T.; Richard, J. P.; Rivas, F. M.; Toth, K. *J. Am. Chem. Soc.* **2004**, *126*, 4366.

(41) Jensen, K. H.; Sigman, M. S. *J. Org. Chem.* **2010**, *75*, 7194.

(42) Klapars, A.; Huang, X.; Buchwald, S. L. *J. Am. Chem. Soc.* **2002**, *124*, 7421.

(43) Dineen, T. A.; Zajac, M. A.; Myers, A. G. *J. Am. Chem. Soc.* **2006**, *128*, 16406.

(44) Glorius, F.; Altenhoff, G.; Goddard, R.; Lehmann, C. *Chemical Communications (Cambridge, United Kingdom)* **2002**, 2704.

(45) Glorius, F. *Angew. Chem., Int. Ed.* **2004**, *43*, 3364.

(46) Perry, M. C.; Cui, X.; Powell, M. T.; Hou, D.-R.; Reibenspies, J. H.; Burgess, K. *J. Am. Chem. Soc.* **2003**, *125*, 113.

(47) Nair, V.; Poonoth, M.; Vellalath, S.; Suresh, E.; Thirumalai, R. *The Journal of Organic Chemistry* **2006**, *71*, 8964.

(48) Enders, D.; Breuer, K.; Runsink, J.; Teles, J. H. *Helv. Chim. Acta* **1996**, *79*, 1899.

(49) Droege, T.; Glorius, F. *Angew. Chem., Int. Ed.* **2010**, *49*, 6940.

APPENDIX A

NMR SPECTRA, IPrCO_2 TGA DATA, AND X-RAY CRYSTAL STRUCTURE REPORTS

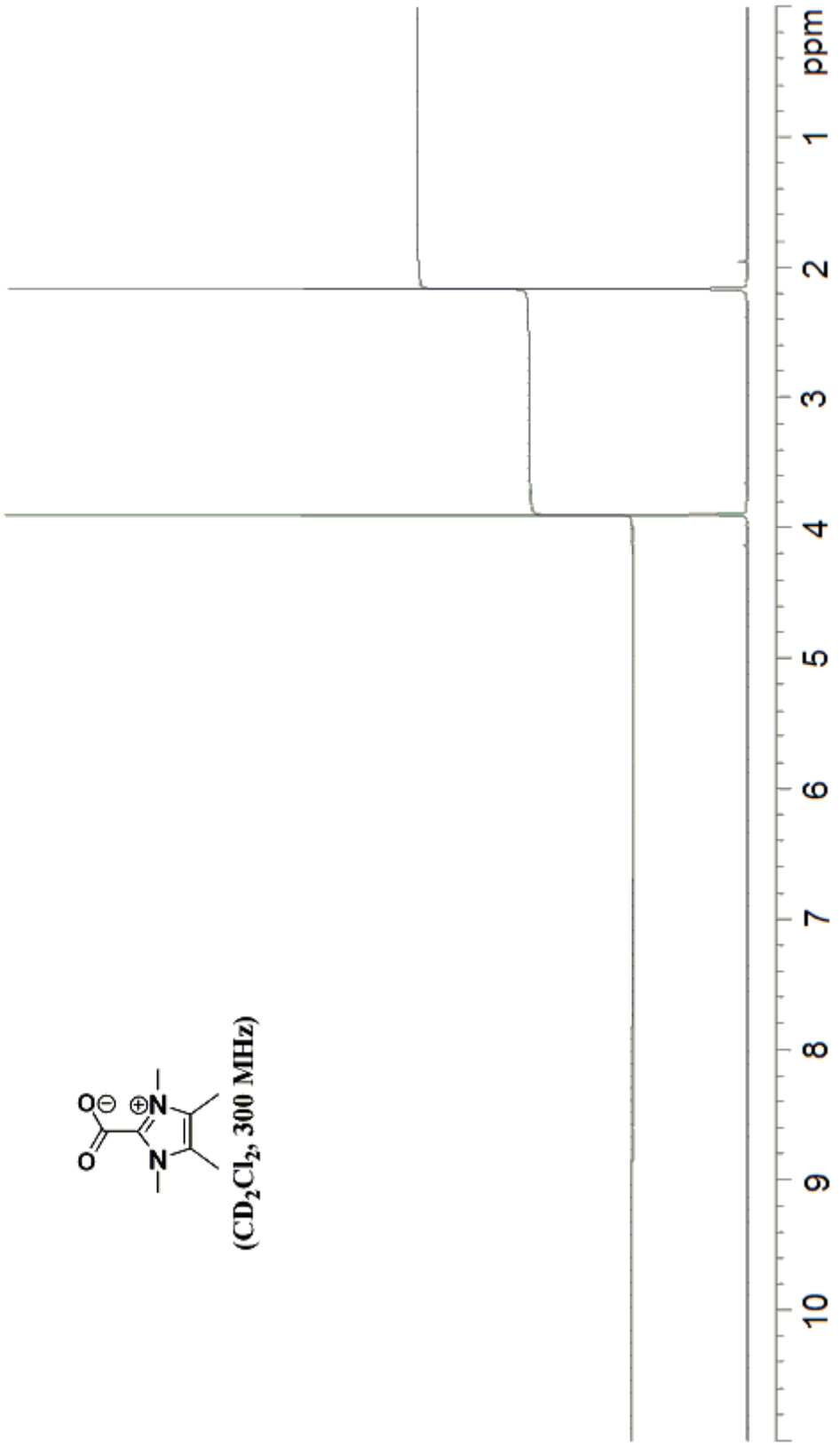

(CD_2Cl_2, 300 MHz)

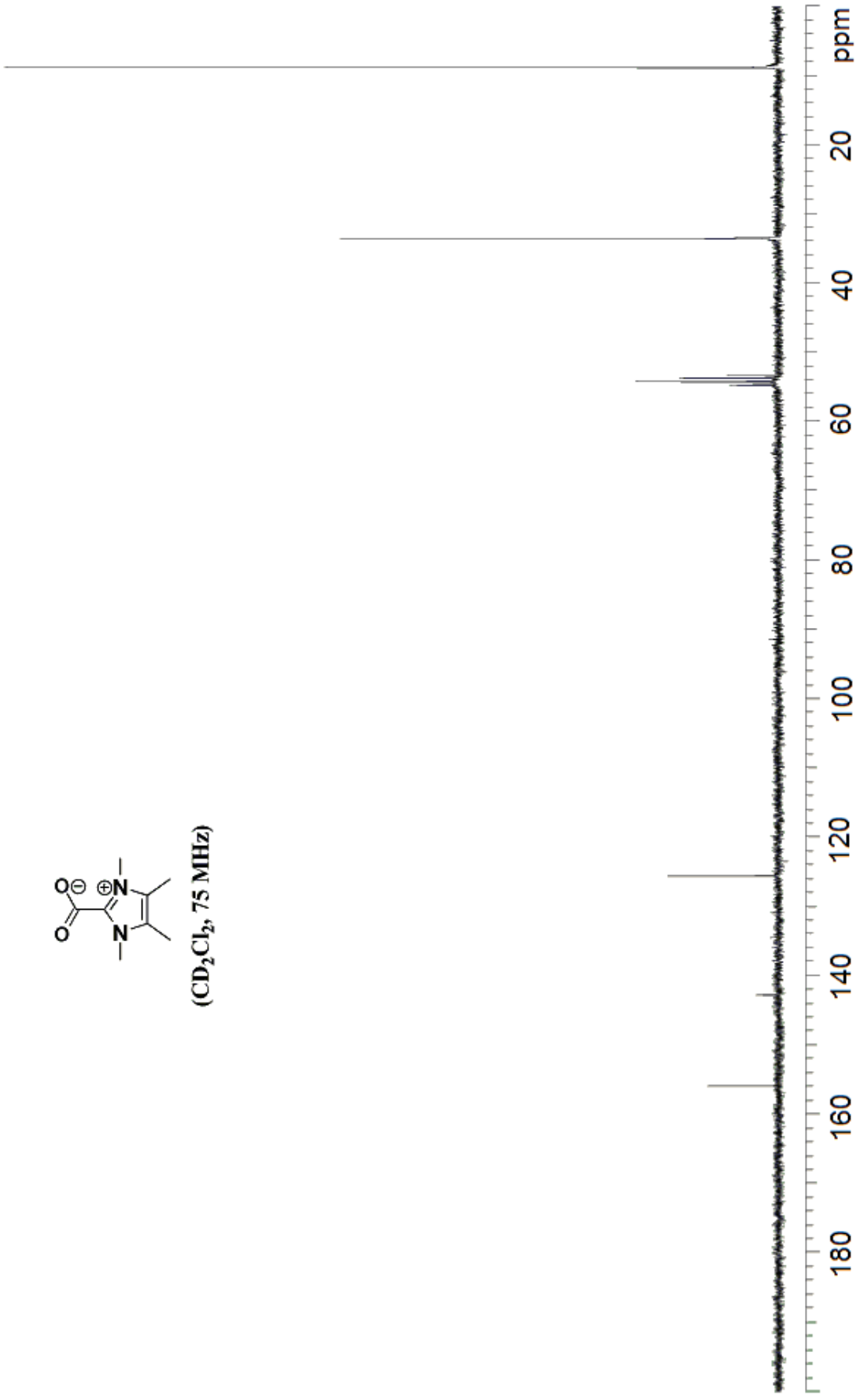

(CD_2Cl_2, 75 MHz)

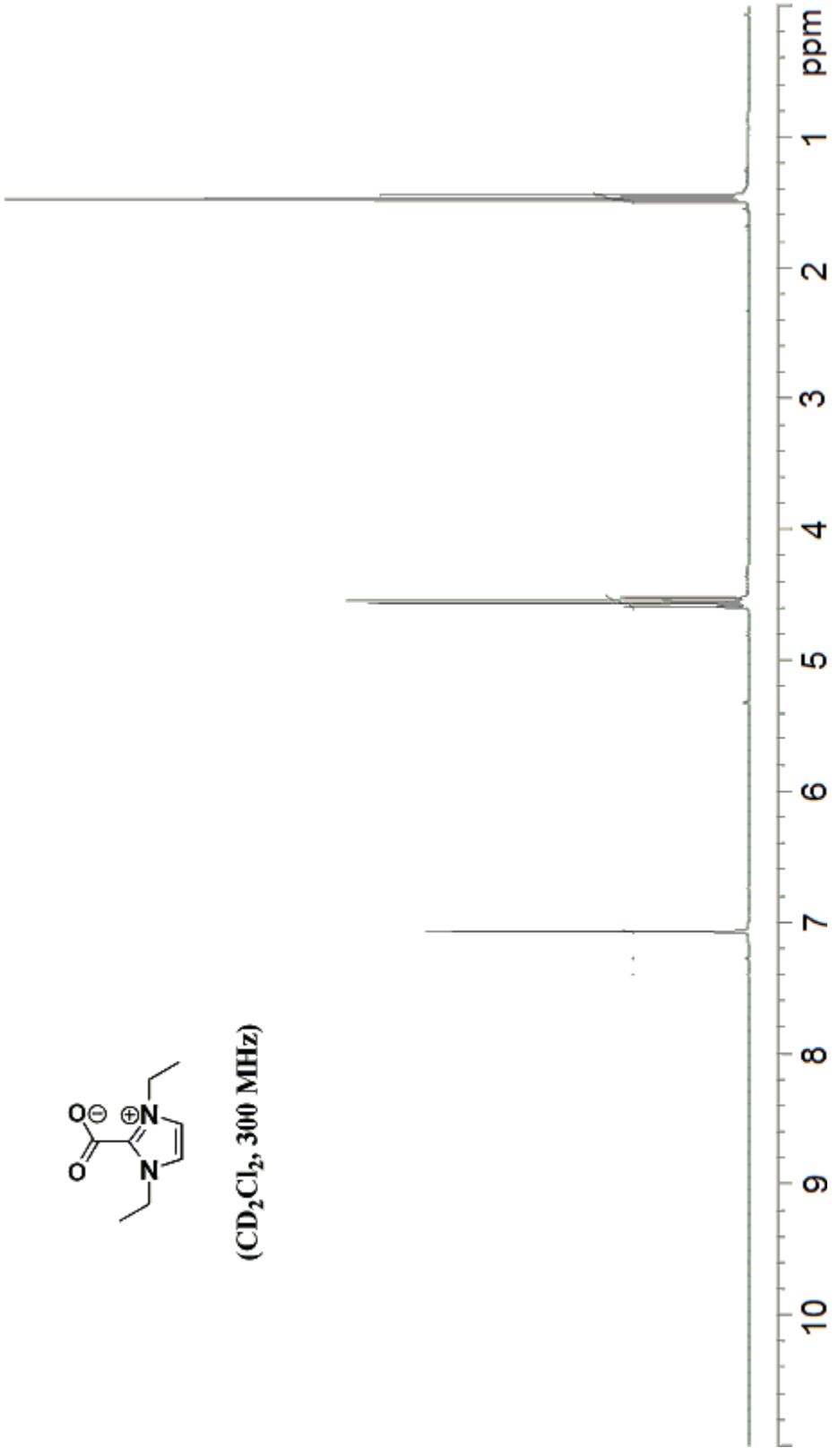

(CD_2Cl_2, 300 MHz)

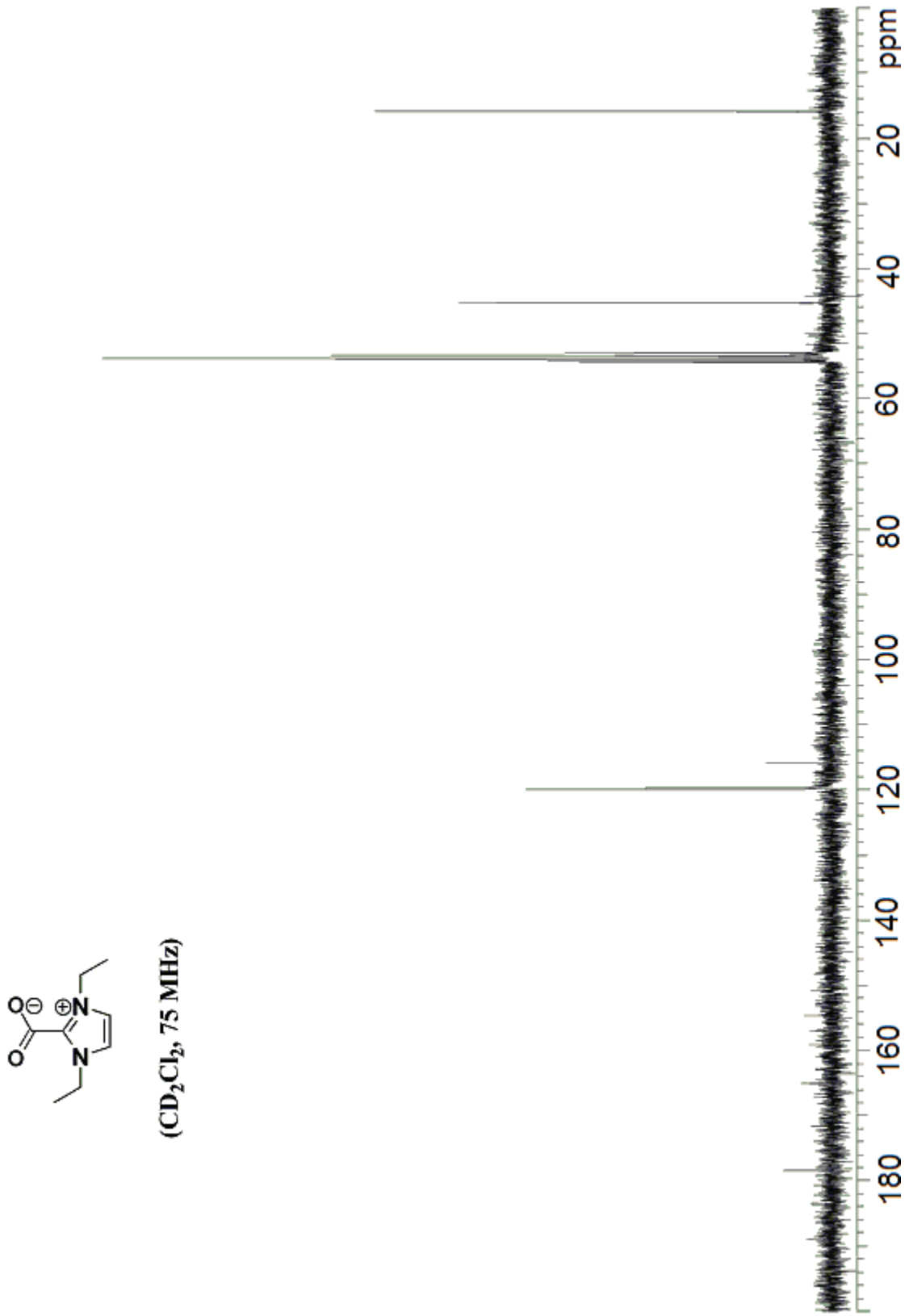

(CD_2Cl_2, 75 MHz)

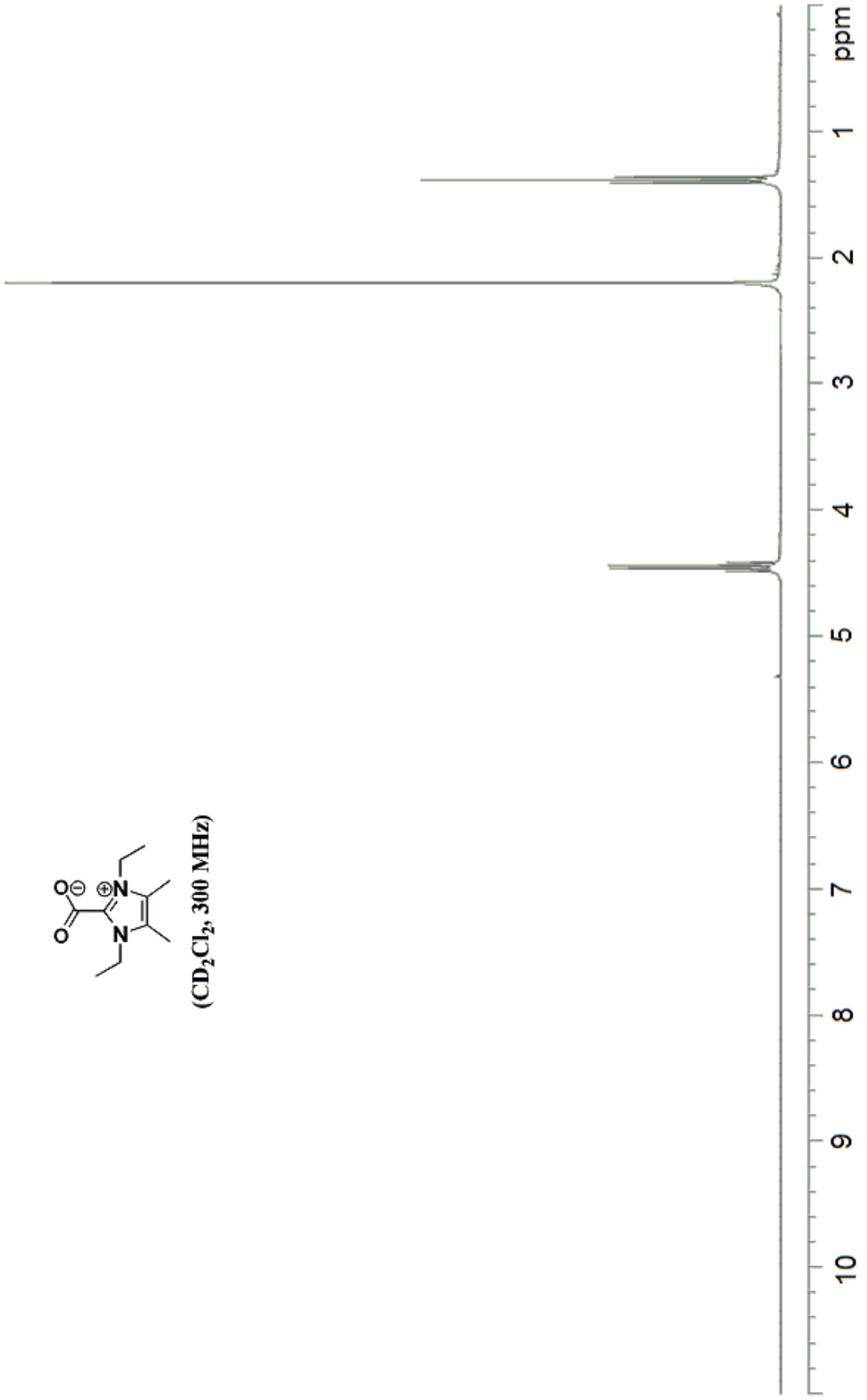

(CD_2Cl_2, 300 MHz)

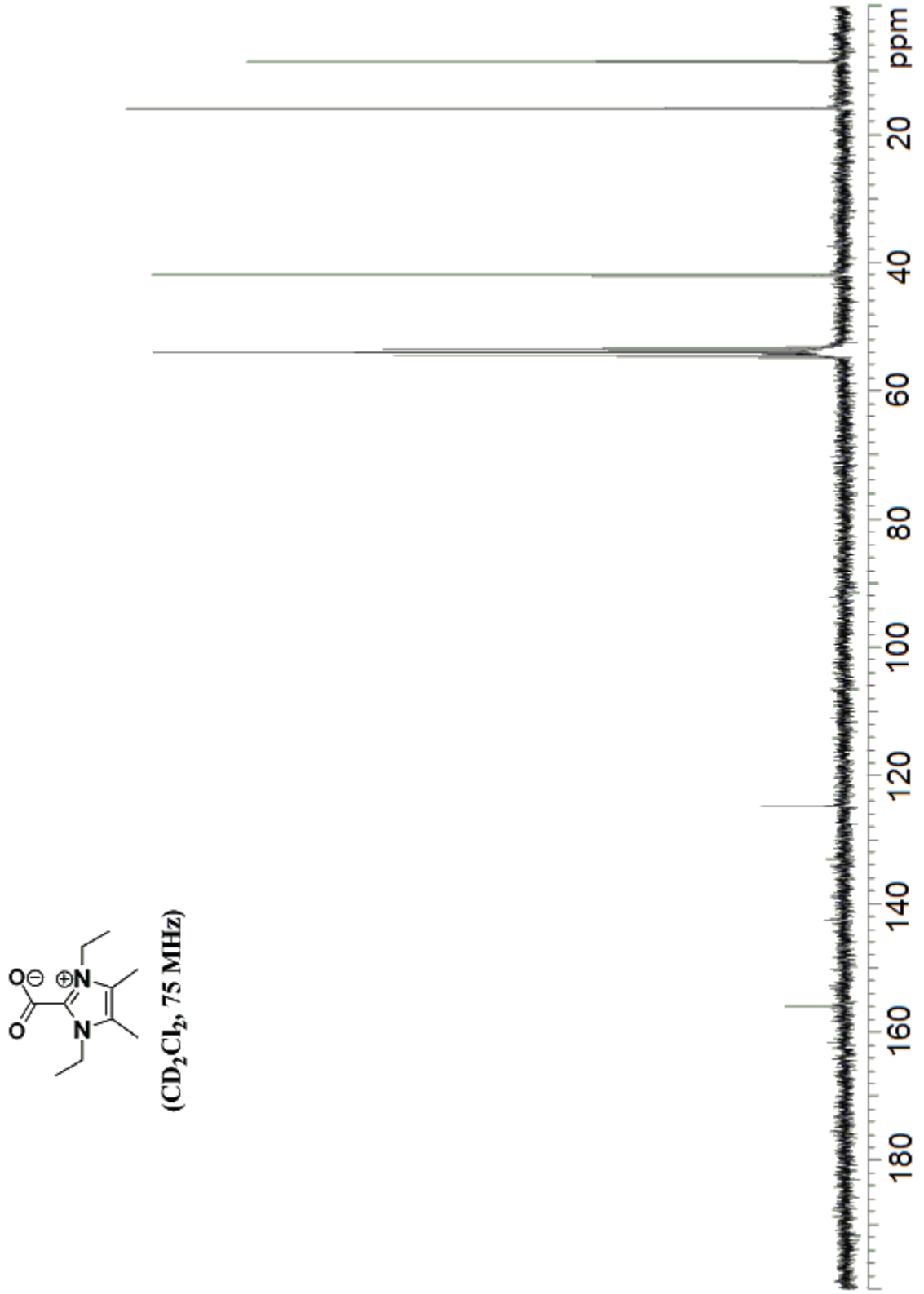

(CD_2Cl_2, 75 MHz)

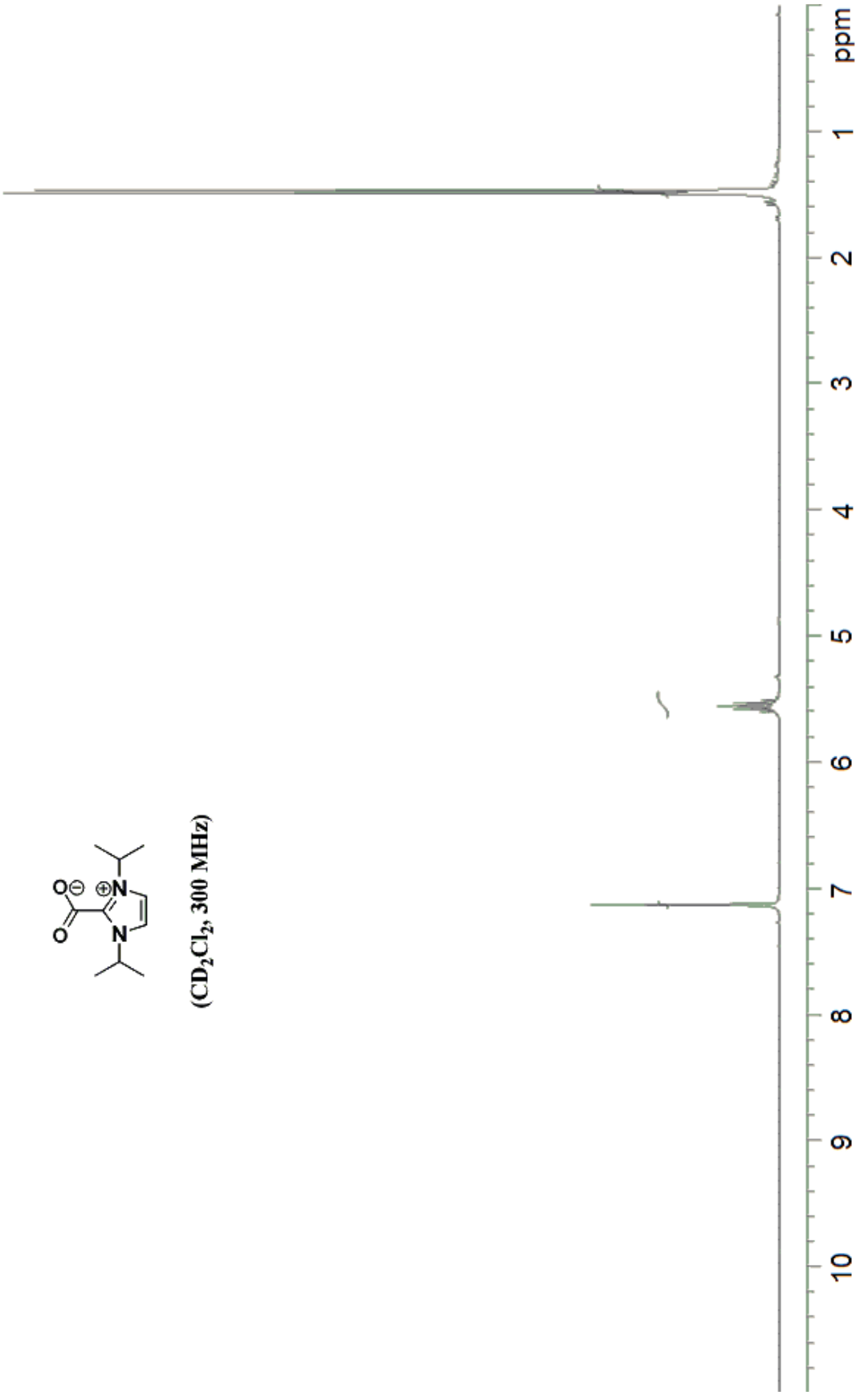

(CD_2Cl_2, 300 MHz)

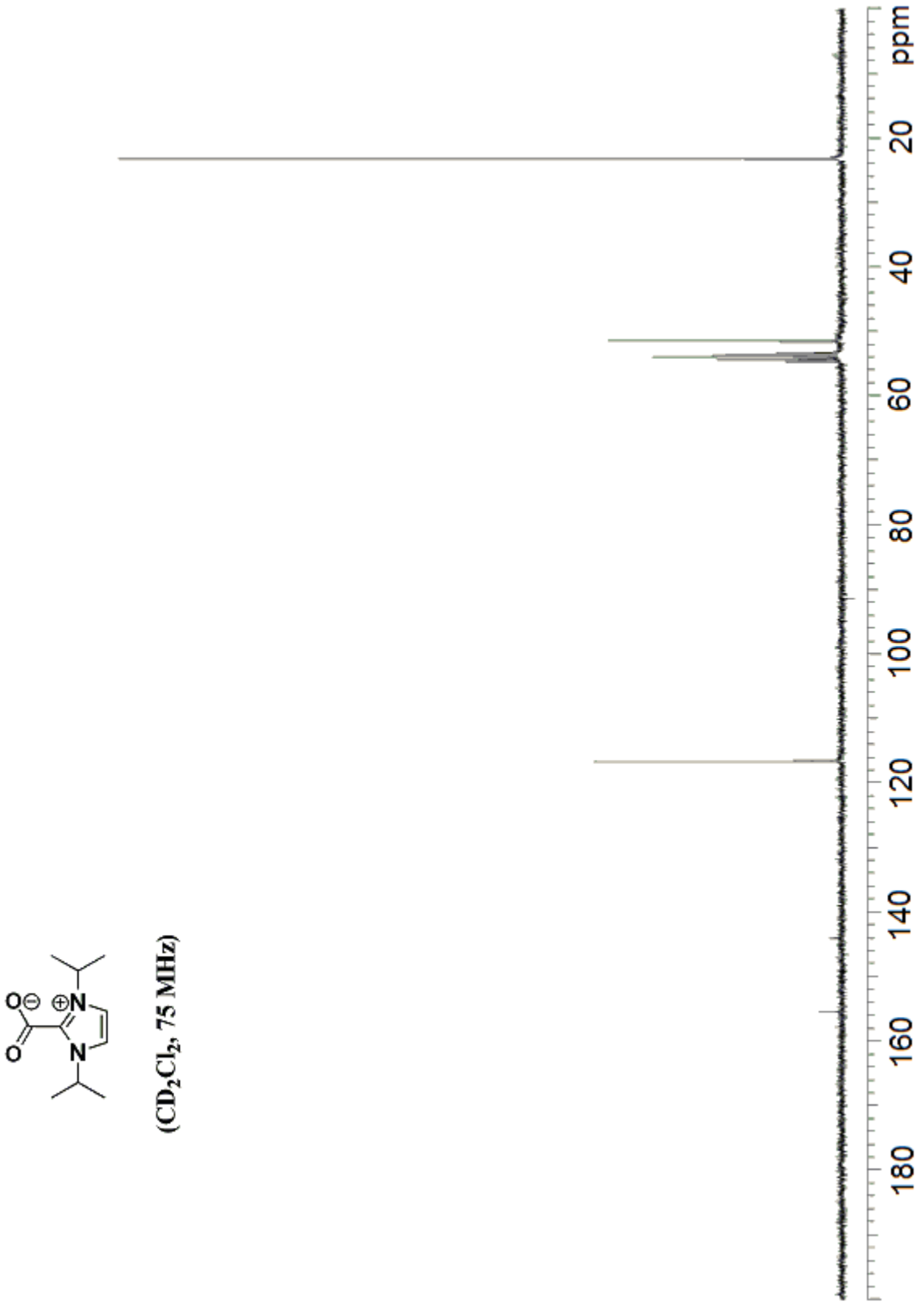

(CD_2Cl_2, 75 MHz)

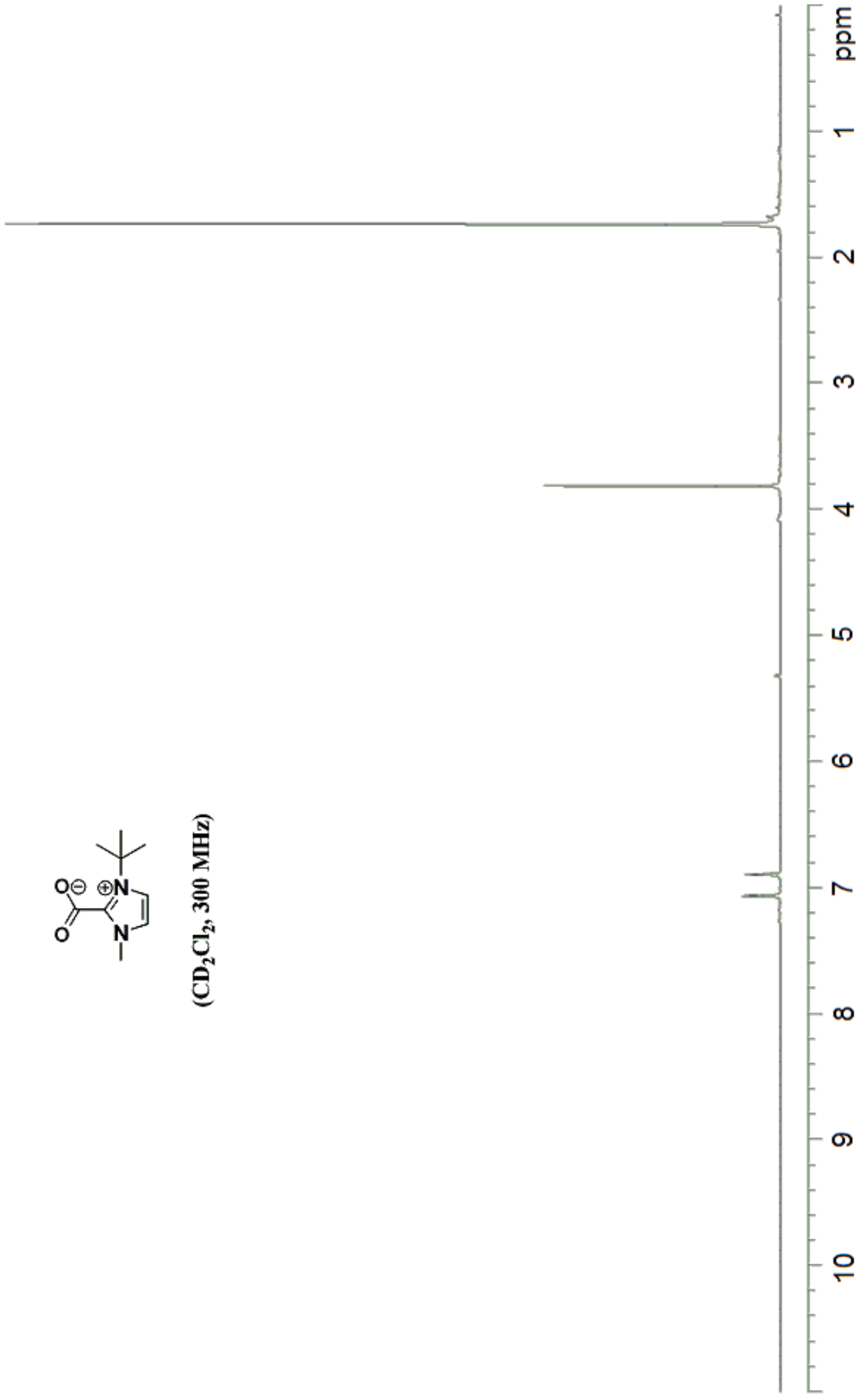

(CD_2Cl_2, 300 MHz)

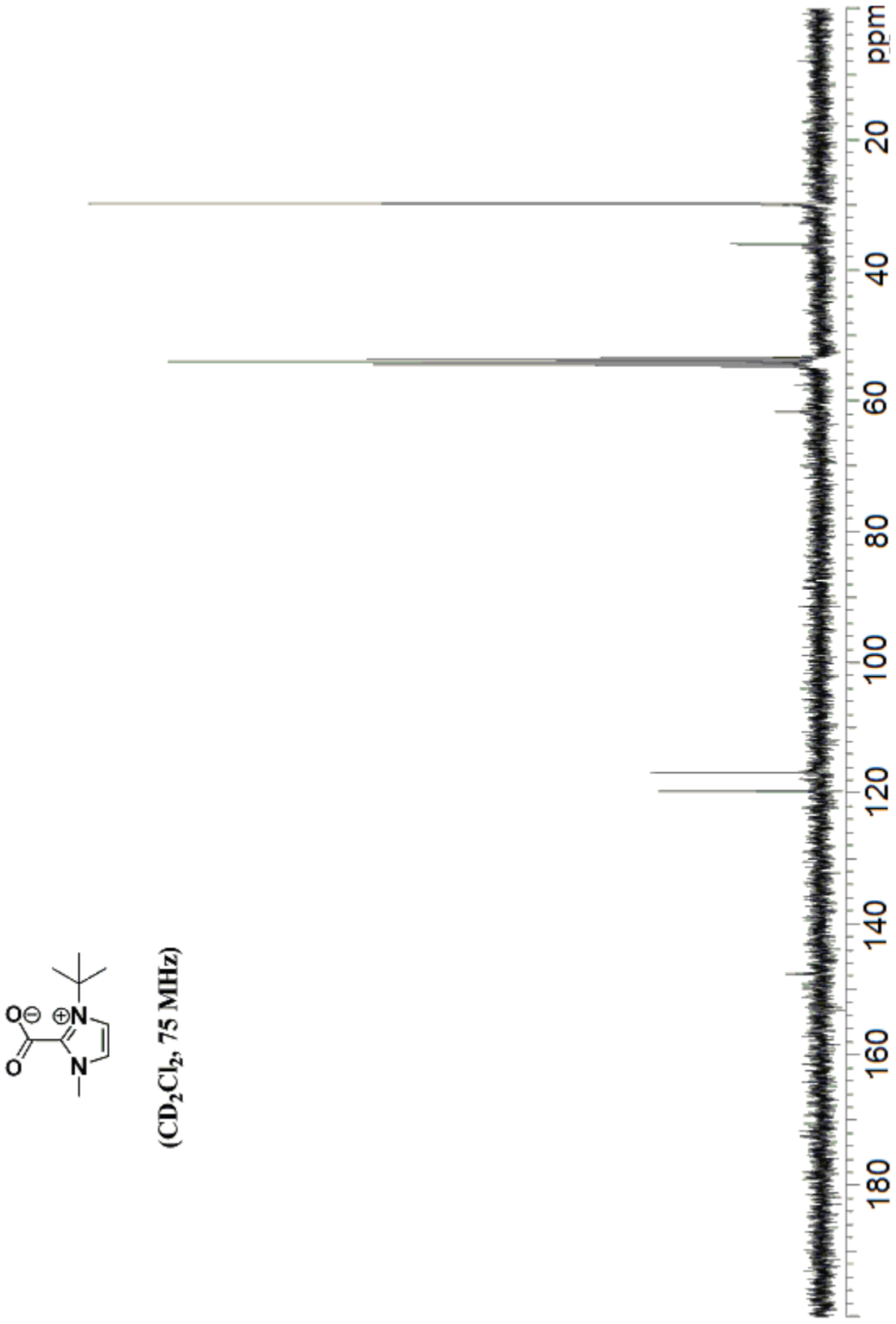

(CD_2Cl_2, 75 MHz)

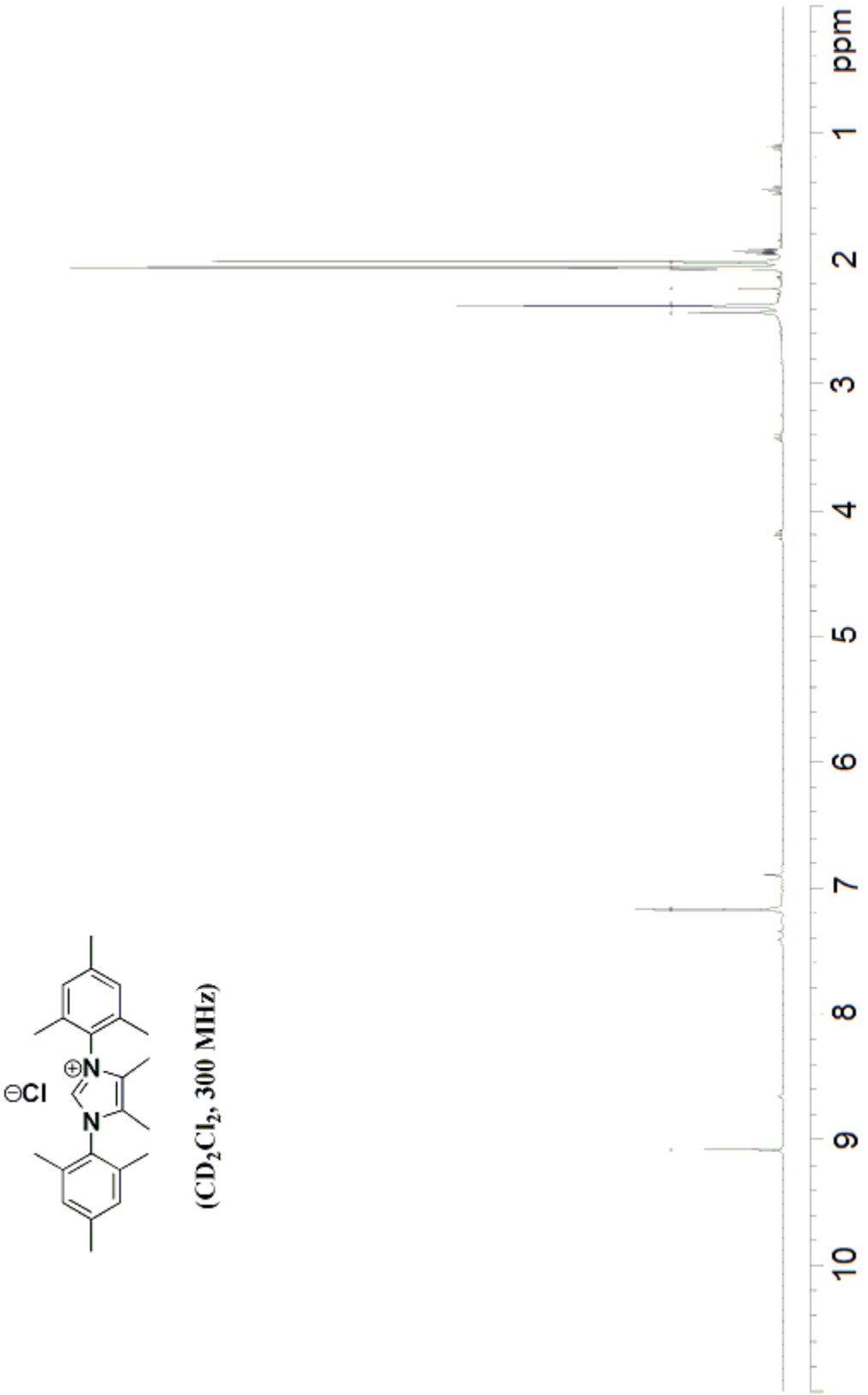
ppm
1
2
3
4
5
6
7
8
9
10
⊕N
⊖Cl
N
(CD2Cl2, 300 MHz)

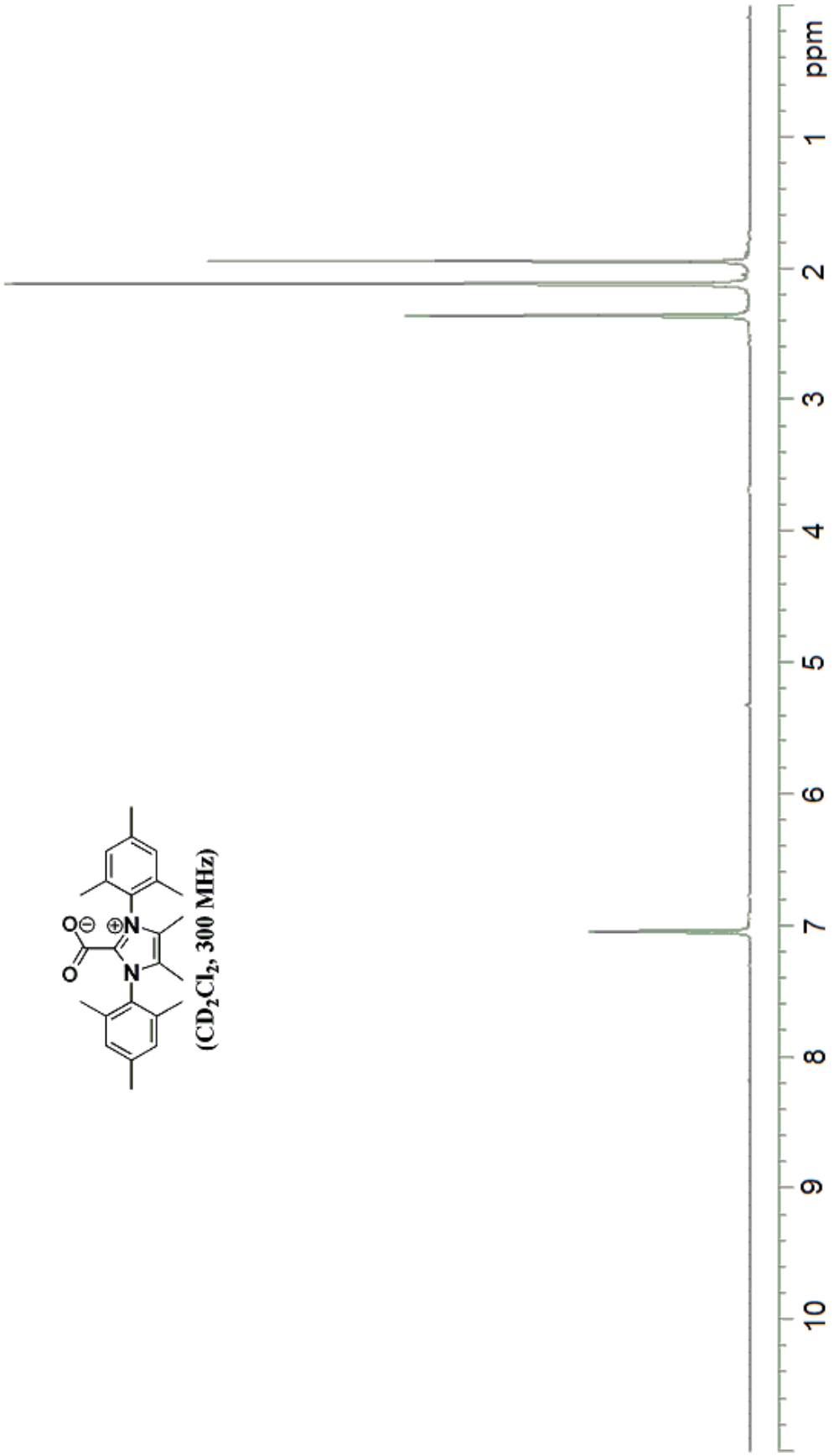

(CD_2Cl_2, 300 MHz)

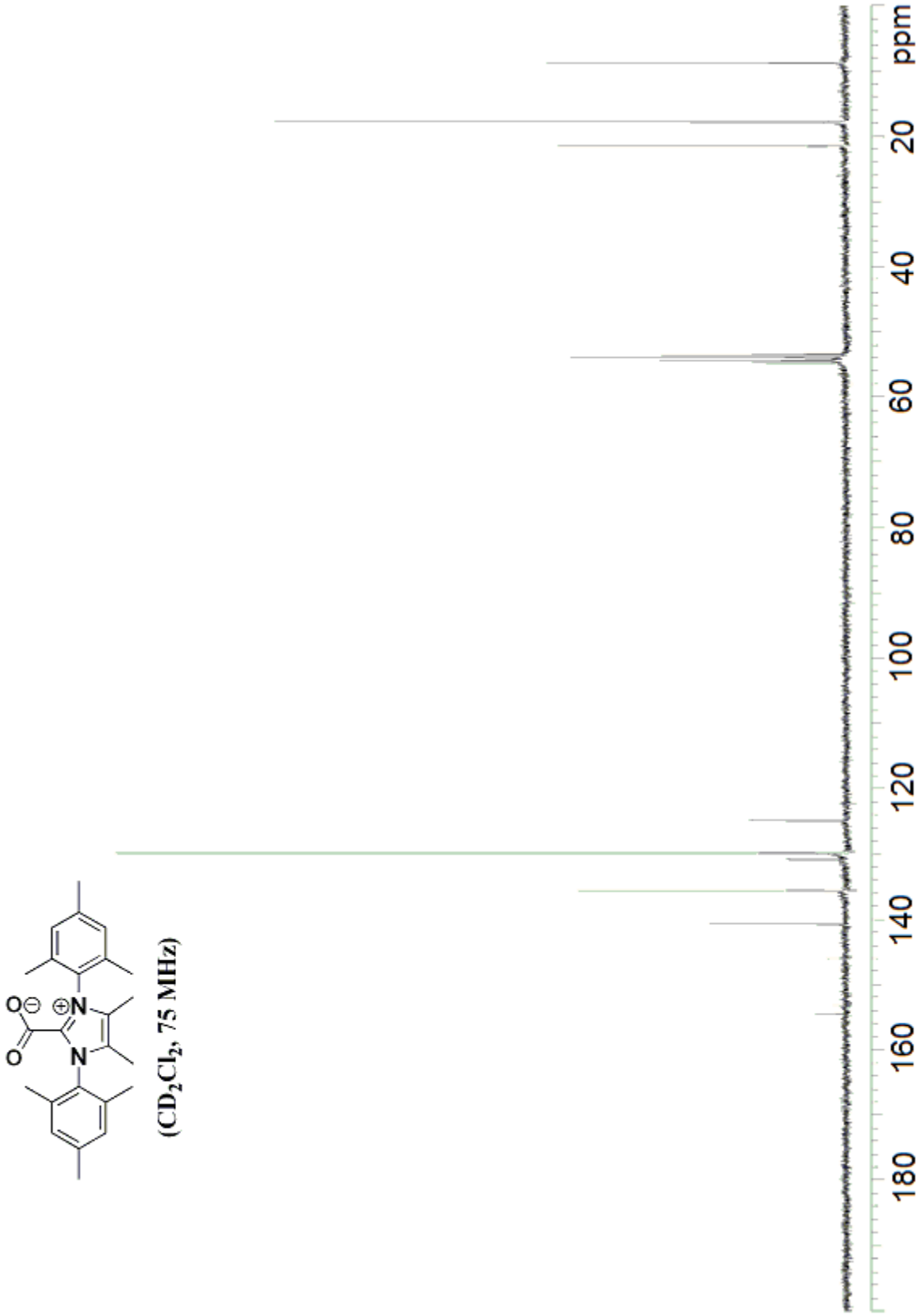
ppm
20
40
60
80
100
120
140
160
180
O
O
N
N
(CD2Cl2, 75 MHz)

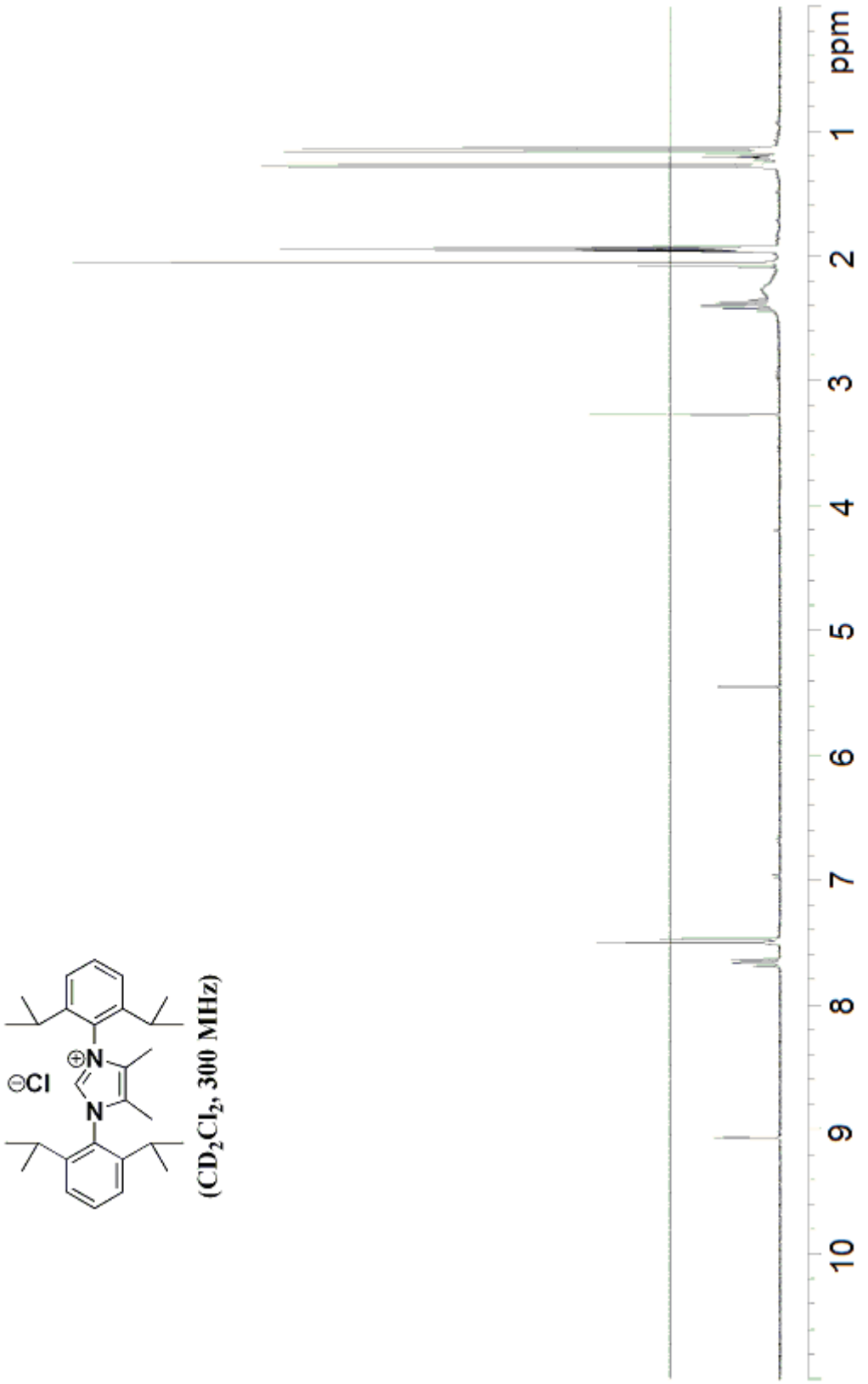
ppm
1
2
3
4
5
6
7
8
9
10
⊕N
⊖Cl
N
(CD2Cl2, 300 MHz)

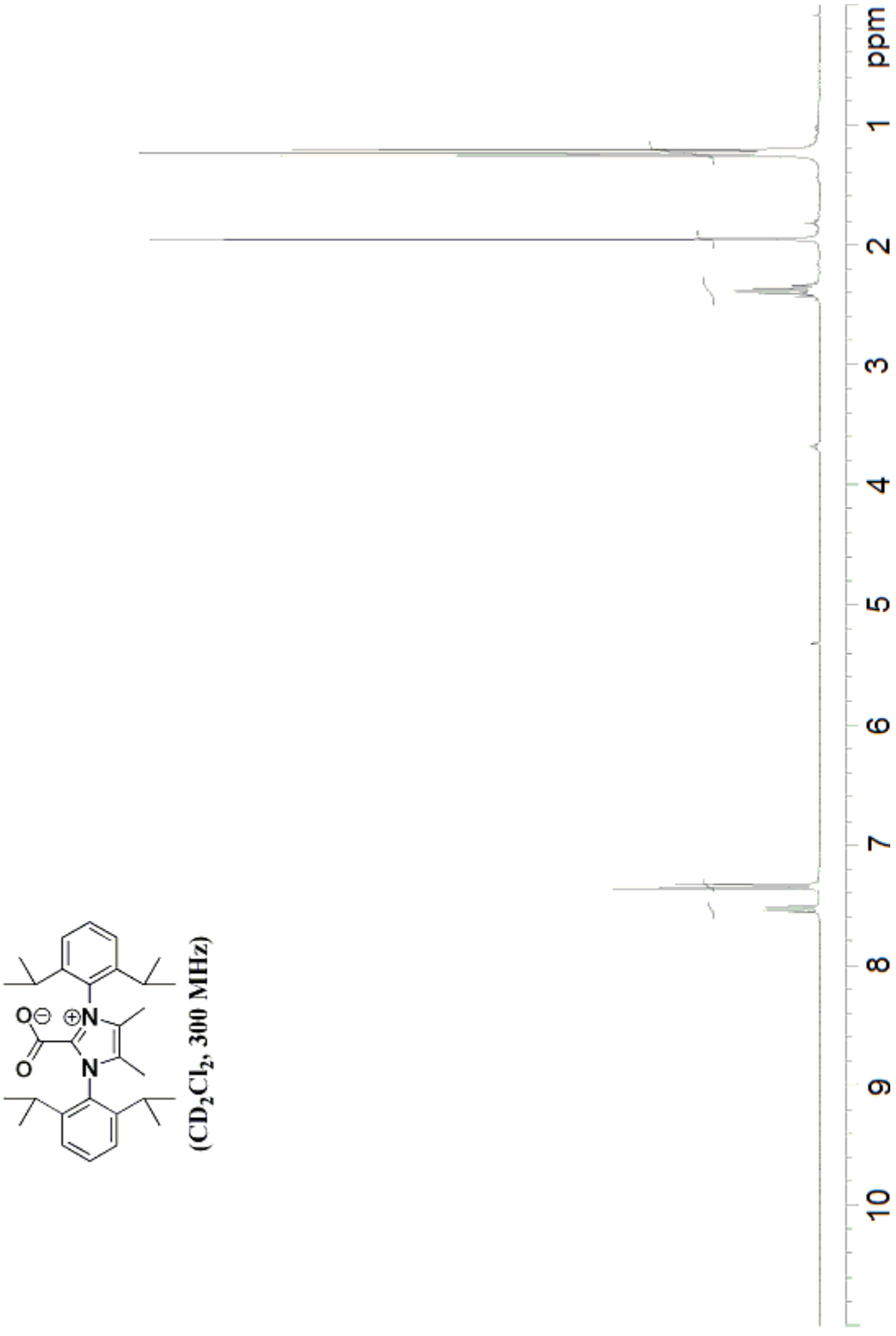

(CD_2Cl_2, 300 MHz)

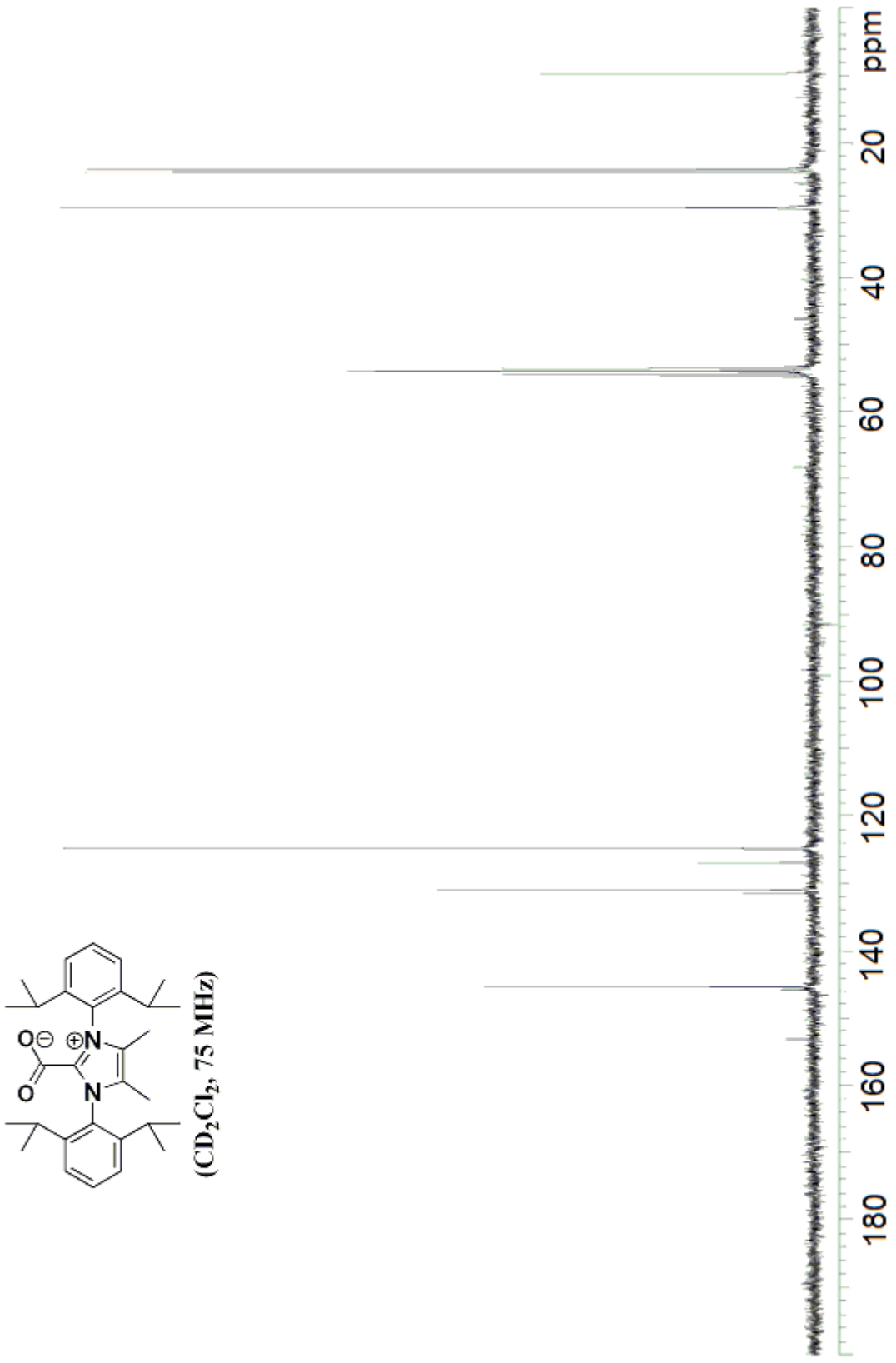

(CD_2Cl_2, 75 MHz)

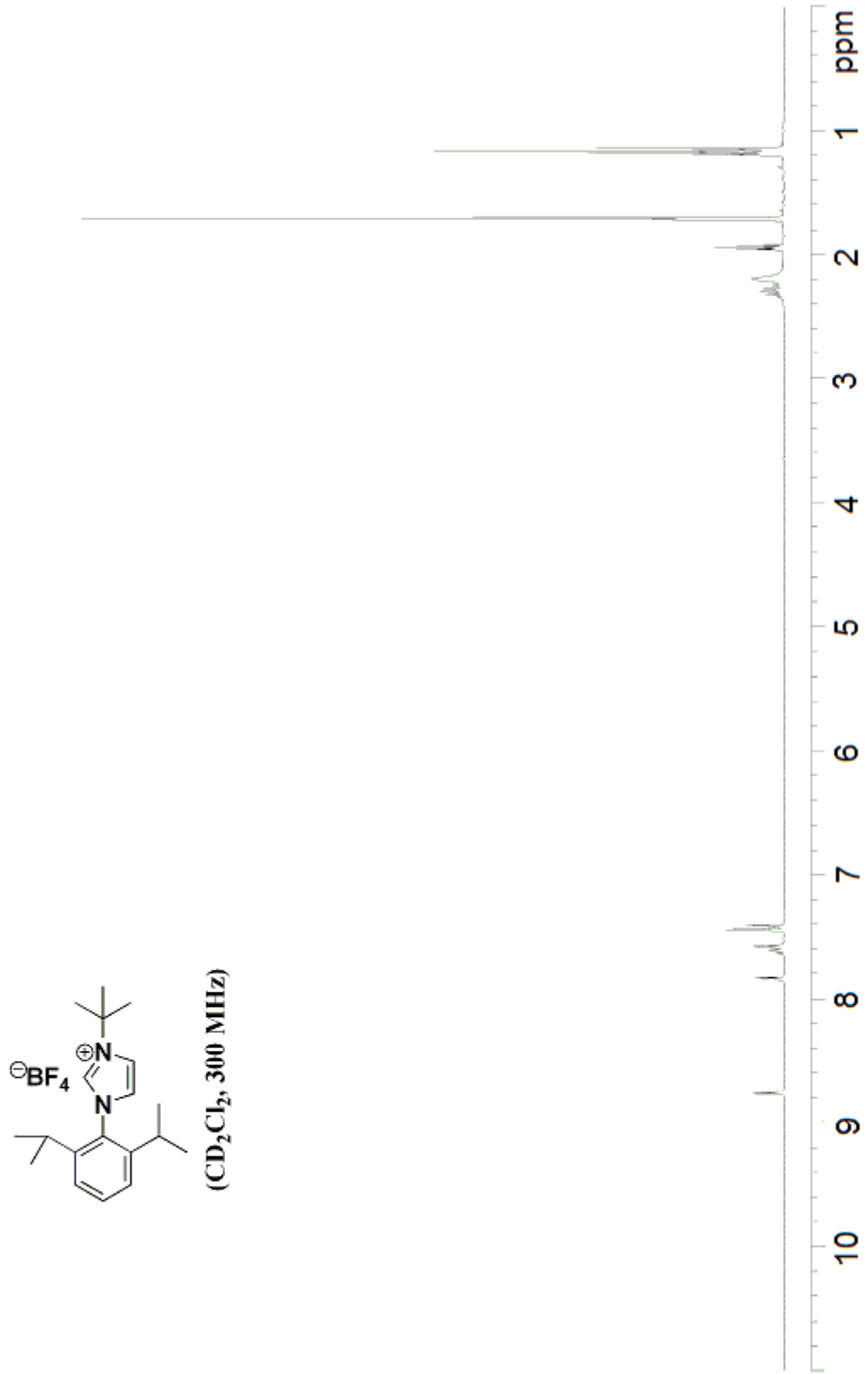

(CD_2Cl_2, 300 MHz)

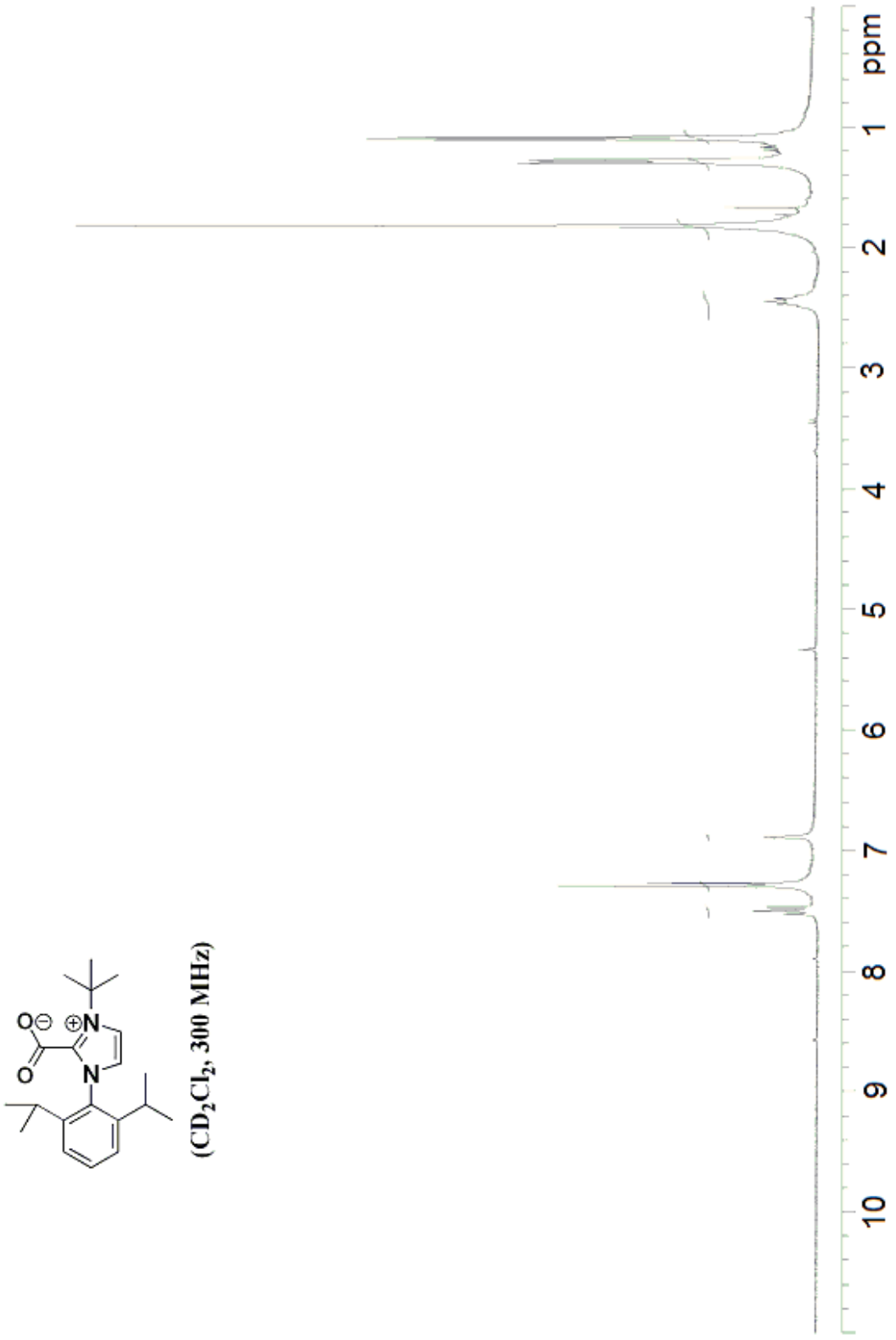

(CD_2Cl_2, 300 MHz)

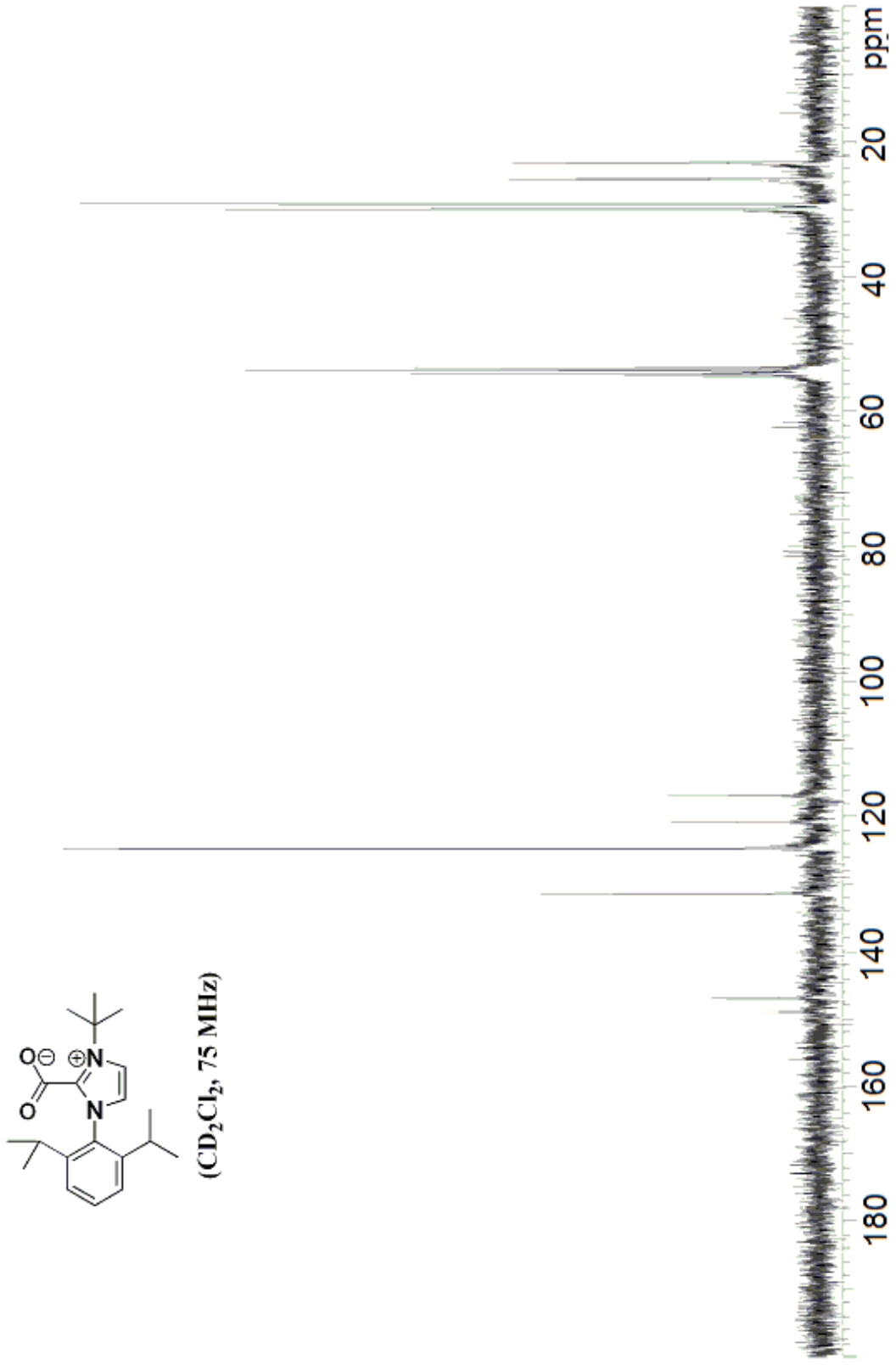

(CD_2Cl_2, 75 MHz)

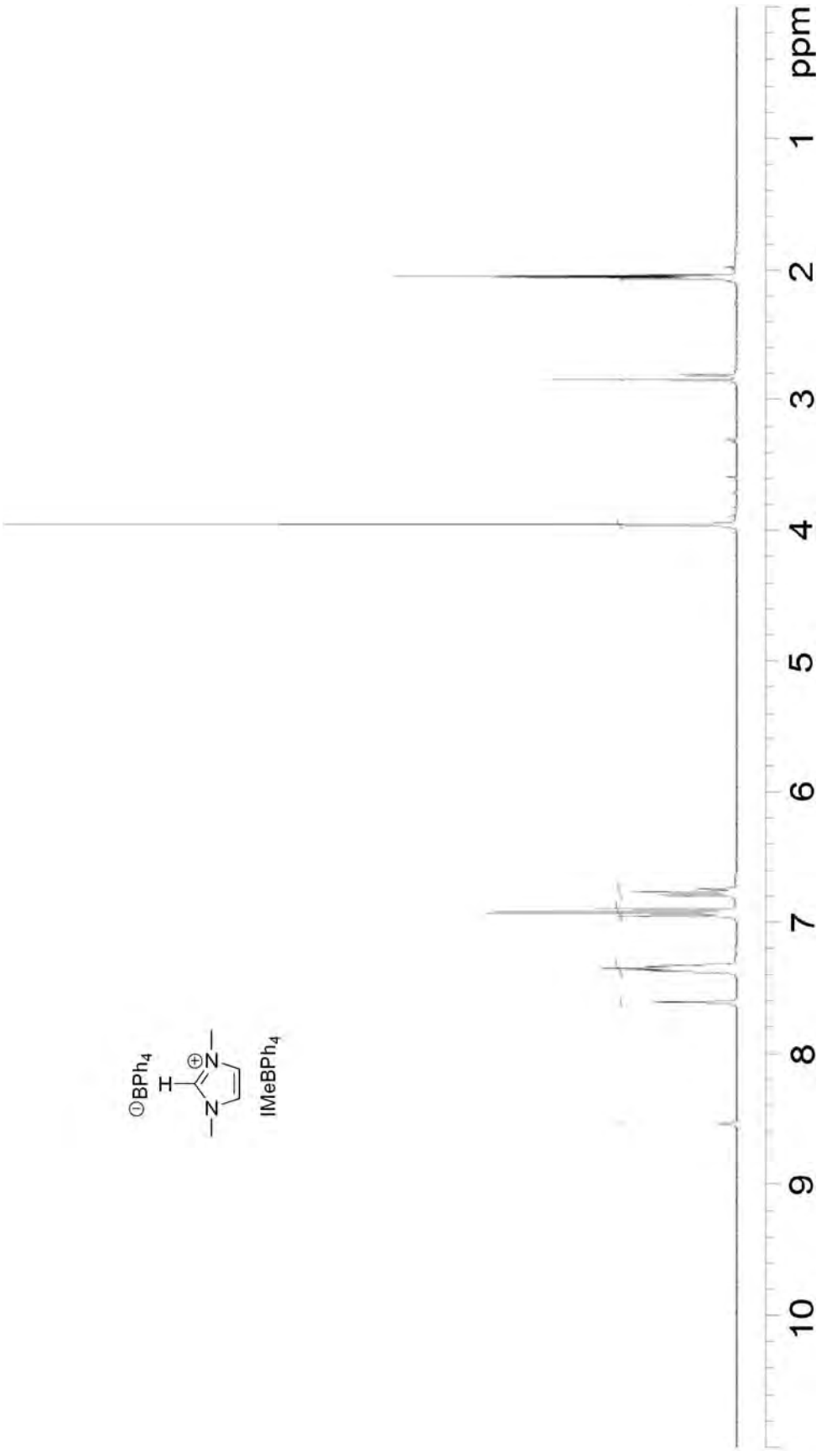
ppm
1
2
3
4
5
6
7
8
9
10
IMeBPh4

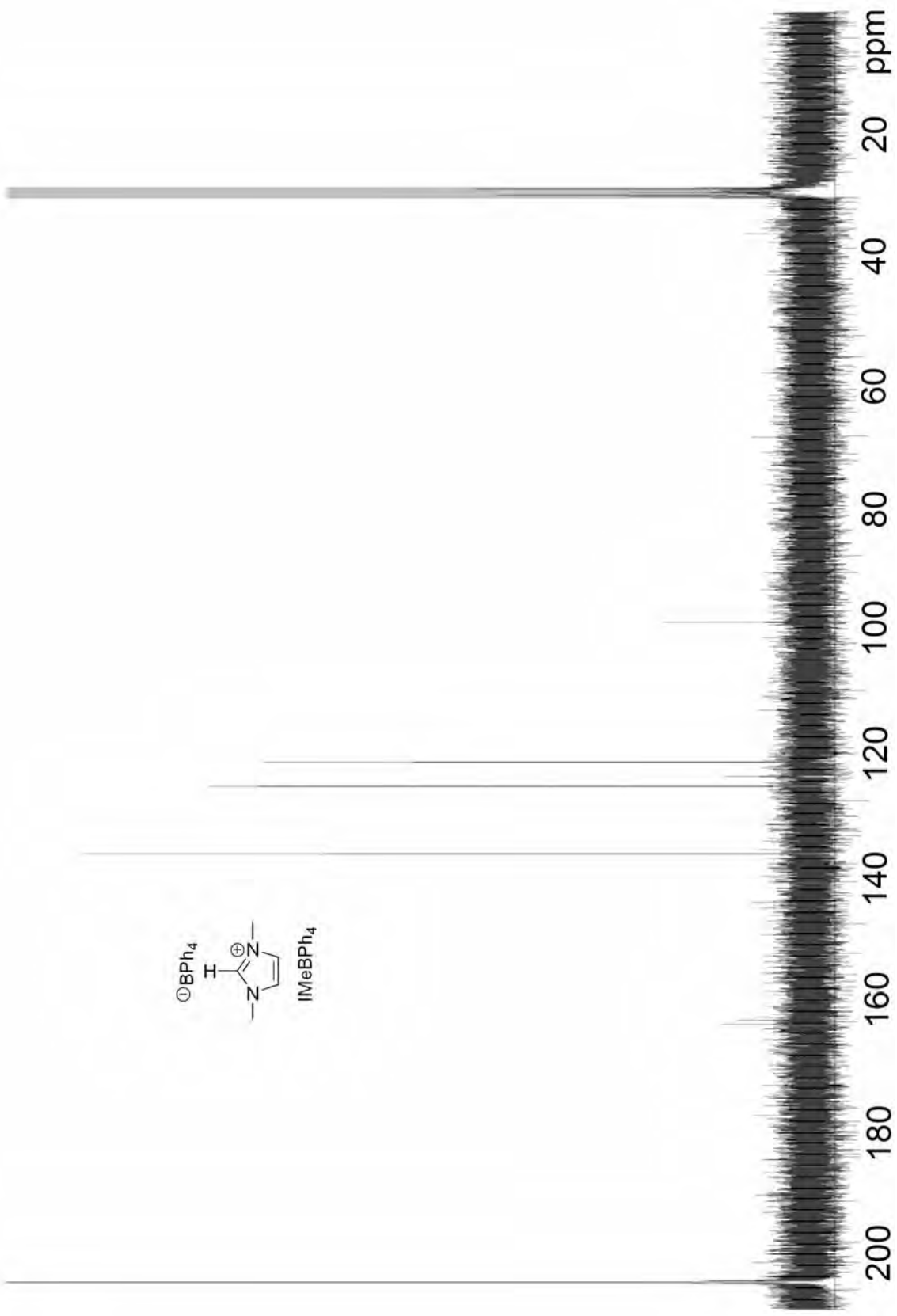
ppm
20
40
60
80
100
120
140
160
180
200
IMeBPh4
⊖BPh4

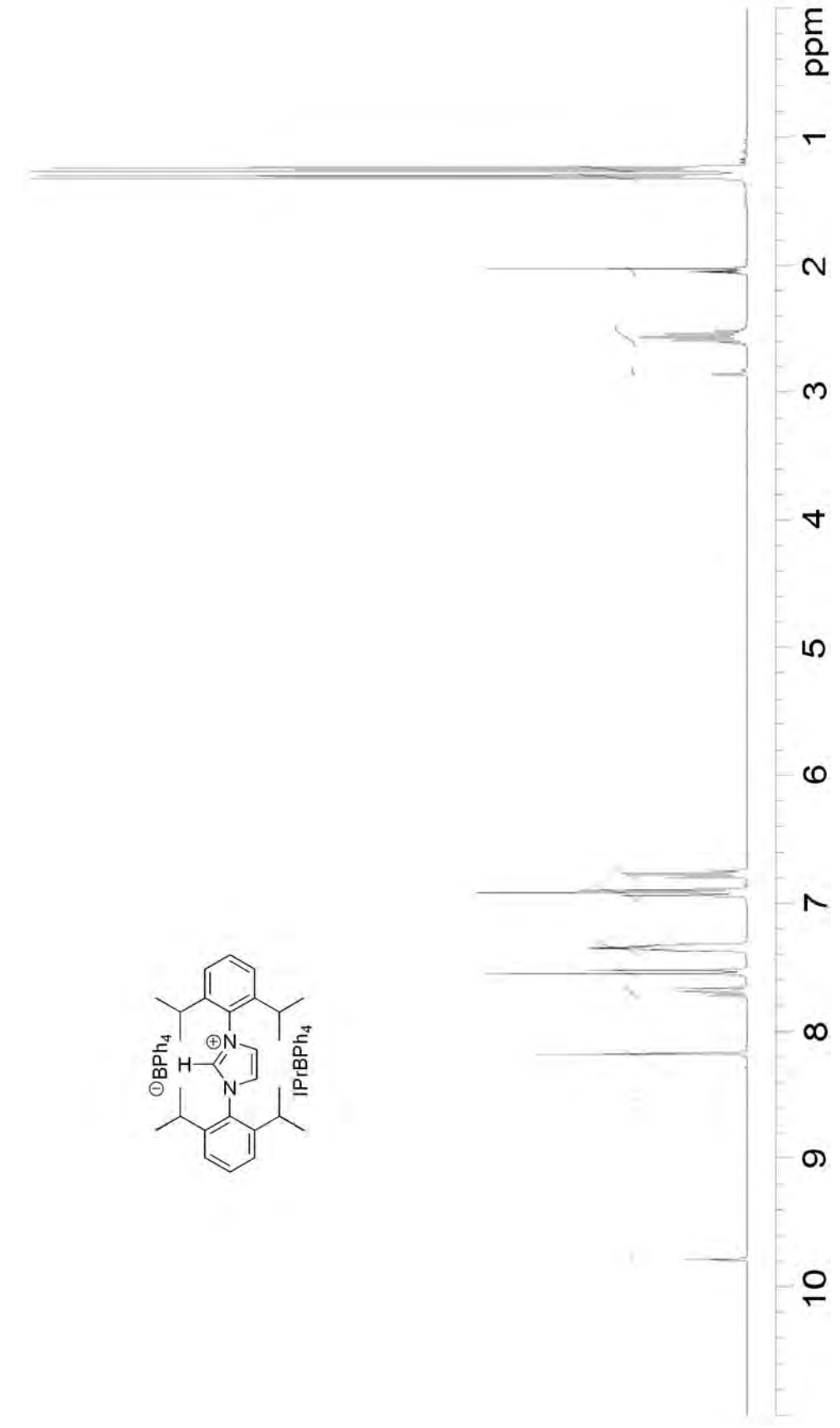
ppm
1
2
3
4
5
6
7
8
9
10
IPrBPh4
BPh4

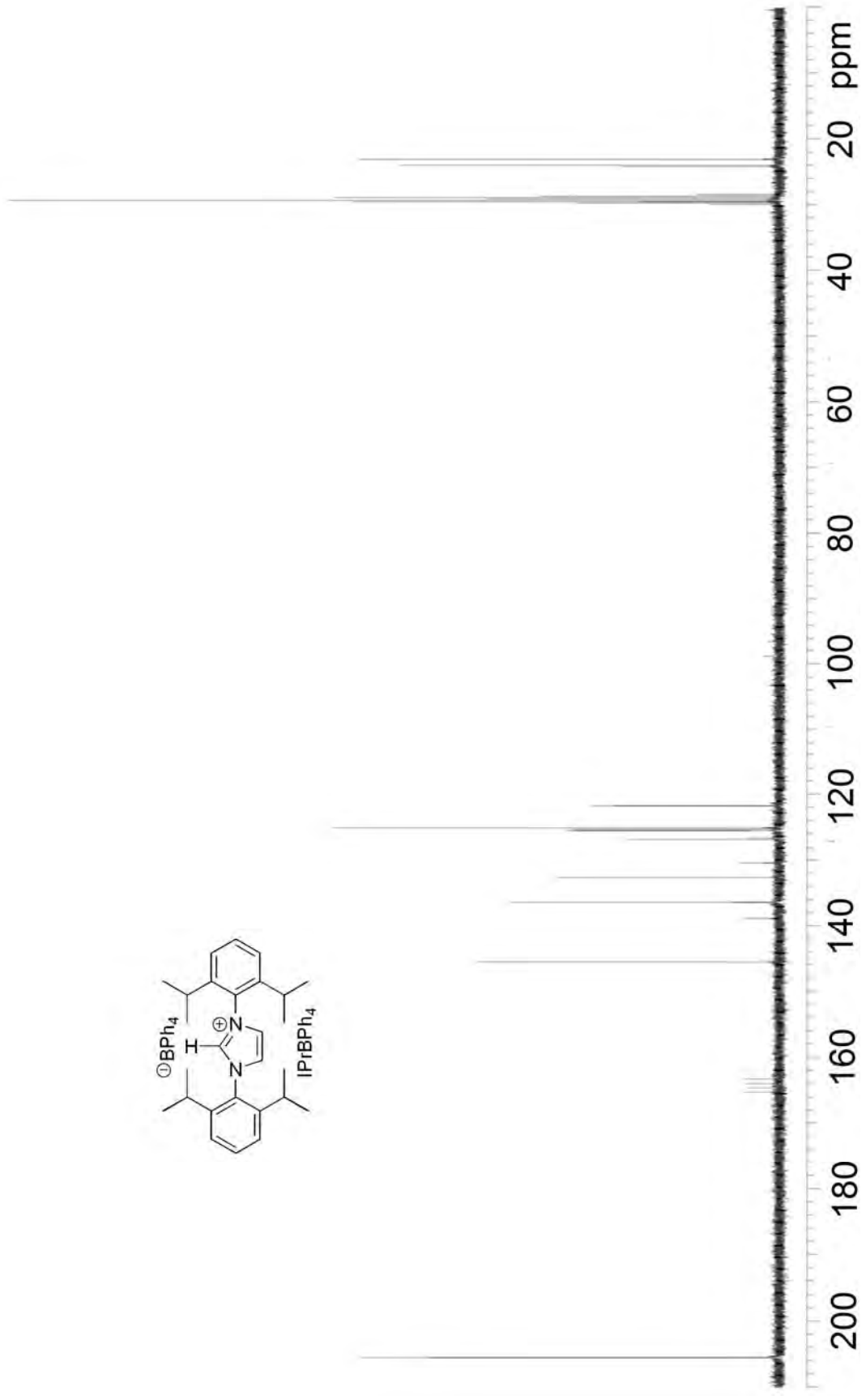
ppm
20
40
60
80
100
120
140
160
180
200
⊖BPh4
IPrBPh4
H
N
N

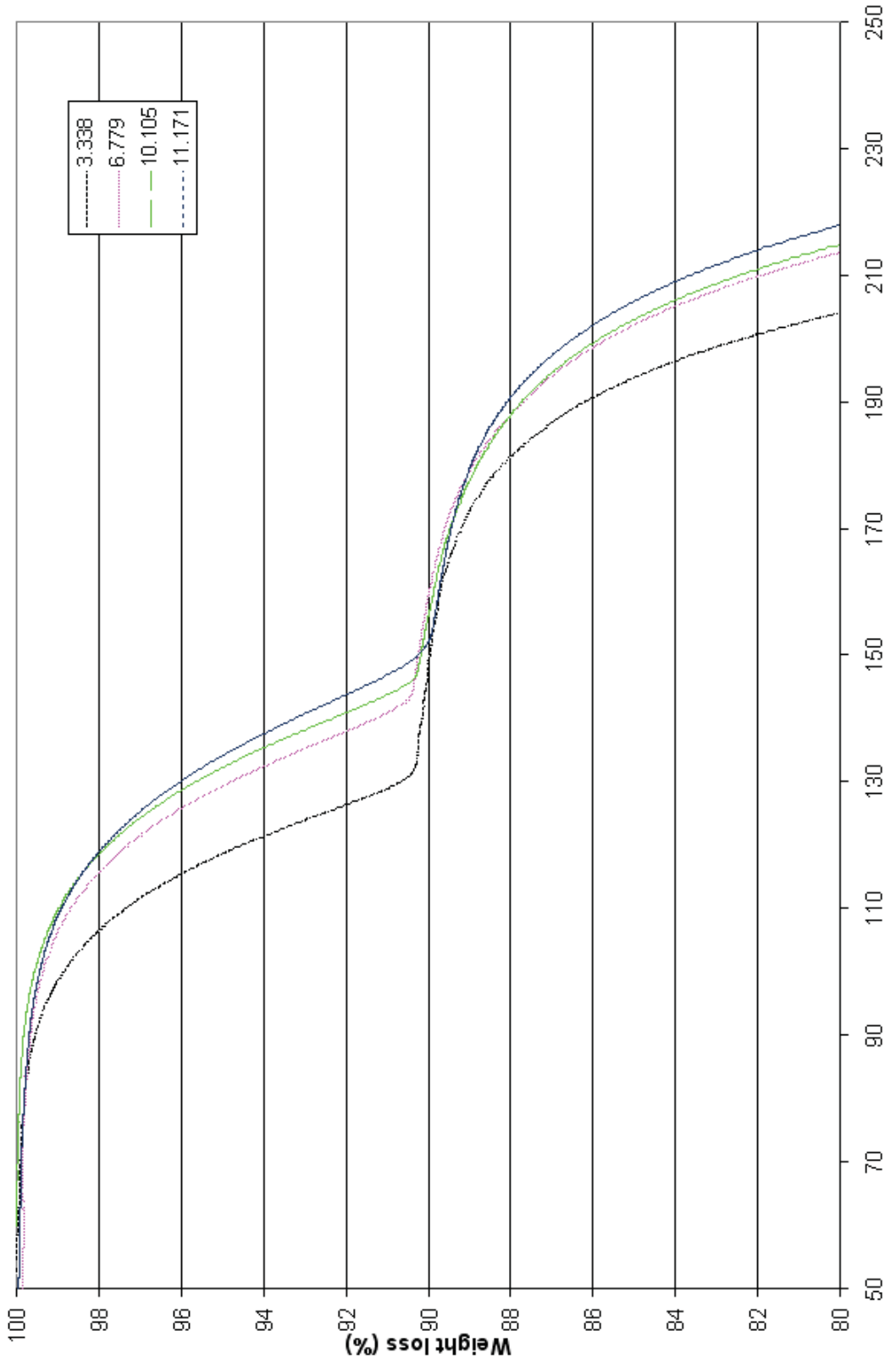

TGA data of $IPrCO_2$ at masses in the TGA instrument

Thermal ellipsoid diagram of **2a$_{Me}$** drawn at 50% probability.

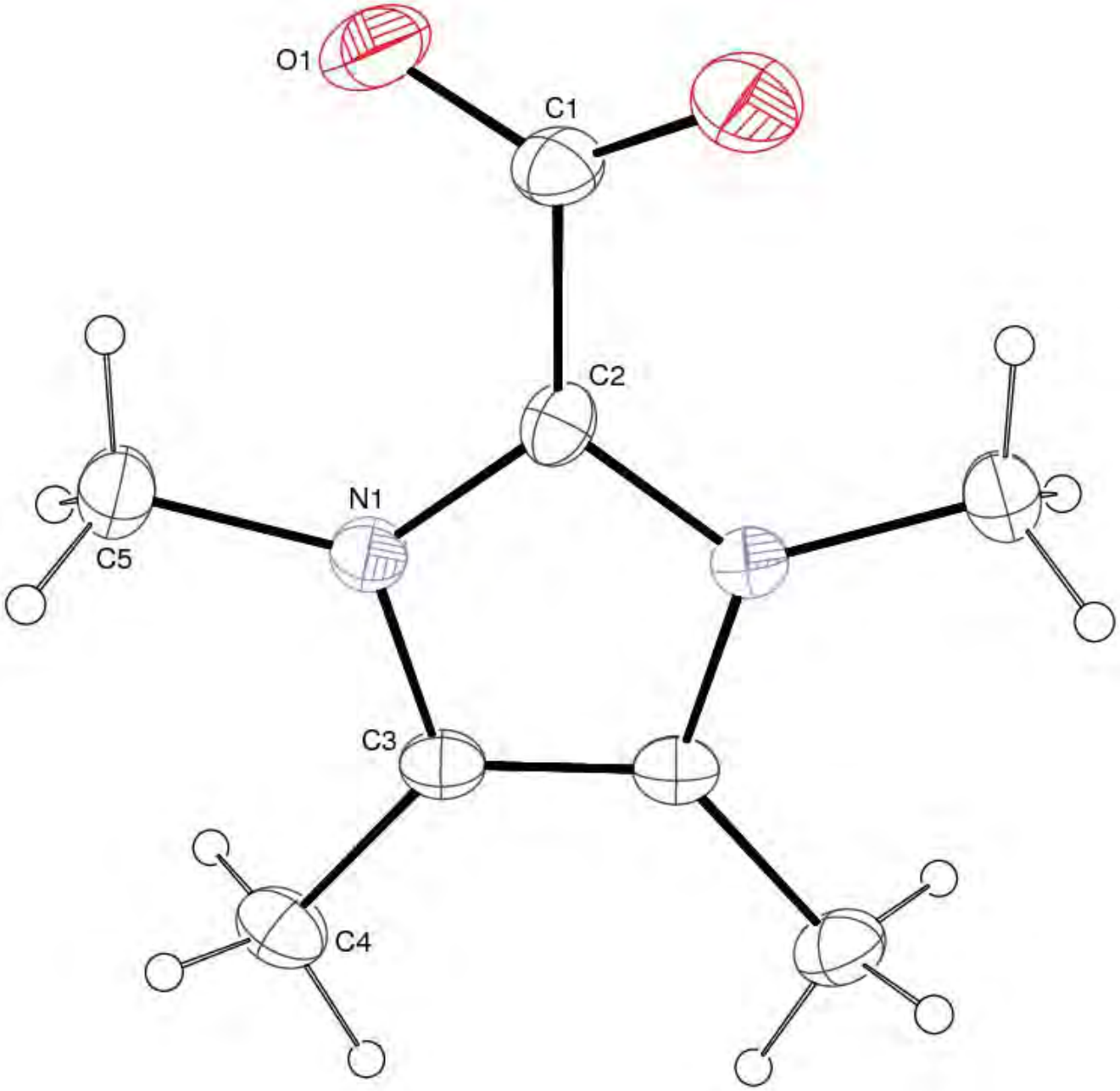

Crystal data and structure refinement for **$2a_{Me}$**.

Crystal Data		
Empirical formula	$C_8 H_{12} N_2 O_2$	
Formula weight	168.20	
Temperature	150(1) K	
Wavelength	0.71073 Å	
Crystal system	Tetragonal	
Space group	$\boldsymbol{P}4_32_12$	
Unit cell dimensions	a = 6.10930(10) Å	α= 90°.
	b = 6.10930(10) Å	β= 90°.
	c = 22.3025(7) Å	γ = 90°.
Volume	832.41(3) $Å^3$	
Z	4	
Density (calculated)	1.342 Mg/m^3	
Absorption coefficient	0.098 mm^{-1}	
F(000)	360	
Data Collection		
Diffractometer	Nonius KappaCCD	
Wavelength	0.71073 Å	
Temperature	150(1)K	
Crystal size	0.35 x 0.35 x 0.25 mm^3	
Theta range for data collection	3.46 to 27.81°	
Index ranges	-8<=h<=8, -5<=k<=5, -20<=l<=29	
Reflections collected	1593	
Independent reflections	977 [R(int) = 0.0216]	
Completeness to theta = 27.81°	98.9 %	
Solution and Refinement		
System Used	SIR 97	
Solution	Direct methods and heavy atom	
Absorption correction	Multi-scan	
Max. and min. transmission	0.9759 and 0.9665	
Refinement method	Full-matrix least-squares on F^2	
Data / restraints / parameters	977 / 0 / 77	
Goodness-of-fit on F^2	1.078	
Final R indices [I>2sigma(I)]	R1 = 0.0346, wR2 = 0.0858	
R indices (all data)	R1 = 0.0382, wR2 = 0.0883	
Absolute structure parameter	0(2)	
Extinction coefficient	0.055(15)	
Largest diff. peak and hole	0.272 and -0.234 $e.Å^{-3}$	

Atomic coordinates (x 10^4) and equivalent isotropic displacement parameters ($Å^2$x 10^3) for **2a$_{Me}$.** U(eq) is defined as one third of the trace of the orthogonalized U^{ij} tensor.

	x	y	z	U(eq)
O(1)	4729(2)	3977(2)	9523(1)	42(1)
N(1)	8468(2)	6881(2)	9625(1)	20(1)
C(1)	4960	4960	10000	24(1)
C(2)	6720	6720	10000	20(1)
C(3)	9708(2)	8715(2)	9765(1)	20(1)
C(4)	11697(2)	9331(3)	9419(1)	27(1)
C(5)	9135(3)	5298(3)	9165(1)	29(1)

Bond lengths [Å] and angles [°] for **2a$_{Me}$.**

O(1)-C(1)	1.2298(11)
N(1)-C(2)	1.3596(11)
N(1)-C(3)	1.3879(17)
N(1)-C(5)	1.4688(18)
C(1)-O(1)#1	1.2298(11)
C(1)-C(2)	1.5205
C(2)-N(1)#1	1.3595(11)
C(3)-C(3)#1	1.354(3)
C(3)-C(4)	1.488(2)
C(4)-H(4A)	0.94(2)
C(4)-H(4B)	0.99(2)
C(4)-H(4C)	1.009(19)
C(5)-H(5A)	0.97(2)
C(5)-H(5B)	0.99(2)
C(5)-H(5C)	0.93(3)

C(2)-N(1)-C(3) 110.43(9)

C(2)-N(1)-C(5) 126.88(11)
C(3)-N(1)-C(5) 122.51(12)
O(1)#1-C(1)-O(1)129.53(11)
O(1)#1-C(1)-C(2)115.23(5)
O(1)-C(1)-C(2) 115.23(5)
N(1)#1-C(2)-N(1)105.31(10)
N(1)#1-C(2)-C(1)127.35(5)
N(1)-C(2)-C(1) 127.34(5)
C(3)#1-C(3)-N(1)106.91(7)
C(3)#1-C(3)-C(4)130.83(8)
N(1)-C(3)-C(4) 122.24(12)
C(3)-C(4)-H(4A)109.1(12)
C(3)-C(4)-H(4B)109.3(12)
H(4A)-C(4)-H(4B)111.1(17)
C(3)-C(4)-H(4C)108.3(11)
H(4A)-C(4)-H(4C)108.0(16)
H(4B)-C(4)-H(4C)110.9(16)
N(1)-C(5)-H(5A)110.8(12)
N(1)-C(5)-H(5B)108.4(13)
H(5A)-C(5)-H(5B)107.4(17)
N(1)-C(5)-H(5C)107.3(14)
H(5A)-C(5)-H(5C)111.7(17)
H(5B)-C(5)-H(5C)111.2(18)

Symmetry transformations used to generate equivalent atoms:
#1 y,x,-z+2

Anisotropic displacement parameters ($Å^2 x\ 10^3$)for **2a$_{Me}$.** The anisotropic displacement factor exponent takes the form: $-2\pi^2[h^2a^{*2}U^{11} + ... + 2\ h\ k\ a^*\ b^*\ U^{12}]$

	U^{11}	U^{22}	U^{33}	U^{23}	U^{13}	U^{12}
O(1)	44(1)	44(1)	38(1)	-14(1)	4(1)	-22(1)
N(1)	20(1)	19(1)	21(1)	0(1)	2(1)	-2(1)
C(1)	24(1)	17	30(1)	0	0	-4(1)
C(2)	25(1)	14	19(1)	0	0	1(1)
C(3)	19(1)	19(1)	23(1)	3(1)	-3(1)	-3(1)
C(4)	22(1)	28(1)	31(1)	4(1)	4(1)	-4(1)
C(5)	31(1)	26(1)	30(1)	-7(1)	7(1)	-2(1)

Hydrogen coordinates ($x\ 10^4$) and isotropic displacement parameters ($Å^2 x\ 10^3$) for **2a$_{Me}$**.

	x	y	z	U(eq)
H(4A)	12680(30)	8150(30)	9417(8)	37(5)
H(4B)	12370(30)	10650(30)	9603(9)	40(5)
H(4C)	11250(30)	9630(30)	8991(8)	39(5)
H(5A)	10540(40)	4650(30)	9263(8)	39(5)
H(5B)	9310(30)	6090(40)	8780(9)	44(6)
H(5C)	8040(40)	4240(40)	9140(10)	52(6)

Torsion angles [°] for **2a$_{Me}$**.

C(3)-N(1)-C(2)-N(1)#1	-0.02(7)
C(5)-N(1)-C(2)-N(1)#1	175.16(15)
C(3)-N(1)-C(2)-C(1)	179.98(7)
C(5)-N(1)-C(2)-C(1)	-4.84(15)
O(1)#1-C(1)-C(2)-N(1)#1	-22.41(10)
O(1)-C(1)-C(2)-N(1)#1	157.59(10)
O(1)#1-C(1)-C(2)-N(1)	157.60(10)
O(1)-C(1)-C(2)-N(1)	-22.41(10)
C(2)-N(1)-C(3)-C(3)#1	0.06(18)
C(5)-N(1)-C(3)-C(3)#1	-175.37(14)
C(2)-N(1)-C(3)-C(4)	-178.56(11)
C(5)-N(1)-C(3)-C(4)	6.0(2)

Symmetry transformations used to generate equivalent atoms:
#1 y,x,-z+2

Thermal ellipsoid diagram of **2b$_{Me}$** drawn at 50% probability.

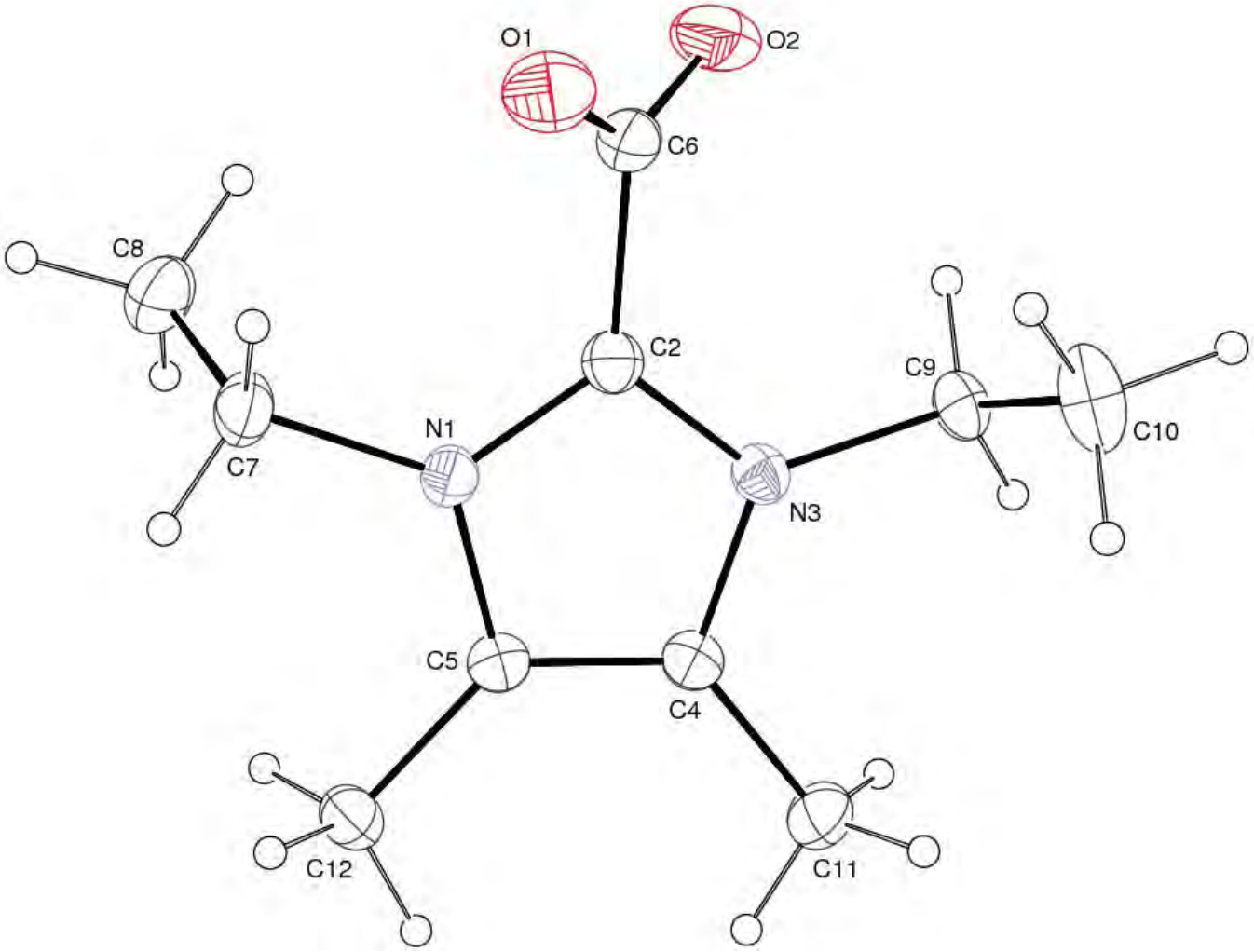

Crystal data and structure refinement for **$2b_{Me}$**.

Crystal Data		
Empirical formula	$C_{10.67}\ H_{17}\ N_{2.33}\ O_2$	
Formula weight	209.93	
Temperature	150(1) K	
Wavelength	0.71073 Å	
Crystal system	Trigonal	
Space group	$R\bar{3}$	
Unit cell dimensions	a = 18.7559(3) Å	α= 90°.
	b = 18.7559(3) Å	β= 90°.
	c = 16.2998(3) Å	γ= 120°.
Volume	4965.79(14) $Å^3$	
Z	18	
Density (calculated)	1.264 Mg/m^3	
Absorption coefficient	0.088 mm^{-1}	
F(000)	2040	
Data Collection		
Diffractometer	Nonius KappaCCD	
Wavelength	0.71073 Å	
Temperature	150(1)K	
Crystal size	0.43 x 0.40 x 0.33 mm^3	
Theta range for data collection	2.17 to 27.48°.	
Index ranges	-23<=h<=24, -20<=k<=20, -18<=l<=21	
Reflections collected	4522	
Independent reflections	2519 [R(int) = 0.0214]	
Completeness to theta = 27.48°	99.4 %	
Solution and Refinement		
System Used	SIR 97	
Solution	Direct methods and heavy atom	
Absorption correction	Multi-scan	
Max. and min. transmission	0.9714 and 0.9630	
Refinement method	Full-matrix least-squares on F^2	
Data / restraints / parameters	2519 / 0 / 204	
Goodness-of-fit on F^2	1.060	
Final R indices [I>2sigma(I)]	R1 = 0.0386, wR2 = 0.0936	
R indices (all data)	R1 = 0.0466, wR2 = 0.0986	
Largest diff. peak and hole	0.247 and -0.220 $e.Å^{-3}$	

Atomic coordinates (x 10^4) and equivalent isotropic displacement parameters (Å^{2}x 10^3) for **2b$_{Me}$.** U(eq) is defined as one third of the trace of the orthogonalized U^{ij} tensor.

	x	y	z	U(eq)
O(1)	3139(1)	1918(1)	3701(1)	35(1)
O(2)	1977(1)	1944(1)	3402(1)	37(1)
N(1)	2204(1)	242(1)	2955(1)	18(1)
N(2)	0	0	1804(2)	57(1)
N(3)	1950(1)	890(1)	2009(1)	18(1)
C(2)	2195(1)	937(1)	2788(1)	19(1)
C(4)	1810(1)	151(1)	1666(1)	18(1)
C(5)	1955(1)	-265(1)	2267(1)	18(1)
C(6)	2463(1)	1678(1)	3360(1)	24(1)
C(7)	2442(1)	45(1)	3752(1)	25(1)
C(8)	1758(1)	-242(1)	4374(1)	34(1)
C(9)	1854(1)	1533(1)	1584(1)	21(1)
C(10)	2666(1)	2227(1)	1291(1)	34(1)
C(11)	1584(1)	-65(1)	789(1)	25(1)
C(12)	1875(1)	-1094(1)	2267(1)	23(1)
C(13)	0	0	2507(3)	50(1)
C(14)	0	0	3382(3)	71(1)

Bond lengths [Å] and angles [°] for **2b$_{Me}$.**

O(1)-C(6)	1.2439(15)
O(2)-C(6)	1.2392(15)
N(1)-C(2)	1.3409(14)
N(1)-C(5)	1.3929(13)
N(1)-C(7)	1.4787(14)
N(2)-C(13)	1.146(5)
N(3)-C(2)	1.3376(14)
N(3)-C(4)	1.3930(14)
N(3)-C(9)	1.4769(13)
C(2)-C(6)	1.5350(15)
C(4)-C(5)	1.3608(15)
C(4)-C(11)	1.4880(15)
C(5)-C(12)	1.4857(15)
C(7)-C(8)	1.5084(18)
C(7)-H(7A)	0.971(15)
C(7)-H(7B)	0.969(15)
C(8)-H(8A)	0.981(18)
C(8)-H(8B)	0.989(18)
C(8)-H(8C)	0.996(16)
C(9)-C(10)	1.5029(17)
C(9)-H(9A)	0.968(15)
C(9)-H(9B)	0.973(14)
C(10)-H(10A)	0.938(17)
C(10)-H(10B)	1.003(17)
C(10)-H(10C)	0.980(19)
C(11)-H(11A)	0.999(15)
C(11)-H(11B)	0.973(16)
C(11)-H(11C)	0.970(15)
C(12)-H(12A)	0.981(16)
C(12)-H(12B)	0.985(15)
C(12)-H(12C)	0.962(15)
C(13)-C(14)	1.426(6)
C(14)-H(14)	1.00(2)

C(2)-N(1)-C(5) 109.65(9)
C(2)-N(1)-C(7) 125.12(9)
C(5)-N(1)-C(7) 125.23(9)
C(2)-N(3)-C(4) 109.51(9)
C(2)-N(3)-C(9) 124.69(9)
C(4)-N(3)-C(9) 125.80(9)
N(3)-C(2)-N(1) 107.49(9)
N(3)-C(2)-C(6) 125.68(9)
N(1)-C(2)-C(6) 126.74(10)
C(5)-C(4)-N(3) 106.85(9)
C(5)-C(4)-C(11) 130.25(10)
N(3)-C(4)-C(11) 122.84(10)
C(4)-C(5)-N(1) 106.47(9)
C(4)-C(5)-C(12) 130.97(10)
N(1)-C(5)-C(12) 122.56(9)
O(2)-C(6)-O(1) 130.69(11)
O(2)-C(6)-C(2) 115.00(10)
O(1)-C(6)-C(2) 114.31(10)
N(1)-C(7)-C(8) 111.73(11)
N(1)-C(7)-H(7A) 105.8(8)
C(8)-C(7)-H(7A) 112.0(8)
N(1)-C(7)-H(7B) 107.2(8)
C(8)-C(7)-H(7B) 112.5(9)
H(7A)-C(7)-H(7B) 107.2(12)
C(7)-C(8)-H(8A) 110.4(10)
C(7)-C(8)-H(8B) 109.1(10)
H(8A)-C(8)-H(8B) 110.3(14)
C(7)-C(8)-H(8C) 109.8(9)
H(8A)-C(8)-H(8C) 107.8(14)
H(8B)-C(8)-H(8C) 109.4(13)
N(3)-C(9)-C(10) 111.82(9)
N(3)-C(9)-H(9A) 105.9(8)
C(10)-C(9)-H(9A) 112.3(9)
N(3)-C(9)-H(9B) 105.9(8)
C(10)-C(9)-H(9B) 111.0(8)
H(9A)-C(9)-H(9B) 109.8(12)

C(9)-C(10)-H(10A)108.3(10)
C(9)-C(10)-H(10B)110.2(9)
H(10A)-C(10)-H(10B)
C(9)-C(10)-H(10C)109.3(11)
H(10A)-C(10)-H(10C)
H(10B)-C(10)-H(10C)
C(4)-C(11)-H(11A)110.9(8)
C(4)-C(11)-H(11B)111.4(9)
H(11A)-C(11)-H(11B)
C(4)-C(11)-H(11C)109.9(8)
H(11A)-C(11)-H(11C)
H(11B)-C(11)-H(11C)
C(5)-C(12)-H(12A)111.8(9)
C(5)-C(12)-H(12B)108.6(9)
H(12A)-C(12)-H(12B)
C(5)-C(12)-H(12C)109.3(9)
H(12A)-C(12)-H(12C)
H(12B)-C(12)-H(12C)
N(2)-C(13)-C(14)180.000(1)
C(13)-C(14)-H(14)109.7(14)

Symmetry transformations used to generate equivalent atoms:
#1 y,x,-z+2

Anisotropic displacement parameters ($Å^2 x\ 10^3$)for **$2b_{Me}$.** The anisotropic displacement factor exponent takes the form: $-2\pi^2[h^2a^{*2}U^{11} + ... + 2\ h\ k\ a^*\ b^*\ U^{12}]$

	U^{11}	U^{22}	U^{33}	U^{23}	U^{13}	U^{12}
O(1)	37(1)	26(1)	33(1)	-9(1)	-11(1)	11(1)
O(2)	51(1)	37(1)	36(1)	-10(1)	-3(1)	31(1)
N(1)	21(1)	17(1)	16(1)	0(1)	-1(1)	9(1)
N(2)	26(1)	26(1)	119(3)	0	0	13(1)
N(3)	17(1)	17(1)	19(1)	0(1)	-1(1)	9(1)
C(2)	19(1)	18(1)	19(1)	1(1)	1(1)	9(1)
C(4)	16(1)	17(1)	20(1)	-1(1)	0(1)	8(1)
C(5)	16(1)	18(1)	18(1)	-1(1)	0(1)	7(1)
C(6)	33(1)	18(1)	18(1)	0(1)	0(1)	11(1)
C(7)	31(1)	21(1)	20(1)	1(1)	-6(1)	11(1)
C(8)	49(1)	31(1)	21(1)	5(1)	4(1)	19(1)
C(9)	23(1)	20(1)	24(1)	3(1)	-2(1)	13(1)
C(10)	27(1)	28(1)	46(1)	15(1)	1(1)	12(1)
C(11)	29(1)	25(1)	19(1)	-2(1)	-4(1)	13(1)
C(12)	26(1)	20(1)	24(1)	-1(1)	-2(1)	13(1)
C(13)	22(1)	22(1)	108(3)	0	0	11(1)
C(14)	49(1)	49(1)	115(3)	0	0	24(1)

Hydrogen coordinates (x 10^4) and isotropic displacement parameters (Å^{2}x 10^3) for **2b$_{Me}$**.

	x	y	z	U(eq)
H(7A)	2933(9)	545(9)	3926(8)	27(4)
H(7B)	2604(9)	-364(9)	3647(8)	31(4)
H(8A)	1623(10)	192(11)	4480(10)	47(5)
H(8B)	1932(10)	-393(10)	4887(11)	47(5)
H(8C)	1253(10)	-732(10)	4159(9)	39(4)
H(9A)	1590(9)	1716(9)	1973(9)	28(4)
H(9B)	1486(9)	1258(9)	1124(9)	28(4)
H(10A)	3014(10)	2451(10)	1746(11)	42(4)
H(10B)	2586(10)	2658(10)	1013(10)	42(4)
H(10C)	2906(11)	2014(11)	892(11)	54(5)
H(11A)	1060(9)	-73(9)	657(8)	30(4)
H(11B)	2012(9)	328(9)	425(9)	34(4)
H(11C)	1521(9)	-601(9)	673(8)	29(4)
H(12A)	2389(10)	-1071(9)	2433(9)	36(4)
H(12B)	1450(9)	-1442(9)	2669(9)	33(4)
H(12C)	1722(9)	-1329(9)	1727(9)	30(4)
H(14)	475(14)	528(14)	3590(14)	91(8)

Torsion angles [°] for **2b$_{Me}$**.

C(4)-N(3)-C(2)-N(1)	-0.85(12)
C(9)-N(3)-C(2)-N(1)	179.82(9)
C(4)-N(3)-C(2)-C(6)	175.85(10)
C(9)-N(3)-C(2)-C(6)	-3.49(17)
C(5)-N(1)-C(2)-N(3)	-0.32(12)
C(7)-N(1)-C(2)-N(3)	179.81(10)
C(5)-N(1)-C(2)-C(6)	-176.97(10)
C(7)-N(1)-C(2)-C(6)	3.16(18)
C(2)-N(3)-C(4)-C(5)	1.70(12)
C(9)-N(3)-C(4)-C(5)	-178.98(10)
C(2)-N(3)-C(4)-C(11)	-175.88(10)
C(9)-N(3)-C(4)-C(11)	3.45(17)
N(3)-C(4)-C(5)-N(1)	-1.82(12)
C(11)-C(4)-C(5)-N(1)	175.51(11)
N(3)-C(4)-C(5)-C(12)	177.42(11)
C(11)-C(4)-C(5)-C(12)	-5.2(2)
C(2)-N(1)-C(5)-C(4)	1.36(12)
C(7)-N(1)-C(5)-C(4)	-178.76(10)
C(2)-N(1)-C(5)-C(12)	-177.96(10)
C(7)-N(1)-C(5)-C(12)	1.92(16)
N(3)-C(2)-C(6)-O(2)	50.79(16)
N(1)-C(2)-C(6)-O(2)	-133.15(12)
N(3)-C(2)-C(6)-O(1)	-128.52(12)
N(1)-C(2)-C(6)-O(1)	47.55(16)
C(2)-N(1)-C(7)-C(8)	78.51(14)
C(5)-N(1)-C(7)-C(8)	-101.35(13)
C(2)-N(3)-C(9)-C(10)	79.95(14)
C(4)-N(3)-C(9)-C(10)	-99.28(13)

Symmetry transformations used to generate equivalent atoms:
#1 y,x,-z+2

Thermal ellipsoid diagram of **2f** drawn at 50% probability.

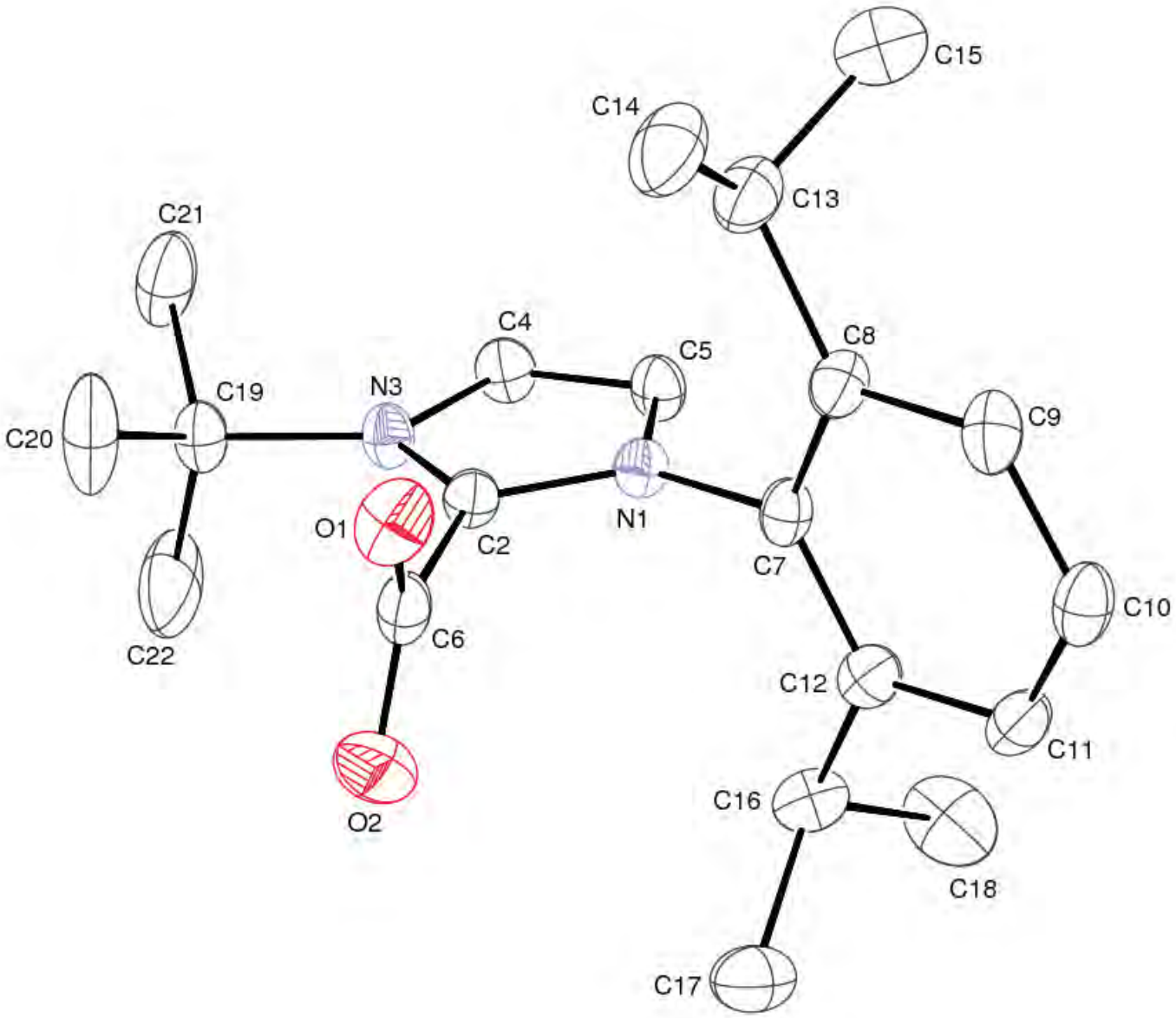

Crystal data and structure refinement for **2f.**

Crystal Data		
Empirical formula	$C_{20}H_{28}N_2O_2$	
Formula weight	328.44	
Temperature	150(1) K	
Wavelength	0.71073 Å	
Crystal system	Tetragonal	
Space group	$P4_1$	
Unit cell dimensions	a = 14.6394(4) Å	α= 90°.
	b = 14.6394(4) Å	β= 90°.
	c = 18.0698(4) Å	γ= 90°.
Volume	3872.58(17) $Å^3$	
Z	8	
Density (calculated)	1.127 Mg/m^3	
Absorption coefficient	0.073 mm^{-1}	
F(000)	1424	
Data Collection		
Diffractometer	Nonius KappaCCD	
Wavelength	0.71073 Å	
Temperature	150(1)K	
Crystal size	0.33 x 0.30 x 0.28 mm^3	
Theta range for data collection	1.39 to 27.47°.	
Index ranges	-18<=h<=19, -13<=k<=13, -23<=l<=21	
Reflections collected	8513	
Independent reflections	8487 [R(int) = 0.0000]	
Completeness to theta = 27.47°	99.9 %	
Solution and Refinement		
System Used	SIR 97	
Solution	Direct methods and heavy atom	
Absorption correction	Multi-scan	
Max. and min. transmission	0.9799 and 0.9764	
Refinement method	Full-matrix least-squares on F^2	
Data / restraints / parameters	8487 / 1 / 435	
Goodness-of-fit on F^2	1.071	
Final R indices [I>2sigma(I)]	R1 = 0.0599, wR2 = 0.1188	
R indices (all data)	R1 = 0.0929, wR2 = 0.1357	
Absolute structure parameter	2.3(17)	
Extinction coefficient	0.0086(7)	
Largest diff. peak and hole	0.179 and -0.166 $e.Å^{-3}$	

Atomic coordinates (x 10^4) and equivalent isotropic displacement parameters ($Å^2$x 10^3) for **2f.** U(eq) is defined as one third of the trace of the orthogonalized U^{ij} tensor.

	x	y	z	U(eq)
O(1)	8094(2)	1997(2)	7604(1)	53(1)
O(2)	6590(2)	1727(2)	7568(2)	64(1)
N(1)	7679(2)	384(2)	8666(1)	33(1)
N(3)	7530(2)	-255(2)	7594(1)	37(1)
C(2)	7553(2)	557(2)	7945(2)	33(1)
C(4)	7636(3)	-950(2)	8118(2)	42(1)
C(5)	7734(2)	-548(2)	8782(2)	40(1)
C(6)	7391(3)	1526(2)	7664(2)	41(1)
C(7)	7779(2)	1088(2)	9230(2)	35(1)
C(8)	8650(2)	1439(2)	9365(2)	39(1)
C(9)	8719(3)	2119(2)	9900(2)	45(1)
C(10)	7969(3)	2424(2)	10283(2)	44(1)
C(11)	7116(2)	2050(2)	10142(2)	42(1)
C(12)	7001(2)	1382(2)	9604(2)	39(1)
C(13)	9499(3)	1096(3)	8974(2)	52(1)
C(14)	10007(3)	1885(3)	8590(2)	65(1)
C(15)	10113(3)	579(3)	9509(3)	74(1)
C(16)	6053(2)	1005(3)	9448(2)	49(1)
C(17)	5414(3)	1767(3)	9185(3)	61(1)
C(18)	5675(3)	526(4)	10128(3)	80(1)
C(19)	7410(3)	-432(2)	6774(2)	43(1)
C(20)	7767(4)	364(3)	6336(2)	83(2)
C(21)	7983(4)	-1273(3)	6584(2)	74(1)
C(22)	6434(4)	-598(6)	6644(3)	126(3)
O(1A)	3063(2)	-3439(2)	10055(1)	54(1)
O(2A)	3124(2)	-1940(2)	10299(2)	56(1)
N(1A)	4625(2)	-2602(2)	9104(1)	32(1)
N(3A)	5221(2)	-2616(2)	10202(1)	33(1)
C(2A)	4432(2)	-2645(2)	9832(2)	30(1)
C(4A)	5931(2)	-2538(2)	9689(2)	39(1)
C(5A)	5567(2)	-2527(2)	9010(2)	38(1)

C(6A)	3432(2)	-2680(3)	10102(2)	40(1)
C(7A)	3954(2)	-2563(2)	8519(2)	33(1)
C(8A)	3647(2)	-3378(2)	8204(2)	36(1)
C(9A)	3014(3)	-3313(3)	7632(2)	46(1)
C(10A)	2709(3)	-2476(3)	7390(2)	49(1)
C(11A)	3029(3)	-1677(3)	7709(2)	48(1)
C(12A)	3658(2)	-1705(2)	8283(2)	39(1)
C(13A)	3997(3)	-4314(2)	8446(2)	47(1)
C(14A)	3207(3)	-4925(3)	8696(2)	63(1)
C(15A)	4547(3)	-4763(3)	7829(2)	66(1)
C(16A)	3995(3)	-822(2)	8618(2)	48(1)
C(17A)	3228(3)	-283(3)	8985(2)	58(1)
C(18A)	4486(3)	-253(3)	8019(3)	75(1)
C(19A)	5365(2)	-2613(2)	11029(2)	39(1)
C(20A)	4571(3)	-3079(3)	11420(2)	49(1)
C(21A)	6232(3)	-3161(4)	11186(2)	67(1)
C(22A)	5455(5)	-1633(3)	11266(2)	85(2)

Bond lengths [Å] and angles [°] for **2f.**

O(1)-C(6)	1.242(4)
O(2)-C(6)	1.223(5)
N(1)-C(2)	1.340(4)
N(1)-C(5)	1.382(4)
N(1)-C(7)	1.456(4)
N(3)-C(2)	1.348(4)
N(3)-C(4)	1.398(4)
N(3)-C(19)	1.515(4)
C(2)-C(6)	1.525(5)
C(4)-C(5)	1.345(5)
C(4)-H(4)	0.9500
C(5)-H(5)	0.9500
C(7)-C(12)	1.392(5)
C(7)-C(8)	1.396(5)

C(8)-C(9)	1.393(5)
C(8)-C(13)	1.515(5)
C(9)-C(10)	1.373(5)
C(9)-H(9)	0.9500
C(10)-C(11)	1.387(5)
C(10)-H(10)	0.9500
C(11)-C(12)	1.390(5)
C(11)-H(11)	0.9500
C(12)-C(16)	1.520(5)
C(13)-C(15)	1.522(6)
C(13)-C(14)	1.539(6)
C(13)-H(13)	1.0000
C(14)-H(14A)	0.9800
C(14)-H(14B)	0.9800
C(14)-H(14C)	0.9800
C(15)-H(15A)	0.9800
C(15)-H(15B)	0.9800
C(15)-H(15C)	0.9800
C(16)-C(18)	1.520(6)
C(16)-C(17)	1.530(6)
C(16)-H(16)	1.0000
C(17)-H(17A)	0.9800
C(17)-H(17B)	0.9800
C(17)-H(17C)	0.9800
C(18)-H(18A)	0.9800
C(18)-H(18B)	0.9800
C(18)-H(18C)	0.9800
C(19)-C(22)	1.468(6)
C(19)-C(20)	1.502(6)
C(19)-C(21)	1.529(6)
C(20)-H(20A)	0.9800
C(20)-H(20B)	0.9800
C(20)-H(20C)	0.9800
C(21)-H(21A)	0.9800
C(21)-H(21B)	0.9800
C(21)-H(21C)	0.9800

C(22)-H(22A)	0.9800
C(22)-H(22B)	0.9800
C(22)-H(22C)	0.9800
O(1A)-C(6A)	1.238(4)
O(2A)-C(6A)	1.227(4)
N(1A)-C(2A)	1.348(4)
N(1A)-C(5A)	1.395(4)
N(1A)-C(7A)	1.444(4)
N(3A)-C(2A)	1.334(4)
N(3A)-C(4A)	1.398(4)
N(3A)-C(19A)	1.509(4)
C(2A)-C(6A)	1.545(4)
C(4A)-C(5A)	1.337(5)
C(4A)-H(4A)	0.9500
C(5A)-H(5A)	0.9500
C(7A)-C(12A)	1.396(5)
C(7A)-C(8A)	1.396(5)
C(8A)-C(9A)	1.392(5)
C(8A)-C(13A)	1.526(5)
C(9A)-C(10A)	1.376(5)
C(9A)-H(9A)	0.9500
C(10A)-C(11A)	1.384(5)
C(10A)-H(10A)	0.9500
C(11A)-C(12A)	1.388(5)
C(11A)-H(11A)	0.9500
C(12A)-C(16A)	1.510(5)
C(13A)-C(15A)	1.525(5)
C(13A)-C(14A)	1.530(5)
C(13A)-H(13A)	1.0000
C(14A)-H(14D)	0.9800
C(14A)-H(14E)	0.9800
C(14A)-H(14F)	0.9800
C(15A)-H(15D)	0.9800
C(15A)-H(15E)	0.9800
C(15A)-H(15F)	0.9800
C(16A)-C(17A)	1.524(6)

C(16A)-C(18A)	1.543(6)
C(16A)-H(16A)	1.0000
C(17A)-H(17D)	0.9800
C(17A)-H(17E)	0.9800
C(17A)-H(17F)	0.9800
C(18A)-H(18D)	0.9800
C(18A)-H(18E)	0.9800
C(18A)-H(18F)	0.9800
C(19A)-C(22A)	1.503(5)
C(19A)-C(20A)	1.521(5)
C(19A)-C(21A)	1.529(5)
C(20A)-H(20D)	0.9800
C(20A)-H(20E)	0.9800
C(20A)-H(20F)	0.9800
C(21A)-H(21D)	0.9800
C(21A)-H(21E)	0.9800
C(21A)-H(21F)	0.9800
C(22A)-H(22D)	0.9800
C(22A)-H(22E)	0.9800
C(22A)-H(22F)	0.9800

C(2)-N(1)-C(5)	109.9(3)
C(2)-N(1)-C(7)	124.1(3)
C(5)-N(1)-C(7)	126.0(3)
C(2)-N(3)-C(4)	108.7(3)
C(2)-N(3)-C(19)	127.9(3)
C(4)-N(3)-C(19)	123.4(3)
N(1)-C(2)-N(3)	107.2(3)
N(1)-C(2)-C(6)	121.3(3)
N(3)-C(2)-C(6)	131.3(3)
C(5)-C(4)-N(3)	107.3(3)
C(5)-C(4)-H(4)	126.3
N(3)-C(4)-H(4)	126.3
C(4)-C(5)-N(1)	106.9(3)
C(4)-C(5)-H(5)	126.5
N(1)-C(5)-H(5)	126.5

O(2)-C(6)-O(1) 130.4(4)
O(2)-C(6)-C(2) 114.9(3)
O(1)-C(6)-C(2) 114.6(3)
C(12)-C(7)-C(8) 123.3(3)
C(12)-C(7)-N(1) 118.4(3)
C(8)-C(7)-N(1) 118.2(3)
C(9)-C(8)-C(7) 116.8(3)
C(9)-C(8)-C(13) 120.1(3)
C(7)-C(8)-C(13) 123.2(3)
C(10)-C(9)-C(8) 121.6(3)
C(10)-C(9)-H(9) 119.2
C(8)-C(9)-H(9) 119.2
C(9)-C(10)-C(11) 120.0(3)
C(9)-C(10)-H(10) 120.0
C(11)-C(10)-H(10) 120.0
C(10)-C(11)-C(12) 121.0(3)
C(10)-C(11)-H(11) 119.5
C(12)-C(11)-H(11) 119.5
C(11)-C(12)-C(7) 117.3(3)
C(11)-C(12)-C(16) 119.7(3)
C(7)-C(12)-C(16) 123.0(3)
C(8)-C(13)-C(15) 110.7(3)
C(8)-C(13)-C(14) 111.0(3)
C(15)-C(13)-C(14) 112.0(3)
C(8)-C(13)-H(13) 107.7
C(15)-C(13)-H(13) 107.7
C(14)-C(13)-H(13) 107.7
C(13)-C(14)-H(14A)
C(13)-C(14)-H(14B)
H(14A)-C(14)-H(14B)
C(13)-C(14)-H(14C)
H(14A)-C(14)-H(14C)
H(14B)-C(14)-H(14C)
C(13)-C(15)-H(15A)
C(13)-C(15)-H(15B)
H(15A)-C(15)-H(15B)

C(13)-C(15)-H(15C)
H(15A)-C(15)-H(15C)
H(15B)-C(15)-H(15C)
C(18)-C(16)-C(12)110.5(3)
C(18)-C(16)-C(17)111.4(3)
C(12)-C(16)-C(17)110.6(3)
C(18)-C(16)-H(16)108.1
C(12)-C(16)-H(16)108.1
C(17)-C(16)-H(16)108.1
C(16)-C(17)-H(17A)
C(16)-C(17)-H(17B)
H(17A)-C(17)-H(17B)
C(16)-C(17)-H(17C)
H(17A)-C(17)-H(17C)
H(17B)-C(17)-H(17C)
C(16)-C(18)-H(18A)
C(16)-C(18)-H(18B)
H(18A)-C(18)-H(18B)
C(16)-C(18)-H(18C)
H(18A)-C(18)-H(18C)
H(18B)-C(18)-H(18C)
C(22)-C(19)-C(20)112.5(4)
C(22)-C(19)-N(3)107.3(3)
C(20)-C(19)-N(3)110.0(3)
C(22)-C(19)-C(21)111.4(4)
C(20)-C(19)-C(21)108.4(4)
N(3)-C(19)-C(21)107.1(3)
C(19)-C(20)-H(20A)
C(19)-C(20)-H(20B)
H(20A)-C(20)-H(20B)
C(19)-C(20)-H(20C)
H(20A)-C(20)-H(20C)
H(20B)-C(20)-H(20C)
C(19)-C(21)-H(21A)
C(19)-C(21)-H(21B)
H(21A)-C(21)-H(21B)

C(19)-C(21)-H(21C)
H(21A)-C(21)-H(21C)
H(21B)-C(21)-H(21C)
C(19)-C(22)-H(22A)
C(19)-C(22)-H(22B)
H(22A)-C(22)-H(22B)
C(19)-C(22)-H(22C)
H(22A)-C(22)-H(22C)
H(22B)-C(22)-H(22C)
C(2A)-N(1A)-C(5A)
C(2A)-N(1A)-C(7A)
C(5A)-N(1A)-C(7A)
C(2A)-N(3A)-C(4A)
C(2A)-N(3A)-C(19A)
C(4A)-N(3A)-C(19A)
N(3A)-C(2A)-N(1A)
N(3A)-C(2A)-C(6A)
N(1A)-C(2A)-C(6A)
C(5A)-C(4A)-N(3A)
C(5A)-C(4A)-H(4A)
N(3A)-C(4A)-H(4A)
C(4A)-C(5A)-N(1A)
C(4A)-C(5A)-H(5A)
N(1A)-C(5A)-H(5A)
O(2A)-C(6A)-O(1A)
O(2A)-C(6A)-C(2A)
O(1A)-C(6A)-C(2A)
C(12A)-C(7A)-C(8A)
C(12A)-C(7A)-N(1A)
C(8A)-C(7A)-N(1A)
C(9A)-C(8A)-C(7A)
C(9A)-C(8A)-C(13A)
C(7A)-C(8A)-C(13A)
C(10A)-C(9A)-C(8A)
C(10A)-C(9A)-H(9A)
C(8A)-C(9A)-H(9A)

C(9A)-C(10A)-C(11A)
C(9A)-C(10A)-H(10A)
C(11A)-C(10A)-H(10A)
C(10A)-C(11A)-C(12A)
C(10A)-C(11A)-H(11A)
C(12A)-C(11A)-H(11A)
C(11A)-C(12A)-C(7A)
C(11A)-C(12A)-C(16A)
C(7A)-C(12A)-C(16A)
C(15A)-C(13A)-C(8A)
C(15A)-C(13A)-C(14A)
C(8A)-C(13A)-C(14A)
C(15A)-C(13A)-H(13A)
C(8A)-C(13A)-H(13A)
C(14A)-C(13A)-H(13A)
C(13A)-C(14A)-H(14D)
C(13A)-C(14A)-H(14E)
H(14D)-C(14A)-H(14E)
C(13A)-C(14A)-H(14F)
H(14D)-C(14A)-H(14F)
H(14E)-C(14A)-H(14F)
C(13A)-C(15A)-H(15D)
C(13A)-C(15A)-H(15E)
H(15D)-C(15A)-H(15E)
C(13A)-C(15A)-H(15F)
H(15D)-C(15A)-H(15F)
H(15E)-C(15A)-H(15F)
C(12A)-C(16A)-C(17A)
C(12A)-C(16A)-C(18A)
C(17A)-C(16A)-C(18A)
C(12A)-C(16A)-H(16A)
C(17A)-C(16A)-H(16A)
C(18A)-C(16A)-H(16A)
C(16A)-C(17A)-H(17D)
C(16A)-C(17A)-H(17E)
H(17D)-C(17A)-H(17E)

C(16A)-C(17A)-H(17F)
H(17D)-C(17A)-H(17F)
H(17E)-C(17A)-H(17F)
C(16A)-C(18A)-H(18D)
C(16A)-C(18A)-H(18E)
H(18D)-C(18A)-H(18E)
C(16A)-C(18A)-H(18F)
H(18D)-C(18A)-H(18F)
H(18E)-C(18A)-H(18F)
C(22A)-C(19A)-N(3A)
C(22A)-C(19A)-C(20A)
N(3A)-C(19A)-C(20A)
C(22A)-C(19A)-C(21A)
N(3A)-C(19A)-C(21A)
C(20A)-C(19A)-C(21A)
C(19A)-C(20A)-H(20D)
C(19A)-C(20A)-H(20E)
H(20D)-C(20A)-H(20E)
C(19A)-C(20A)-H(20F)
H(20D)-C(20A)-H(20F)
H(20E)-C(20A)-H(20F)
C(19A)-C(21A)-H(21D)
C(19A)-C(21A)-H(21E)
H(21D)-C(21A)-H(21E)
C(19A)-C(21A)-H(21F)
H(21D)-C(21A)-H(21F)
H(21E)-C(21A)-H(21F)
C(19A)-C(22A)-H(22D)
C(19A)-C(22A)-H(22E)
H(22D)-C(22A)-H(22E)
C(19A)-C(22A)-H(22F)
H(22D)-C(22A)-H(22F)
H(22E)-C(22A)-H(22F)

Symmetry transformations used to generate equivalent atoms:
#1 y,x,-z+2

Anisotropic displacement parameters ($Å^2 x\ 10^3$)for **2f.** The anisotropic displacement factor exponent takes the form: $-2\pi^2[h^2 a^{*2} U^{11} + ... + 2 h k a^* b^* U^{12}]$

U^{11}	U^{22}	U^{33}	U^{23}	U^{13}	U^{12}	
O(1)	67(2)	37(1)	54(2)	4(1)	13(1)	-7(1)
O(2)	64(2)	59(2)	68(2)	11(1)	-6(2)	17(2)
N(1)	38(2)	29(1)	32(1)	-1(1)	0(1)	-2(1)
N(3)	49(2)	31(1)	30(1)	-1(1)	-2(1)	-2(1)
C(2)	40(2)	28(2)	32(2)	0(1)	1(1)	2(1)
C(4)	54(2)	29(2)	43(2)	1(1)	-3(2)	1(2)
C(5)	54(2)	32(2)	33(2)	4(1)	-2(1)	2(2)
C(6)	61(2)	35(2)	27(2)	-2(1)	2(2)	5(2)
C(7)	48(2)	29(2)	27(2)	1(1)	1(1)	-2(1)
C(8)	41(2)	43(2)	32(2)	-3(1)	5(1)	-3(2)
C(9)	54(2)	48(2)	32(2)	-4(2)	-1(2)	-12(2)
C(10)	68(2)	32(2)	32(2)	-3(1)	2(2)	-2(2)
C(11)	51(2)	38(2)	37(2)	0(2)	11(2)	9(2)
C(12)	43(2)	34(2)	39(2)	3(1)	6(1)	1(2)
C(13)	45(2)	65(3)	46(2)	-15(2)	7(2)	-10(2)
C(14)	55(3)	90(3)	50(2)	-12(2)	15(2)	-21(2)
C(15)	61(3)	80(3)	80(3)	-4(3)	8(2)	10(3)
C(16)	44(2)	41(2)	61(2)	-3(2)	8(2)	0(2)
C(17)	46(2)	59(3)	78(3)	-11(2)	-3(2)	5(2)
C(18)	61(3)	86(3)	92(3)	32(3)	1(3)	-27(3)
C(19)	58(2)	40(2)	31(2)	-2(1)	-3(2)	-3(2)
C(20)	169(6)	51(3)	30(2)	1(2)	1(3)	-4(3)
C(21)	126(4)	55(3)	41(2)	-4(2)	14(2)	14(3)
C(22)	65(3)	271(10)	44(2)	-28(4)	-9(2)	-40(4)
O(1A)	49(2)	72(2)	42(1)	6(1)	0(1)	-25(1)
O(2A)	44(2)	70(2)	55(2)	-1(1)	7(1)	13(1)
N(1A)	30(1)	38(2)	27(1)	-2(1)	2(1)	0(1)
N(3A)	29(1)	38(2)	32(1)	1(1)	-2(1)	1(1)
C(2A)	31(2)	31(2)	28(1)	0(1)	-2(1)	1(1)
C(4A)	27(2)	51(2)	40(2)	-2(2)	3(1)	0(2)
C(5A)	30(2)	51(2)	34(2)	-3(2)	1(1)	-2(2)

C(6A)	29(2)	62(2)	30(2)	2(2)	-1(1)	-1(2)
C(7A)	28(2)	45(2)	26(1)	2(1)	-1(1)	-2(1)
C(8A)	34(2)	48(2)	27(2)	0(1)	1(1)	-1(2)
C(9A)	47(2)	59(2)	33(2)	-8(2)	-6(2)	-7(2)
C(10A)	50(2)	66(3)	30(2)	2(2)	-9(2)	6(2)
C(11A)	50(2)	54(2)	40(2)	11(2)	-4(2)	9(2)
C(12A)	38(2)	48(2)	32(2)	6(1)	0(1)	-1(2)
C(13A)	55(2)	42(2)	42(2)	-4(2)	-7(2)	-7(2)
C(14A)	76(3)	53(2)	59(2)	6(2)	-18(2)	-15(2)
C(15A)	81(3)	57(3)	61(2)	-11(2)	-9(2)	21(2)
C(16A)	52(2)	43(2)	49(2)	0(2)	-9(2)	1(2)
C(17A)	65(3)	48(2)	61(2)	0(2)	-3(2)	5(2)
C(18A)	74(3)	63(3)	87(3)	-1(2)	15(3)	-18(2)
C(19A)	41(2)	48(2)	26(2)	1(1)	-9(1)	-2(2)
C(20A)	47(2)	69(3)	31(2)	2(2)	-2(2)	4(2)
C(21A)	41(2)	106(4)	53(2)	24(2)	-6(2)	10(2)
C(22A)	161(5)	58(3)	36(2)	-5(2)	-15(3)	-25(3)

Hydrogen coordinates (x 10^4) and isotropic displacement parameters (Å^{2}x 10^3) for **2f**.

	x	y	z	U(eq)
H(4)	7638	-1588	8022	50
H(5)	7823	-847	9243	48
H(9)	9300	2379	10003	54
H(10)	8034	2891	10644	53
H(11)	6602	2254	10418	51
H(13)	9300	658	8581	62
H(14A)	10552	1647	8341	98
H(14B)	10189	2340	8959	98
H(14C)	9603	2171	8224	98

H(15A)	10658	363	9246	110
H(15B)	9780	54	9711	110
H(15C)	10297	985	9913	110
H(16)	6106	545	9041	59
H(17A)	4807	1512	9087	92
H(17B)	5658	2039	8731	92
H(17C)	5368	2236	9570	92
H(18A)	5065	287	10018	119
H(18B)	5637	962	10539	119
H(18C)	6080	21	10265	119
H(20A)	8419	445	6440	125
H(20B)	7435	918	6477	125
H(20C)	7681	247	5807	125
H(21A)	8630	-1140	6672	111
H(21B)	7894	-1431	6062	111
H(21C)	7793	-1787	6895	111
H(22A)	6235	-1124	6937	190
H(22B)	6333	-723	6117	190
H(22C)	6084	-57	6790	190
H(4A)	6563	-2500	9803	47
H(5A)	5888	-2478	8555	46
H(9A)	2790	-3854	7405	56
H(10A)	2274	-2445	7001	58
H(11A)	2815	-1105	7532	58
H(13A)	4413	-4222	8879	56
H(14D)	2867	-4621	9093	94
H(14E)	3449	-5507	8877	94
H(14F)	2798	-5038	8276	94
H(15D)	4768	-5360	7997	99
H(15E)	5068	-4374	7701	99
H(15F)	4157	-4844	7393	99
H(16A)	4454	-978	9008	58
H(17D)	3475	284	9192	87
H(17E)	2957	-650	9381	87
H(17F)	2759	-137	8616	87
H(18D)	4706	320	8236	112

H(18E)	4058	-117	7616	112
H(18F)	5004	-601	7823	112
H(20D)	4530	-3716	11255	74
H(20E)	4002	-2760	11300	74
H(20F)	4671	-3062	11956	74
H(21D)	6147	-3793	11022	100
H(21E)	6359	-3152	11718	100
H(21F)	6747	-2888	10918	100
H(22D)	5972	-1351	11008	127
H(22E)	5560	-1607	11802	127
H(22F)	4893	-1302	11145	127

Torsion angles [°] for **2f**.

C(5)-N(1)-C(2)-N(3)	-0.2(4)
C(7)-N(1)-C(2)-N(3)	177.5(3)
C(5)-N(1)-C(2)-C(6)	175.0(3)
C(7)-N(1)-C(2)-C(6)	-7.3(5)
C(4)-N(3)-C(2)-N(1)	0.6(4)
C(19)-N(3)-C(2)-N(1)	-179.5(3)
C(4)-N(3)-C(2)-C(6)	-174.0(4)
C(19)-N(3)-C(2)-C(6)	6.0(6)
C(2)-N(3)-C(4)-C(5)	-0.7(4)
C(19)-N(3)-C(4)-C(5)	179.3(3)
N(3)-C(4)-C(5)-N(1)	0.6(4)
C(2)-N(1)-C(5)-C(4)	-0.2(4)
C(7)-N(1)-C(5)-C(4)	-177.9(3)
N(1)-C(2)-C(6)-O(2)	-97.2(4)
N(3)-C(2)-C(6)-O(2)	76.7(5)
N(1)-C(2)-C(6)-O(1)	79.5(4)
N(3)-C(2)-C(6)-O(1)	-106.6(4)
C(2)-N(1)-C(7)-C(12)	92.7(4)

C(5)-N(1)-C(7)-C(12)	-89.9(4)
C(2)-N(1)-C(7)-C(8)	-86.9(4)
C(5)-N(1)-C(7)-C(8)	90.5(4)
C(12)-C(7)-C(8)-C(9)	-0.4(5)
N(1)-C(7)-C(8)-C(9)	179.2(3)
C(12)-C(7)-C(8)-C(13)	178.0(3)
N(1)-C(7)-C(8)-C(13)	-2.4(5)
C(7)-C(8)-C(9)-C(10)	0.7(5)
C(13)-C(8)-C(9)-C(10)	-177.8(3)
C(8)-C(9)-C(10)-C(11)	0.3(5)
C(9)-C(10)-C(11)-C(12)	-1.5(5)
C(10)-C(11)-C(12)-C(7)	1.7(5)
C(10)-C(11)-C(12)-C(16)	-178.3(3)
C(8)-C(7)-C(12)-C(11)	-0.8(5)
N(1)-C(7)-C(12)-C(11)	179.6(3)
C(8)-C(7)-C(12)-C(16)	179.2(3)
N(1)-C(7)-C(12)-C(16)	-0.4(5)
C(9)-C(8)-C(13)-C(15)	67.8(5)
C(7)-C(8)-C(13)-C(15)	-110.5(4)
C(9)-C(8)-C(13)-C(14)	-57.2(4)
C(7)-C(8)-C(13)-C(14)	124.5(4)
C(11)-C(12)-C(16)-C(18)	-62.9(5)
C(7)-C(12)-C(16)-C(18)	117.1(4)
C(11)-C(12)-C(16)-C(17)	60.8(4)
C(7)-C(12)-C(16)-C(17)	-119.2(4)
C(2)-N(3)-C(19)-C(22)	-94.8(5)
C(4)-N(3)-C(19)-C(22)	85.1(5)
C(2)-N(3)-C(19)-C(20)	27.9(5)
C(4)-N(3)-C(19)-C(20)	-152.2(4)
C(2)-N(3)-C(19)-C(21)	145.5(4)
C(4)-N(3)-C(19)-C(21)	-34.6(5)
C(4A)-N(3A)-C(2A)-N(1A)	0.9(3)
C(19A)-N(3A)-C(2A)-N(1A)	177.9(3)
C(4A)-N(3A)-C(2A)-C(6A)	-176.6(3)
C(19A)-N(3A)-C(2A)-C(6A)	0.3(5)
C(5A)-N(1A)-C(2A)-N(3A)	-1.1(4)

C(7A)-N(1A)-C(2A)-N(3A)	-176.3(3)
C(5A)-N(1A)-C(2A)-C(6A)	176.8(3)
C(7A)-N(1A)-C(2A)-C(6A)	1.6(5)
C(2A)-N(3A)-C(4A)-C(5A)	-0.4(4)
C(19A)-N(3A)-C(4A)-C(5A)	-177.5(3)
N(3A)-C(4A)-C(5A)-N(1A)	-0.2(4)
C(2A)-N(1A)-C(5A)-C(4A)	0.8(4)
C(7A)-N(1A)-C(5A)-C(4A)	176.0(3)
N(3A)-C(2A)-C(6A)-O(2A)	79.2(4)
N(1A)-C(2A)-C(6A)-O(2A)	-98.1(4)
N(3A)-C(2A)-C(6A)-O(1A)	-103.7(4)
N(1A)-C(2A)-C(6A)-O(1A)	79.0(4)
C(2A)-N(1A)-C(7A)-C(12A)	90.5(4)
C(5A)-N(1A)-C(7A)-C(12A)	-84.0(4)
C(2A)-N(1A)-C(7A)-C(8A)	-91.1(4)
C(5A)-N(1A)-C(7A)-C(8A)	94.5(4)
C(12A)-C(7A)-C(8A)-C(9A)	-0.4(5)
N(1A)-C(7A)-C(8A)-C(9A)	-178.7(3)
C(12A)-C(7A)-C(8A)-C(13A)	177.8(3)
N(1A)-C(7A)-C(8A)-C(13A)	-0.5(4)
C(7A)-C(8A)-C(9A)-C(10A)	0.1(5)
C(13A)-C(8A)-C(9A)-C(10A)	-178.1(3)
C(8A)-C(9A)-C(10A)-C(11A)	0.4(6)
C(9A)-C(10A)-C(11A)-C(12A)	-0.6(6)
C(10A)-C(11A)-C(12A)-C(7A)	0.3(5)
C(10A)-C(11A)-C(12A)-C(16A)	179.9(3)
C(8A)-C(7A)-C(12A)-C(11A)	0.2(5)
N(1A)-C(7A)-C(12A)-C(11A)	178.5(3)
C(8A)-C(7A)-C(12A)-C(16A)	-179.4(3)
N(1A)-C(7A)-C(12A)-C(16A)	-1.1(5)
C(9A)-C(8A)-C(13A)-C(15A)	65.3(4)
C(7A)-C(8A)-C(13A)-C(15A)	-112.9(4)
C(9A)-C(8A)-C(13A)-C(14A)	-58.7(4)
C(7A)-C(8A)-C(13A)-C(14A)	123.2(3)
C(11A)-C(12A)-C(16A)-C(17A)	63.2(4)
C(7A)-C(12A)-C(16A)-C(17A)	-117.3(4)

C(11A)-C(12A)-C(16A)-C(18A)	-61.3(5)
C(7A)-C(12A)-C(16A)-C(18A)	118.3(4)
C(2A)-N(3A)-C(19A)-C(22A)	-95.1(4)
C(4A)-N(3A)-C(19A)-C(22A)	81.4(4)
C(2A)-N(3A)-C(19A)-C(20A)	26.5(5)
C(4A)-N(3A)-C(19A)-C(20A)	-157.0(3)
C(2A)-N(3A)-C(19A)-C(21A)	144.4(3)
C(4A)-N(3A)-C(19A)-C(21A)	-39.1(4)

Symmetry transformations used to generate equivalent atoms:

#1 y,x,-z+2

Thermal ellipsoid diagram of **2h$_{Me}$** drawn at 50% probability.

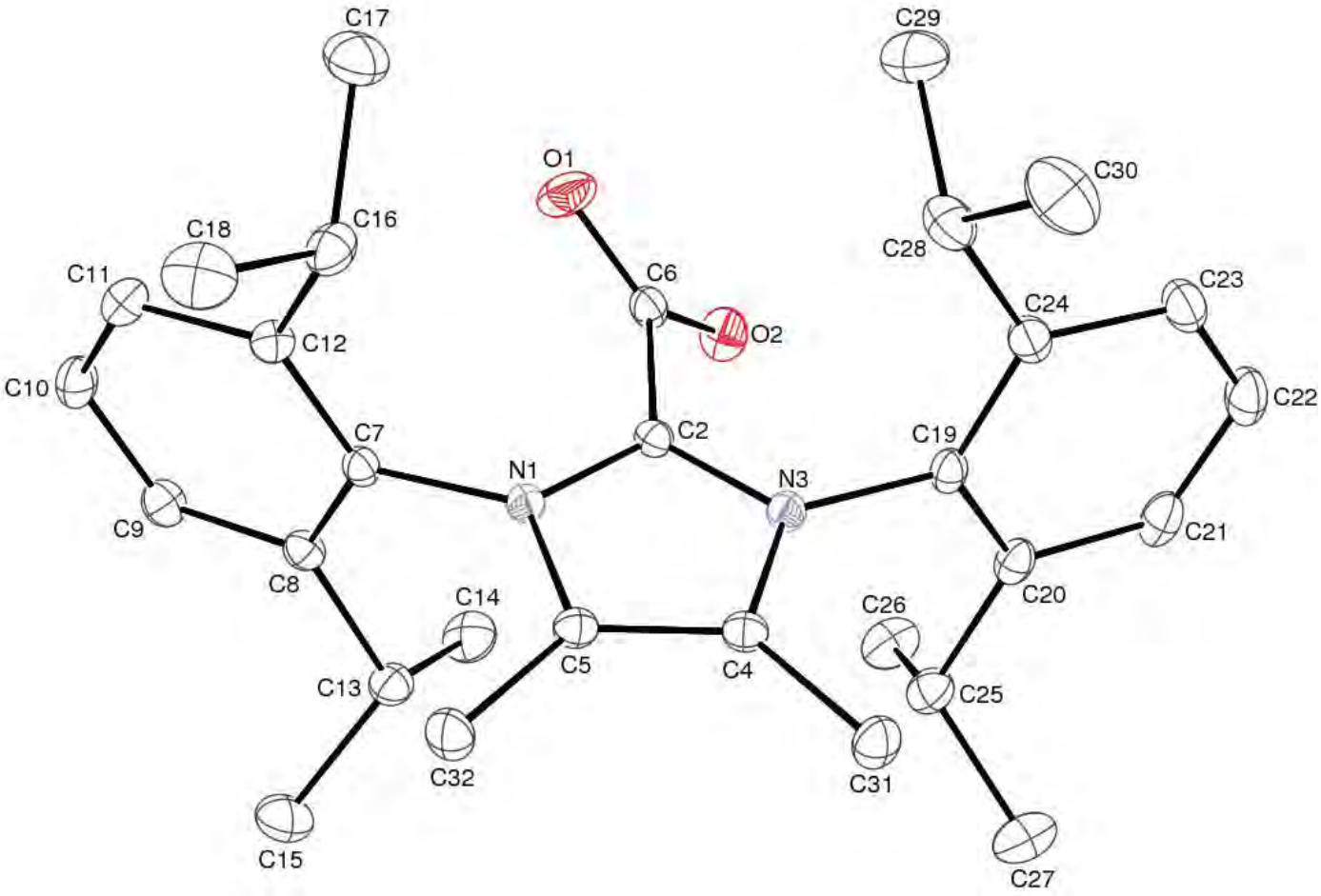

Crystal data and structure refinement for **$2h_{Me}$**.

Crystal Data		
Empirical formula	$C_{30}\ H_{40}\ N_2\ O_2$	
Formula weight	460.64	
Temperature	150(1) K	
Wavelength	0.71073 Å	
Crystal system	Monoclinic	
Space group	$P2_1/n$	
Unit cell dimensions	a = 12.4100(2) Å	α= 90°.
	b = 16.4677(2) Å	β= 102.8772(9)°.
	c = 13.3409(3) Å	γ = 90°.
Volume	2657.83(8) $Å^3$	
Z	4	
Density (calculated)	1.151 Mg/m^3	
Absorption coefficient	0.071 mm^{-1}	
F(000)	1000	
Data Collection		
Diffractometer	Nonius KappaCCD	
Wavelength	0.71073 Å	
Temperature	150(1)K	
Crystal size	0.33 x 0.25 x 0.15 mm^3	
Theta range for data collection	2.00 to 27.47°.	
Index ranges	-16<=h<=16, -21<=k<=20, -17<=l<=17	
Reflections collected	11239	
Independent reflections	6082 [R(int) = 0.0244]	
Completeness to theta = 27.47°	99.8 %	
Solution and Refinement		
System Used	SIR 97	
Solution	Direct methods and heavy atom	
Absorption correction	Multi-scan	
Max. and min. transmission	0.9894 and 0.9768	
Refinement method	Full-matrix least-squares on F^2	
Data / restraints / parameters	6082 / 0 / 468	
Goodness-of-fit on F^2	1.025	
Final R indices [I>2sigma(I)]	R1 = 0.0411, wR2 = 0.0946	
R indices (all data)	R1 = 0.0667, wR2 = 0.1065	
Extinction coefficient	0.0101(11)	
Largest diff. peak and hole	0.230 and -0.208 $e.Å^{-3}$	

Atomic coordinates (x 10^4) and equivalent isotropic displacement parameters ($Å^2$x 10^3) for **$2h_{Me}$.** U(eq) is defined as one third of the trace of the orthogonalized U^{ij} tensor.

	x	y	z	U(eq)
O(1)	7661(1)	-114(1)	7735(1)	39(1)
O(2)	9391(1)	6(1)	7502(1)	33(1)
N(1)	7940(1)	1640(1)	8224(1)	18(1)
N(3)	8586(1)	1684(1)	6852(1)	19(1)
C(2)	8351(1)	1184(1)	7565(1)	18(1)
C(4)	8311(1)	2483(1)	7058(1)	21(1)
C(5)	7915(1)	2456(1)	7927(1)	20(1)
C(6)	8484(1)	253(1)	7604(1)	22(1)
C(7)	7694(1)	1326(1)	9166(1)	19(1)
C(8)	8567(1)	1285(1)	10034(1)	22(1)
C(9)	8358(1)	895(1)	10899(1)	26(1)
C(10)	7318(1)	592(1)	10895(1)	29(1)
C(11)	6459(1)	688(1)	10042(1)	28(1)
C(12)	6620(1)	1059(1)	9152(1)	23(1)
C(13)	9695(1)	1658(1)	10051(1)	26(1)
C(14)	10552(1)	1021(1)	9939(1)	37(1)
C(15)	10105(2)	2157(1)	11029(1)	45(1)
C(16)	5659(1)	1183(1)	8238(1)	30(1)
C(17)	5143(1)	377(1)	7798(1)	42(1)
C(18)	4782(1)	1728(1)	8536(1)	43(1)
C(19)	8992(1)	1435(1)	5957(1)	21(1)
C(20)	10128(1)	1492(1)	6004(1)	25(1)
C(21)	10485(1)	1239(1)	5135(1)	32(1)
C(22)	9756(1)	962(1)	4265(1)	36(1)
C(23)	8639(1)	930(1)	4244(1)	33(1)
C(24)	8228(1)	1158(1)	5091(1)	26(1)
C(25)	10954(1)	1783(1)	6951(1)	30(1)
C(26)	11681(1)	1081(1)	7457(1)	41(1)
C(27)	11666(1)	2477(1)	6697(2)	45(1)
C(28)	7001(1)	1059(1)	5070(1)	33(1)
C(29)	6712(1)	153(1)	5053(2)	47(1)

C(30)	6267(2)	1501(1)	4161(1)	51(1)
C(31)	8468(1)	3179(1)	6389(1)	29(1)
C(32)	7519(1)	3106(1)	8529(1)	29(1)

Bond lengths [Å] and angles [°] for **2h$_{Me}$**.

O(1)-C(6)	1.2322(15)
O(2)-C(6)	1.2330(14)
N(1)-C(2)	1.3408(14)
N(1)-C(5)	1.3987(14)
N(1)-C(7)	1.4530(14)
N(3)-C(2)	1.3383(14)
N(3)-C(4)	1.4009(14)
N(3)-C(19)	1.4543(14)
C(2)-C(6)	1.5415(16)
C(4)-C(5)	1.3567(17)
C(4)-C(31)	1.4917(17)
C(5)-C(32)	1.4856(17)
C(7)-C(8)	1.3992(16)
C(7)-C(12)	1.3995(16)
C(8)-C(9)	1.3949(17)
C(8)-C(13)	1.5244(16)
C(9)-C(10)	1.3834(18)
C(9)-H(9)	0.969(14)
C(10)-C(11)	1.3838(19)
C(10)-H(10)	0.972(15)
C(11)-C(12)	1.3901(17)
C(11)-H(11)	0.965(14)
C(12)-C(16)	1.5173(17)
C(13)-C(14)	1.5254(19)
C(13)-C(15)	1.5296(19)
C(13)-H(13)	0.982(14)

C(14)-H(14A)	1.024(18)
C(14)-H(14B)	1.002(17)
C(14)-H(14C)	1.017(18)
C(15)-H(15A)	0.994(19)
C(15)-H(15B)	0.998(16)
C(15)-H(15C)	0.979(18)
C(16)-C(18)	1.530(2)
C(16)-C(17)	1.532(2)
C(16)-H(16)	0.981(14)
C(17)-H(17A)	1.00(2)
C(17)-H(17B)	1.013(18)
C(17)-H(17C)	1.030(18)
C(18)-H(18A)	1.034(19)
C(18)-H(18B)	1.02(2)
C(18)-H(18C)	1.005(17)
C(19)-C(24)	1.3974(17)
C(19)-C(20)	1.4008(17)
C(20)-C(21)	1.3934(18)
C(20)-C(25)	1.5166(18)
C(21)-C(22)	1.381(2)
C(21)-H(21)	1.008(15)
C(22)-C(23)	1.382(2)
C(22)-H(22)	0.988(17)
C(23)-C(24)	1.3914(18)
C(23)-H(23)	1.002(16)
C(24)-C(28)	1.5256(18)
C(25)-C(27)	1.5275(19)
C(25)-C(26)	1.529(2)
C(25)-H(25)	1.002(14)
C(26)-H(26A)	1.015(17)
C(26)-H(26B)	1.028(17)
C(26)-H(26C)	1.002(17)
C(27)-H(27A)	1.017(18)
C(27)-H(27B)	1.008(18)
C(27)-H(27C)	0.990(18)
C(28)-C(30)	1.529(2)

C(28)-C(29)	1.534(2)
C(28)-H(28)	0.989(15)
C(29)-H(29A)	1.04(2)
C(29)-H(29B)	1.03(2)
C(29)-H(29C)	0.985(18)
C(30)-H(30A)	0.98(2)
C(30)-H(30B)	0.983(19)
C(30)-H(30C)	1.05(2)
C(31)-H(31A)	0.980(18)
C(31)-H(31B)	1.004(16)
C(31)-H(31C)	0.981(16)
C(32)-H(32A)	0.967(17)
C(32)-H(32B)	0.999(18)
C(32)-H(32C)	1.023(17)

C(2)-N(1)-C(5)	109.88(9)
C(2)-N(1)-C(7)	123.47(9)
C(5)-N(1)-C(7)	126.26(9)
C(2)-N(3)-C(4)	109.69(9)
C(2)-N(3)-C(19)	125.40(9)
C(4)-N(3)-C(19)	124.78(9)
N(3)-C(2)-N(1)	107.22(9)
N(3)-C(2)-C(6)	126.70(10)
N(1)-C(2)-C(6)	126.04(10)
C(5)-C(4)-N(3)	106.72(10)
C(5)-C(4)-C(31)	131.02(11)
N(3)-C(4)-C(31)	122.26(11)
C(4)-C(5)-N(1)	106.48(10)
C(4)-C(5)-C(32)	131.64(11)
N(1)-C(5)-C(32)	121.88(11)
O(1)-C(6)-O(2)	131.31(11)
O(1)-C(6)-C(2)	114.02(10)
O(2)-C(6)-C(2)	114.68(10)
C(8)-C(7)-C(12)	123.70(11)
C(8)-C(7)-N(1)	117.36(10)
C(12)-C(7)-N(1)	118.91(10)

C(9)-C(8)-C(7) 117.06(11)
C(9)-C(8)-C(13)120.77(11)
C(7)-C(8)-C(13)122.16(11)
C(10)-C(9)-C(8)120.56(12)
C(10)-C(9)-H(9)120.5(8)
C(8)-C(9)-H(9) 118.9(8)
C(9)-C(10)-C(11)120.59(12)
C(9)-C(10)-H(10)119.1(8)
C(11)-C(10)-H(10)120.3(8)
C(10)-C(11)-C(12)121.46(12)
C(10)-C(11)-H(11)118.5(9)
C(12)-C(11)-H(11)120.1(9)
C(11)-C(12)-C(7)116.42(11)
C(11)-C(12)-C(16)120.53(11)
C(7)-C(12)-C(16)123.02(11)
C(8)-C(13)-C(14)112.32(11)
C(8)-C(13)-C(15)111.09(11)
C(14)-C(13)-C(15)110.33(12)
C(8)-C(13)-H(13)108.4(8)
C(14)-C(13)-H(13)107.4(8)
C(15)-C(13)-H(13)107.0(8)
C(13)-C(14)-H(14A)
C(13)-C(14)-H(14B)
H(14A)-C(14)-H(14B)
C(13)-C(14)-H(14C)
H(14A)-C(14)-H(14C)
H(14B)-C(14)-H(14C)
C(13)-C(15)-H(15A)
C(13)-C(15)-H(15B)
H(15A)-C(15)-H(15B)
C(13)-C(15)-H(15C)
H(15A)-C(15)-H(15C)
H(15B)-C(15)-H(15C)
C(12)-C(16)-C(18)110.33(12)
C(12)-C(16)-C(17)112.29(12)
C(18)-C(16)-C(17)110.32(12)

C(12)-C(16)-H(16)108.5(8)
C(18)-C(16)-H(16)107.6(8)
C(17)-C(16)-H(16)107.6(8)
C(16)-C(17)-H(17A)
C(16)-C(17)-H(17B)
H(17A)-C(17)-H(17B)
C(16)-C(17)-H(17C)
H(17A)-C(17)-H(17C)
H(17B)-C(17)-H(17C)
C(16)-C(18)-H(18A)
C(16)-C(18)-H(18B)
H(18A)-C(18)-H(18B)
C(16)-C(18)-H(18C)
H(18A)-C(18)-H(18C)
H(18B)-C(18)-H(18C)
C(24)-C(19)-C(20)123.31(11)
C(24)-C(19)-N(3)118.41(10)
C(20)-C(19)-N(3)118.28(10)
C(21)-C(20)-C(19)116.53(12)
C(21)-C(20)-C(25)120.39(11)
C(19)-C(20)-C(25)123.05(11)
C(22)-C(21)-C(20)121.87(13)
C(22)-C(21)-H(21)119.3(9)
C(20)-C(21)-H(21)118.8(9)
C(21)-C(22)-C(23)119.73(13)
C(21)-C(22)-H(22)119.9(9)
C(23)-C(22)-H(22)120.4(9)
C(22)-C(23)-C(24)121.42(13)
C(22)-C(23)-H(23)119.6(9)
C(24)-C(23)-H(23)119.0(9)
C(23)-C(24)-C(19)117.12(12)
C(23)-C(24)-C(28)120.07(12)
C(19)-C(24)-C(28)122.73(11)
C(20)-C(25)-C(27)111.66(12)
C(20)-C(25)-C(26)110.57(11)
C(27)-C(25)-C(26)110.51(12)

C(20)-C(25)-H(25)109.4(8)
C(27)-C(25)-H(25)106.8(8)
C(26)-C(25)-H(25)107.8(8)
C(25)-C(26)-H(26A)
C(25)-C(26)-H(26B)
H(26A)-C(26)-H(26B)
C(25)-C(26)-H(26C)
H(26A)-C(26)-H(26C)
H(26B)-C(26)-H(26C)
C(25)-C(27)-H(27A)
C(25)-C(27)-H(27B)
H(27A)-C(27)-H(27B)
C(25)-C(27)-H(27C)
H(27A)-C(27)-H(27C)
H(27B)-C(27)-H(27C)
C(24)-C(28)-C(30)112.31(13)
C(24)-C(28)-C(29)109.52(12)
C(30)-C(28)-C(29)110.84(13)
C(24)-C(28)-H(28)108.4(8)
C(30)-C(28)-H(28)108.0(9)
C(29)-C(28)-H(28)107.7(9)
C(28)-C(29)-H(29A)
C(28)-C(29)-H(29B)
H(29A)-C(29)-H(29B)
C(28)-C(29)-H(29C)
H(29A)-C(29)-H(29C)
H(29B)-C(29)-H(29C)
C(28)-C(30)-H(30A)
C(28)-C(30)-H(30B)
H(30A)-C(30)-H(30B)
C(28)-C(30)-H(30C)
H(30A)-C(30)-H(30C)
H(30B)-C(30)-H(30C)
C(4)-C(31)-H(31A)111.1(10)
C(4)-C(31)-H(31B)112.8(9)
H(31A)-C(31)-H(31B)

C(4)-C(31)-H(31C)109.9(9)
H(31A)-C(31)-H(31C)
H(31B)-C(31)-H(31C)
C(5)-C(32)-H(32A)109.4(9)
C(5)-C(32)-H(32B)110.0(10)
H(32A)-C(32)-H(32B)
C(5)-C(32)-H(32C)109.8(10)
H(32A)-C(32)-H(32C)
H(32B)-C(32)-H(32C)

Symmetry transformations used to generate equivalent atoms:
#1 y,x,-z+2

Anisotropic displacement parameters ($Å^2$x 10^3)for **$2h_{Me}$.** The anisotropic displacement factor exponent takes the form: $-2\pi^2[h^2a^{*2}U^{11} + ... + 2 h k a^* b^* U^{12}]$

	U^{11}	U^{22}	U^{33}	U^{23}	U^{13}	U^{12}
O(1)	41(1)	21(1)	61(1)	-5(1)	23(1)	-8(1)
O(2)	37(1)	26(1)	39(1)	2(1)	16(1)	10(1)
N(1)	20(1)	17(1)	18(1)	0(1)	5(1)	-1(1)
N(3)	21(1)	18(1)	20(1)	0(1)	6(1)	0(1)
C(2)	18(1)	19(1)	18(1)	-1(1)	3(1)	0(1)
C(4)	21(1)	17(1)	24(1)	-1(1)	4(1)	1(1)
C(5)	21(1)	18(1)	22(1)	0(1)	4(1)	0(1)
C(6)	31(1)	18(1)	19(1)	-1(1)	7(1)	1(1)
C(7)	24(1)	16(1)	18(1)	-1(1)	7(1)	1(1)
C(8)	24(1)	19(1)	22(1)	-2(1)	5(1)	1(1)
C(9)	28(1)	28(1)	21(1)	2(1)	2(1)	3(1)
C(10)	35(1)	29(1)	24(1)	6(1)	11(1)	2(1)

C(11)	27(1)	28(1)	31(1)	3(1)	10(1)	-3(1)
C(12)	24(1)	22(1)	24(1)	-1(1)	6(1)	-1(1)
C(13)	24(1)	29(1)	23(1)	1(1)	2(1)	-4(1)
C(14)	24(1)	43(1)	45(1)	0(1)	7(1)	1(1)
C(15)	40(1)	52(1)	42(1)	-16(1)	6(1)	-16(1)
C(16)	24(1)	38(1)	26(1)	6(1)	3(1)	-4(1)
C(17)	32(1)	51(1)	41(1)	-12(1)	2(1)	-7(1)
C(18)	31(1)	44(1)	50(1)	1(1)	-1(1)	7(1)
C(19)	28(1)	18(1)	21(1)	2(1)	11(1)	3(1)
C(20)	28(1)	21(1)	27(1)	5(1)	11(1)	2(1)
C(21)	37(1)	29(1)	37(1)	7(1)	21(1)	4(1)
C(22)	52(1)	31(1)	31(1)	-1(1)	23(1)	6(1)
C(23)	48(1)	29(1)	23(1)	-4(1)	10(1)	0(1)
C(24)	35(1)	21(1)	22(1)	0(1)	7(1)	1(1)
C(25)	26(1)	30(1)	34(1)	1(1)	10(1)	-2(1)
C(26)	32(1)	40(1)	48(1)	10(1)	3(1)	-1(1)
C(27)	38(1)	37(1)	58(1)	7(1)	10(1)	-10(1)
C(28)	31(1)	40(1)	26(1)	-5(1)	2(1)	1(1)
C(29)	38(1)	51(1)	50(1)	-4(1)	4(1)	-14(1)
C(30)	48(1)	58(1)	39(1)	-3(1)	-6(1)	14(1)
C(31)	39(1)	21(1)	31(1)	5(1)	14(1)	3(1)
C(32)	41(1)	20(1)	30(1)	-1(1)	14(1)	4(1)

Hydrogen coordinates (x 10^4) and isotropic displacement parameters (Å^{2}x 10^3) for **2h$_{Me}$**.

	x	y	z	U(eq)
H(9)	8957(11)	832(8)	11499(11)	28(3)
H(10)	7194(11)	316(9)	11504(11)	34(4)
H(11)	5735(12)	492(9)	10077(11)	35(4)
H(13)	9620(11)	2033(8)	9468(11)	29(3)
H(14A)	10290(13)	679(10)	9289(14)	53(5)
H(14B)	11263(14)	1290(9)	9891(12)	47(4)
H(14C)	10686(13)	653(10)	10567(14)	52(5)
H(15A)	10239(15)	1799(11)	11644(15)	61(5)
H(15B)	10801(14)	2448(9)	10995(12)	44(4)
H(15C)	9574(15)	2584(11)	11089(13)	56(5)
H(16)	5933(11)	1460(8)	7693(11)	31(4)
H(17A)	4826(16)	89(12)	8325(16)	71(6)
H(17B)	5715(14)	30(10)	7564(13)	54(5)
H(17C)	4527(14)	505(11)	7160(14)	59(5)
H(18A)	4425(14)	1446(11)	9074(14)	61(5)
H(18B)	5099(15)	2275(12)	8819(14)	65(5)
H(18C)	4180(14)	1845(10)	7912(13)	50(5)
H(21)	11301(13)	1243(9)	5154(11)	43(4)
H(22)	10038(13)	774(10)	3668(13)	50(5)
H(23)	8112(12)	726(9)	3613(12)	40(4)
H(25)	10548(11)	2001(8)	7463(11)	31(4)
H(26A)	12188(14)	1257(10)	8129(13)	48(4)
H(26B)	12156(13)	880(10)	6966(13)	49(5)
H(26C)	11210(13)	622(10)	7604(13)	51(5)
H(27A)	12195(14)	2666(10)	7351(14)	51(5)
H(27B)	12138(14)	2281(11)	6221(13)	55(5)
H(27C)	11216(14)	2944(11)	6372(13)	58(5)
H(28)	6856(12)	1293(9)	5710(12)	39(4)
H(29A)	7186(15)	-135(11)	5693(15)	66(6)
H(29B)	6830(15)	-113(12)	4390(16)	66(6)

H(29C)	5923(16)	120(11)	5066(14)	63(5)
H(30A)	6477(15)	2071(12)	4150(13)	59(5)
H(30B)	6371(15)	1258(11)	3516(15)	63(5)
H(30C)	5431(17)	1457(12)	4199(15)	74(6)
H(31A)	8172(14)	3053(11)	5662(14)	58(5)
H(31B)	9266(14)	3326(9)	6460(12)	46(4)
H(31C)	8114(12)	3667(10)	6590(12)	45(4)
H(32A)	7479(12)	3614(10)	8158(12)	45(4)
H(32B)	8033(14)	3161(10)	9217(14)	54(5)
H(32C)	6749(14)	2965(10)	8631(13)	55(5)

Torsion angles [°] for **2h**$_{\mathbf{Me}}$.

C(4)-N(3)-C(2)-N(1)	-0.34(12)
C(19)-N(3)-C(2)-N(1)	-176.36(10)
C(4)-N(3)-C(2)-C(6)	177.51(11)
C(19)-N(3)-C(2)-C(6)	1.49(18)
C(5)-N(1)-C(2)-N(3)	-0.20(12)
C(7)-N(1)-C(2)-N(3)	-173.42(9)
C(5)-N(1)-C(2)-C(6)	-178.07(10)
C(7)-N(1)-C(2)-C(6)	8.71(17)
C(2)-N(3)-C(4)-C(5)	0.77(13)
C(19)-N(3)-C(4)-C(5)	176.81(10)
C(2)-N(3)-C(4)-C(31)	-179.39(11)
C(19)-N(3)-C(4)-C(31)	-3.34(17)
N(3)-C(4)-C(5)-N(1)	-0.85(12)
C(31)-C(4)-C(5)-N(1)	179.32(12)
N(3)-C(4)-C(5)-C(32)	178.45(12)
C(31)-C(4)-C(5)-C(32)	-1.4(2)
C(2)-N(1)-C(5)-C(4)	0.68(13)

C(7)-N(1)-C(5)-C(4)	173.66(10)
C(2)-N(1)-C(5)-C(32)	-178.71(11)
C(7)-N(1)-C(5)-C(32)	-5.73(17)
N(3)-C(2)-C(6)-O(1)	-130.73(12)
N(1)-C(2)-C(6)-O(1)	46.73(16)
N(3)-C(2)-C(6)-O(2)	49.45(16)
N(1)-C(2)-C(6)-O(2)	-133.08(12)
C(2)-N(1)-C(7)-C(8)	84.17(13)
C(5)-N(1)-C(7)-C(8)	-87.91(13)
C(2)-N(1)-C(7)-C(12)	-93.85(13)
C(5)-N(1)-C(7)-C(12)	94.07(13)
C(12)-C(7)-C(8)-C(9)	5.37(17)
N(1)-C(7)-C(8)-C(9)	-172.55(10)
C(12)-C(7)-C(8)-C(13)	-173.76(11)
N(1)-C(7)-C(8)-C(13)	8.32(16)
C(7)-C(8)-C(9)-C(10)	-2.28(17)
C(13)-C(8)-C(9)-C(10)	176.87(11)
C(8)-C(9)-C(10)-C(11)	-1.55(19)
C(9)-C(10)-C(11)-C(12)	2.6(2)
C(10)-C(11)-C(12)-C(7)	0.22(18)
C(10)-C(11)-C(12)-C(16)	-178.03(12)
C(8)-C(7)-C(12)-C(11)	-4.34(17)
N(1)-C(7)-C(12)-C(11)	173.55(10)
C(8)-C(7)-C(12)-C(16)	173.86(11)
N(1)-C(7)-C(12)-C(16)	-8.25(16)
C(9)-C(8)-C(13)-C(14)	77.81(15)
C(7)-C(8)-C(13)-C(14)	-103.08(14)
C(9)-C(8)-C(13)-C(15)	-46.29(17)
C(7)-C(8)-C(13)-C(15)	132.81(13)
C(11)-C(12)-C(16)-C(18)	61.45(16)
C(7)-C(12)-C(16)-C(18)	-116.68(14)
C(11)-C(12)-C(16)-C(17)	-62.06(16)
C(7)-C(12)-C(16)-C(17)	119.80(14)
C(2)-N(3)-C(19)-C(24)	81.69(14)
C(4)-N(3)-C(19)-C(24)	-93.74(13)
C(2)-N(3)-C(19)-C(20)	-98.91(13)

C(4)-N(3)-C(19)-C(20)	85.66(14)
C(24)-C(19)-C(20)-C(21)	-1.25(17)
N(3)-C(19)-C(20)-C(21)	179.38(10)
C(24)-C(19)-C(20)-C(25)	-179.28(11)
N(3)-C(19)-C(20)-C(25)	1.35(17)
C(19)-C(20)-C(21)-C(22)	1.26(18)
C(25)-C(20)-C(21)-C(22)	179.34(12)
C(20)-C(21)-C(22)-C(23)	-0.2(2)
C(21)-C(22)-C(23)-C(24)	-1.1(2)
C(22)-C(23)-C(24)-C(19)	1.05(19)
C(22)-C(23)-C(24)-C(28)	-175.71(12)
C(20)-C(19)-C(24)-C(23)	0.13(18)
N(3)-C(19)-C(24)-C(23)	179.50(10)
C(20)-C(19)-C(24)-C(28)	176.80(11)
N(3)-C(19)-C(24)-C(28)	-3.83(17)
C(21)-C(20)-C(25)-C(27)	55.43(16)
C(19)-C(20)-C(25)-C(27)	-126.62(13)
C(21)-C(20)-C(25)-C(26)	-68.05(15)
C(19)-C(20)-C(25)-C(26)	109.91(14)
C(23)-C(24)-C(28)-C(30)	-56.33(17)
C(19)-C(24)-C(28)-C(30)	127.10(14)
C(23)-C(24)-C(28)-C(29)	67.28(16)
C(19)-C(24)-C(28)-C(29)	-109.29(14)

Symmetry transformations used to generate equivalent atoms:

#1 y,x,-z+2

Thermal ellipsoid diagram of **2j** drawn at 50% probability.

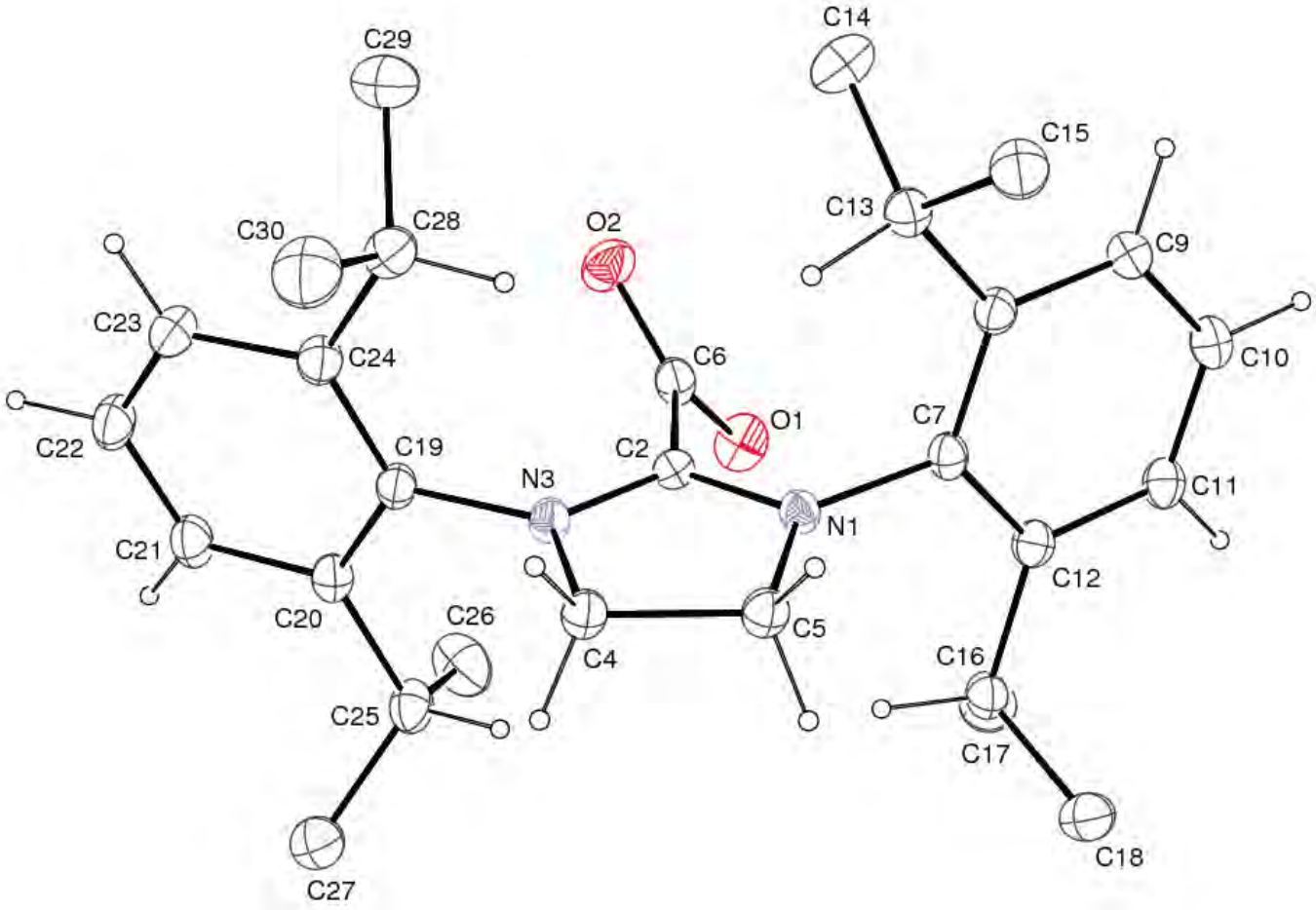

Crystal data and structure refinement for **2j.**

Crystal Data		
Empirical formula	C30 H41 N3 O2	
Formula weight	475.66	
Temperature	150(1) K	
Wavelength	0.71073 Å	
Crystal system	Monoclinic	
Space group	$P2_1/c$	
Unit cell dimensions	a = 13.0159(4) Å	α= 90°.
	b = 16.1571(5) Å	β= 110.0289(17)°.
	c = 14.0635(3) Å	γ= 90°.
Volume	2778.67(13) $Å^3$	
Z	4	
Density (calculated)	1.137 Mg/m^3	
Absorption coefficient	0.071 mm^{-1}	
F(000)	1032	
Data Collection		
Diffractometer	Nonius KappaCCD	
Wavelength	0.71073 Å	
Temperature	150(1)K	
Crystal size	0.33 x 0.23 x 0.10 mm^3	
Theta range for data collection	1.99 to 27.48°.	
Index ranges	-16<=h<=16, -20<=k<=19, -18<=l<=18	
Reflections collected	11038	
Independent reflections	6359 [R(int) = 0.0351]	
Completeness to theta = 27.48°	99.8 %	
Solution and Refinement		
System Used	SIR 97	
Solution	Direct methods and heavy atom	
Absorption correction	Multi-scan	
Max. and min. transmission	0.9929 and 0.9769	
Refinement method	Full-matrix least-squares on F^2	
Data / restraints / parameters	6359 / 0 / 481	
Goodness-of-fit on F^2	1.012	
Final R indices [I>2sigma(I)]	R1 = 0.0503, wR2 = 0.1096	
R indices (all data)	R1 = 0.0947, wR2 = 0.1296	
Extinction coefficient	0.0133(12)	
Largest diff. peak and hole	0.199 and -0.209 $e.Å^{-3}$	

Atomic coordinates (x 10^4) and equivalent isotropic displacement parameters ($Å^2$x 10^3) for **2j.** U(eq) is defined as one third of the trace of the orthogonalized U^{ij} tensor.

	x	y	z	U(eq)
O(1)	967(1)	2872(1)	10341(1)	41(1)
O(2)	2643(1)	3363(1)	10515(1)	44(1)
N(1)	682(1)	3176(1)	8190(1)	25(1)
N(2)	6206(2)	729(2)	7804(2)	82(1)
N(3)	2108(1)	2356(1)	8605(1)	25(1)
C(2)	1520(1)	2868(1)	8938(1)	24(1)
C(4)	1663(1)	2287(1)	7487(1)	28(1)
C(5)	645(1)	2837(1)	7201(1)	30(1)
C(6)	1737(1)	3061(1)	10058(1)	30(1)
C(7)	-16(1)	3828(1)	8330(1)	26(1)
C(8)	358(1)	4646(1)	8387(1)	28(1)
C(9)	-274(1)	5256(1)	8625(1)	31(1)
C(10)	-1259(1)	5063(1)	8747(1)	33(1)
C(11)	-1627(1)	4253(1)	8635(1)	31(1)
C(12)	-1017(1)	3614(1)	8433(1)	28(1)
C(13)	1380(1)	4894(1)	8163(1)	32(1)
C(14)	2274(2)	5253(2)	9084(2)	47(1)
C(15)	1085(2)	5516(1)	7287(2)	40(1)
C(16)	-1444(1)	2734(1)	8318(1)	32(1)
C(17)	-1777(2)	2461(2)	9212(2)	45(1)
C(18)	-2403(2)	2644(1)	7316(2)	43(1)
C(19)	3117(1)	1957(1)	9204(1)	27(1)
C(20)	3064(1)	1183(1)	9628(1)	29(1)
C(21)	4056(1)	820(1)	10212(1)	36(1)
C(22)	5040(2)	1207(1)	10333(1)	40(1)
C(23)	5066(2)	1960(1)	9879(1)	40(1)
C(24)	4103(1)	2361(1)	9304(1)	32(1)
C(25)	1996(1)	746(1)	9500(1)	36(1)
C(26)	1719(2)	809(2)	10473(2)	56(1)
C(27)	2006(2)	-160(1)	9195(2)	44(1)
C(28)	4158(2)	3189(1)	8814(1)	40(1)

C(29)	4838(2)	3817(2)	9586(2)	58(1)
C(30)	4589(2)	3088(2)	7934(2)	56(1)
C(31)	5291(2)	678(1)	7641(1)	45(1)
C(32)	4137(2)	608(2)	7461(2)	49(1)

Bond lengths [Å] and angles [°] for **2j.**

O(1)-C(6)	1.237(2)
O(2)-C(6)	1.234(2)
N(1)-C(2)	1.3264(19)
N(1)-C(7)	1.447(2)
N(1)-C(5)	1.4802(19)
N(2)-C(31)	1.137(3)
N(3)-C(2)	1.3171(19)
N(3)-C(19)	1.446(2)
N(3)-C(4)	1.4815(19)
C(2)-C(6)	1.535(2)
C(4)-C(5)	1.531(2)
C(4)-H(4A)	0.997(17)
C(4)-H(4B)	0.98(2)
C(5)-H(5A)	0.980(18)
C(5)-H(5B)	0.997(19)
C(7)-C(8)	1.401(2)
C(7)-C(12)	1.403(2)
C(8)-C(9)	1.396(2)
C(8)-C(13)	1.523(2)
C(9)-C(10)	1.385(2)
C(9)-H(9)	1.007(19)
C(10)-C(11)	1.383(3)

C(10)-H(10)	0.99(2)
C(11)-C(12)	1.390(2)
C(11)-H(11)	1.00(2)
C(12)-C(16)	1.515(2)
C(13)-C(14)	1.528(3)
C(13)-C(15)	1.533(2)
C(13)-H(13)	1.036(18)
C(14)-H(14A)	1.01(2)
C(14)-H(14B)	1.04(2)
C(14)-H(14C)	0.99(2)
C(15)-H(15A)	1.03(2)
C(15)-H(15B)	0.99(2)
C(15)-H(15C)	1.02(2)
C(16)-C(17)	1.529(2)
C(16)-C(18)	1.536(3)
C(16)-H(16)	0.997(17)
C(17)-H(17A)	1.02(2)
C(17)-H(17B)	1.02(2)
C(17)-H(17C)	1.00(2)
C(18)-H(18A)	1.05(2)
C(18)-H(18B)	1.03(2)
C(18)-H(18C)	0.97(2)
C(19)-C(20)	1.397(2)
C(19)-C(24)	1.403(2)
C(20)-C(21)	1.400(2)
C(20)-C(25)	1.516(2)
C(21)-C(22)	1.382(3)
C(21)-H(21)	0.97(2)
C(22)-C(23)	1.380(3)
C(22)-H(22)	0.99(2)
C(23)-C(24)	1.397(2)
C(23)-H(23)	0.98(2)
C(24)-C(28)	1.518(3)
C(25)-C(27)	1.525(3)
C(25)-C(26)	1.533(3)
C(25)-H(25)	0.992(17)

C(26)-H(26A)	0.97(3)
C(26)-H(26B)	1.04(3)
C(26)-H(26C)	1.01(3)
C(27)-H(27A)	1.01(2)
C(27)-H(27B)	1.00(2)
C(27)-H(27C)	0.98(2)
C(28)-C(29)	1.527(3)
C(28)-C(30)	1.532(3)
C(28)-H(26)	0.993(19)
C(29)-H(29A)	1.01(3)
C(29)-H(29B)	0.97(3)
C(29)-H(29C)	1.04(2)
C(30)-H(30A)	1.00(2)
C(30)-H(30B)	0.97(2)
C(30)-H(30C)	1.02(3)
C(31)-C(32)	1.439(3)
C(32)-H(32A)	0.97(3)
C(32)-H(32B)	1.02(3)
C(32)-H(32C)	0.97(3)

C(2)-N(1)-C(7)	123.28(12)
C(2)-N(1)-C(5)	111.07(12)
C(7)-N(1)-C(5)	125.29(12)
C(2)-N(3)-C(19)	126.49(13)
C(2)-N(3)-C(4)	111.20(13)
C(19)-N(3)-C(4)	122.11(12)
N(3)-C(2)-N(1)	111.94(13)
N(3)-C(2)-C(6)	124.60(13)
N(1)-C(2)-C(6)	123.41(13)
N(3)-C(4)-C(5)	102.91(12)
N(3)-C(4)-H(4A)	111.0(9)
C(5)-C(4)-H(4A)	112.7(10)
N(3)-C(4)-H(4B)	109.4(10)
C(5)-C(4)-H(4B)	113.3(11)
H(4A)-C(4)-H(4B)	107.5(14)
N(1)-C(5)-C(4)	102.79(12)

N(1)-C(5)-H(5A)109.4(10)
C(4)-C(5)-H(5A)113.7(10)
N(1)-C(5)-H(5B)109.9(10)
C(4)-C(5)-H(5B)111.1(11)
H(5A)-C(5)-H(5B)109.6(14)
O(2)-C(6)-O(1) 131.78(15)
O(2)-C(6)-C(2) 114.97(14)
O(1)-C(6)-C(2) 113.24(14)
C(8)-C(7)-C(12)122.89(14)
C(8)-C(7)-N(1) 118.18(13)
C(12)-C(7)-N(1)118.90(14)
C(9)-C(8)-C(7) 117.24(15)
C(9)-C(8)-C(13)119.50(15)
C(7)-C(8)-C(13)123.22(15)
C(10)-C(9)-C(8)121.15(17)
C(10)-C(9)-H(9)120.4(10)
C(8)-C(9)-H(9) 118.4(10)
C(11)-C(10)-C(9)119.83(17)
C(11)-C(10)-H(10)120.6(11)
C(9)-C(10)-H(10)119.6(11)
C(10)-C(11)-C(12)121.75(16)
C(10)-C(11)-H(11)119.7(11)
C(12)-C(11)-H(11)118.5(11)
C(11)-C(12)-C(7)116.99(15)
C(11)-C(12)-C(16)120.35(14)
C(7)-C(12)-C(16)122.65(15)
C(8)-C(13)-C(14)112.95(14)
C(8)-C(13)-C(15)110.01(14)
C(14)-C(13)-C(15)109.99(16)
C(8)-C(13)-H(13)110.1(10)
C(14)-C(13)-H(13)106.7(9)
C(15)-C(13)-H(13)106.8(10)
C(13)-C(14)-H(14A)
C(13)-C(14)-H(14B)
H(14A)-C(14)-H(14B)
C(13)-C(14)-H(14C)

H(14A)-C(14)-H(14C)
H(14B)-C(14)-H(14C)
C(13)-C(15)-H(15A)
C(13)-C(15)-H(15B)
H(15A)-C(15)-H(15B)
C(13)-C(15)-H(15C)
H(15A)-C(15)-H(15C)
H(15B)-C(15)-H(15C)
C(12)-C(16)-C(17)112.26(15)
C(12)-C(16)-C(18)109.88(15)
C(17)-C(16)-C(18)110.92(16)
C(12)-C(16)-H(16)107.1(10)
C(17)-C(16)-H(16)105.2(9)
C(18)-C(16)-H(16)111.4(9)
C(16)-C(17)-H(17A)
C(16)-C(17)-H(17B)
H(17A)-C(17)-H(17B)
C(16)-C(17)-H(17C)
H(17A)-C(17)-H(17C)
H(17B)-C(17)-H(17C)
C(16)-C(18)-H(18A)
C(16)-C(18)-H(18B)
H(18A)-C(18)-H(18B)
C(16)-C(18)-H(18C)
H(18A)-C(18)-H(18C)
H(18B)-C(18)-H(18C)
C(20)-C(19)-C(24)123.38(15)
C(20)-C(19)-N(3)118.74(14)
C(24)-C(19)-N(3)117.86(15)
C(19)-C(20)-C(21)117.11(16)
C(19)-C(20)-C(25)122.98(14)
C(21)-C(20)-C(25)119.90(16)
C(22)-C(21)-C(20)120.79(18)
C(22)-C(21)-H(21)118.5(11)
C(20)-C(21)-H(21)120.7(12)
C(23)-C(22)-C(21)120.75(17)

C(23)-C(22)-H(22)120.5(11)
C(21)-C(22)-H(22)118.8(11)
C(22)-C(23)-C(24)121.10(18)
C(22)-C(23)-H(23)120.6(12)
C(24)-C(23)-H(23)118.3(12)
C(23)-C(24)-C(19)116.83(17)
C(23)-C(24)-C(28)119.93(16)
C(19)-C(24)-C(28)123.24(15)
C(20)-C(25)-C(27)112.63(15)
C(20)-C(25)-C(26)110.45(17)
C(27)-C(25)-C(26)110.05(17)
C(20)-C(25)-H(25)107.9(10)
C(27)-C(25)-H(25)108.3(10)
C(26)-C(25)-H(25)107.4(9)
C(25)-C(26)-H(26A)
C(25)-C(26)-H(26B)
H(26A)-C(26)-H(26B)
C(25)-C(26)-H(26C)
H(26A)-C(26)-H(26C)
H(26B)-C(26)-H(26C)
C(25)-C(27)-H(27A)
C(25)-C(27)-H(27B)
H(27A)-C(27)-H(27B)
C(25)-C(27)-H(27C)
H(27A)-C(27)-H(27C)
H(27B)-C(27)-H(27C)
C(24)-C(28)-C(29)111.66(17)
C(24)-C(28)-C(30)111.05(17)
C(29)-C(28)-C(30)111.19(19)
C(24)-C(28)-H(26)108.1(11)
C(29)-C(28)-H(26)107.6(11)
C(30)-C(28)-H(26)107.0(10)
C(28)-C(29)-H(29A)
C(28)-C(29)-H(29B)
H(29A)-C(29)-H(29B)
C(28)-C(29)-H(29C)

H(29A)-C(29)-H(29C)
H(29B)-C(29)-H(29C)
C(28)-C(30)-H(30A)
C(28)-C(30)-H(30B)
H(30A)-C(30)-H(30B)
C(28)-C(30)-H(30C)
H(30A)-C(30)-H(30C)
H(30B)-C(30)-H(30C)
N(2)-C(31)-C(32)178.6(2)
C(31)-C(32)-H(32A)
C(31)-C(32)-H(32B)
H(32A)-C(32)-H(32B)
C(31)-C(32)-H(32C)
H(32A)-C(32)-H(32C)
H(32B)-C(32)-H(32C)

Symmetry transformations used to generate equivalent atoms:
#1 y,x,-z+2

Anisotropic displacement parameters ($Å^2 x\ 10^3$)for **2j.** The anisotropic displacement factor exponent takes the form: $-2\pi^2[h^2 a^{*2} U^{11} + ... + 2 h k a^* b^* U^{12}]$

	U^{11}	U^{22}	U^{33}	U^{23}	U^{13}	U^{12}
O(1)	41(1)	56(1)	30(1)	1(1)	16(1)	2(1)
O(2)	34(1)	57(1)	37(1)	-16(1)	6(1)	-2(1)
N(1)	26(1)	25(1)	23(1)	-1(1)	7(1)	4(1)
N(2)	45(1)	96(2)	108(2)	31(1)	29(1)	2(1)
N(3)	24(1)	29(1)	22(1)	-2(1)	7(1)	3(1)
C(2)	22(1)	24(1)	27(1)	-1(1)	8(1)	-1(1)
C(4)	27(1)	34(1)	23(1)	-2(1)	7(1)	3(1)
C(5)	29(1)	34(1)	25(1)	-2(1)	8(1)	2(1)
C(6)	31(1)	31(1)	26(1)	-1(1)	8(1)	7(1)
C(7)	26(1)	28(1)	22(1)	1(1)	7(1)	6(1)
C(8)	25(1)	29(1)	27(1)	1(1)	6(1)	3(1)
C(9)	31(1)	27(1)	34(1)	0(1)	10(1)	2(1)
C(10)	33(1)	32(1)	34(1)	2(1)	13(1)	8(1)
C(11)	28(1)	35(1)	34(1)	2(1)	14(1)	5(1)
C(12)	27(1)	30(1)	26(1)	3(1)	9(1)	2(1)
C(13)	29(1)	28(1)	40(1)	0(1)	13(1)	1(1)
C(14)	33(1)	61(2)	45(1)	0(1)	10(1)	-10(1)
C(15)	39(1)	40(1)	45(1)	6(1)	19(1)	-1(1)
C(16)	28(1)	29(1)	39(1)	1(1)	13(1)	3(1)
C(17)	47(1)	44(1)	49(1)	5(1)	23(1)	-5(1)
C(18)	40(1)	38(1)	45(1)	-2(1)	7(1)	-6(1)
C(19)	23(1)	31(1)	25(1)	-3(1)	6(1)	4(1)
C(20)	28(1)	32(1)	28(1)	1(1)	10(1)	5(1)
C(21)	34(1)	35(1)	34(1)	2(1)	7(1)	10(1)
C(22)	28(1)	45(1)	40(1)	-1(1)	4(1)	10(1)
C(23)	25(1)	44(1)	45(1)	-6(1)	7(1)	0(1)
C(24)	28(1)	34(1)	33(1)	-4(1)	9(1)	3(1)
C(25)	31(1)	34(1)	42(1)	10(1)	14(1)	5(1)
C(26)	65(2)	48(2)	74(2)	1(1)	48(1)	-1(1)
C(27)	41(1)	43(1)	47(1)	0(1)	13(1)	-2(1)
C(28)	31(1)	37(1)	49(1)	2(1)	10(1)	-2(1)

C(29)	53(2)	42(1)	74(2)	-5(1)	14(1)	-10(1)
C(30)	53(1)	55(2)	64(1)	12(1)	28(1)	-3(1)
C(31)	38(1)	49(1)	48(1)	11(1)	15(1)	4(1)
C(32)	33(1)	60(2)	50(1)	4(1)	10(1)	4(1)

Hydrogen coordinates (x 10^4) and isotropic displacement parameters (Å^{2}x 10^3) for **2j**.

	x	y	z	U(eq)
H(4A)	2207(14)	2479(11)	7180(12)	28(4)
H(4B)	1499(14)	1707(13)	7297(13)	37(5)
H(5A)	656(13)	3293(12)	6746(12)	31(4)
H(5B)	-35(15)	2504(12)	6897(13)	36(5)
H(9)	-3(14)	5844(12)	8698(12)	32(4)
H(10)	-1690(15)	5506(13)	8917(13)	42(5)
H(11)	-2332(16)	4114(12)	8737(14)	46(5)
H(13)	1715(14)	4383(12)	7934(13)	35(5)
H(14A)	2523(18)	4835(15)	9655(17)	65(7)
H(14B)	1975(17)	5768(15)	9348(16)	60(6)
H(14C)	2921(17)	5400(13)	8902(14)	49(6)
H(15A)	502(16)	5276(13)	6655(15)	52(6)
H(15B)	828(16)	6044(14)	7484(15)	52(6)
H(15C)	1759(16)	5639(12)	7100(14)	47(5)
H(16)	-823(13)	2365(11)	8336(11)	26(4)
H(17A)	-2026(16)	1859(15)	9119(15)	54(6)
H(17B)	-2413(18)	2808(14)	9253(15)	56(6)
H(17C)	-1139(19)	2511(14)	9851(18)	66(7)
H(18A)	-3055(17)	3035(14)	7296(15)	55(6)
H(18B)	-2157(18)	2817(14)	6719(18)	66(7)
H(18C)	-2684(18)	2081(16)	7222(16)	63(7)
H(21)	4067(15)	296(13)	10558(14)	47(5)

H(22)	5725(16)	934(12)	10750(14)	47(5)
H(23)	5764(17)	2225(12)	9949(15)	47(5)
H(25)	1408(13)	1034(11)	8959(12)	29(4)
H(26)	3403(16)	3412(12)	8525(13)	39(5)
H(26A)	1689(19)	1386(18)	10665(18)	79(8)
H(26B)	2290(20)	476(16)	11050(19)	74(7)
H(26C)	980(20)	561(16)	10351(18)	77(8)
H(27A)	2568(17)	-464(13)	9761(15)	50(6)
H(27B)	2194(16)	-189(13)	8561(16)	56(6)
H(27C)	1270(20)	-378(15)	9066(17)	69(7)
H(29A)	4570(20)	3867(16)	10170(20)	85(8)
H(29B)	4789(19)	4355(18)	9269(19)	76(8)
H(29C)	5650(20)	3631(15)	9855(17)	69(7)
H(30A)	5360(20)	2872(15)	8197(17)	67(7)
H(30B)	4581(17)	3624(16)	7619(17)	62(7)
H(30C)	4090(20)	2689(16)	7411(19)	73(8)
H(32A)	3940(20)	30(20)	7328(19)	93(9)
H(32B)	3980(20)	765(16)	8110(20)	87(8)
H(32C)	3720(20)	947(16)	6890(20)	78(8)

Torsion angles [°] for **2j**.

C(19)-N(3)-C(2)-N(1)	175.42(14)
C(4)-N(3)-C(2)-N(1)	0.66(19)
C(19)-N(3)-C(2)-C(6)	-7.0(3)
C(4)-N(3)-C(2)-C(6)	178.21(15)
C(7)-N(1)-C(2)-N(3)	-172.18(14)
C(5)-N(1)-C(2)-N(3)	1.33(19)
C(7)-N(1)-C(2)-C(6)	10.2(2)
C(5)-N(1)-C(2)-C(6)	-176.26(15)
C(2)-N(3)-C(4)-C(5)	-2.22(18)
C(19)-N(3)-C(4)-C(5)	-177.24(14)
C(2)-N(1)-C(5)-C(4)	-2.60(18)

C(7)-N(1)-C(5)-C(4)	170.76(14)
N(3)-C(4)-C(5)-N(1)	2.72(17)
N(3)-C(2)-C(6)-O(2)	59.8(2)
N(1)-C(2)-C(6)-O(2)	-122.87(17)
N(3)-C(2)-C(6)-O(1)	-119.30(17)
N(1)-C(2)-C(6)-O(1)	58.0(2)
C(2)-N(1)-C(7)-C(8)	80.28(19)
C(5)-N(1)-C(7)-C(8)	-92.30(18)
C(2)-N(1)-C(7)-C(12)	-97.91(18)
C(5)-N(1)-C(7)-C(12)	89.51(19)
C(12)-C(7)-C(8)-C(9)	4.5(2)
N(1)-C(7)-C(8)-C(9)	-173.61(13)
C(12)-C(7)-C(8)-C(13)	-173.14(14)
N(1)-C(7)-C(8)-C(13)	8.8(2)
C(7)-C(8)-C(9)-C(10)	-3.4(2)
C(13)-C(8)-C(9)-C(10)	174.36(15)
C(8)-C(9)-C(10)-C(11)	0.2(2)
C(9)-C(10)-C(11)-C(12)	2.2(2)
C(10)-C(11)-C(12)-C(7)	-1.2(2)
C(10)-C(11)-C(12)-C(16)	179.80(15)
C(8)-C(7)-C(12)-C(11)	-2.3(2)
N(1)-C(7)-C(12)-C(11)	175.81(13)
C(8)-C(7)-C(12)-C(16)	176.73(14)
N(1)-C(7)-C(12)-C(16)	-5.2(2)
C(9)-C(8)-C(13)-C(14)	66.2(2)
C(7)-C(8)-C(13)-C(14)	-116.24(19)
C(9)-C(8)-C(13)-C(15)	-57.1(2)
C(7)-C(8)-C(13)-C(15)	120.45(17)
C(11)-C(12)-C(16)-C(17)	-52.4(2)
C(7)-C(12)-C(16)-C(17)	128.63(17)
C(11)-C(12)-C(16)-C(18)	71.55(19)
C(7)-C(12)-C(16)-C(18)	-107.44(18)
C(2)-N(3)-C(19)-C(20)	90.3(2)
C(4)-N(3)-C(19)-C(20)	-95.48(18)
C(2)-N(3)-C(19)-C(24)	-91.51(19)
C(4)-N(3)-C(19)-C(24)	82.72(19)

C(24)-C(19)-C(20)-C(21)	2.6(2)
N(3)-C(19)-C(20)-C(21)	-179.34(14)
C(24)-C(19)-C(20)-C(25)	-178.87(15)
N(3)-C(19)-C(20)-C(25)	-0.8(2)
C(19)-C(20)-C(21)-C(22)	-1.8(2)
C(25)-C(20)-C(21)-C(22)	179.62(15)
C(20)-C(21)-C(22)-C(23)	-0.1(3)
C(21)-C(22)-C(23)-C(24)	1.4(3)
C(22)-C(23)-C(24)-C(19)	-0.6(3)
C(22)-C(23)-C(24)-C(28)	179.95(16)
C(20)-C(19)-C(24)-C(23)	-1.4(2)
N(3)-C(19)-C(24)-C(23)	-179.49(14)
C(20)-C(19)-C(24)-C(28)	178.02(16)
N(3)-C(19)-C(24)-C(28)	-0.1(2)
C(19)-C(20)-C(25)-C(27)	132.37(17)
C(21)-C(20)-C(25)-C(27)	-49.1(2)
C(19)-C(20)-C(25)-C(26)	-104.14(19)
C(21)-C(20)-C(25)-C(26)	74.4(2)
C(23)-C(24)-C(28)-C(29)	-53.8(2)
C(19)-C(24)-C(28)-C(29)	126.78(19)
C(23)-C(24)-C(28)-C(30)	70.9(2)
C(19)-C(24)-C(28)-C(30)	-108.5(2)

Symmetry transformations used to generate equivalent atoms:

#1 y,x,-z+2

APPENDIX B

NMR SPECTRA AND X-RAY CRYSTAL STRUCTURE REPORTS FOR CHAPTER 2

^{1}H NMR spectrum of 4

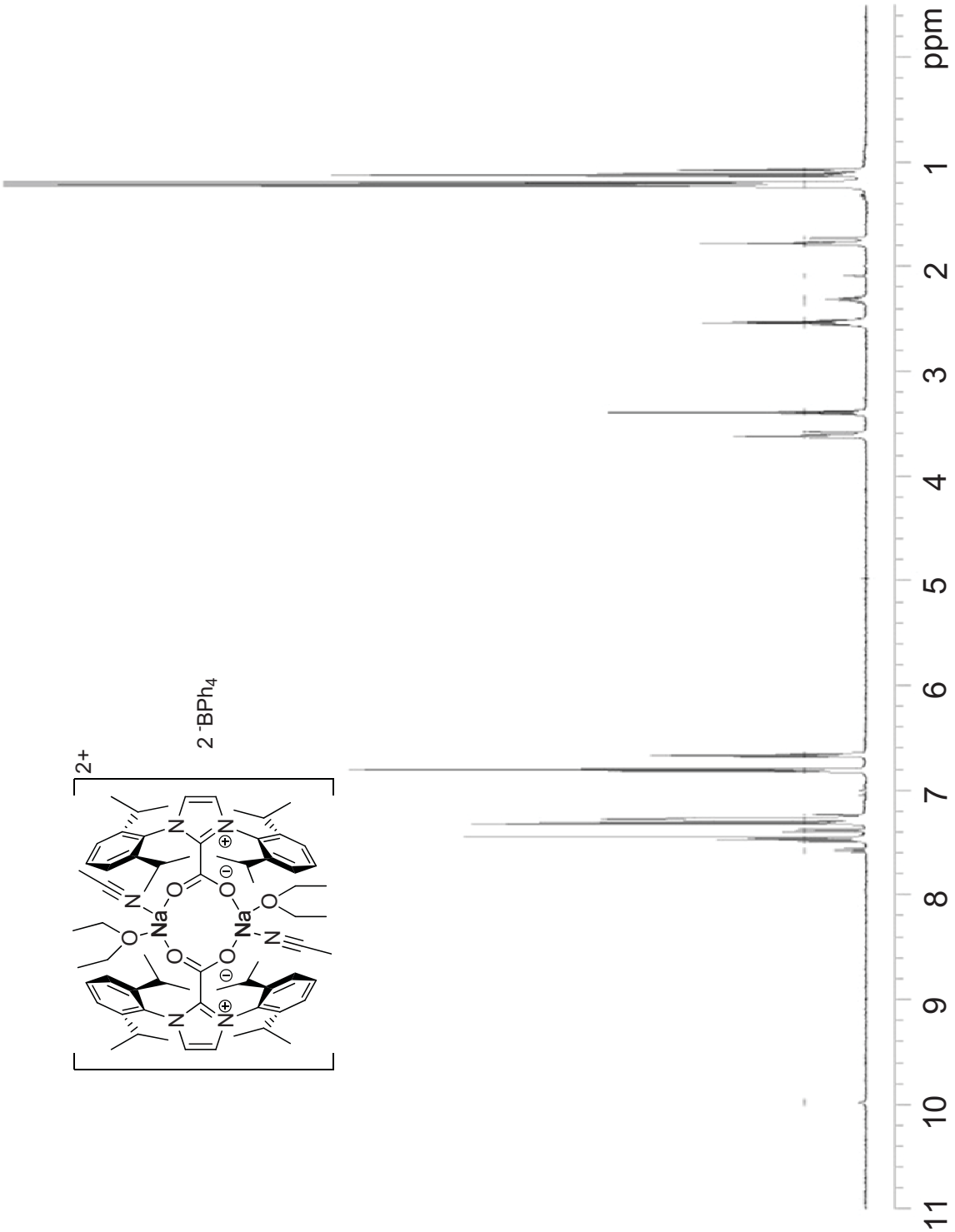

^{13}C NMR spectrum of 4

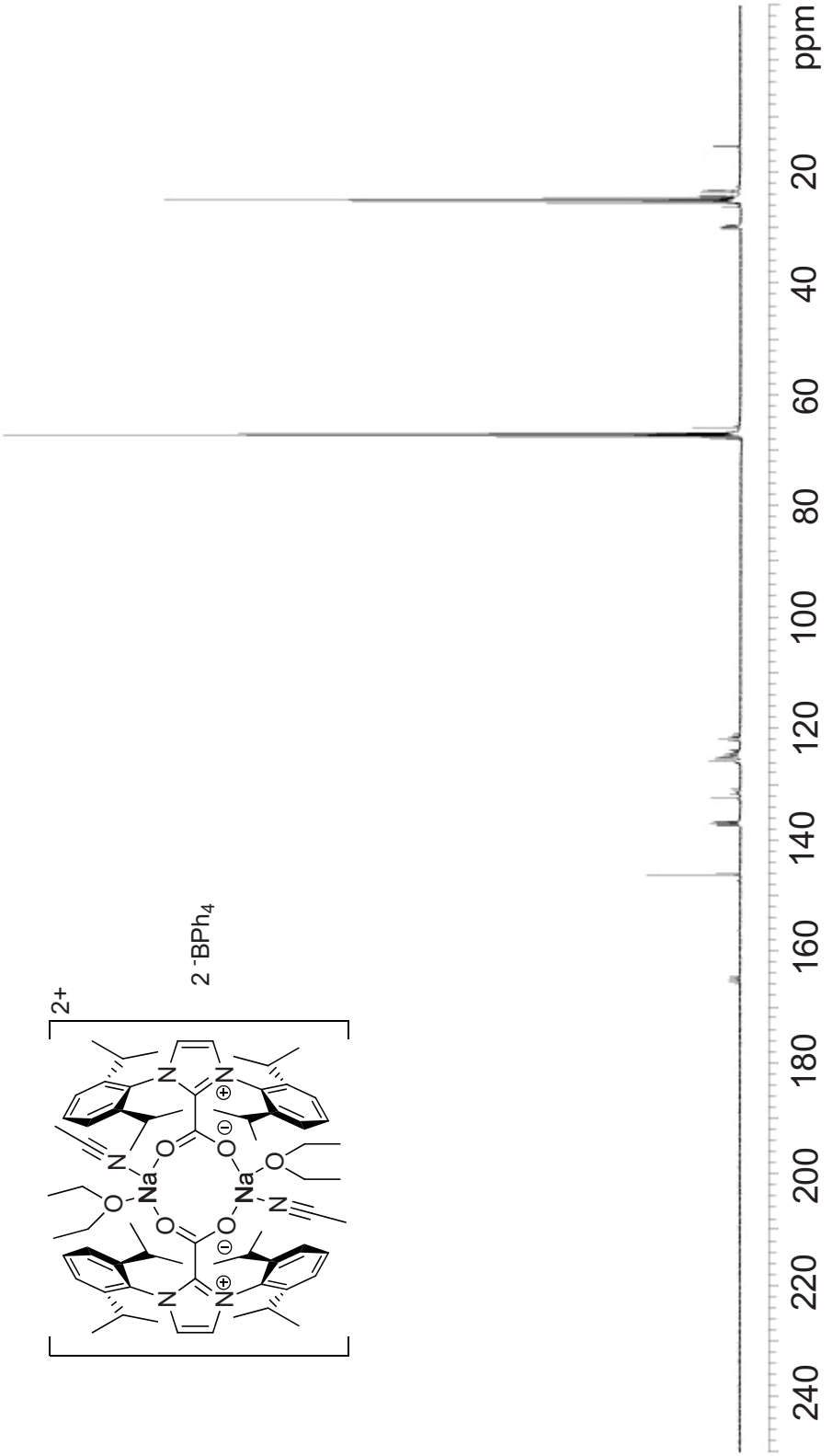

^{1}H NMR spectrum of 5

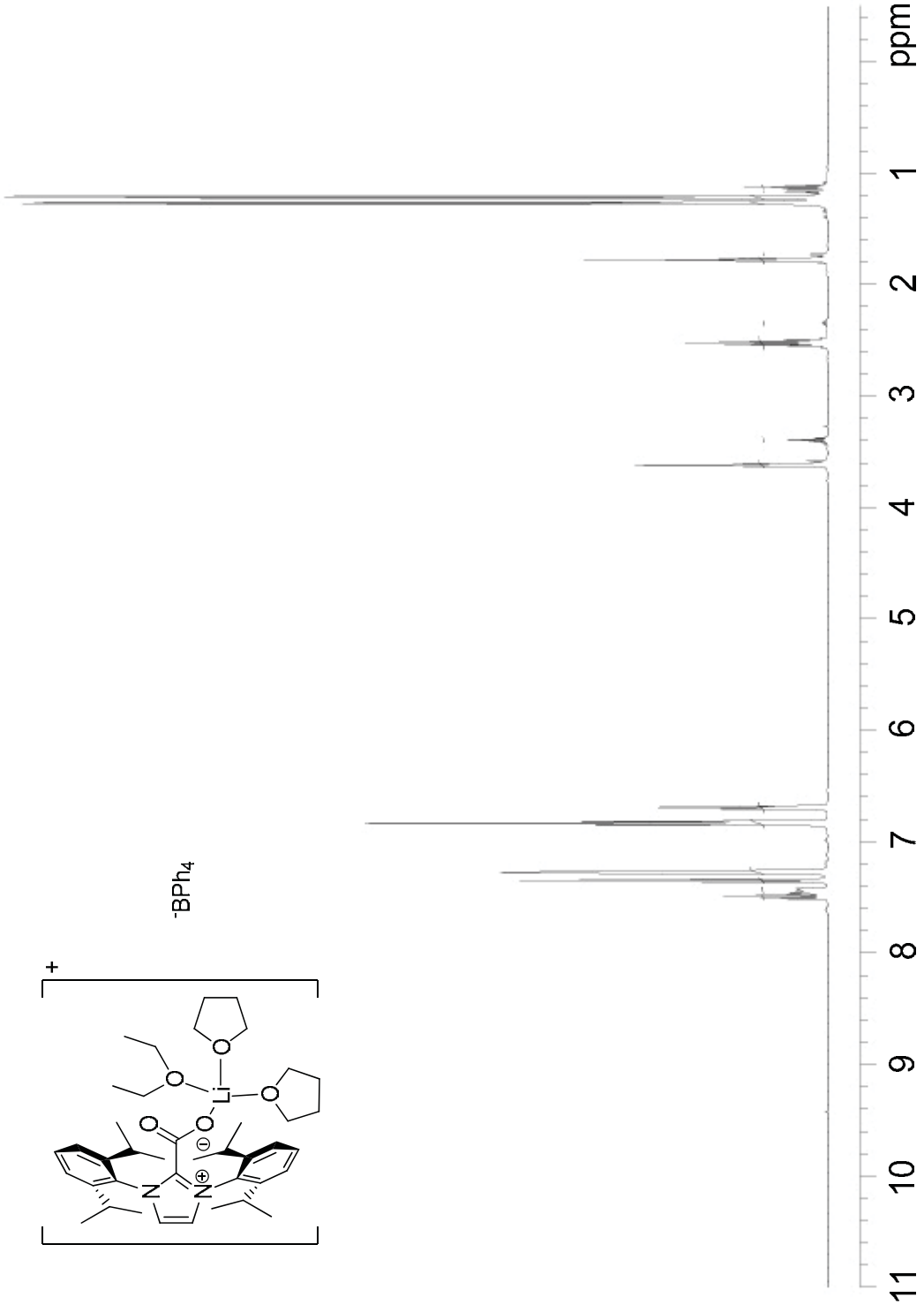

^{13}C NMR spectrum of 5

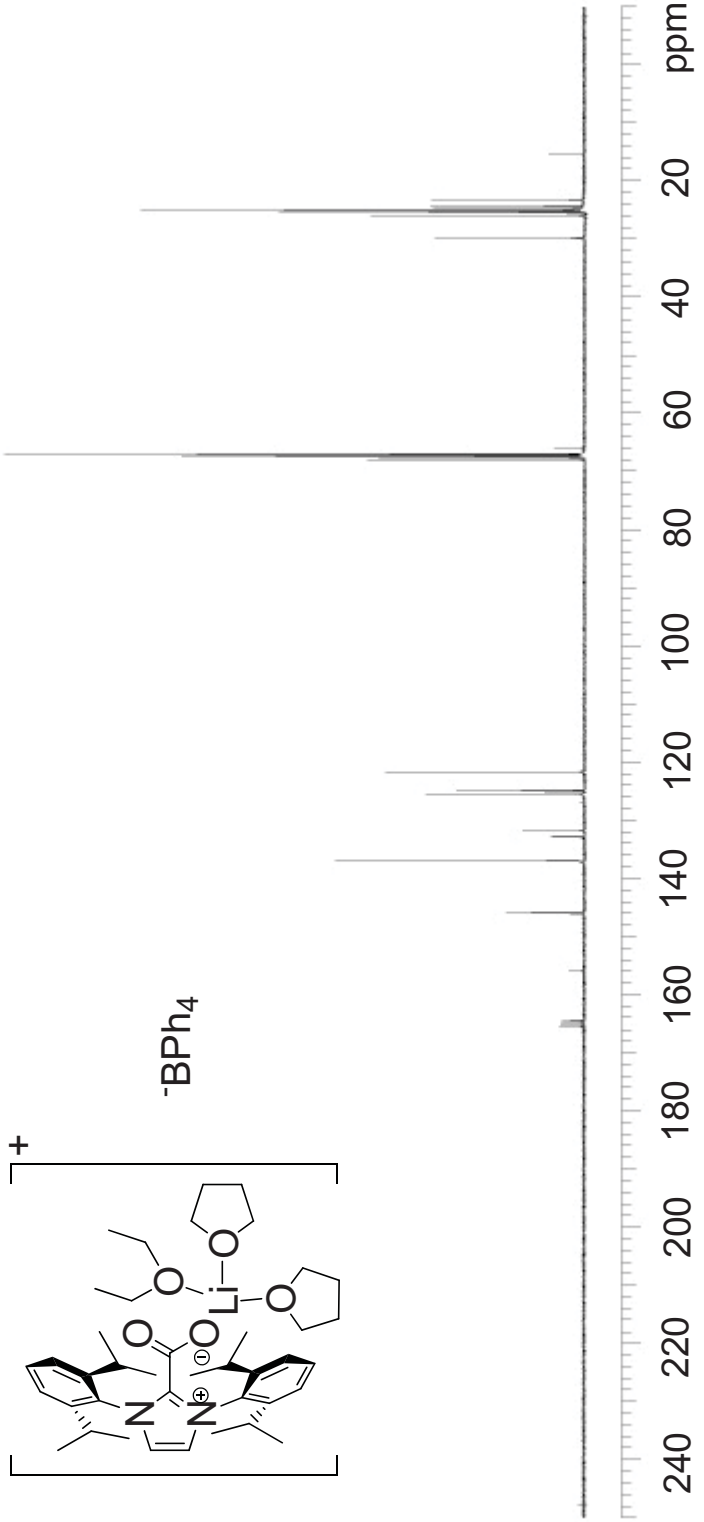

^{1}H NMR spectrum of *iso*-structural 6–crystal grown with THF in lieu of MeCN

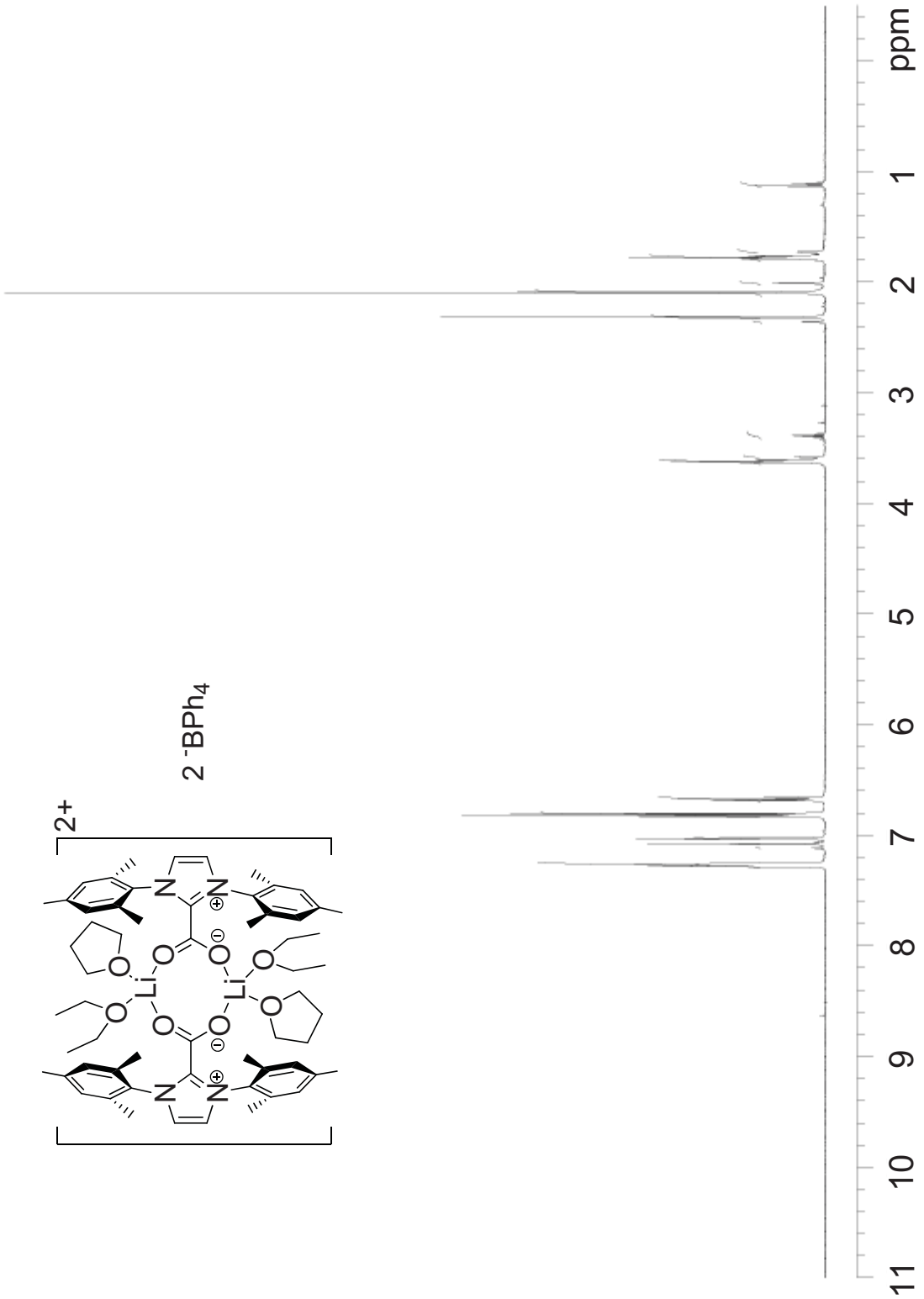

^{13}C NMR spectrum of *iso*-structural 6–crystal grown with THF in lieu of MeCN

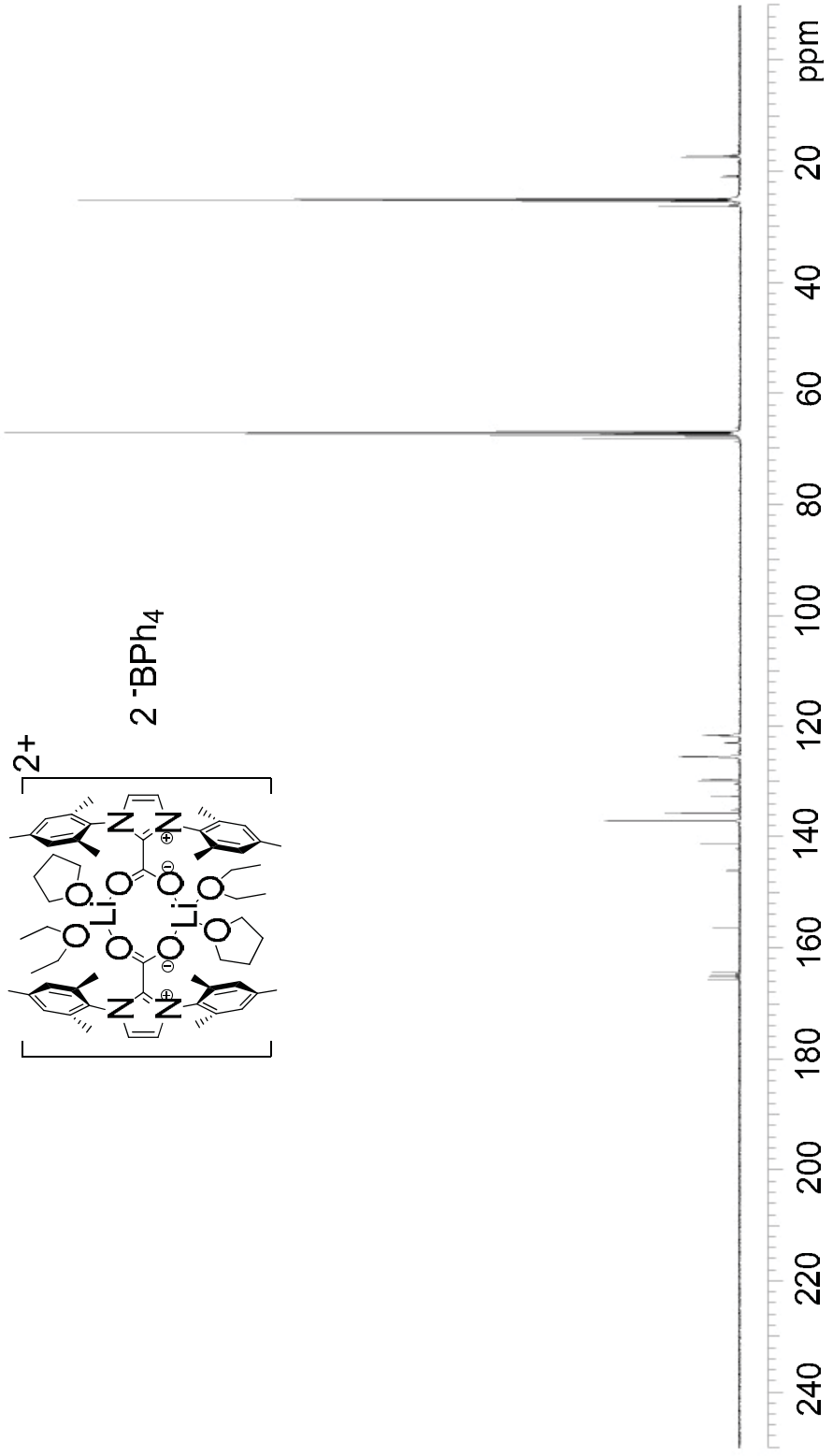

^{1}H NMR spectrum of IPrCO$_2$+KBPh$_4$

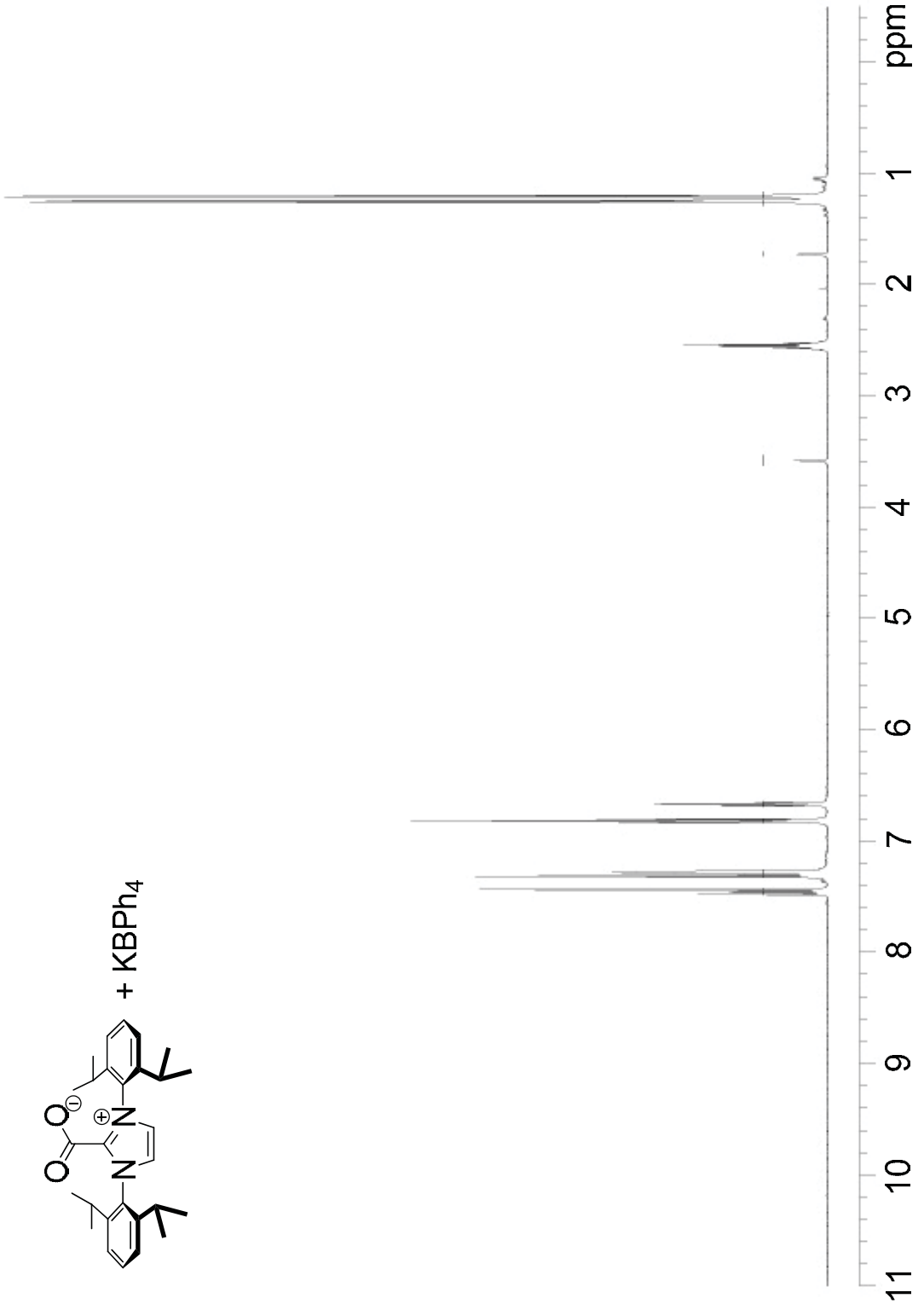

^{13}C NMR spectrum of IPrCO$_2$+KBPh$_4$

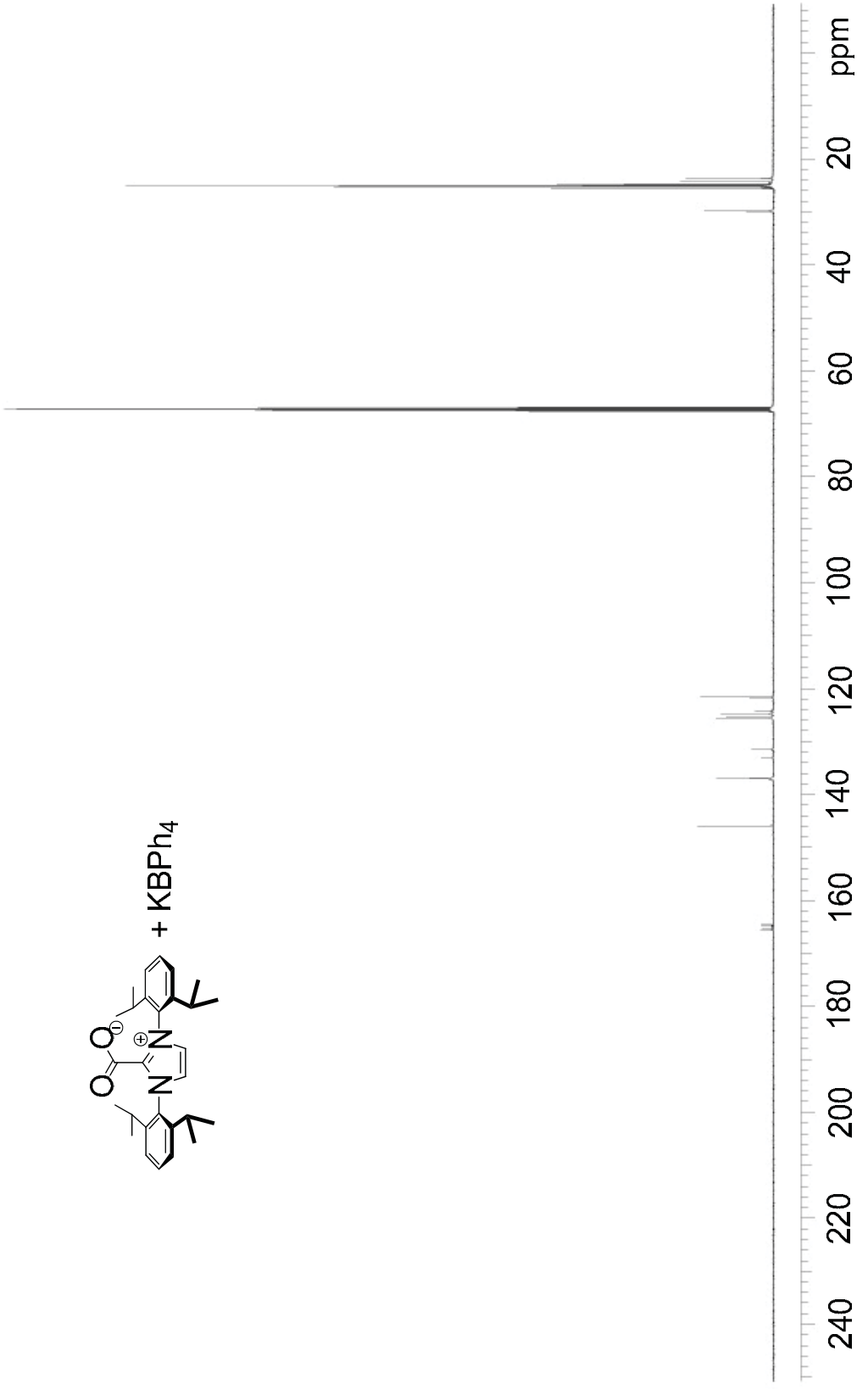

^{1}H NMR spectrum of IPrCO$_2$+LiBF$_4$

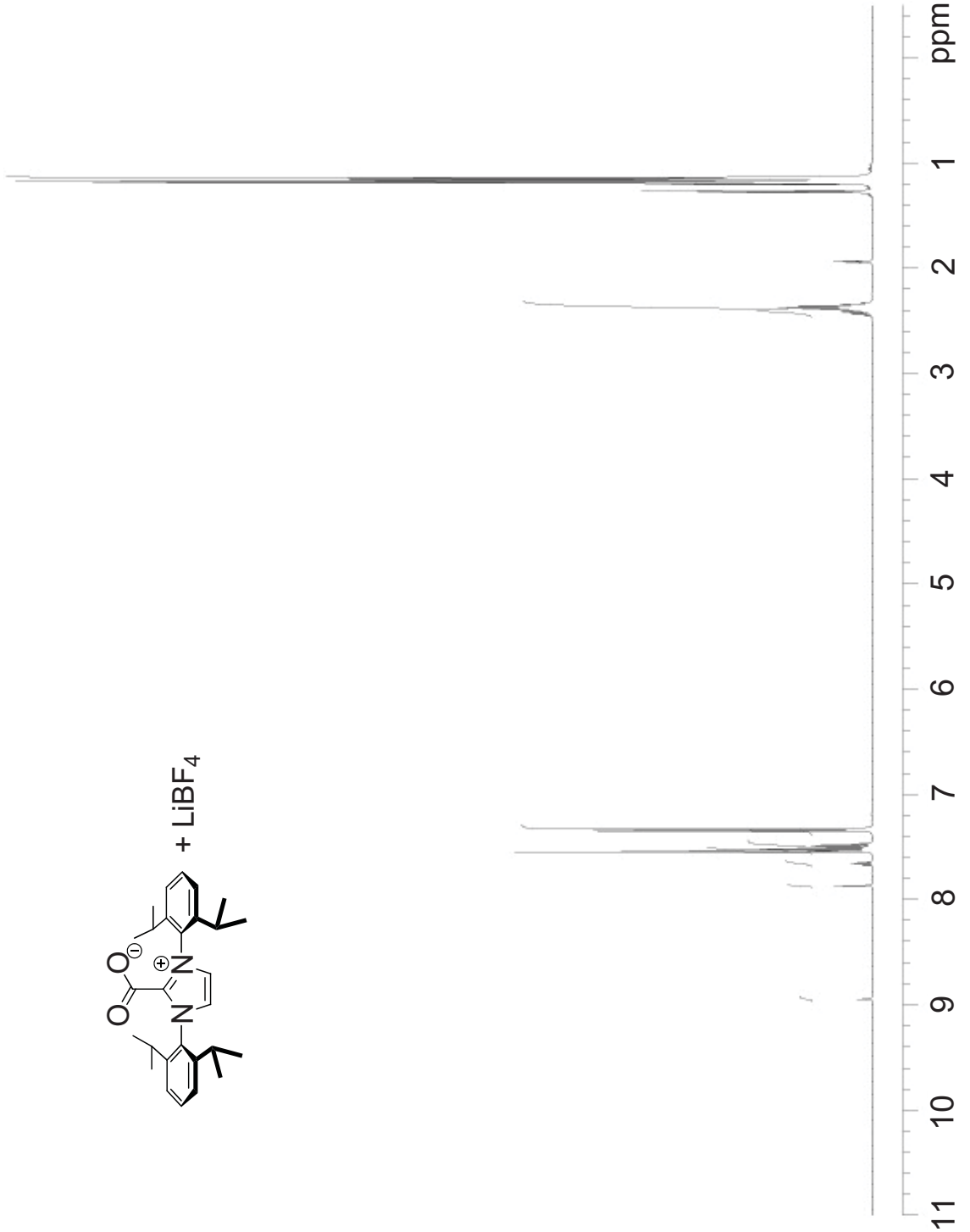

^{13}C NMR spectrum of IPrCO$_2$+LiBF$_4$

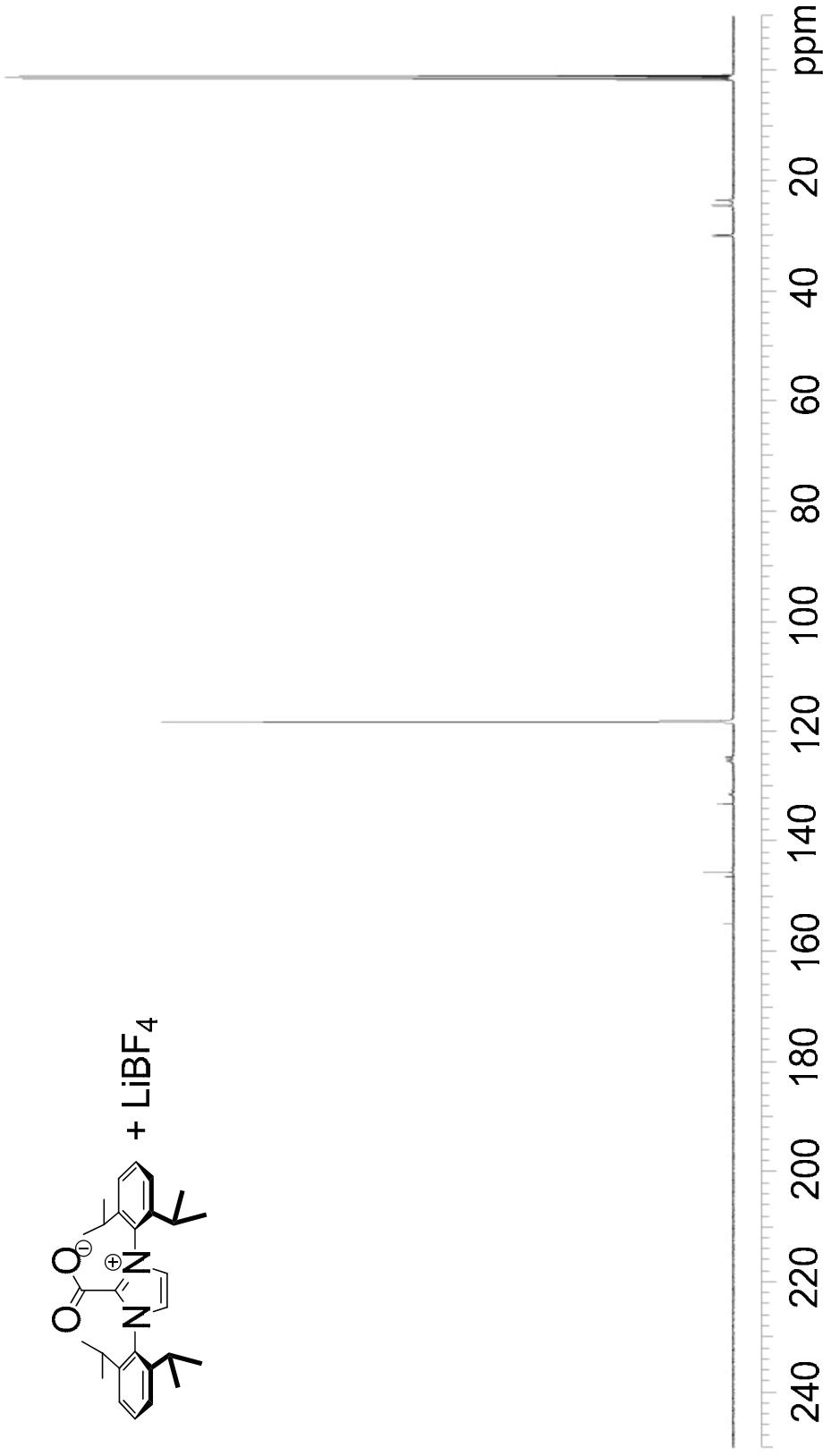

^{1}H NMR spectrum of IPrCO$_2$+LiI

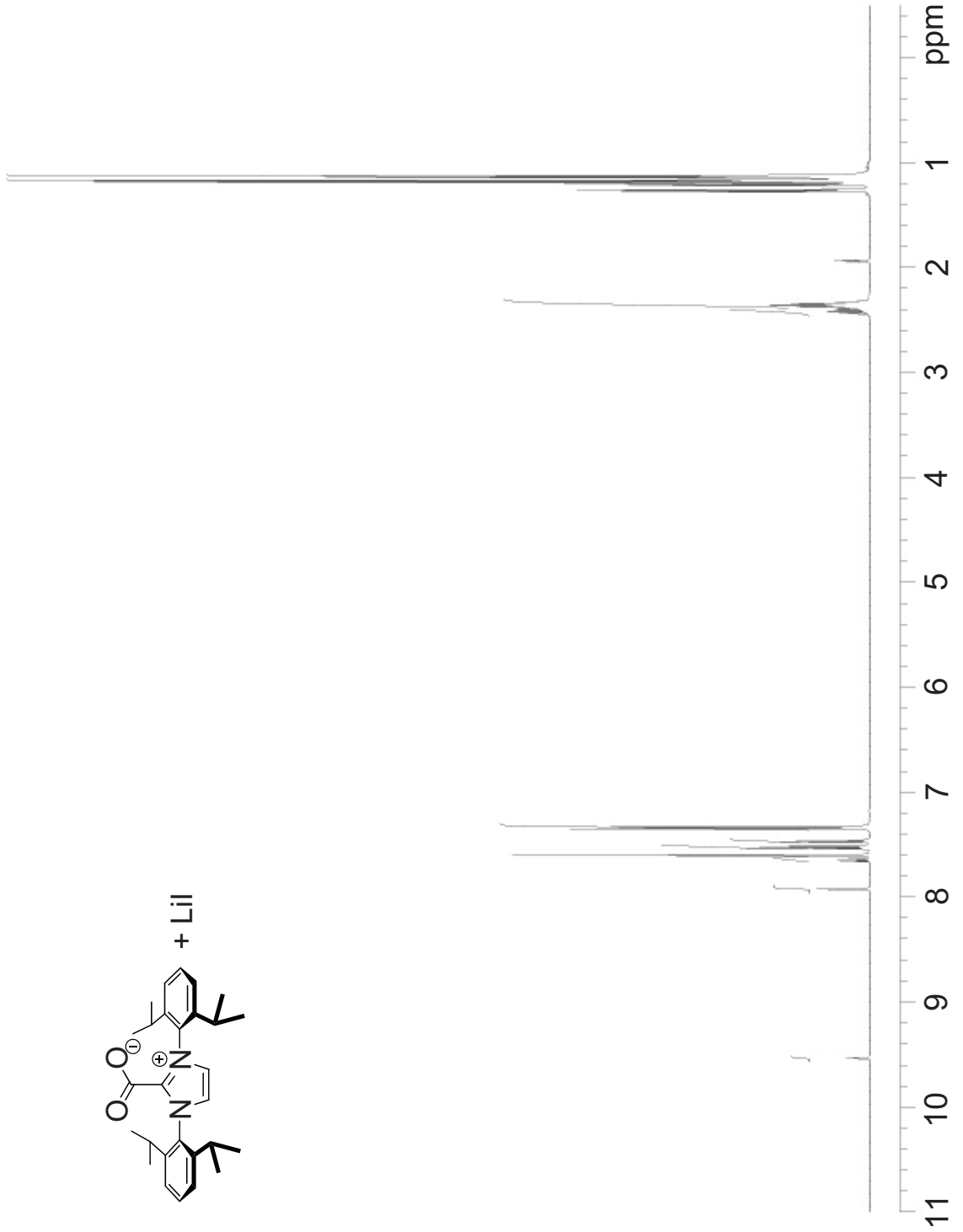

^{13}C NMR spectrum of IPrCO$_2$+LiI

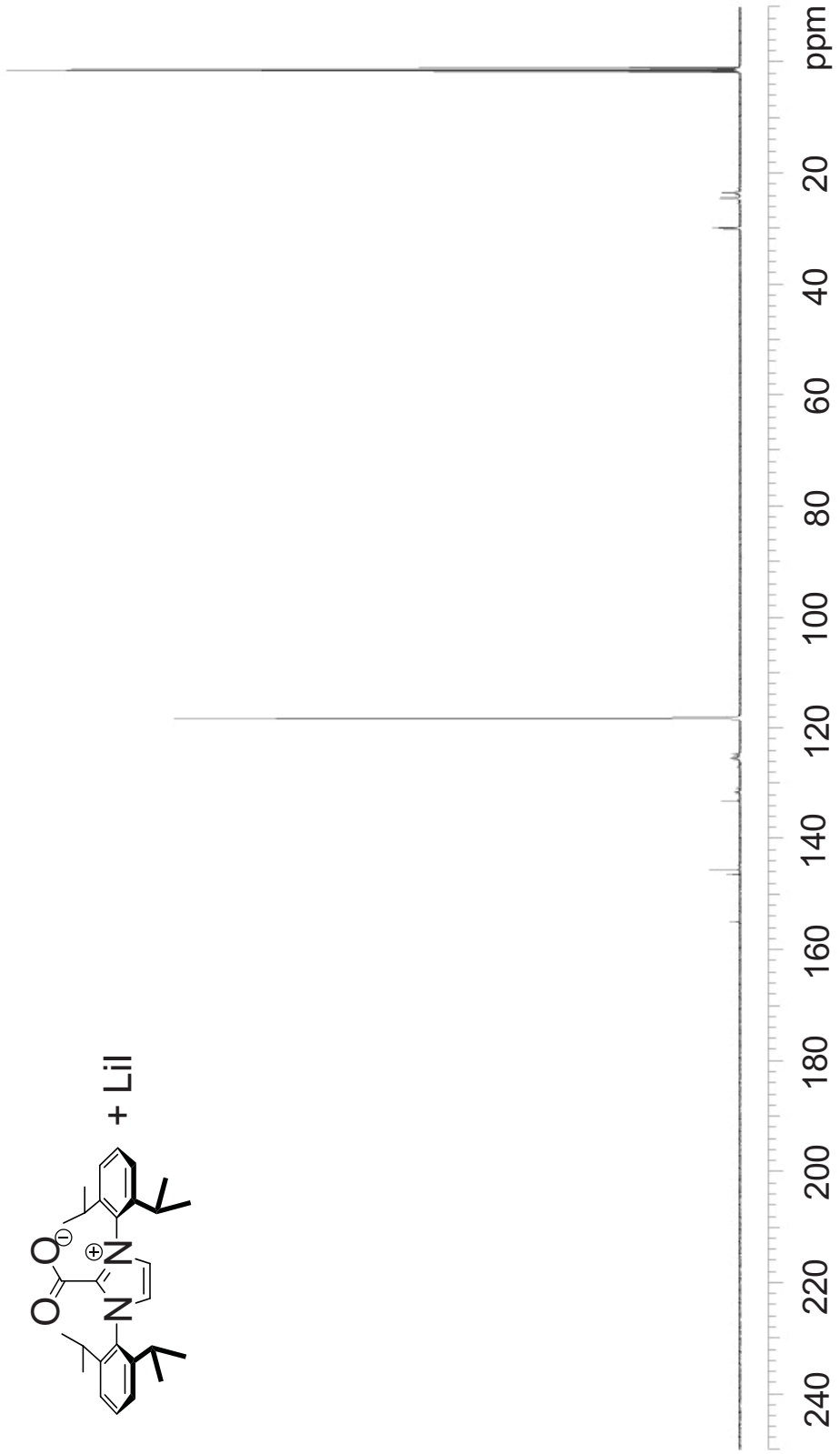

^{1}H NMR spectrum of IPrCO$_2$+NaI

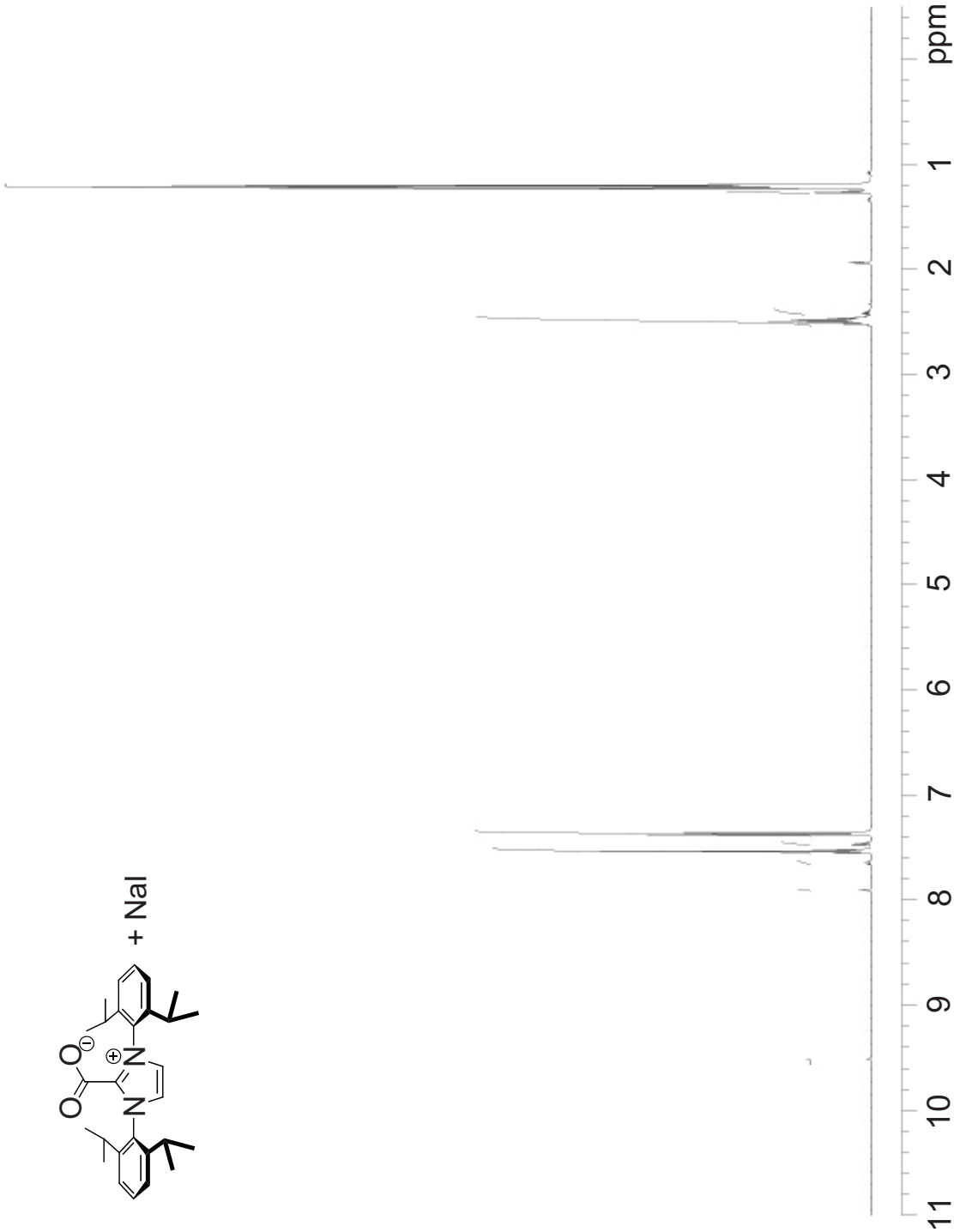

^{13}C NMR spectrum of IPrCO_2+NaI

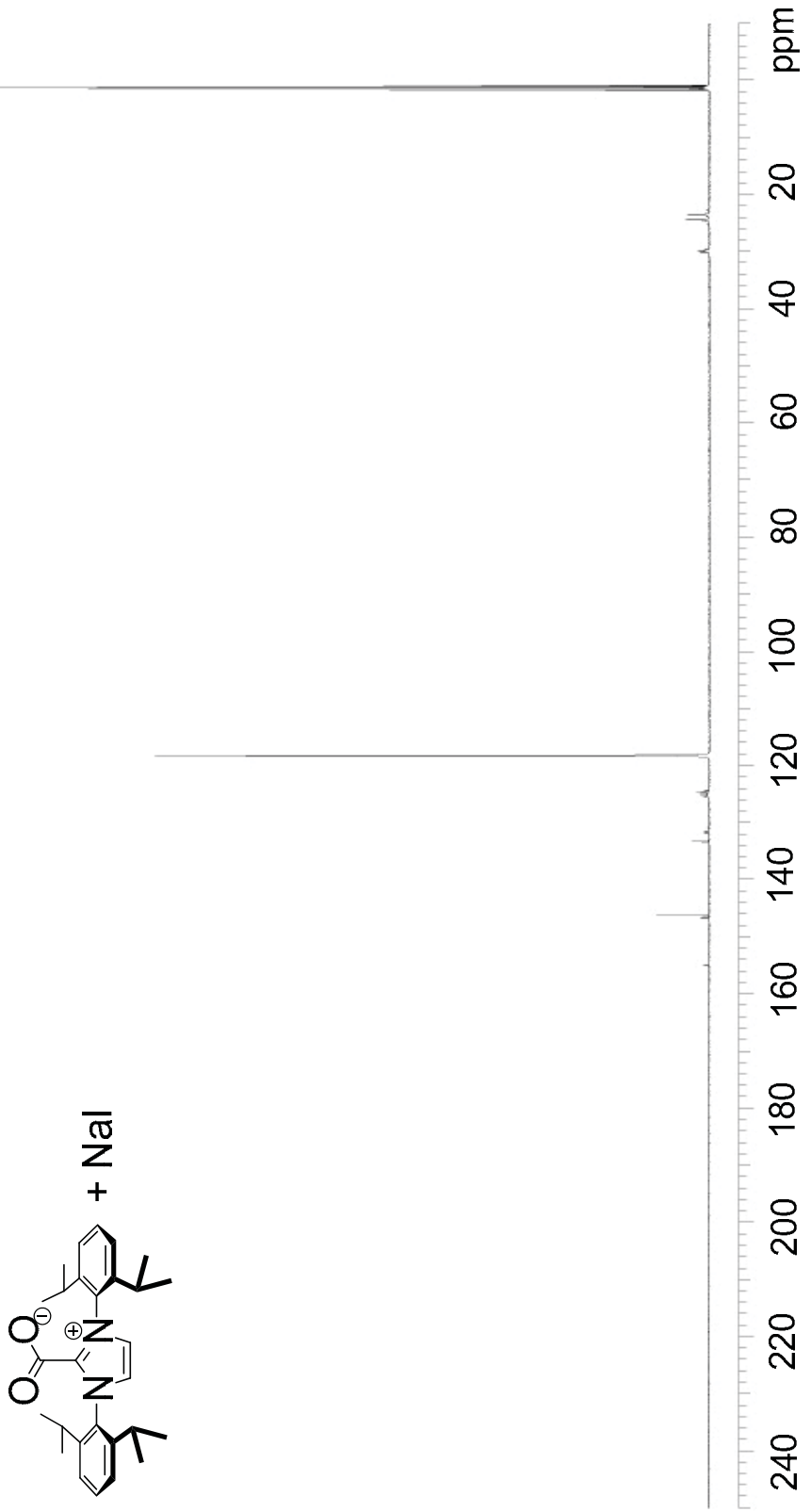

^{1}H NMR spectrum of IPrCO$_2$+LiI

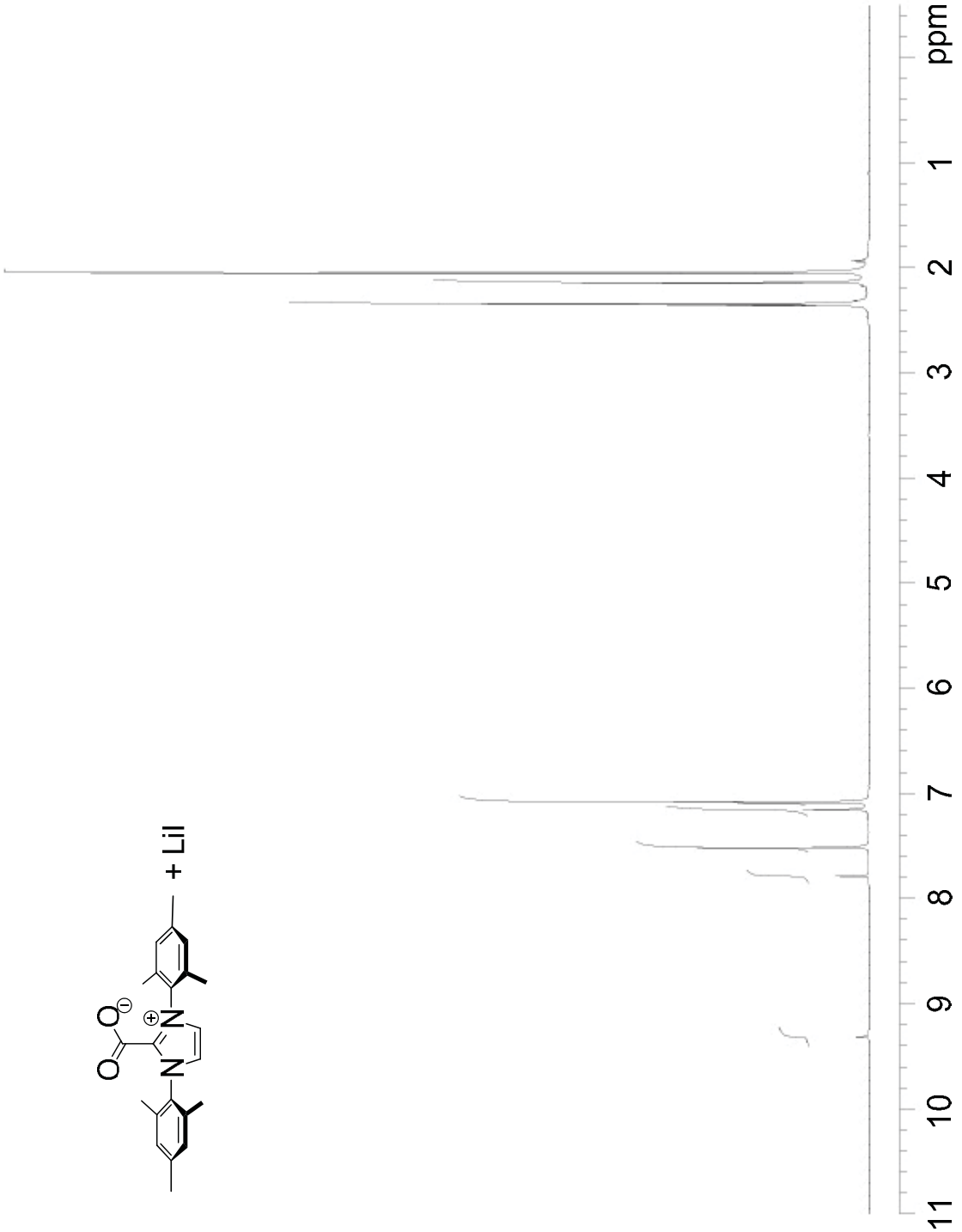

^{13}C NMR spectrum of IPrCO$_2$+LiI

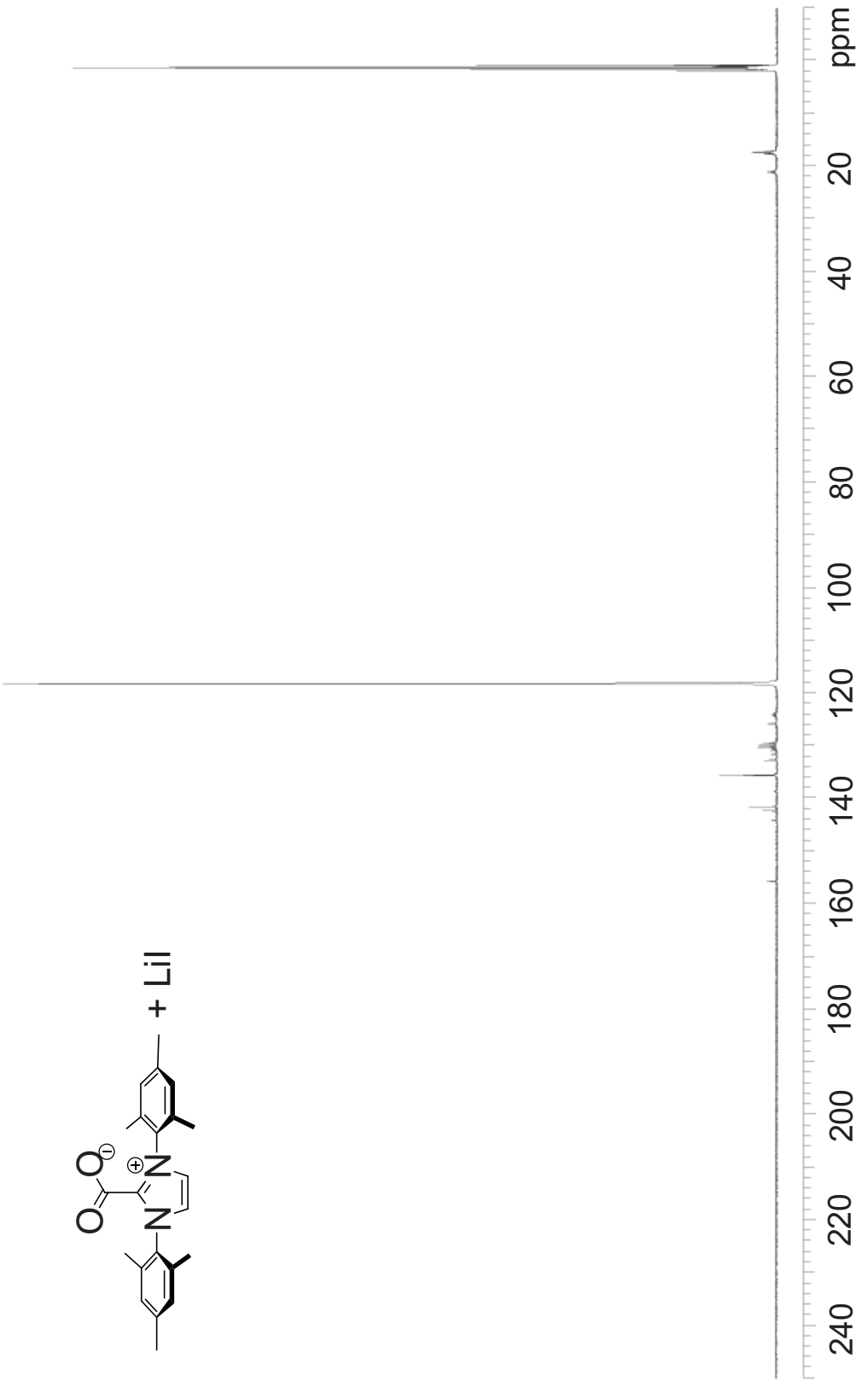

^{1}H NMR spectrum of I^{t}BuCO$_2$+LiBPh$_4$(DME)$_3$

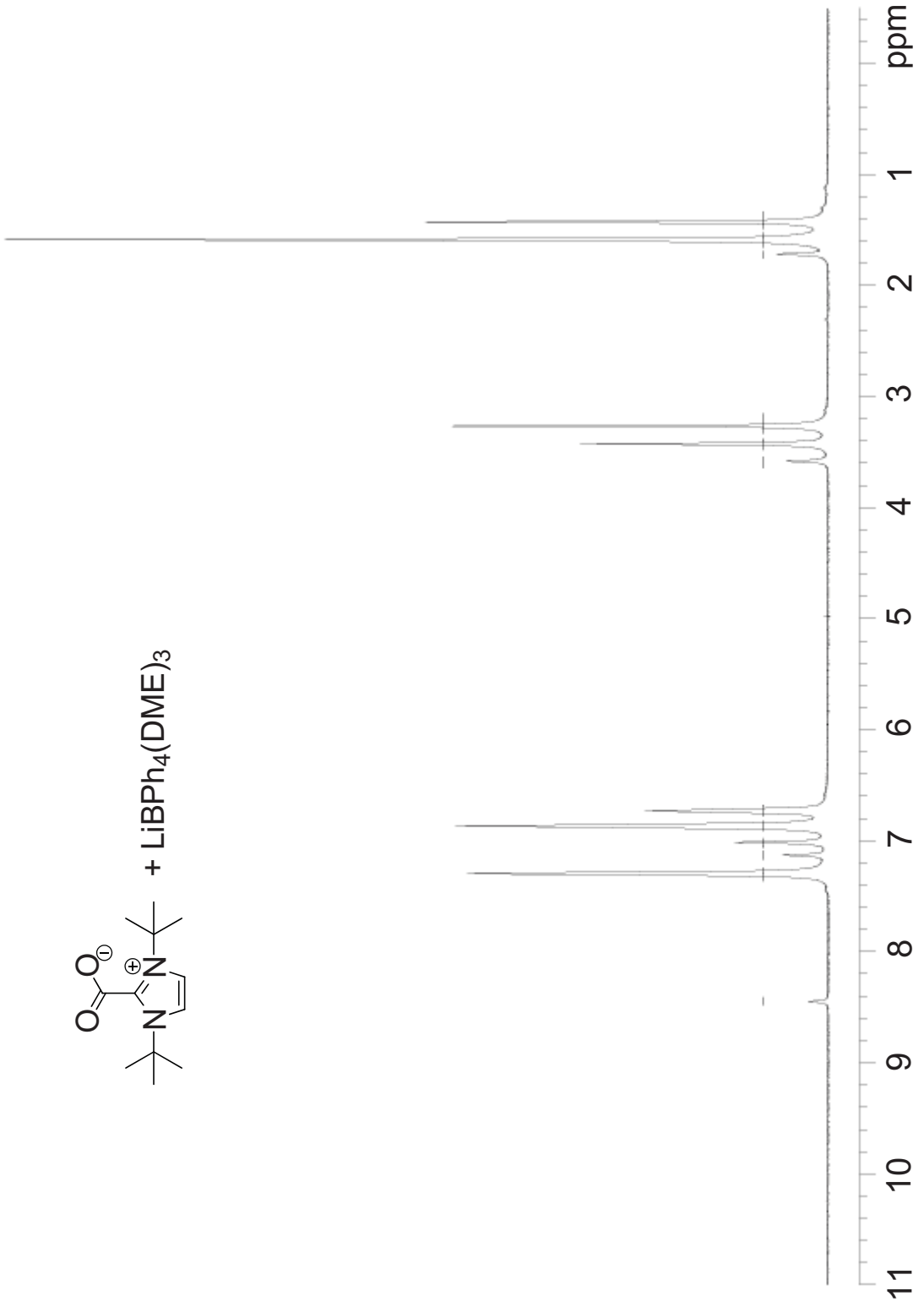

^{13}C NMR spectrum of I^{t}BuCO$_2$+LiBPh$_4$(DME)$_3$

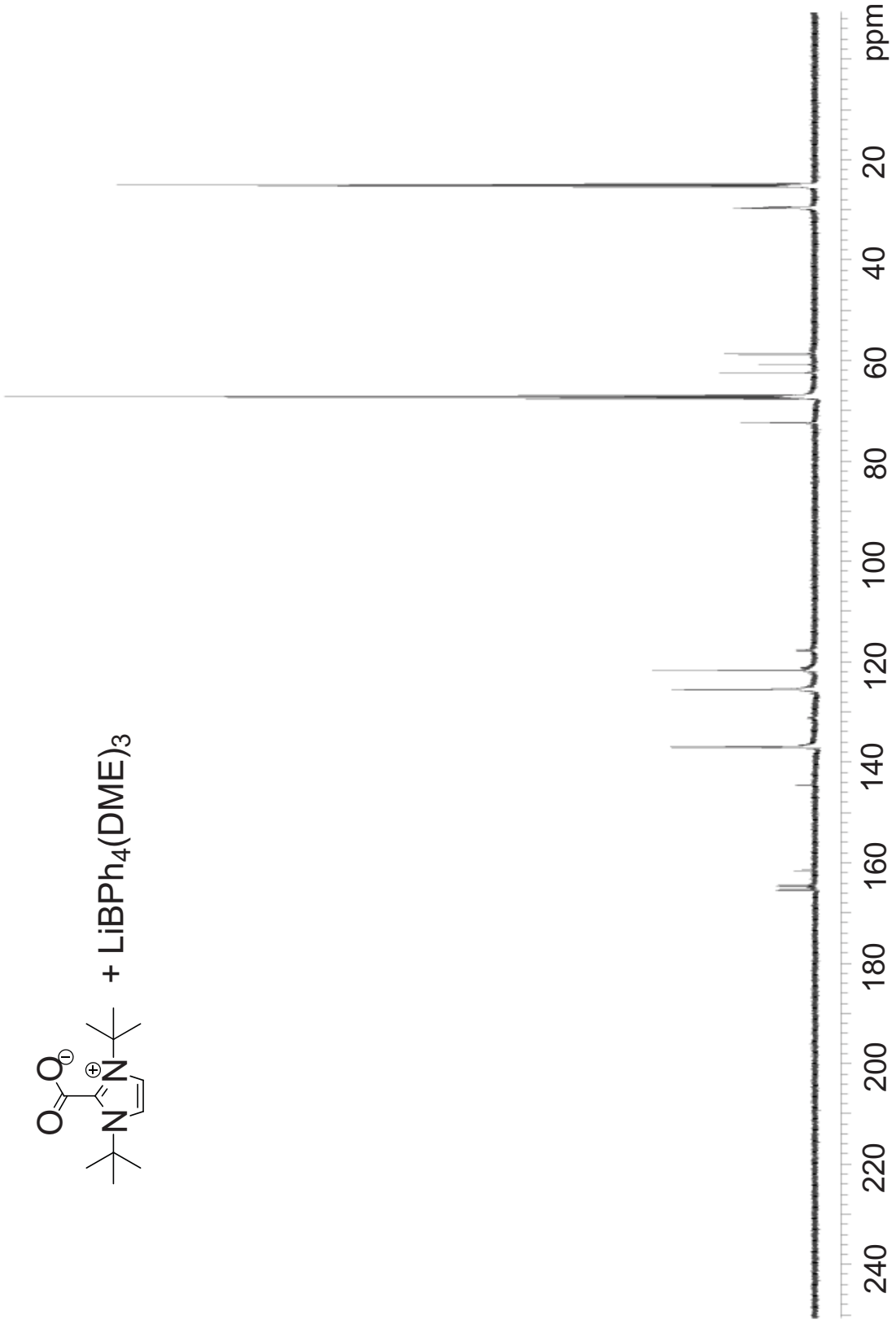

^{1}H NMR spectrum of I^{t}BuCO$_2$+NaBPh$_4$

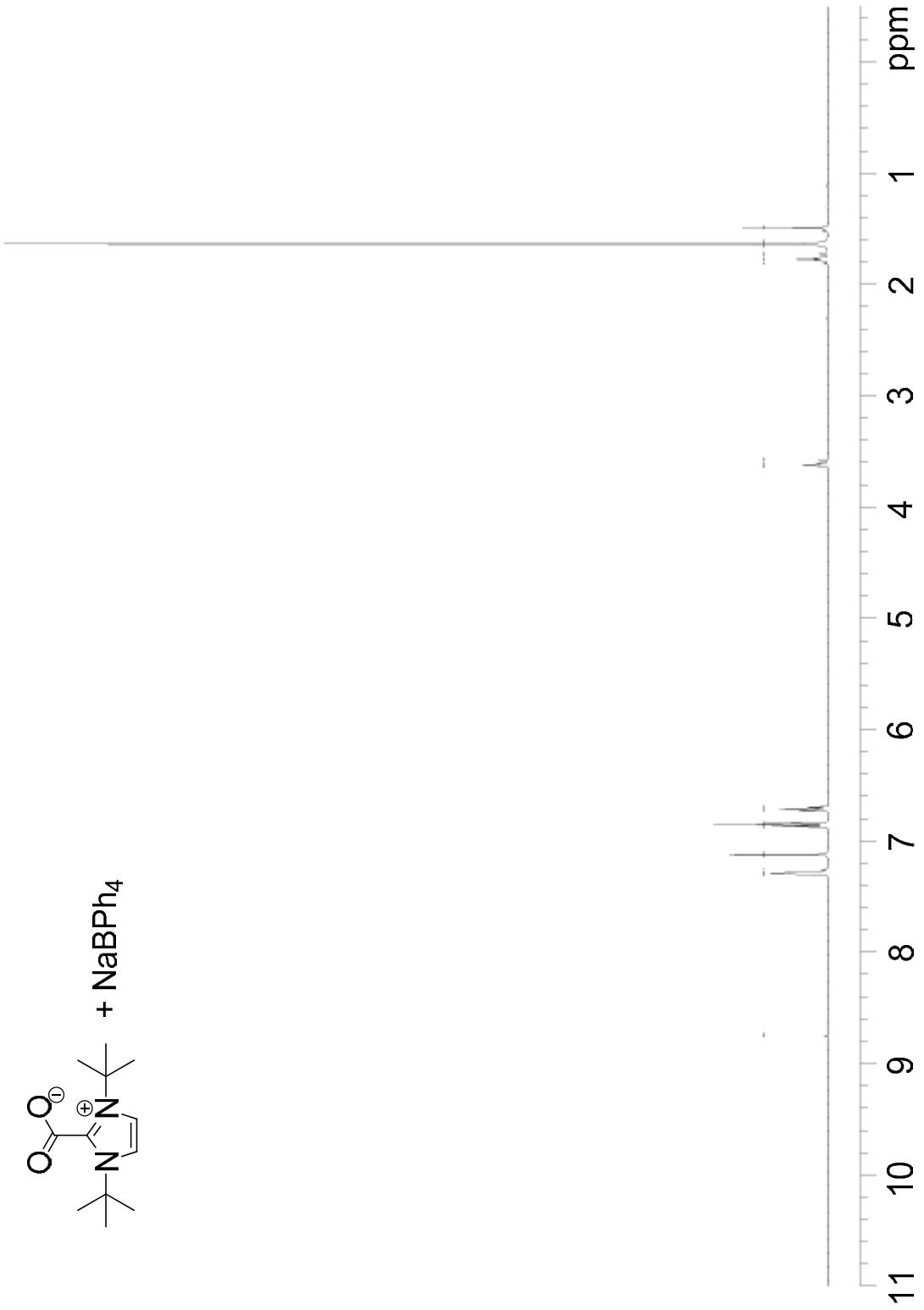

^{13}C NMR spectrum of I^{t}BuCO$_2$+NaBPh$_4$

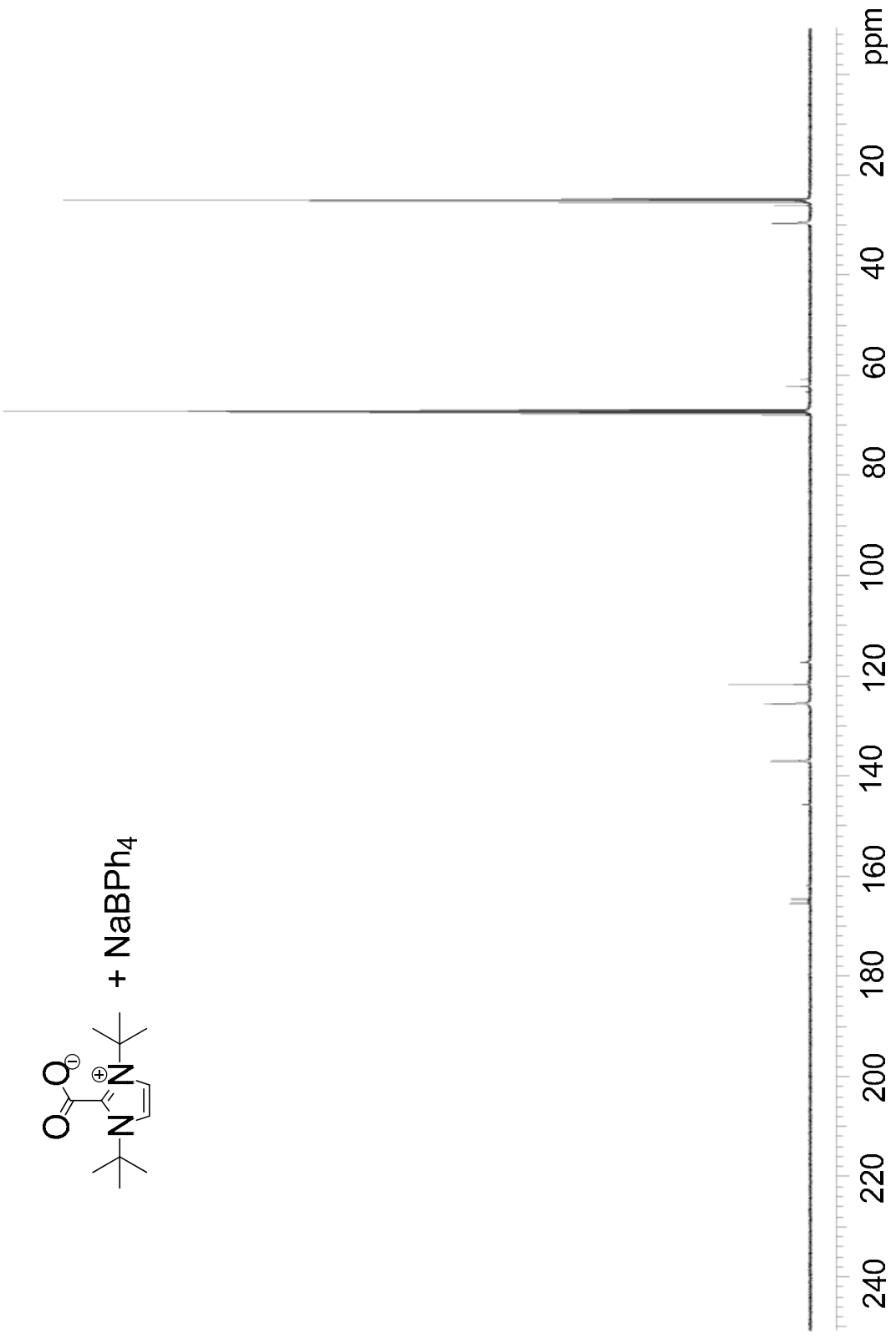

^{1}H NMR spectrum of I^{t}BuCO$_2$+KBPh$_4$

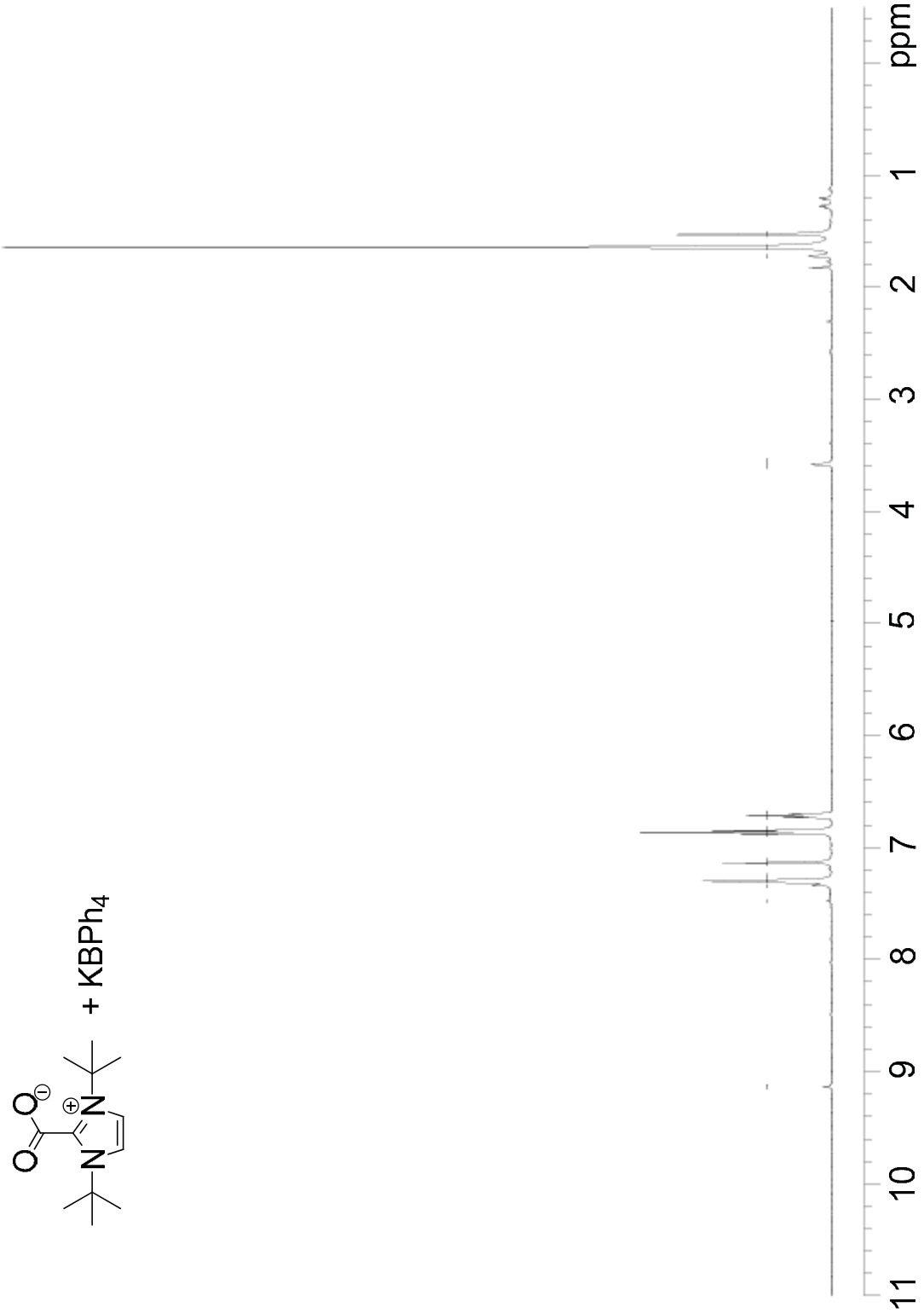

^{13}C NMR spectrum of I^{t}BuCO$_2$+KBPh$_4$

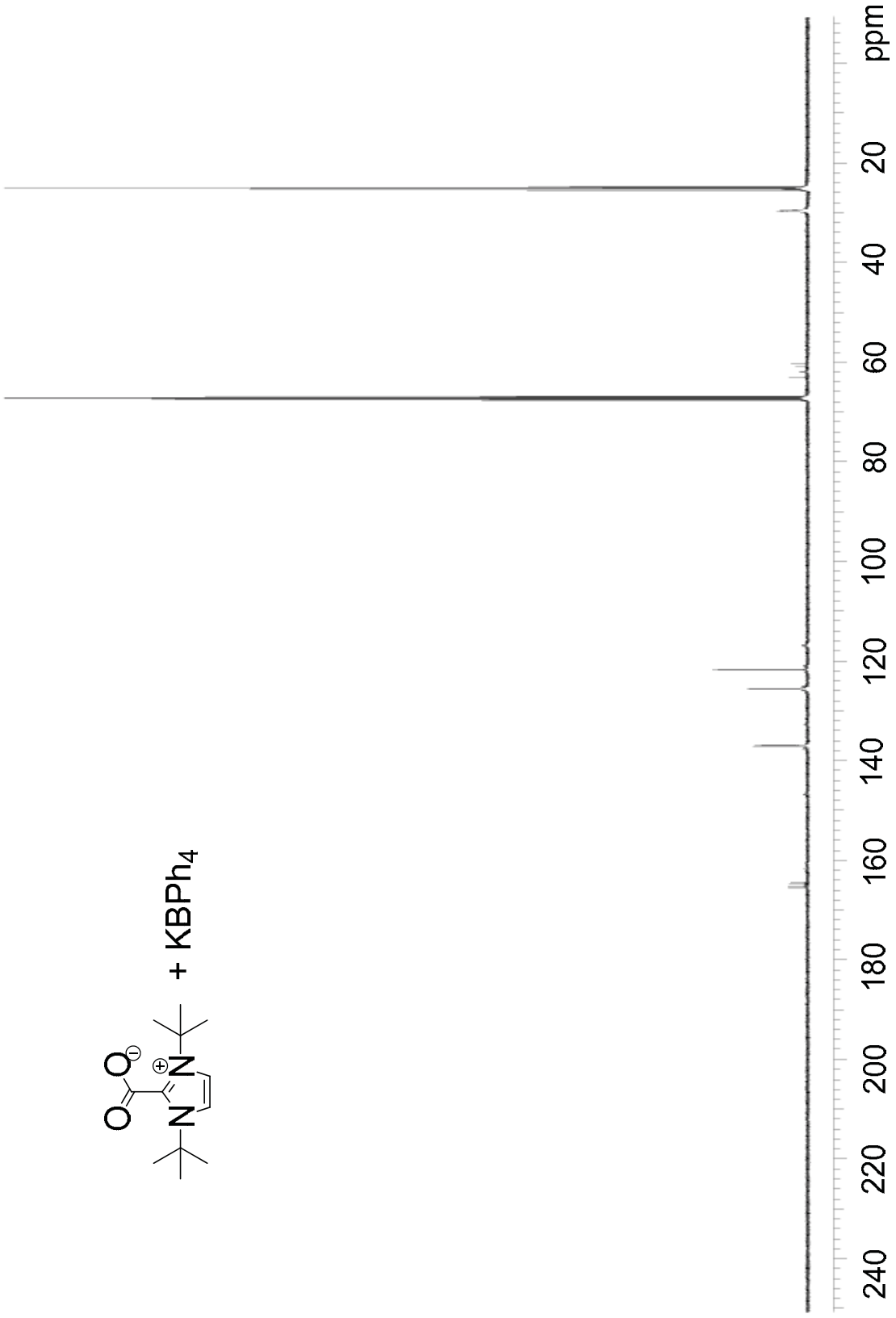

^{1}H NMR spectrum of Compound 11

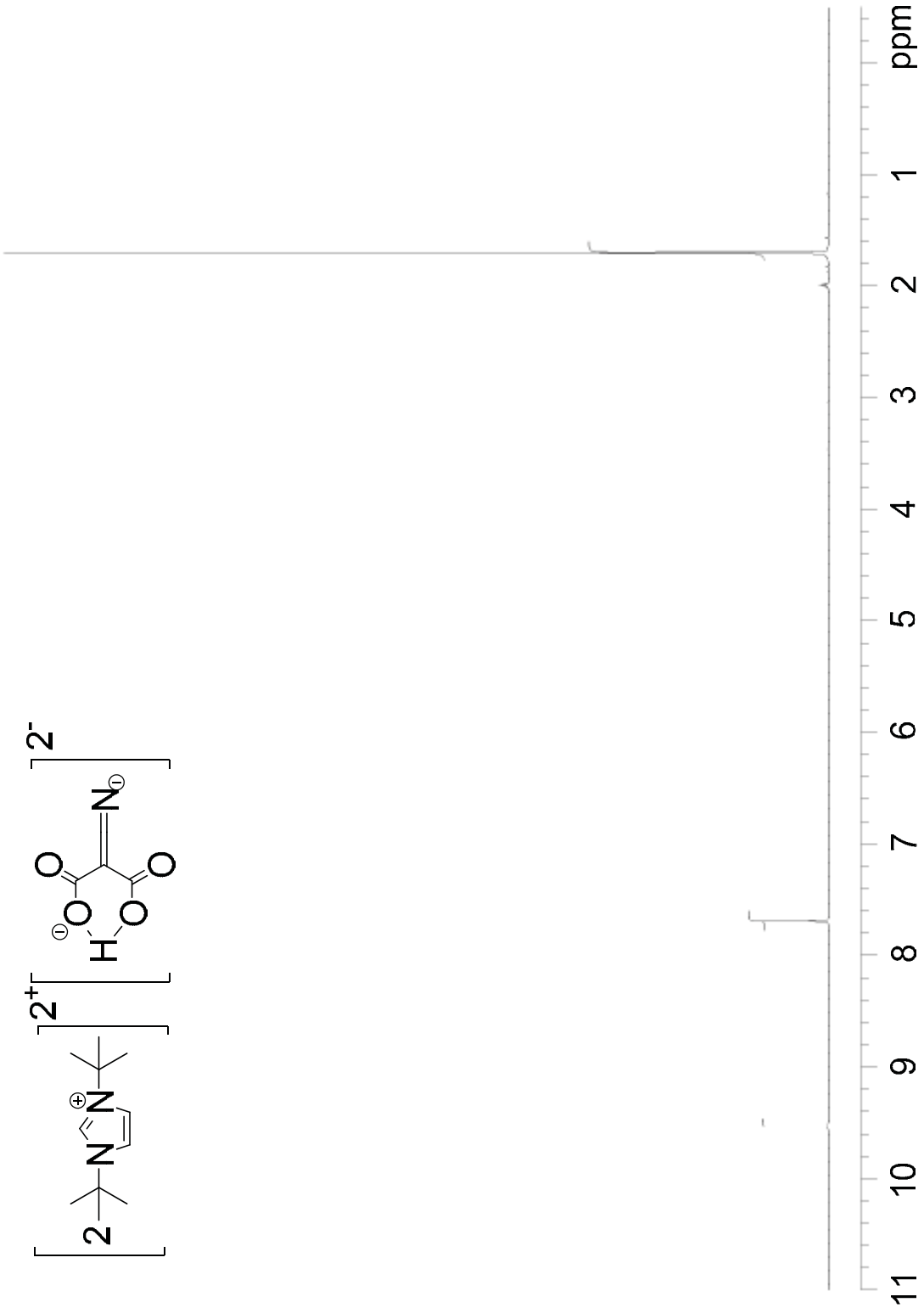

^{13}C NMR spectrum of Compound 15

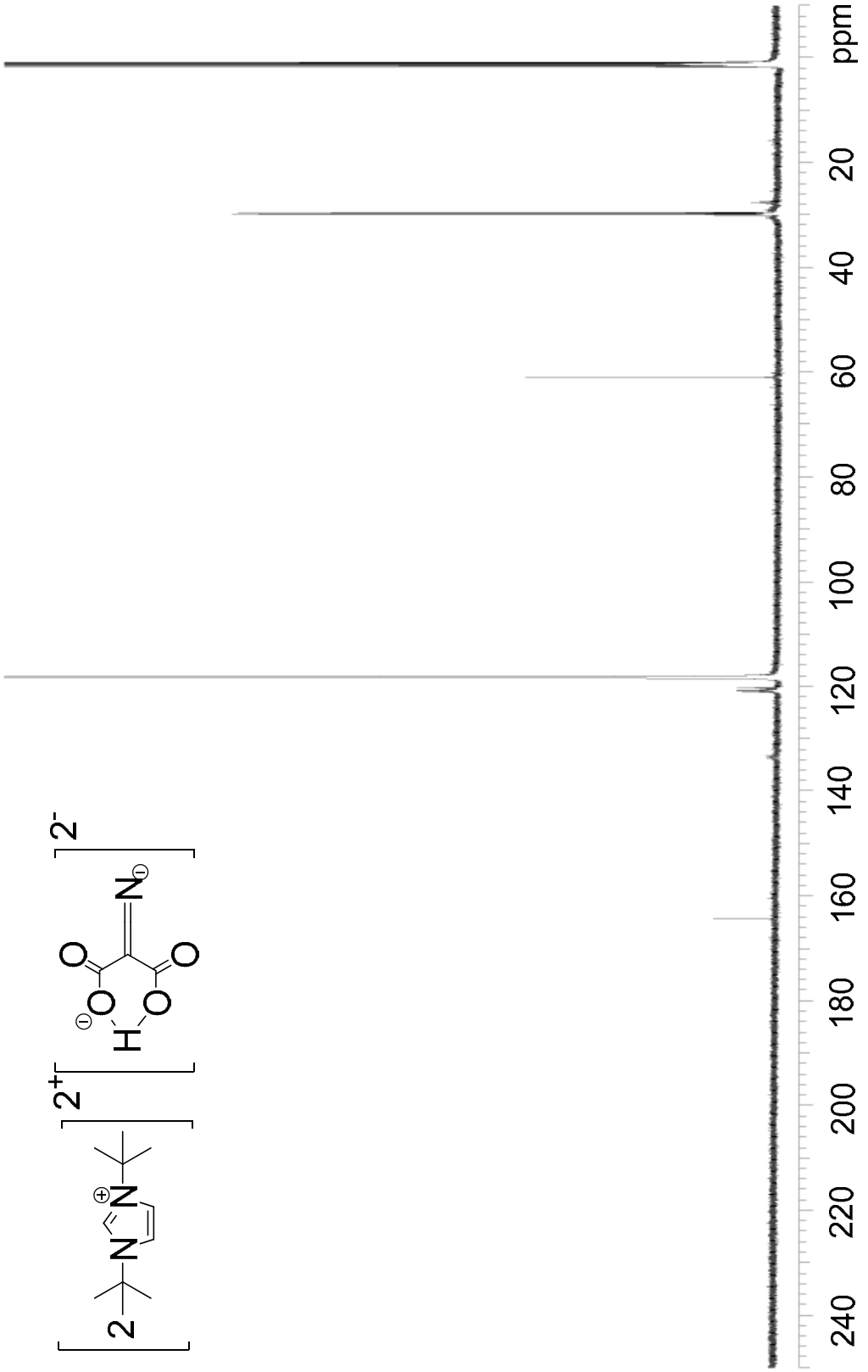

Example of Acetophenone and d^3-Acetophenone scrambling with IPr carbene-time 0

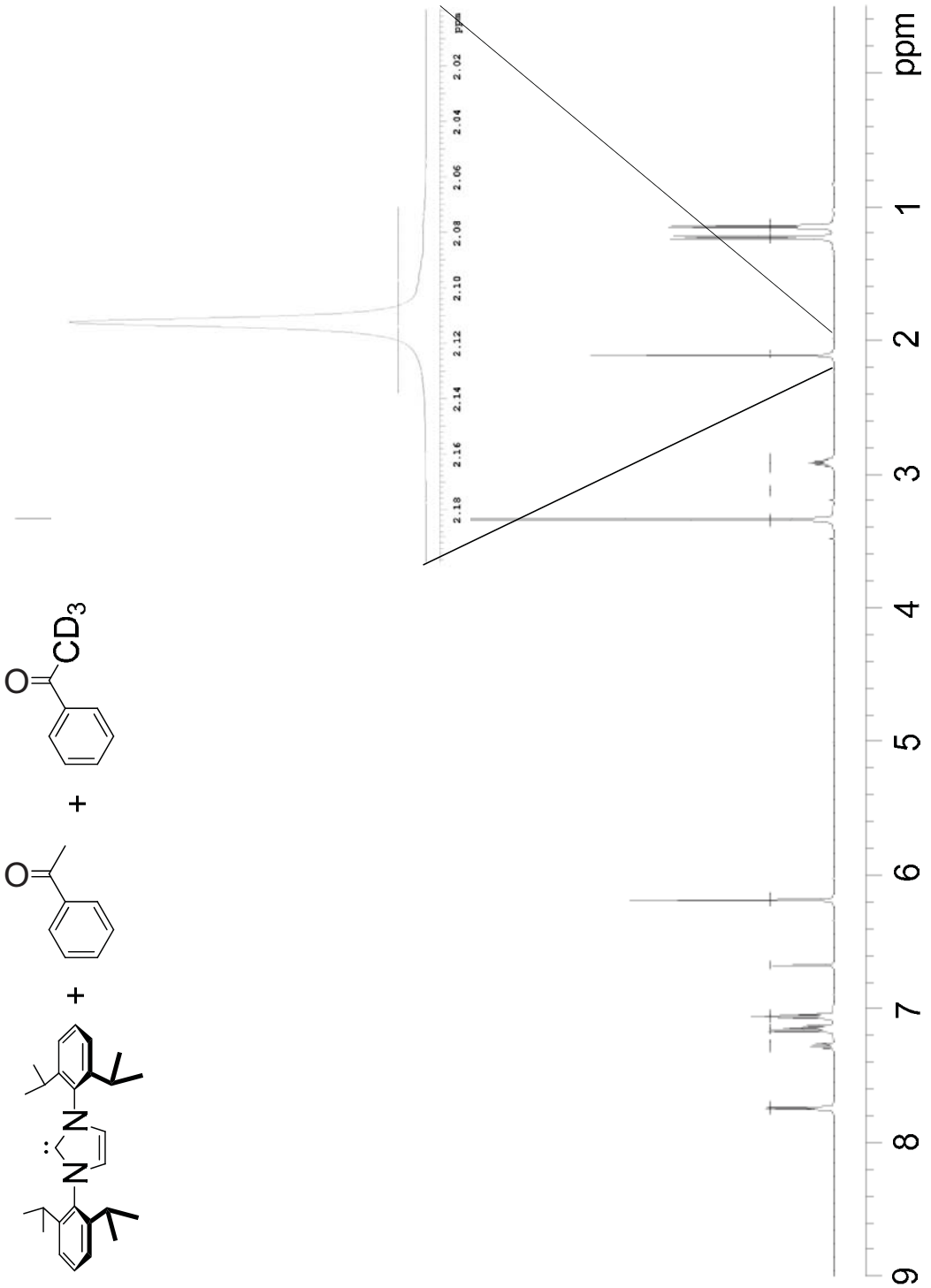

Acetophenone and d^3-Acetophenone scrambling with IPr carbene – time 180 min

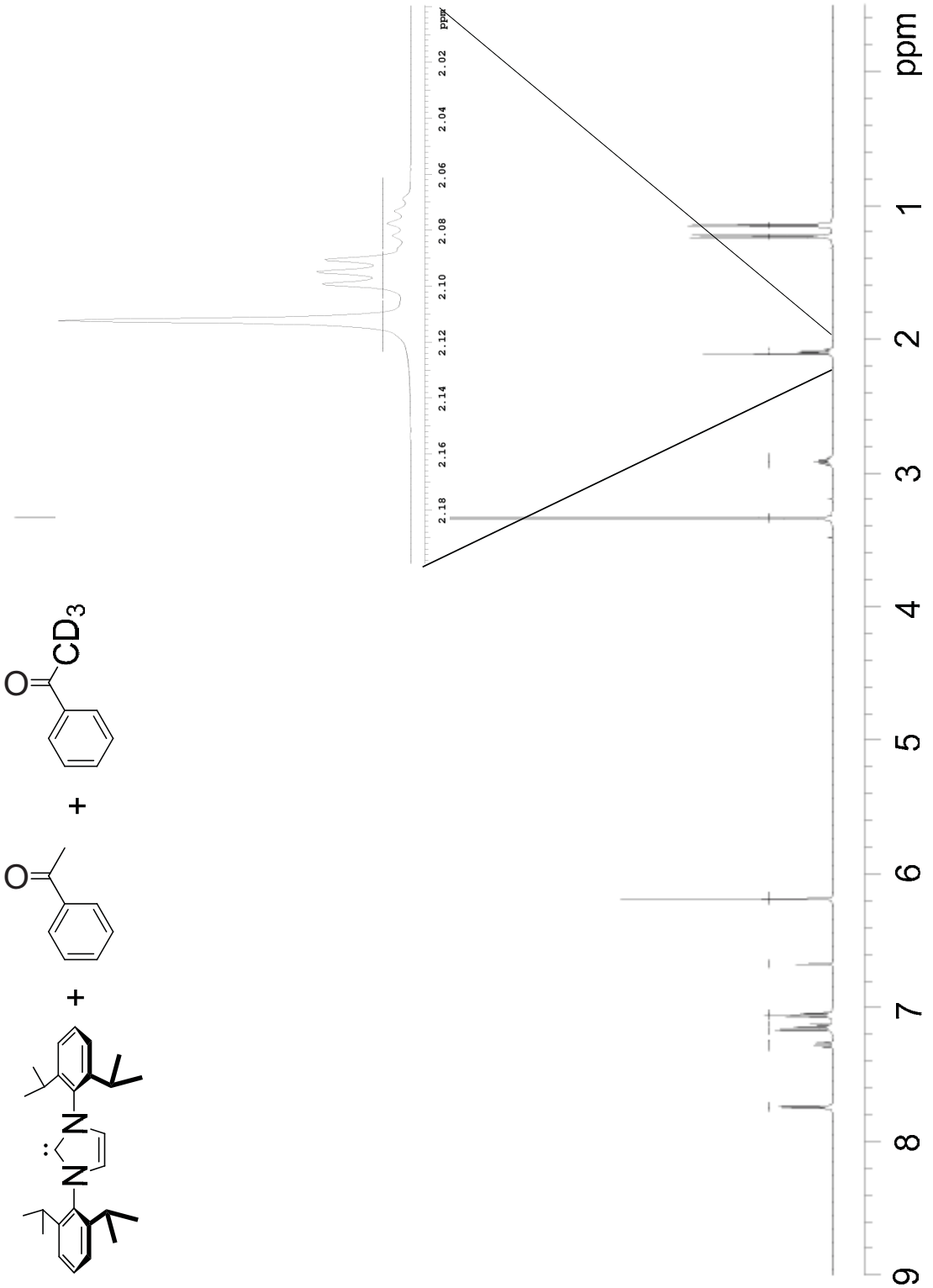

ORTEP Diagram for 4

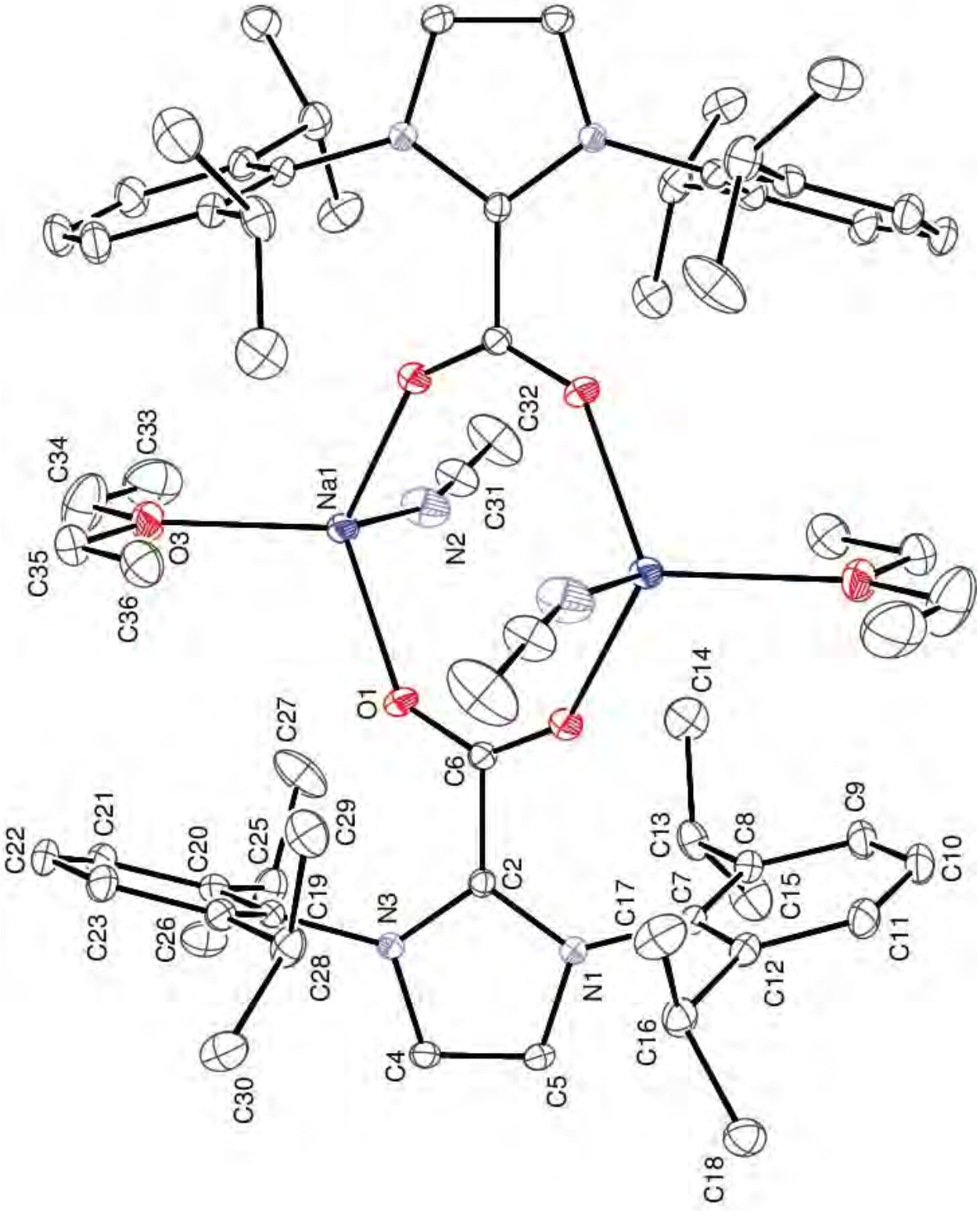

ORTEP Diagram for 5

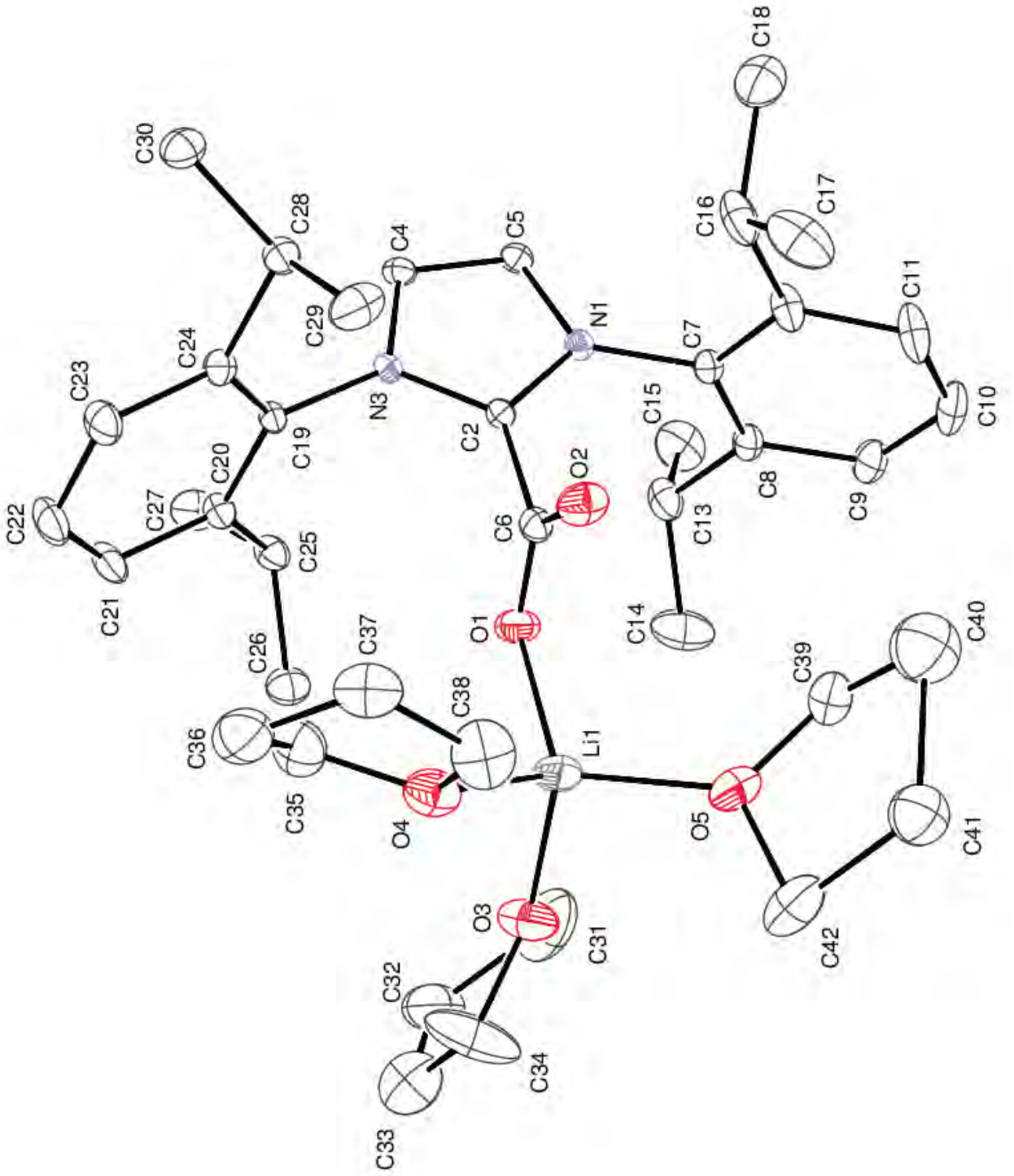

ORTEP Diagram for 6

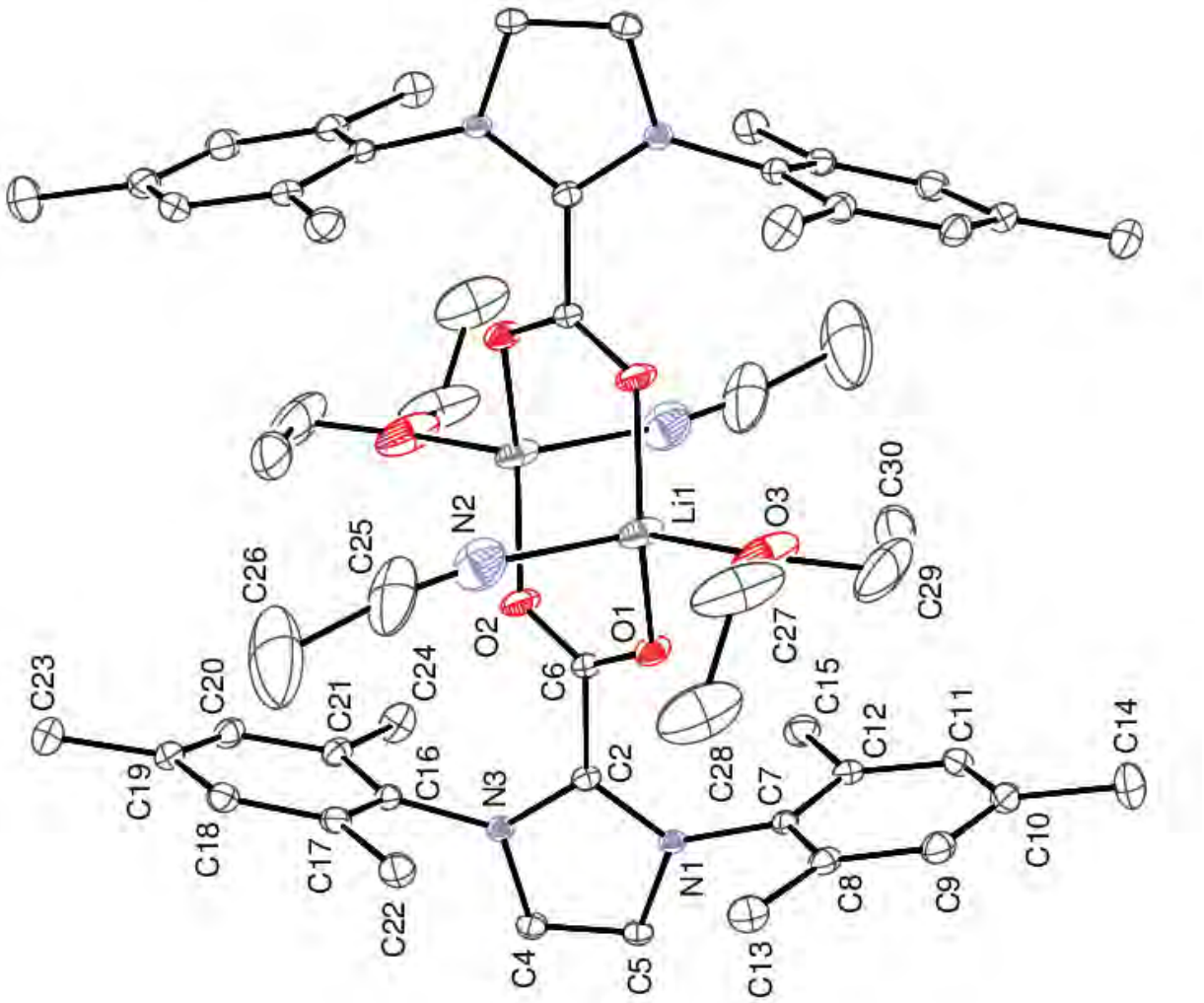

ORTEP Diagram for 11

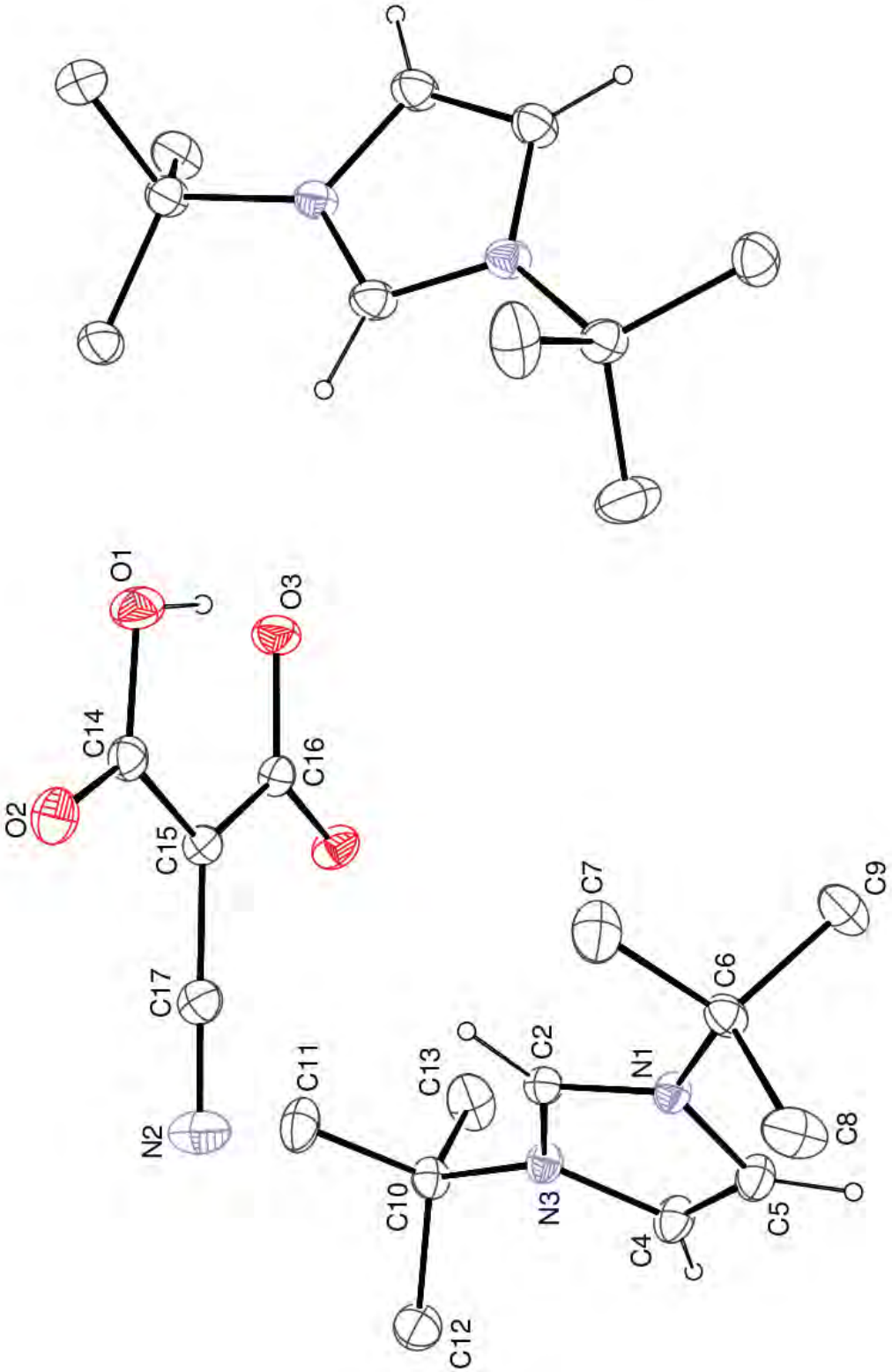

APPENDIX C

NMR SPECTRA AND X-RAY CRYSTAL STRUCTURE REPORTS FOR CHAPTER 3

^{1}H NMR spectrum of 21

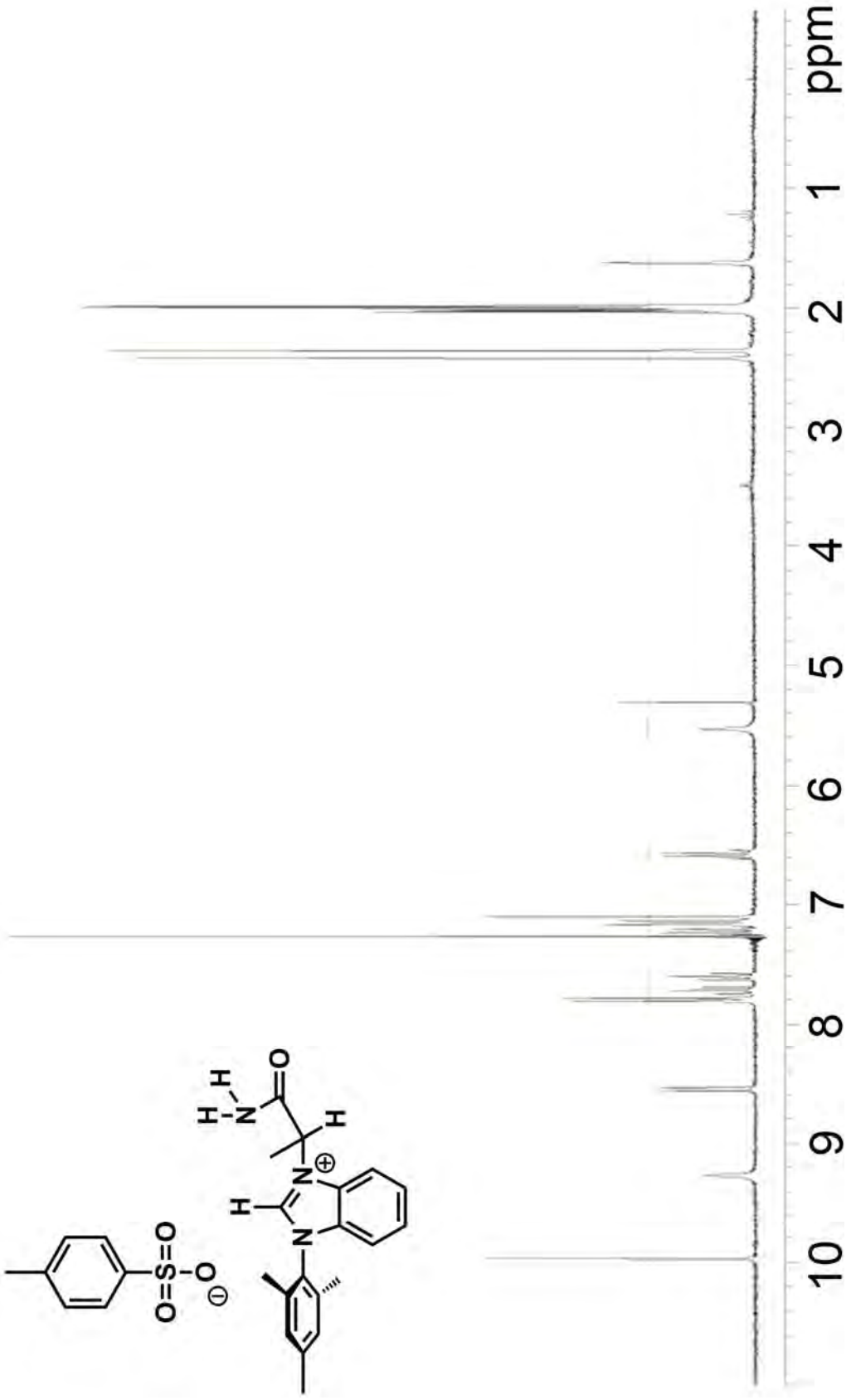

^{13}C NMR spectrum of 21

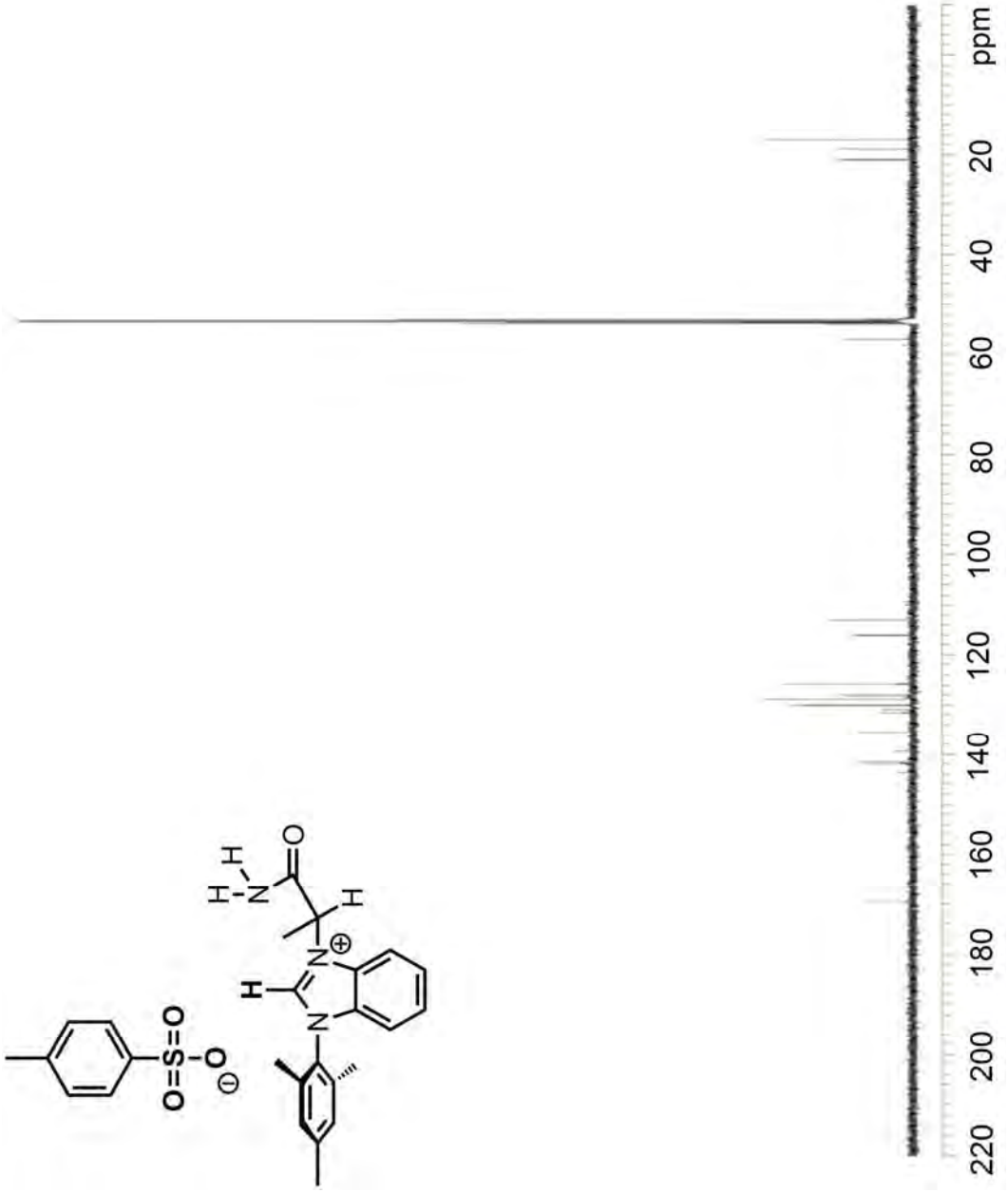

^{1}H NMR spectrum of 22

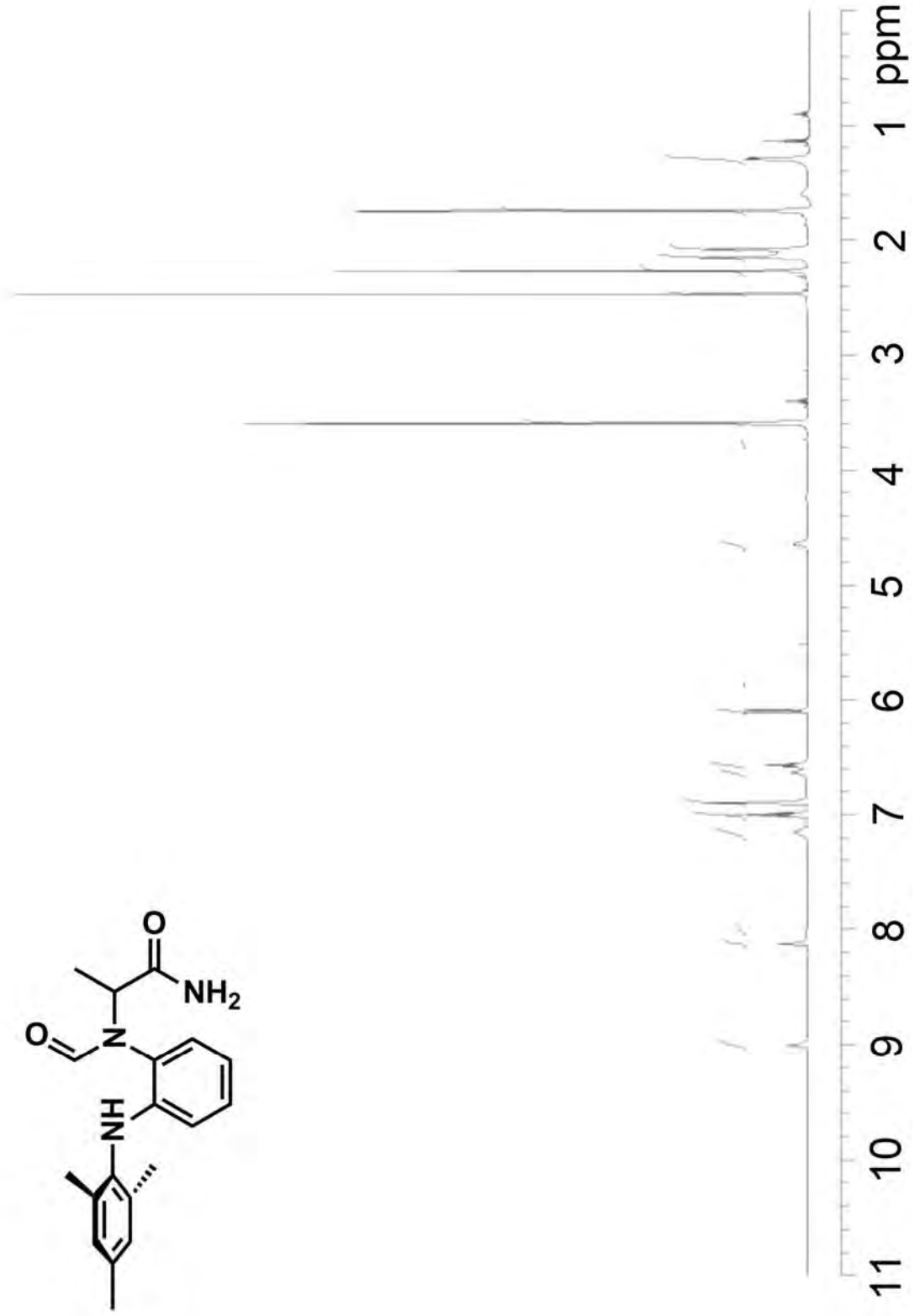

^{13}C NMR spectrum of 22

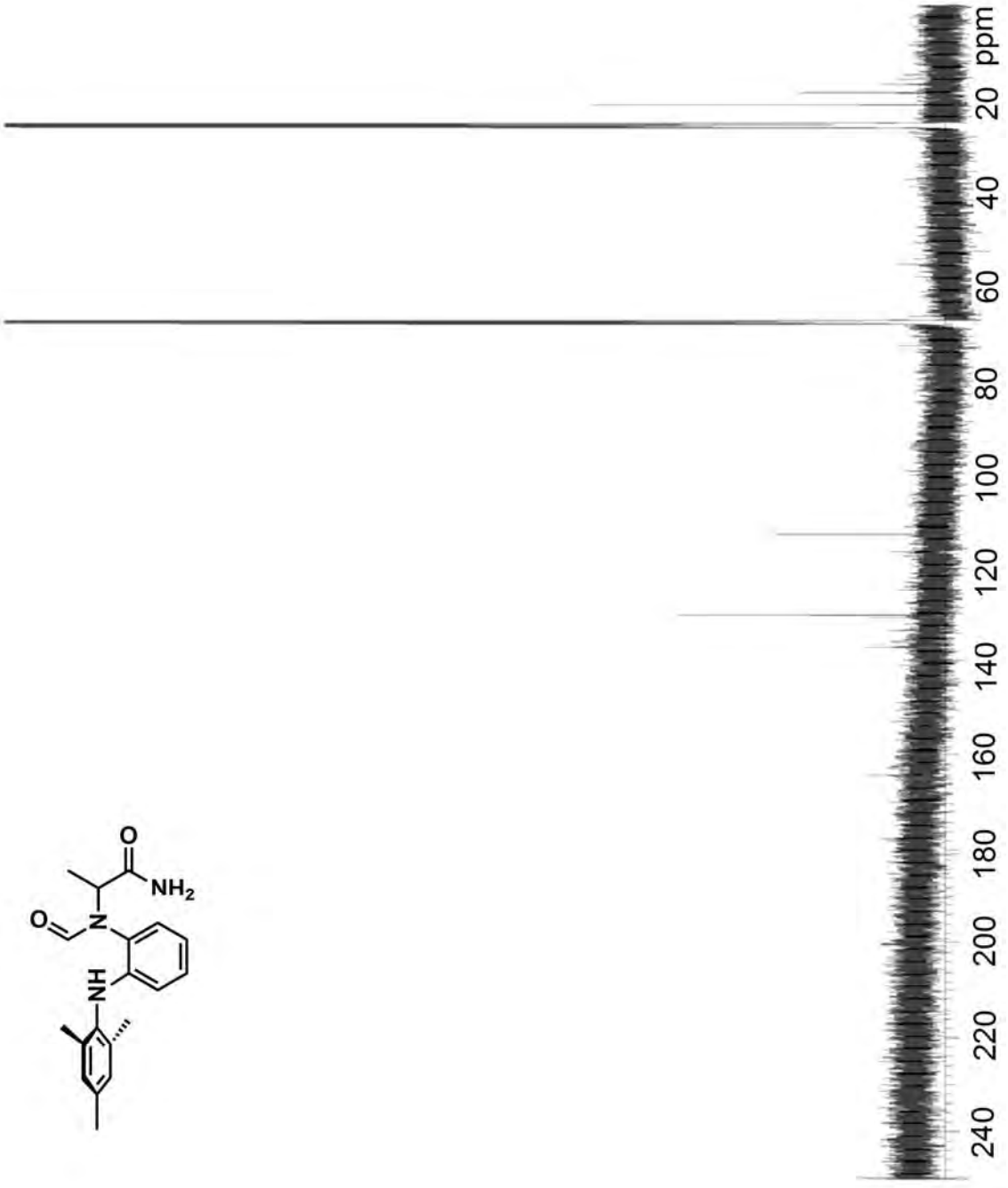

^{1}H NMR spectrum of 23

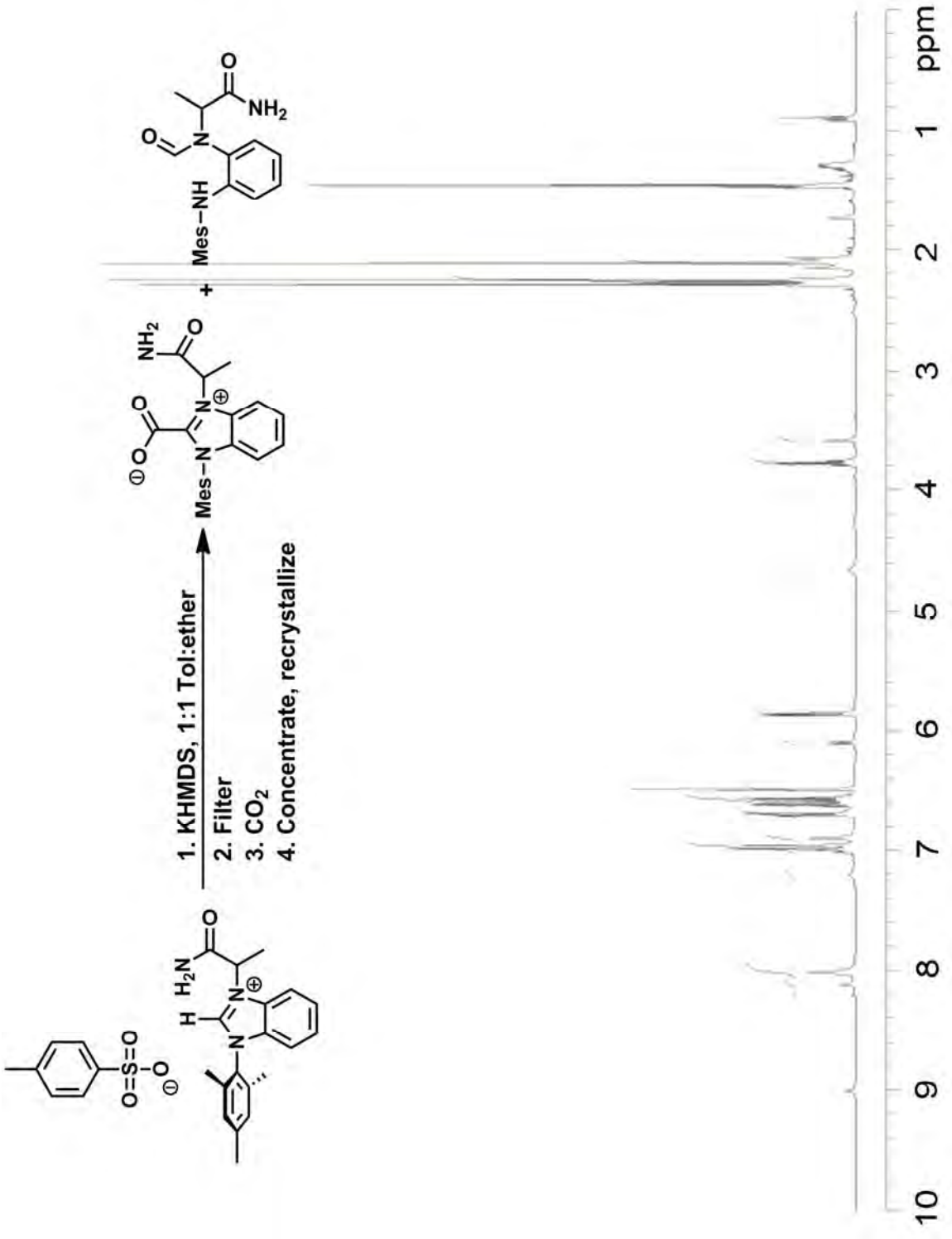

Crystal Structure Report

Experimental:

A colorless plate shaped crystal 0.30 x 0.28 x 0.05 mm in size was mounted on a glass fiber with traces of viscous oil and then transferred to a Nonius KappaCCD diffractometer equipped with Mo Kα radiation (λ = 0.71073 Å). Ten frames of data were collected at 150(1) K with an oscillation range of *1* deg/frame and an exposure time of 20 sec/frame. [REF1] Indexing and unit cell refinement based on all observed reflection from those ten frames, indicated a monoclinic ***P*** lattice. A total of 16671 reflections (Θ_{max} = 25°) were indexed, integrated and corrected for Lorentz, polarization and absorption effects using DENZO-SMN and SCALEPAC. [REF 2] Post refinement of the unit cell gave *a* = 13.580(2) Å, b = 13.3873(14) Å, c = 17.254(2) Å, β =112.412(10), and V = 2899.8(7) Å^3. Axial photographs and systematic absences were consistent with the compound having crystallized in the monoclinic space group ***P*** $2_1/c$.

The structure was solved by a combination of direct methods and heavy atom using SIR 97. [REF 3]
All of the non-hydrogen atoms were refined with anisotropic displacement coefficients. Hydrogen atoms were either located and refined isotropically or assigned isotropic displacement coefficients U(H) = 1.2U(C) or 1.5U(Cmethyl), and their coordinates were allowed to ride on their respective carbons using SHELXL97. [REF 4] The asymmetric unit contains a disordered Methlyene Chloride solvent molecule. The weighting scheme employed was $w = 1/[\sigma^2(F_o^2) + (0.0932P)^2 + 0.2873P]$ where $P = (F_o^2 + 2F_c^2)/3$. The refinement converged to R1 = 0.0617, wR2 = 0.1574, and S = 1.052 for 3028 reflections with $1 > 2\sigma(I)$, and R1 = 0.1201, wR2 = 0.1842, and S = 1.052 for 5059 unique reflections and 414 parameters. [REF 5] The maximum Δ/σ in the final cycle of the least-squares was 0.001, and the residual peaks on the final difference-Fourier map ranged from -0.726 to 0.509 e/Å^3. Scattering factors were taken from the International Tables for Crystallography, Volume C. [REF 6, REF 7]

REF 1 COLLECT Data Collection Software. Nonius B.V. 1998.

REF 2 Otwinowski, Z.; Minor, W., "Processing of X-ray Diffraction Data Collected in Oscillation Mode", Methods Enzymol. 1997, 276, 307-326.

REF 3 SIR97 (Release 1.02) - A program for automatic solution and refinement of crystal structure. A. Altomare, M.C. Burla, M. Camalli, G. Cascarano, C. Giacovazzo, A. Guagliardi, A.G. G. Moliteni, G. Polidori, and R. Spagna.

REF 4 SHELX97 [Includes SHELXS97, SHELXL97, CIFTAB] - Sheldrick, G. M. (1997). Programs for Crystal Structure Analysis (Release 97-2). University of Göttingen, Germany.

REF 5 $R1 = \Sigma(\| F_o | - |F_c \|) / \Sigma |F_o|$, $wR2 = [\Sigma(w(F_o^2 - F_c^2)2) / \Sigma(F_o^2)^2]^{1/2}$, and S = Goodness-of-fit on $F^2 = [\Sigma(w(F_o^2 - F_c^2)^2 / (n-p)]^{1/2}$, where n is the number of reflections and p is the number of parameters refined.

REF 6 Maslen, E. N.; Fox, A. G.; O'Keefe, M. A., International Tables for Crystallography: Mathemetical, Physical and Chemical Tables, Vol. C, Chapter 6, Wilson, A. J. C., Ed.; Kluwer, Dordrecht, The Netherlands, 1992; pp. 476-516.

REF 7 Creagh, D. C.; McAuley, W. J., International Tables for Crystallography: mathematical, Physical and Chemical tables, Vol. C, Chapter 4 Wilson, A. J. C., Ed.; Kluwer, Dordrecht, The Netherlands, 1992; pp. 206-222.

REF8 ORTEP3 for Windows - L. J. Farrugia, *J. Appl. Crystallogr*. **1997**, *30*, 565.

REF9 WinGX A Windows Program for Crystal Structure Analysis. L. J. Farrugia, University of Glasgow, Glasgow, 1998.

Thermal ellipsoid diagram of **20** drawn at 50% probability.

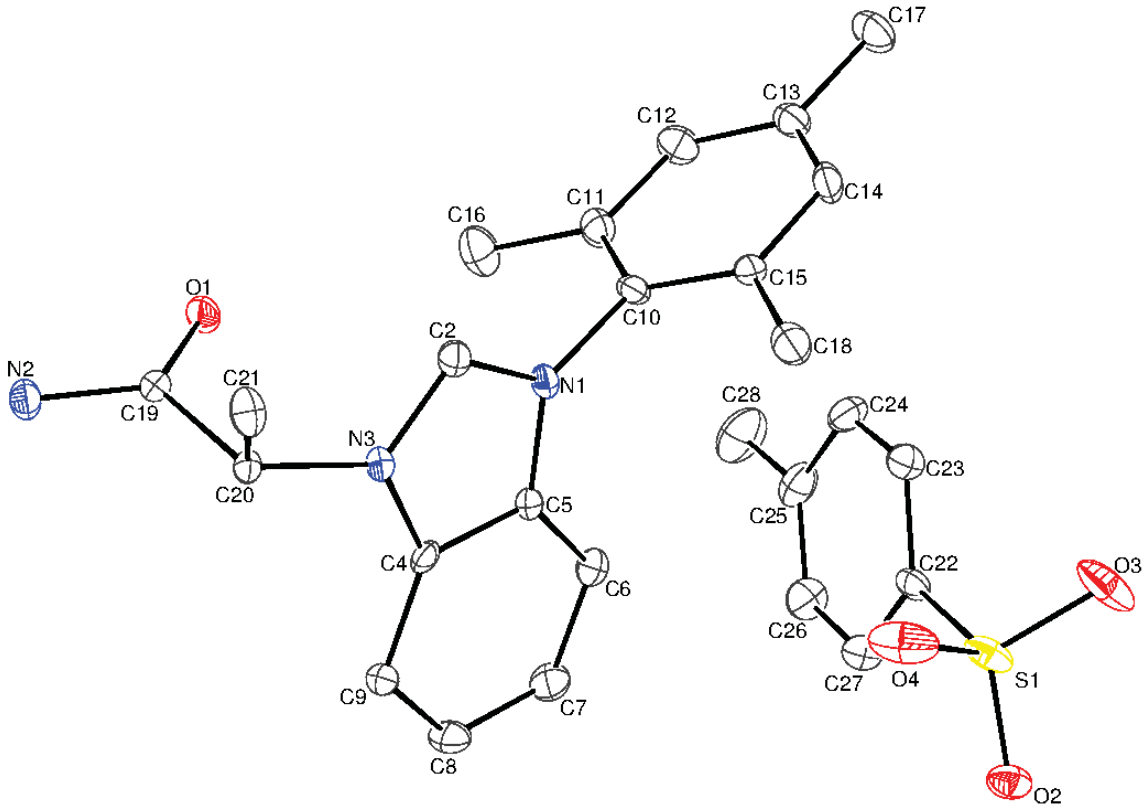

Crystal data and structure refinement for **20**.

Identification code	jl041	
Empirical formula	C27 H31 Cl2 N3 O4 S	
Formula weight	564.51	
Temperature	150(1) K	
Wavelength	0.71073 Å	
Crystal system	Monoclinic	
Space group	***P*** $2_1/c$	
Unit cell dimensions	a = 13.580(2) Å	□= 90°.
	b = 13.3873(14) Å	□= 112.412(10)°.
	c = 17.254(2) Å	□ = 90°.
Volume	2899.8(7) $Å^3$	
Z	4	
Density (calculated)	1.293 Mg/m^3	
Absorption coefficient	0.332 mm^{-1}	
F(000)	1184	
Crystal size	0.30 x 0.28 x 0.05 mm^3	
Theta range for data collection	4.80 to 25.00°.	
Index ranges	-16<=h<=16, -15<=k<=15, -20<=l<=18	
Reflections collected	16671	
Independent reflections	5059 [R(int) = 0.1000]	
Completeness to theta = 25.00°	99.3 %	
Absorption correction	Multi-scan	
Max. and min. transmission	0.9836 and 0.9070	
Refinement method	Full-matrix least-squares on F^2	
Data / restraints / parameters	5059 / 0 / 414	
Goodness-of-fit on F^2	1.052	
Final R indices [I>2sigma(I)]	R1 = 0.0617, wR2 = 0.1574	
R indices (all data)	R1 = 0.1201, wR2 = 0.1842	
Extinction coefficient	0.0083(16)	
Largest diff. peak and hole	0.509 and -0.726 $e.Å^{-3}$	

Atomic coordinates (x 10^4) and equivalent isotropic displacement parameters ($Å^2$x 10^3) for **20**. U(eq) is defined as one third of the trace of the orthogonalized U^{ij} tensor.

	x	y	z	U(eq)
Cl(1)	-169(1)	1297(2)	5985(1)	100(1)
Cl(2)	228(1)	1493(1)	4443(1)	91(1)
S(1)	2831(1)	2600(1)	7395(1)	32(1)
O(1)	4891(2)	8870(2)	9441(1)	29(1)
O(2)	2479(2)	1834(2)	7830(2)	33(1)
O(3)	2919(2)	2230(3)	6630(2)	54(1)
O(4)	3780(2)	3116(3)	7940(2)	52(1)
N(1)	4207(2)	6560(2)	8238(2)	22(1)
N(2)	6066(3)	9176(3)	10759(2)	27(1)
N(3)	5263(2)	6927(2)	9517(2)	21(1)
C(2)	5085(3)	7041(3)	8713(2)	23(1)
C(4)	4439(3)	6364(2)	9581(2)	20(1)
C(5)	3768(3)	6117(3)	8762(2)	20(1)
C(6)	2858(3)	5540(3)	8591(2)	29(1)
C(7)	2651(3)	5236(3)	9280(3)	34(1)
C(8)	3318(3)	5485(3)	10097(3)	32(1)
C(9)	4223(3)	6049(3)	10273(2)	25(1)
C(10)	3740(3)	6571(3)	7324(2)	24(1)
C(11)	2977(3)	7290(3)	6938(2)	29(1)
C(12)	2554(3)	7299(3)	6066(2)	33(1)
C(13)	2869(3)	6619(3)	5591(2)	30(1)
C(14)	3630(3)	5922(3)	6018(2)	30(1)
C(15)	4101(3)	5876(3)	6887(2)	23(1)
C(16)	2617(4)	8030(4)	7436(3)	44(1)
C(17)	2379(3)	6655(3)	4645(2)	40(1)
C(18)	4941(3)	5124(3)	7336(2)	36(1)
C(19)	5602(3)	8594(3)	10107(2)	21(1)
C(20)	6022(3)	7523(3)	10198(2)	21(1)
C(21)	7139(3)	7484(3)	10199(2)	29(1)
C(22)	1803(3)	3507(3)	7068(2)	25(1)
C(23)	1776(3)	4218(3)	6476(2)	33(1)

C(24)	1009(4)	4951(3)	6244(3)	41(1)
C(25)	232(4)	4990(3)	6598(3)	42(1)
C(26)	270(3)	4275(3)	7177(3)	40(1)
C(27)	1032(3)	3532(3)	7417(3)	32(1)
C(28)	-606(4)	5791(4)	6346(4)	71(2)
C(29A)	753(8)	1136(10)	5546(7)	68(3)
C(29B)	410(8)	1979(9)	5281(9)	75(4)

Bond lengths [Å] and angles [°] for **20**.

Cl(1)-C(29A)	1.707(10)
Cl(1)-C(29B)	1.911(13)
Cl(2)-C(29B)	1.517(12)
Cl(2)-C(29A)	1.822(12)
S(1)-O(4)	1.448(3)
S(1)-O(2)	1.454(3)
S(1)-O(3)	1.458(3)
S(1)-C(22)	1.771(4)
O(1)-C(19)	1.242(4)
N(1)-C(2)	1.327(4)
N(1)-C(5)	1.393(4)
N(1)-C(10)	1.457(4)
N(2)-C(19)	1.315(5)
N(2)-H(2A)	0.87(4)
N(2)-H(2B)	0.77(5)
N(3)-C(2)	1.323(4)
N(3)-C(4)	1.388(4)
N(3)-C(20)	1.469(4)
C(2)-H(2)	0.89(4)
C(4)-C(5)	1.398(5)
C(4)-C(9)	1.399(5)
C(5)-C(6)	1.390(5)

C(6)-C(7)	1.383(5)
C(6)-H(6)	1.03(4)
C(7)-C(8)	1.394(6)
C(7)-H(7)	0.90(4)
C(8)-C(9)	1.374(5)
C(8)-H(8)	0.91(4)
C(9)-H(9)	1.00(4)
C(10)-C(11)	1.384(5)
C(10)-C(15)	1.400(5)
C(11)-C(12)	1.392(5)
C(11)-C(16)	1.510(5)
C(12)-C(13)	1.396(6)
C(12)-H(12)	0.89(4)
C(13)-C(14)	1.378(6)
C(13)-C(17)	1.510(5)
C(14)-C(15)	1.390(5)
C(14)-H(14)	0.87(4)
C(15)-C(18)	1.497(5)
C(16)-H(16A)	0.9800
C(16)-H(16B)	0.9800
C(16)-H(16C)	0.9800
C(17)-H(17A)	0.9800
C(17)-H(17B)	0.9800
C(17)-H(17C)	0.9800
C(18)-H(18A)	0.9800
C(18)-H(18B)	0.9800
C(18)-H(18C)	0.9800
C(19)-C(20)	1.529(5)
C(20)-C(21)	1.516(5)
C(20)-H(20)	0.94(3)
C(21)-H(21A)	0.9800
C(21)-H(21B)	0.9800
C(21)-H(21C)	0.9800
C(22)-C(23)	1.386(5)
C(22)-C(27)	1.393(5)
C(23)-C(24)	1.375(6)

C(23)-H(23)	0.89(4)
C(24)-C(25)	1.407(6)
C(24)-H(24)	0.99(4)
C(25)-C(26)	1.370(6)
C(25)-C(28)	1.503(6)
C(26)-C(27)	1.379(6)
C(26)-H(26)	0.94(5)
C(27)-H(27)	0.95(4)
C(28)-H(28A)	0.9800
C(28)-H(28B)	0.9800
C(28)-H(28C)	0.9800
C(29A)-H(29A)	0.9900
C(29A)-H(29B)	0.9900
C(29B)-H(29C)	0.9900
C(29B)-H(29D)	0.9900

C(29A)-Cl(1)-C(29B)	39.6(5)
C(29B)-Cl(2)-C(29A)	42.4(6)
O(4)-S(1)-O(2)	112.80(16)
O(4)-S(1)-O(3)	112.88(19)
O(2)-S(1)-O(3)	112.55(19)
O(4)-S(1)-C(22)	106.19(19)
O(2)-S(1)-C(22)	105.90(16)
O(3)-S(1)-C(22)	105.78(16)
C(2)-N(1)-C(5)	108.1(3)
C(2)-N(1)-C(10)	125.6(3)
C(5)-N(1)-C(10)	126.1(3)
C(19)-N(2)-H(2A)	115(3)
C(19)-N(2)-H(2B)	116(3)
H(2A)-N(2)-H(2B)	126(4)
C(2)-N(3)-C(4)	108.4(3)
C(2)-N(3)-C(20)	124.6(3)
C(4)-N(3)-C(20)	125.0(3)
N(3)-C(2)-N(1)	110.7(3)
N(3)-C(2)-H(2)	126(2)
N(1)-C(2)-H(2)	122(2)

N(3)-C(4)-C(5)	106.4(3)
N(3)-C(4)-C(9)	132.0(3)
C(5)-C(4)-C(9)	121.6(3)
C(6)-C(5)-N(1)	131.7(3)
C(6)-C(5)-C(4)	122.0(3)
N(1)-C(5)-C(4)	106.3(3)
C(7)-C(6)-C(5)	115.9(3)
C(7)-C(6)-H(6)	122(2)
C(5)-C(6)-H(6)	122(2)
C(6)-C(7)-C(8)	122.1(4)
C(6)-C(7)-H(7)	118(3)
C(8)-C(7)-H(7)	119(3)
C(9)-C(8)-C(7)	122.5(4)
C(9)-C(8)-H(8)	118(2)
C(7)-C(8)-H(8)	120(2)
C(8)-C(9)-C(4)	115.9(3)
C(8)-C(9)-H(9)	125(2)
C(4)-C(9)-H(9)	119(2)
C(11)-C(10)-C(15)	123.7(3)
C(11)-C(10)-N(1)	117.7(3)
C(15)-C(10)-N(1)	118.6(3)
C(10)-C(11)-C(12)	116.8(4)
C(10)-C(11)-C(16)	121.9(3)
C(12)-C(11)-C(16)	121.3(4)
C(11)-C(12)-C(13)	122.4(4)
C(11)-C(12)-H(12)	117(2)
C(13)-C(12)-H(12)	121(2)
C(14)-C(13)-C(12)	117.6(3)
C(14)-C(13)-C(17)	122.1(4)
C(12)-C(13)-C(17)	120.3(4)
C(13)-C(14)-C(15)	123.4(4)
C(13)-C(14)-H(14)	117(2)
C(15)-C(14)-H(14)	119(3)
C(14)-C(15)-C(10)	116.1(3)
C(14)-C(15)-C(18)	122.4(3)
C(10)-C(15)-C(18)	121.5(3)

C(11)-C(16)-H(16A)	109.5
C(11)-C(16)-H(16B)	109.5
H(16A)-C(16)-H(16B)	109.5
C(11)-C(16)-H(16C)	109.5
H(16A)-C(16)-H(16C)	109.5
H(16B)-C(16)-H(16C)	109.5
C(13)-C(17)-H(17A)	109.5
C(13)-C(17)-H(17B)	109.5
H(17A)-C(17)-H(17B)	109.5
C(13)-C(17)-H(17C)	109.5
H(17A)-C(17)-H(17C)	109.5
H(17B)-C(17)-H(17C)	109.5
C(15)-C(18)-H(18A)	109.5
C(15)-C(18)-H(18B)	109.5
H(18A)-C(18)-H(18B)	109.5
C(15)-C(18)-H(18C)	109.5
H(18A)-C(18)-H(18C)	109.5
H(18B)-C(18)-H(18C)	109.5
O(1)-C(19)-N(2)	124.4(4)
O(1)-C(19)-C(20)	120.2(3)
N(2)-C(19)-C(20)	115.4(3)
N(3)-C(20)-C(21)	112.3(3)
N(3)-C(20)-C(19)	107.9(3)
C(21)-C(20)-C(19)	111.5(3)
N(3)-C(20)-H(20)	105(2)
C(21)-C(20)-H(20)	110(2)
C(19)-C(20)-H(20)	110(2)
C(20)-C(21)-H(21A)	109.5
C(20)-C(21)-H(21B)	109.5
H(21A)-C(21)-H(21B)	109.5
C(20)-C(21)-H(21C)	109.5
H(21A)-C(21)-H(21C)	109.5
H(21B)-C(21)-H(21C)	109.5
C(23)-C(22)-C(27)	119.2(4)
C(23)-C(22)-S(1)	120.1(3)
C(27)-C(22)-S(1)	120.7(3)

C(24)-C(23)-C(22)	120.6(4)
C(24)-C(23)-H(23)	122(3)
C(22)-C(23)-H(23)	117(2)
C(23)-C(24)-C(25)	120.6(4)
C(23)-C(24)-H(24)	117(3)
C(25)-C(24)-H(24)	122(3)
C(26)-C(25)-C(24)	117.7(4)
C(26)-C(25)-C(28)	121.5(4)
C(24)-C(25)-C(28)	120.8(4)
C(25)-C(26)-C(27)	122.5(4)
C(25)-C(26)-H(26)	120(3)
C(27)-C(26)-H(26)	118(3)
C(26)-C(27)-C(22)	119.3(4)
C(26)-C(27)-H(27)	119(2)
C(22)-C(27)-H(27)	122(2)
C(25)-C(28)-H(28A)	109.5
C(25)-C(28)-H(28B)	109.5
H(28A)-C(28)-H(28B)	109.5
C(25)-C(28)-H(28C)	109.5
H(28A)-C(28)-H(28C)	109.5
H(28B)-C(28)-H(28C)	109.5
Cl(1)-C(29A)-Cl(2)	111.7(6)
Cl(1)-C(29A)-H(29A)	109.3
Cl(2)-C(29A)-H(29A)	109.3
Cl(1)-C(29A)-H(29B)	109.3
Cl(2)-C(29A)-H(29B)	109.3
H(29A)-C(29A)-H(29B)	107.9
Cl(2)-C(29B)-Cl(1)	116.4(6)
Cl(2)-C(29B)-H(29C)	108.2
Cl(1)-C(29B)-H(29C)	108.2
Cl(2)-C(29B)-H(29D)	108.2
Cl(1)-C(29B)-H(29D)	108.2
H(29C)-C(29B)-H(29D)	107.4

Symmetry transformations used to generate equivalent atoms:

Anisotropic displacement parameters ($Å^2 x\ 10^3$)for **20**. The anisotropic displacement factor exponent takes the form: $-2\pi^2[h^2a^{*2}U^{11} + ... + 2\ h\ k\ a^*\ b^*\ U^{12}]$

	U^{11}	U^{22}	U^{33}	U^{23}	U^{13}	U^{12}
Cl(1)	87(1)	101(2)	120(2)	-28(1)	50(1)	-22(1)
Cl(2)	67(1)	91(1)	122(2)	5(1)	44(1)	2(1)
S(1)	25(1)	52(1)	19(1)	9(1)	8(1)	8(1)
O(1)	41(2)	21(2)	16(1)	2(1)	3(1)	5(1)
O(2)	33(2)	36(2)	27(1)	10(1)	10(1)	7(1)
O(3)	51(2)	93(3)	27(2)	12(2)	23(1)	35(2)
O(4)	24(2)	80(3)	37(2)	25(2)	-5(1)	-12(2)
N(1)	27(2)	22(2)	18(2)	-6(1)	9(1)	-6(1)
N(2)	37(2)	19(2)	19(2)	-3(2)	2(2)	2(2)
N(3)	27(2)	19(2)	17(2)	-3(1)	7(1)	-2(1)
C(2)	25(2)	23(2)	23(2)	-3(2)	9(2)	-3(2)
C(4)	26(2)	10(2)	26(2)	-1(2)	11(2)	0(2)
C(5)	25(2)	17(2)	20(2)	-3(2)	11(2)	-1(2)
C(6)	33(2)	25(2)	28(2)	-5(2)	9(2)	-8(2)
C(7)	34(2)	33(3)	39(2)	-2(2)	20(2)	-11(2)
C(8)	39(2)	32(3)	32(2)	6(2)	21(2)	-3(2)
C(9)	37(2)	20(2)	21(2)	1(2)	13(2)	2(2)
C(10)	28(2)	29(2)	16(2)	-2(2)	9(2)	-10(2)
C(11)	29(2)	32(2)	25(2)	-4(2)	9(2)	-3(2)
C(12)	30(2)	40(3)	29(2)	3(2)	10(2)	3(2)
C(13)	31(2)	36(3)	22(2)	-2(2)	11(2)	-9(2)
C(14)	36(2)	31(3)	27(2)	-11(2)	17(2)	-5(2)
C(15)	29(2)	21(2)	20(2)	-1(2)	12(2)	-7(2)
C(16)	47(3)	49(3)	35(2)	-5(2)	13(2)	13(2)
C(17)	45(3)	53(3)	21(2)	-1(2)	10(2)	-3(2)
C(18)	49(3)	33(3)	27(2)	0(2)	16(2)	6(2)
C(19)	29(2)	17(2)	19(2)	-1(2)	10(2)	-3(2)
C(20)	28(2)	16(2)	16(2)	-2(2)	5(2)	-4(2)
C(21)	26(2)	33(3)	25(2)	-9(2)	5(2)	-2(2)
C(22)	27(2)	31(2)	14(2)	0(2)	5(2)	-1(2)
C(23)	38(2)	33(3)	30(2)	-1(2)	16(2)	-4(2)

C(24) 57(3)	24(3)	37(2)	5(2)	12(2)	-4(2)
C(25) 42(3)	28(3)	49(3)	-1(2)	9(2)	4(2)
C(26) 36(2)	40(3)	47(3)	1(2)	19(2)	3(2)
C(27) 31(2)	36(3)	31(2)	5(2)	13(2)	2(2)
C(28) 73(4)	40(3)	93(4)	8(3)	23(3)	23(3)
C(29A)36(6)	71(9)	99(9)	-3(7)	28(6)	-18(6)
C(29B)38(6)	42(7)	142(12)	-35(8)	31(7)	-16(5)

Hydrogen coordinates (x 10^4) and isotropic displacement parameters ($Å^2$x 10^3)
for **20**.

	x	y	z	U(eq)
H(16A)	2197	8558	7062	73(16)
H(16B)	3241	8325	7876	61(14)
H(16C)	2179	7688	7692	53(14)
H(17A)	2533	7303	4451	61
H(17B)	1606	6567	4455	61
H(17C)	2678	6119	4415	61
H(18A)	5040	4667	6928	64(14)
H(18B)	4719	4743	7727	49(13)
H(18C)	5613	5468	7648	68(15)
H(21A)	7639	7790	10714	33(10)
H(21B)	7157	7849	9712	34(11)
H(21C)	7341	6786	10170	55(14)
H(28A)	-898	5864	6782	106
H(28B)	-1178	5607	5815	106
H(28C)	-288	6426	6277	106
H(29A)	975	427	5597	82
H(29B)	1391	1544	5854	82
H(29C)	102	2660	5174	90

H(29D)	1187	2051	5594	90
H(2)	5520(30)	7320(30)	8500(20)	30(11)
H(2A)	6470(30)	8870(30)	11220(30)	30(11)
H(2B)	5820(40)	9700(40)	10730(30)	39(14)
H(6)	2380(30)	5330(30)	7990(20)	28(10)
H(7)	2030(30)	4930(30)	9190(20)	38(12)
H(8)	3180(30)	5240(30)	10540(20)	26(10)
H(20)	6010(20)	7240(30)	10690(20)	19(9)
H(9)	4710(30)	6260(30)	10850(20)	28(10)
H(12)	2040(30)	7740(30)	5820(20)	32(11)
H(14)	3820(30)	5500(30)	5720(20)	27(10)
H(23)	2290(30)	4190(30)	6270(20)	27(10)
H(24)	1030(30)	5450(30)	5820(30)	50(13)
H(26)	-240(40)	4280(40)	7430(30)	72(16)
H(27)	1020(30)	3060(30)	7830(30)	40(11)

Torsion angles [°] for **20**.

C(4)-N(3)-C(2)-N(1)	-2.0(4)
C(20)-N(3)-C(2)-N(1)	-166.3(3)
C(5)-N(1)-C(2)-N(3)	1.2(4)
C(10)-N(1)-C(2)-N(3)	176.3(3)
C(2)-N(3)-C(4)-C(5)	1.9(4)
C(20)-N(3)-C(4)-C(5)	166.1(3)
C(2)-N(3)-C(4)-C(9)	-178.3(4)
C(20)-N(3)-C(4)-C(9)	-14.1(6)
C(2)-N(1)-C(5)-C(6)	179.6(4)
C(10)-N(1)-C(5)-C(6)	4.6(6)
C(2)-N(1)-C(5)-C(4)	0.0(4)
C(10)-N(1)-C(5)-C(4)	-175.0(3)
N(3)-C(4)-C(5)-C(6)	179.2(3)
C(9)-C(4)-C(5)-C(6)	-0.6(5)

N(3)-C(4)-C(5)-N(1)	-1.1(4)
C(9)-C(4)-C(5)-N(1)	179.0(3)
N(1)-C(5)-C(6)-C(7)	-178.8(4)
C(4)-C(5)-C(6)-C(7)	0.8(6)
C(5)-C(6)-C(7)-C(8)	-0.5(6)
C(6)-C(7)-C(8)-C(9)	0.1(7)
C(7)-C(8)-C(9)-C(4)	0.1(6)
N(3)-C(4)-C(9)-C(8)	-179.6(4)
C(5)-C(4)-C(9)-C(8)	0.2(5)
C(2)-N(1)-C(10)-C(11)	-91.7(4)
C(5)-N(1)-C(10)-C(11)	82.5(4)
C(2)-N(1)-C(10)-C(15)	86.9(4)
C(5)-N(1)-C(10)-C(15)	-98.9(4)
C(15)-C(10)-C(11)-C(12)	0.4(6)
N(1)-C(10)-C(11)-C(12)	178.9(3)
C(15)-C(10)-C(11)-C(16)	-179.6(4)
N(1)-C(10)-C(11)-C(16)	-1.1(5)
C(10)-C(11)-C(12)-C(13)	0.4(6)
C(16)-C(11)-C(12)-C(13)	-179.7(4)
C(11)-C(12)-C(13)-C(14)	-0.1(6)
C(11)-C(12)-C(13)-C(17)	179.5(4)
C(12)-C(13)-C(14)-C(15)	-0.9(6)
C(17)-C(13)-C(14)-C(15)	179.5(4)
C(13)-C(14)-C(15)-C(10)	1.6(6)
C(13)-C(14)-C(15)-C(18)	-178.8(4)
C(11)-C(10)-C(15)-C(14)	-1.4(5)
N(1)-C(10)-C(15)-C(14)	-179.8(3)
C(11)-C(10)-C(15)-C(18)	179.1(4)
N(1)-C(10)-C(15)-C(18)	0.6(5)
C(2)-N(3)-C(20)-C(21)	-55.9(5)
C(4)-N(3)-C(20)-C(21)	142.3(3)
C(2)-N(3)-C(20)-C(19)	67.3(4)
C(4)-N(3)-C(20)-C(19)	-94.4(4)
O(1)-C(19)-C(20)-N(3)	-15.5(4)
N(2)-C(19)-C(20)-N(3)	166.5(3)
O(1)-C(19)-C(20)-C(21)	108.2(4)

N(2)-C(19)-C(20)-C(21)	-69.8(4)
O(4)-S(1)-C(22)-C(23)	74.5(3)
O(2)-S(1)-C(22)-C(23)	-165.3(3)
O(3)-S(1)-C(22)-C(23)	-45.7(4)
O(4)-S(1)-C(22)-C(27)	-103.7(3)
O(2)-S(1)-C(22)-C(27)	16.4(4)
O(3)-S(1)-C(22)-C(27)	136.1(3)
C(27)-C(22)-C(23)-C(24)	1.1(6)
S(1)-C(22)-C(23)-C(24)	-177.2(3)
C(22)-C(23)-C(24)-C(25)	-0.4(6)
C(23)-C(24)-C(25)-C(26)	-0.1(6)
C(23)-C(24)-C(25)-C(28)	179.9(4)
C(24)-C(25)-C(26)-C(27)	0.0(7)
C(28)-C(25)-C(26)-C(27)	180.0(4)
C(25)-C(26)-C(27)-C(22)	0.7(7)
C(23)-C(22)-C(27)-C(26)	-1.2(6)
S(1)-C(22)-C(27)-C(26)	177.1(3)
C(29B)-Cl(1)-C(29A)-Cl(2)	-45.9(7)
C(29B)-Cl(2)-C(29A)-Cl(1)	58.8(8)
C(29A)-Cl(2)-C(29B)-Cl(1)	-52.4(7)
C(29A)-Cl(1)-C(29B)-Cl(2)	63.4(8)

Symmetry transformations used to generate equivalent atoms:

Hydrogen bonds for **20** [Å and °].

D-H...A	d(D-H)	d(H...A)	d(D...A)	<(DHA)
N(2)-H(2B)...O(1)#1	0.77(5)	2.11(5)	2.882(5)	176(4)
N(2)-H(2A)...O(2)#2	0.87(4)	1.96(4)	2.828(5)	172(4)

Symmetry transformations used to generate equivalent atoms:

#1 -x+1,-y+2,-z+2 #2 -x+1,-y+1,-z+2

Crystal data and structure refinement for **22**.

Identification code	jl045	
Empirical formula	C23 H31 N3 O3	
Formula weight	397.51	
Temperature	150(1) K	
Wavelength	0.71073 Å	
Crystal system	Triclinic	
Space group	$P\bar{1}$	
Unit cell dimensions	a = 8.2018(2) Å	α= 78.0402(15)°.
	b = 10.5178(3) Å	β= 74.4868(18)°.
	c = 14.3064(3) Å	γ = 71.0229(15)°.
Volume	1114.71(5) $Å^3$	
Z	2	
Density (calculated)	1.184 Mg/m^3	
Absorption coefficient	0.079 mm^{-1}	
F(000)	428	
Crystal size	0.35 x 0.28 x 0.20 mm^3	
Theta range for data collection	2.38 to 27.51°.	
Index ranges	-10<=h<=10, -13<=k<=13, -18<=l<=18	
Reflections collected	9662	
Independent reflections	5111 [R(int) = 0.0176]	
Completeness to theta = 27.51°	99.3 %	
Absorption correction	Multi-scan	
Max. and min. transmission	0.9844 and 0.9729	
Refinement method	Full-matrix least-squares on F^2	
Data / restraints / parameters	5111 / 0 / 358	
Goodness-of-fit on F^2	1.028	
Final R indices [I>2sigma(I)]	R1 = 0.0510, wR2 = 0.1272	
R indices (all data)	R1 = 0.0749, wR2 = 0.1443	
Largest diff. peak and hole	0.340 and -0.272 $e.Å^{-3}$	

Atomic coordinates (x 10^4) and equivalent isotropic displacement parameters ($Å^2$x 10^3) for **22**. U(eq) is defined as one third of the trace of the orthogonalized U^{ij} tensor.

	x	y	z	U(eq)
O(1)	7485(2)	842(1)	4619(1)	43(1)
O(2)	5520(2)	3405(1)	5798(1)	36(1)
O(3)	11458(2)	3209(2)	3826(1)	42(1)
O(3')	10930(20)	3970(20)	3940(9)	39(4)
N(1)	6428(2)	1566(1)	7517(1)	34(1)
N(2)	3942(2)	3919(1)	4624(1)	35(1)
N(3)	5496(2)	705(1)	6065(1)	29(1)
C(2)	7118(2)	354(2)	5476(1)	35(1)
C(4)	5222(2)	35(1)	7057(1)	29(1)
C(5)	5731(2)	480(1)	7769(1)	29(1)
C(6)	5511(2)	-220(2)	8721(1)	35(1)
C(7)	4797(2)	-1303(2)	8949(1)	38(1)
C(8)	4297(2)	-1729(2)	8240(1)	39(1)
C(9)	4518(2)	-1052(2)	7292(1)	34(1)
C(10)	7207(2)	1963(2)	8139(1)	34(1)
C(11)	8791(2)	1101(2)	8373(1)	43(1)
C(12)	9559(3)	1532(2)	8967(2)	59(1)
C(13)	8824(3)	2781(3)	9307(1)	61(1)
C(14)	7270(3)	3610(2)	9056(1)	52(1)
C(15)	6430(2)	3223(2)	8479(1)	40(1)
C(16)	9664(3)	-231(2)	7977(2)	59(1)
C(17)	9722(4)	3230(3)	9925(2)	95(1)
C(18)	4723(3)	4137(2)	8230(2)	52(1)
C(19)	4615(2)	3106(2)	5353(1)	30(1)
C(20)	4109(2)	1775(2)	5657(1)	32(1)
C(21)	2336(2)	2020(2)	6379(1)	42(1)
C(22)	9639(2)	3351(2)	4282(1)	50(1)
C(23)	8654(3)	3692(2)	3482(2)	59(1)
C(24)	9881(3)	4186(3)	2592(2)	68(1)
C(25)	11561(5)	3496(5)	2777(3)	45(1)
C(25')	11431(6)	4227(6)	2946(3)	50(1)

Table 3. Bond lengths [Å] and angles [°] for **22**.

O(1)-C(2)	1.2239(18)
O(2)-C(19)	1.2418(17)
O(3)-C(22)	1.431(2)
O(3)-C(25)	1.452(4)
O(3')-C(22)	1.353(13)
O(3')-C(25')	1.365(13)
N(1)-C(5)	1.3804(19)
N(1)-C(10)	1.4162(19)
N(1)-H(6)	0.84(2)
N(2)-C(19)	1.3250(19)
N(2)-H(2A)	0.89(2)
N(2)-H(2B)	0.92(2)
N(3)-C(2)	1.352(2)
N(3)-C(4)	1.4423(17)
N(3)-C(20)	1.4667(19)
C(2)-H(2)	1.024(17)
C(4)-C(9)	1.386(2)
C(4)-C(5)	1.408(2)
C(5)-C(6)	1.403(2)
C(6)-C(7)	1.386(2)
C(6)-H(7)	0.961(19)
C(7)-C(8)	1.388(2)
C(7)-H(8)	0.96(2)
C(8)-C(9)	1.390(2)
C(8)-H(9)	0.981(19)
C(9)-H(1N)	0.953(18)
C(10)-C(15)	1.397(2)
C(10)-C(11)	1.401(2)
C(11)-C(12)	1.398(3)
C(11)-C(16)	1.501(3)
C(12)-C(13)	1.385(3)
C(12)-H(12)	0.99(2)
C(13)-C(14)	1.380(3)
C(13)-C(17)	1.516(3)

C(14)-C(15)	1.395(2)
C(14)-H(14)	0.95(2)
C(15)-C(18)	1.504(3)
C(16)-H(16A)	1.00(3)
C(16)-H(16B)	1.03(3)
C(16)-H(16C)	1.02(3)
C(17)-H(17A)	0.9800
C(17)-H(17B)	0.9800
C(17)-H(17C)	0.9800
C(17)-H(17D)	0.9800
C(17)-H(17E)	0.9800
C(17)-H(17F)	0.9800
C(18)-H(18A)	0.98(3)
C(18)-H(18C)	0.95(3)
C(18)-H(18B)	0.99(2)
C(19)-C(20)	1.532(2)
C(20)-C(21)	1.520(2)
C(20)-H(20)	1.002(18)
C(21)-H(21A)	1.00(2)
C(21)-H(21B)	1.02(2)
C(21)-H(21C)	0.99(2)
C(22)-C(23)	1.493(3)
C(22)-H(22A)	0.9900
C(22)-H(22B)	0.9900
C(23)-C(24)	1.511(3)
C(23)-H(23A)	0.9900
C(23)-H(23B)	0.9900
C(24)-C(25)	1.400(5)
C(24)-C(25')	1.504(5)
C(24)-H(24A)	0.9900
C(24)-H(24B)	0.9900
C(25)-H(25A)	0.9900
C(25)-H(25B)	0.9900
C(25')-H(25C)	0.9900
C(25')-H(25D)	0.9900

C(22)-O(3)-C(25)	106.65(19)
C(22)-O(3')-C(25')	116.0(9)
C(5)-N(1)-C(10)	123.91(12)
C(5)-N(1)-H(6)	118.7(13)
C(10)-N(1)-H(6)	116.6(13)
C(19)-N(2)-H(2A)	116.6(13)
C(19)-N(2)-H(2B)	120.1(13)
H(2A)-N(2)-H(2B)	122.5(18)
C(2)-N(3)-C(4)	118.92(12)
C(2)-N(3)-C(20)	117.55(12)
C(4)-N(3)-C(20)	123.52(12)
O(1)-C(2)-N(3)	124.18(15)
O(1)-C(2)-H(2)	122.4(10)
N(3)-C(2)-H(2)	113.4(10)
C(9)-C(4)-C(5)	121.02(13)
C(9)-C(4)-N(3)	120.13(13)
C(5)-C(4)-N(3)	118.82(12)
N(1)-C(5)-C(6)	122.34(13)
N(1)-C(5)-C(4)	119.94(12)
C(6)-C(5)-C(4)	117.72(13)
C(7)-C(6)-C(5)	120.74(14)
C(7)-C(6)-H(7)	121.3(11)
C(5)-C(6)-H(7)	118.0(11)
C(6)-C(7)-C(8)	120.96(14)
C(6)-C(7)-H(8)	120.0(12)
C(8)-C(7)-H(8)	119.0(12)
C(7)-C(8)-C(9)	119.02(14)
C(7)-C(8)-H(9)	119.4(11)
C(9)-C(8)-H(9)	121.5(11)
C(4)-C(9)-C(8)	120.54(14)
C(4)-C(9)-H(1N)	118.8(11)
C(8)-C(9)-H(1N)	120.6(11)
C(15)-C(10)-C(11)	120.92(15)
C(15)-C(10)-N(1)	119.91(14)
C(11)-C(10)-N(1)	119.13(15)
C(12)-C(11)-C(10)	118.03(18)

C(12)-C(11)-C(16)	120.94(18)
C(10)-C(11)-C(16)	121.01(16)
C(13)-C(12)-C(11)	122.17(19)
C(13)-C(12)-H(12)	118.9(13)
C(11)-C(12)-H(12)	118.9(13)
C(14)-C(13)-C(12)	118.33(17)
C(14)-C(13)-C(17)	121.0(2)
C(12)-C(13)-C(17)	120.7(2)
C(13)-C(14)-C(15)	122.0(2)
C(13)-C(14)-H(14)	120.2(13)
C(15)-C(14)-H(14)	117.8(14)
C(14)-C(15)-C(10)	118.57(17)
C(14)-C(15)-C(18)	120.89(17)
C(10)-C(15)-C(18)	120.54(15)
C(11)-C(16)-H(16A)	114.9(14)
C(11)-C(16)-H(16B)	111.3(15)
H(16A)-C(16)-H(16B)	105(2)
C(11)-C(16)-H(16C)	110.6(15)
H(16A)-C(16)-H(16C)	106.7(19)
H(16B)-C(16)-H(16C)	108(2)
C(13)-C(17)-H(17A)	109.5
C(13)-C(17)-H(17B)	109.5
H(17A)-C(17)-H(17B)	109.5
C(13)-C(17)-H(17C)	109.5
H(17A)-C(17)-H(17C)	109.5
H(17B)-C(17)-H(17C)	109.5
C(13)-C(17)-H(17D)	109.5
H(17A)-C(17)-H(17D)	141.1
H(17B)-C(17)-H(17D)	56.3
H(17C)-C(17)-H(17D)	56.3
C(13)-C(17)-H(17E)	109.5
H(17A)-C(17)-H(17E)	56.3
H(17B)-C(17)-H(17E)	141.1
H(17C)-C(17)-H(17E)	56.3
H(17D)-C(17)-H(17E)	109.5
C(13)-C(17)-H(17F)	109.5

H(17A)-C(17)-H(17F)	56.3
H(17B)-C(17)-H(17F)	56.3
H(17C)-C(17)-H(17F)	141.1
H(17D)-C(17)-H(17F)	109.5
H(17E)-C(17)-H(17F)	109.5
C(15)-C(18)-H(18A)	108.2(15)
C(15)-C(18)-H(18C)	108.8(15)
H(18A)-C(18)-H(18C)	109(2)
C(15)-C(18)-H(18B)	113.4(14)
H(18A)-C(18)-H(18B)	108(2)
H(18C)-C(18)-H(18B)	109(2)
O(2)-C(19)-N(2)	123.57(13)
O(2)-C(19)-C(20)	121.46(12)
N(2)-C(19)-C(20)	114.89(13)
N(3)-C(20)-C(21)	112.02(12)
N(3)-C(20)-C(19)	110.53(12)
C(21)-C(20)-C(19)	109.02(13)
N(3)-C(20)-H(20)	110.2(10)
C(21)-C(20)-H(20)	109.1(10)
C(19)-C(20)-H(20)	105.7(10)
C(20)-C(21)-H(21A)	108.8(11)
C(20)-C(21)-H(21B)	109.3(11)
H(21A)-C(21)-H(21B)	110.6(15)
C(20)-C(21)-H(21C)	113.1(13)
H(21A)-C(21)-H(21C)	106.7(16)
H(21B)-C(21)-H(21C)	108.4(17)
O(3')-C(22)-O(3)	33.5(8)
O(3')-C(22)-C(23)	104.9(5)
O(3)-C(22)-C(23)	107.04(15)
O(3')-C(22)-H(22A)	80.5
O(3)-C(22)-H(22A)	110.3
C(23)-C(22)-H(22A)	110.3
O(3')-C(22)-H(22B)	137.0
O(3)-C(22)-H(22B)	110.3
C(23)-C(22)-H(22B)	110.3
H(22A)-C(22)-H(22B)	108.6

C(22)-C(23)-C(24)	104.38(16)
C(22)-C(23)-H(23A)	110.9
C(24)-C(23)-H(23A)	110.9
C(22)-C(23)-H(23B)	110.9
C(24)-C(23)-H(23B)	110.9
H(23A)-C(23)-H(23B)	108.9
C(25)-C(24)-C(25')	32.5(2)
C(25)-C(24)-C(23)	103.4(2)
C(25')-C(24)-C(23)	106.2(2)
C(25)-C(24)-H(24A)	111.1
C(25')-C(24)-H(24A)	134.1
C(23)-C(24)-H(24A)	111.1
C(25)-C(24)-H(24B)	111.1
C(25')-C(24)-H(24B)	80.3
C(23)-C(24)-H(24B)	111.1
H(24A)-C(24)-H(24B)	109.0
C(24)-C(25)-O(3)	109.8(3)
C(24)-C(25)-H(25A)	109.7
O(3)-C(25)-H(25A)	109.7
C(24)-C(25)-H(25B)	109.7
O(3)-C(25)-H(25B)	109.7
H(25A)-C(25)-H(25B)	108.2
O(3')-C(25')-C(24)	103.5(6)
O(3')-C(25')-H(25C)	111.1
C(24)-C(25')-H(25C)	111.1
O(3')-C(25')-H(25D)	111.1
C(24)-C(25')-H(25D)	111.1
H(25C)-C(25')-H(25D)	109.0

Symmetry transformations used to generate equivalent atoms:

Anisotropic displacement parameters ($Å^2 x\ 10^3$)for **22**. The anisotropic displacement factor exponent takes the form: $-2\pi^2[\ h^2a^{*2}U^{11} + ... + 2\ h\ k\ a^*\ b^*\ U^{12}\ ]$

	U^{11}	U^{22}	U^{33}	U^{23}	U^{13}	U^{12}
O(1)	56(1)	45(1)	27(1)	-3(1)	0(1)	-23(1)
O(2)	53(1)	28(1)	34(1)	4(1)	-18(1)	-19(1)
O(3)	34(1)	54(1)	41(1)	2(1)	-11(1)	-17(1)
N(1)	50(1)	32(1)	27(1)	5(1)	-12(1)	-21(1)
N(2)	46(1)	29(1)	35(1)	5(1)	-16(1)	-18(1)
N(3)	41(1)	24(1)	24(1)	0(1)	-6(1)	-14(1)
C(2)	47(1)	29(1)	29(1)	-5(1)	-4(1)	-15(1)
C(4)	37(1)	23(1)	26(1)	1(1)	-4(1)	-10(1)
C(5)	34(1)	25(1)	27(1)	0(1)	-4(1)	-11(1)
C(6)	44(1)	37(1)	25(1)	0(1)	-5(1)	-18(1)
C(7)	48(1)	37(1)	27(1)	6(1)	-4(1)	-19(1)
C(8)	50(1)	30(1)	38(1)	5(1)	-7(1)	-21(1)
C(9)	45(1)	28(1)	32(1)	-2(1)	-7(1)	-16(1)
C(10)	45(1)	37(1)	25(1)	5(1)	-8(1)	-24(1)
C(11)	45(1)	48(1)	39(1)	13(1)	-11(1)	-26(1)
C(12)	60(1)	78(2)	49(1)	26(1)	-27(1)	-45(1)
C(13)	90(2)	85(2)	35(1)	17(1)	-26(1)	-67(1)
C(14)	87(2)	56(1)	29(1)	3(1)	-13(1)	-48(1)
C(15)	60(1)	41(1)	26(1)	2(1)	-8(1)	-29(1)
C(16)	44(1)	49(1)	75(2)	11(1)	-9(1)	-16(1)
C(17)	145(3)	139(3)	55(1)	26(2)	-51(2)	-111(2)
C(18)	65(1)	39(1)	51(1)	-7(1)	-11(1)	-14(1)
C(19)	38(1)	27(1)	28(1)	0(1)	-7(1)	-13(1)
C(20)	42(1)	29(1)	28(1)	2(1)	-10(1)	-17(1)
C(21)	41(1)	37(1)	45(1)	6(1)	-7(1)	-14(1)
C(22)	37(1)	59(1)	50(1)	0(1)	-5(1)	-14(1)
C(23)	45(1)	70(1)	65(1)	1(1)	-18(1)	-24(1)
C(24)	69(1)	87(2)	56(1)	8(1)	-27(1)	-35(1)
C(25)	35(2)	59(3)	38(2)	-2(2)	-5(1)	-15(2)
C(25')	48(2)	66(3)	39(2)	3(2)	-9(2)	-27(2)

Hydrogen coordinates (x 10^4) and isotropic displacement parameters (Å^{2}x 10^3) for **22**.

	x	y	z	U(eq)
H(17A)	9139	4188	10003	143
H(17B)	10967	3114	9602	143
H(17C)	9641	2681	10570	143
H(17D)	10692	2467	10113	143
H(17E)	8864	3541	10515	143
H(17F)	10190	3974	9547	143
H(22A)	9184	4082	4704	60
H(22B)	9501	2494	4692	60
H(23A)	7527	4409	3639	70
H(23B)	8400	2882	3375	70
H(24A)	9744	3951	1988	81
H(24B)	9658	5180	2529	81
H(25A)	12375	4057	2471	54
H(25B)	12029	2636	2488	54
H(25C)	12514	3524	2690	60
H(25D)	11646	5128	2742	60
H(1N)	4180(20)	-1324(18)	6793(13)	37(4)
H(2)	8020(20)	-389(18)	5810(12)	34(4)
H(2A)	4100(30)	4740(20)	4485(15)	53(6)
H(2B)	3200(30)	3680(20)	4355(15)	53(6)
H(6)	6240(20)	2110(20)	7007(14)	40(5)
H(7)	5880(20)	66(19)	9206(14)	43(5)
H(8)	4640(30)	-1770(20)	9604(15)	47(5)
H(9)	3810(20)	-2507(19)	8417(13)	43(5)
H(12)	10690(30)	940(20)	9130(16)	65(6)
H(14)	6750(30)	4480(30)	9269(16)	65(7)
H(16A)	9020(30)	-940(30)	8252(17)	73(7)
H(16B)	9780(30)	-110(30)	7230(20)	82(8)
H(16C)	10900(40)	-640(30)	8114(18)	78(7)
H(18A)	4270(30)	4860(30)	8643(19)	83(8)
H(18C)	3900(30)	3630(30)	8372(17)	71(7)

H(18B)	4850(30)	4560(20)	7539(18)	71(7)
H(20)	3980(20)	1533(18)	5043(13)	40(5)
H(21A)	1430(30)	2740(20)	6060(14)	48(5)
H(21B)	2450(20)	2310(20)	6992(15)	48(5)
H(21C)	1900(30)	1210(20)	6578(16)	61(6)

Torsion angles [°] for **22**.

C(4)-N(3)-C(2)-O(1)	178.78(14)
C(20)-N(3)-C(2)-O(1)	-2.3(2)
C(2)-N(3)-C(4)-C(9)	-97.12(17)
C(20)-N(3)-C(4)-C(9)	84.04(18)
C(2)-N(3)-C(4)-C(5)	80.96(17)
C(20)-N(3)-C(4)-C(5)	-97.89(16)
C(10)-N(1)-C(5)-C(6)	9.1(2)
C(10)-N(1)-C(5)-C(4)	-170.57(14)
C(9)-C(4)-C(5)-N(1)	-179.96(14)
N(3)-C(4)-C(5)-N(1)	2.0(2)
C(9)-C(4)-C(5)-C(6)	0.4(2)
N(3)-C(4)-C(5)-C(6)	-177.71(13)
N(1)-C(5)-C(6)-C(7)	179.64(15)
C(4)-C(5)-C(6)-C(7)	-0.7(2)
C(5)-C(6)-C(7)-C(8)	0.6(3)
C(6)-C(7)-C(8)-C(9)	-0.1(3)
C(5)-C(4)-C(9)-C(8)	0.1(2)
N(3)-C(4)-C(9)-C(8)	178.13(14)
C(7)-C(8)-C(9)-C(4)	-0.2(2)
C(5)-N(1)-C(10)-C(15)	-115.64(17)
C(5)-N(1)-C(10)-C(11)	66.8(2)
C(15)-C(10)-C(11)-C(12)	0.8(2)
N(1)-C(10)-C(11)-C(12)	178.32(14)
C(15)-C(10)-C(11)-C(16)	-177.70(16)
N(1)-C(10)-C(11)-C(16)	-0.2(2)

C(10)-C(11)-C(12)-C(13)	-1.4(3)
C(16)-C(11)-C(12)-C(13)	177.15(18)
C(11)-C(12)-C(13)-C(14)	0.8(3)
C(11)-C(12)-C(13)-C(17)	-178.23(17)
C(12)-C(13)-C(14)-C(15)	0.3(3)
C(17)-C(13)-C(14)-C(15)	179.33(17)
C(13)-C(14)-C(15)-C(10)	-0.8(3)
C(13)-C(14)-C(15)-C(18)	179.04(17)
C(11)-C(10)-C(15)-C(14)	0.2(2)
N(1)-C(10)-C(15)-C(14)	-177.26(14)
C(11)-C(10)-C(15)-C(18)	-179.60(16)
N(1)-C(10)-C(15)-C(18)	2.9(2)
C(2)-N(3)-C(20)-C(21)	177.20(14)
C(4)-N(3)-C(20)-C(21)	-3.93(19)
C(2)-N(3)-C(20)-C(19)	-61.01(16)
C(4)-N(3)-C(20)-C(19)	117.86(14)
O(2)-C(19)-C(20)-N(3)	-31.7(2)
N(2)-C(19)-C(20)-N(3)	151.49(13)
O(2)-C(19)-C(20)-C(21)	91.85(17)
N(2)-C(19)-C(20)-C(21)	-84.97(17)
C(25')-O(3')-C(22)-O(3)	74.0(14)
C(25')-O(3')-C(22)-C(23)	-24.5(16)
C(25)-O(3)-C(22)-O(3')	-89.7(9)
C(25)-O(3)-C(22)-C(23)	1.6(3)
O(3')-C(22)-C(23)-C(24)	16.5(9)
O(3)-C(22)-C(23)-C(24)	-18.3(3)
C(22)-C(23)-C(24)-C(25)	28.4(3)
C(22)-C(23)-C(24)-C(25')	-5.1(3)
C(25')-C(24)-C(25)-O(3)	70.5(5)
C(23)-C(24)-C(25)-O(3)	-28.7(4)
C(22)-O(3)-C(25)-C(24)	17.7(4)
C(22)-O(3')-C(25')-C(24)	20.9(16)
C(25)-C(24)-C(25')-O(3')	-97.5(11)
C(23)-C(24)-C(25')-O(3')	-7.9(10)

Symmetry transformations used to generate equivalent atoms:

Hydrogen bonds for **22** [Å and °].

D-H...A	d(D-H)	d(H...A)	d(D...A)	<(DHA)
N(1)-H(6)...O(2)	0.84(2)	2.06(2)	2.9017(16)	174.1(17)
N(2)-H(2A)...O(2)#1	0.89(2)	2.02(2)	2.9058(17)	178.5(19)
N(2)-H(2B)...O(3)#2	0.92(2)	2.01(2)	2.933(2)	176.8(19)

Symmetry transformations used to generate equivalent atoms:

#1 -x+1,-y+1,-z+1 #2 x-1,y,z